THE UNIVERSITY *of* EDINBURGH

A comparison of the infection biology and transcriptome of wild-type and single gene deletion strains of *Fusarium graminearum*

Neil Andrew Brown

Supervisors:

Prof. Kim Hammond-Kosack / Rothamsted Research

Dr Allison van de Meene / Rothamsted Research

Prof. Nick Read / University of Edinburgh

Dr Sarah Perfect / Syngenta

Name of Degree: Doctor of Philosophy

The University of Edinburgh

Year of presentation: 2011

Abstract

Fusarium Ear Blight is a devastating fungal disease of cereals and due to the contamination of the harvested grain with a range of trichothecene mycotoxins presents a risk to human and animal health. The re-emergence of *Fusarium graminearum* on wheat and maize, the evolution of more aggressive fungal strains and the lack of an effective control strategy, has increased the need for a greater understanding of the disease aetiology. This project aimed to enhance the understanding of the interaction between *F. graminearum* and wheat (*Triticum aestivum*), through the utilisation of microscopy and molecular pathogenomics.

A detailed investigation of the infection process revealed a prolonged latent period of intercellular infection that preceded host cell death, intracellular colonisation and the onset of disease symptoms. Phenotypic differences in colonisation and mycotoxin gene expression implied that hyphae within the two phases of infection were transcriptionally distinct, while a bioinformatic analysis described the fungal secretome. The two fungal gene-deficient strains assessed, *top1* and *tri5*, were unable to establish symptomless infection or spread throughout the wheat ear, in the presence or absence of mycotoxin production, suggesting the existence of additional virulence factors.

Subsequently, a genome wide transcriptome investigation of the two phases of infection, using both Affymetrix and RNA-sequencing technologies, revealed the unique expression profile, and secretome, of the advancing hyphal front of the symptomless infections. This greater understanding of the biphasic interaction will provide a benchmark for comparison with the single gene deficient strains. Finally, a laser capture microdissection procedure was developed to enable future cell-type specific transcriptome experiments.

Collectively, I have discovered and developed a model of how *F. graminearum* establishes symptomless and symptomatic infection. In doing so, this study has enhanced the understanding of this non-biotrophic pathosystem, providing many new lines of investigation, which could greatly improve crop protection strategies.

Acknowledgements

I would like to thank all my supervisors for their guidance and for giving me this opportunity. I am especially thankful to Kim Hammond-Kosack and Martin Urban for their excellent advice, support and encouragement. Thank you to Allison van de Meene, Sarah Perfect and Nick Read for their useful discussion and assistance during manuscript preparations. I would also like to thank Jean Devonshire for her technical guidance and assistance during the microscopy analysis as well as, John Lucas and Jason Rudd for their editorial assistance during manuscript preparations. I am grateful to all of my helpful colleagues in the Plant Pathology and Microbiology department at Rothamsted who created a stimulating environment and were great company every day. Thank you to all the support staff for maintaining the controlled environment facilities, equipment and a reliable supply of wheat plants for experiments. Thank you to Nicola Seymour, Lynda Castle and Graham Shephard in the Visual Communications unit for the preparation of conference posters. This project was jointly funded by a BBSRC-Syngenta Industrial-CASE studentship. All experiments involving *F. graminearum* isolate PH-1 and the transgenic reporter strain were conducted in biological containment facilities under FERA licence number PHL 174G/6222. Finally, to my wife, without you this would not have been possible. Thank you.

Table of contents

List of abbreviations

1-MCP	1-methylcyclopropene
AMP	Adenosine monophosphate
ATP	Adenosine triphosphate
Avr	Avirulence gene
BLAST	Basic local alignment search tool
cAMP	Cyclic adenosine monophosphate
CO_2	Carbon dioxide
CYS	Cysteine residues
d H_2O	Sterile distilled water
DNA	Deoxyribonucleic acid
DON	Deoxynivalenol
DPI	Days post inoculation
EST	Expressed sequence tags
ET	Ethylene
ETI	Effector-triggered immunity
ETS	Effector-triggered susceptibility
FAO	Food and agriculture organisation
FEB	Fusarium ear blight
gDNA	genomic DNA
GFP	Green fluorescent protein
GUS	β-glucuronidase enzyme
H_2O_2	Hydrogen peroxide
HPI	Hours post inoculation
HR	Hypersensitive response
HST	Host selective toxin
IR	Infra red
JA	Jasmonic acid
KEGG	Kyoto encyclopedia of genes and genomes
LCM	Laser capture microdissection
LCP	Laser pulse catapulting
MAPK	Mitogen activated protein kinase
MAPKK	Mitogen activated protein kinase kinase
MAPKKK	Mitogen activated protein kinase kinase kinase
MIPS	Munich information centre for protein sequences
MUG	4-methylumbelliferyl-b-D-glucuronide
NGS	Next generation sequencing
NIV	Nivalenol
NLS	Nuclear localisation signal
O_2	Oxygen

PAMP	Pathogen associated molecular patterns
PCD	Programmed cell death
PCR	Polymerase chain reaction
PCWDEs	Plant cell wall degrading enzymes
PI-3-P	Phosphotidyl-inositol-3-phosphate
PKA	cAMP-dependent protein kinase A
PR	Pathogenicity-related
PRR	Pattern recognition receptors
PTI	PAMP-triggered immunity
qPCR	Quantitative PCR
QTL	Quantitative trait loci
R	Resistance gene
RI	Rachis internode
RIP	Repeat-induced point mutation
RNA	Ribonucleic acid
ROS	Reactive oxygen species
RT	Reverse transcription
SA	Salicylic acid
SAR	Systemic acquired resistance
SEM	Scanning electron microscopy
SNPs	Single nucleotide polymorphisms
TBO	Toluidine blue O
UV	Ultraviolet light
VIGS	Virus induced gene silencing
ZEA	Zearalenone

List of units

cm	Centimetre
mm	Millimetre
µm	Micrometre
nm	Nanometre
L	Litre
ml	Millilitre
µl	Microlitre
g	Gram
mg	Milligram
µg	Microgram
ng	Nanogram
pg	Picogram
M	Mole
mM	Millimole
nM	Nanomole
pM	Picomole
N	Normality
U	Units
sec	Second
min	Minute
h	Hour
Mb	Megabase pairs
Kb	Kilobase pairs
bp	Base pairs
ppm	Parts per million
%	Percent
^{o}C	Degrees celsius
rpm	Revolutions per minute
£	Pounds sterling

Chapter 1. Introduction

1.1. The current pressures on global agriculture

The era of cheap food is at an end. Rising fossil fuel prices, plummeting water tables, limited availability of fertile land, fears that finite resources are running out and the anticipated impact of climate change all depict a worsening situation. This is exaggerated by the growth of the world's population, which is forecast to reach nine billion by 2050. Food is the single most influential factor on human health and now food security has become prevalent on the world's political agenda. Globalisation and the distribution of resources or wealth has made tackling the issue of food security, and providing a 70 % increase in agricultural output by 2050 (Food and Agriculture Organisation (FAO), 2010), a global problem that can only be solved by multinational cooperation.

Cereal crops are the most important provider of human calories. Wheat and maize prices rose in the last 12 months by 69 % and 74 %, respectively (www.worldbank.org/foodcrisis/foodpricewatch/april_2011.html). Two large spikes in the price of cereal grain in the last four years are of serious concern, particularly in the developing world and non-cereal producing countries where price rises push people into poverty, spark food riots and have also played a part in the political uprising in the Middle East during 2011. In addition, the nationalistic views of exporters banning grain sales and rich nations purchasing land within poorer countries to sustain their demand for food, present worrying moral issues. It will be difficult to increase food supply at a similar rate to that which was achieved over the last 50 years by the Green Revolution (Khush, 2001) and the invention of synthetic fertilisers, but this is what is required.

Monitoring global consumption of wheat, rice and maize generally tracks the global demand for food. The yields of these three crops, especially wheat and rice, are growing at a slower rate than the human population (FAO, 2009). In North America maize outputs have increased at a greater pace than the other cereals as a result of the acceptance of biotechnology. In developed countries there is a trend for farmers to use fewer inputs, due to the environmental and economic benefits. In these situations the actual yield increase may be greater than reported. It may therefore be

possible to quickly increase the agricultural output of these efficient systems by applying additional inputs. This is dependent on food prices rising faster than the cost of inputs, which is unlikely, as in recent years fertiliser prices rose higher than food (FAO, 2009), due to the cost of fuel and fears that phosphorus will run out (Cordell *et al.*, 2009). In many current agricultural systems increased fertiliser use would also be counterproductive and cause profound ecological damage to our water systems. The majority of the land available for agriculture is already in use, of which 28.3 % is used for arable farming (FAO, 2009), while the free land, mainly in Latin America and Africa, is exposed to land grabs by rich nations, threatening the food security of the local inhabitants. For the first time in history more people live in cities than they do in the countryside (http://esa.un.org/unpd/wup/). These thirsty cities are competing with agriculture for a limited water supply and water tables are already plummeting. Drip-feed irrigation and no-till agriculture would help to reduce water loss in agricultural systems. However, reduced tilling can be detrimental to crop management. Consequently, the option of simply using more inputs on a larger scale to increase food production is not viable.

In addition to increasing agricultural output, production systems need to limit losses incurred through pests, pathogens and severe weather events linked to climate change. Plants are constantly under attack by insect herbivores, and nematodes which can transmit viral diseases, as well as fungal, oomycete and bacterial infections. The application of chemical pesticides, the use of resistant plant varieties and / or specific cultural practices often only partially mitigates these problems. Some pathogens have only recently emerged as global threats, whilst others have remained difficult to control after decades of research. But more distressing is the rise in pest and pathogens resistant to pesticides, which were widely introduction in the late 1940s. Climate change is forecast to cause more frequent extreme weather events and in combination with a 2^{o}C rise in temperature, which is a modest prediction, will reduce cereal output, particularly in Africa (Parry *et al.*, 2005). The negative impacts will more than counteract any benefits derived from increased photosynthetic rate of plants associated with higher atmospheric CO_2 levels. Additionally, the geo-thermal boundaries of pests and pathogen distribution will be altered, possibly resulting in the emergence of new, or exaggeration of existing, disease problems.

Besides the production of higher yielding, more stress resistant varieties of existing crops, phenotypic variations within land races represents a large genetic resource to be exploited with the domestication of new crops. Through genetic and traditional approaches, stress and disease tolerance could be adapted to individual microenvironments. The development of new uses for existing agricultural produce, such as the use of molecular genetics to enhance willow (*Salix spp.*) lignocellulosic biomass and bioethanol production, will also contribute to an overall increase in agricultural output. Together the diversifying use of existing and new crops will help meet the demands of a changing world.

The popularised political slogan from Sir John Beddington (Chief Scientific Adviser to the UK Government, 2008-present) of 'doing more with less' effectively summarises the situation faced by industrial agriculture and modern biological sciences. While traditional or organic farming could feed the wealthy, it would not be able to sustain a world of nine billion people. The development and dissemination of better technology, across the world, reducing the productivity gap between efficient and inefficient producers, represents the best way to rise to the demand for agricultural produce. The introduction of the semi-dwarfing *RHT* genes into cereals during the Green Revolution reduced plant height and increased yield (Peng *et al.*, 1999, Reynolds & Borlaug, 2006). This sustained population growth since the 1960s and helped people avoid starvation. The conversion of the acidic grasslands of Brazil into the heart of soyabean production via the identification of suitable nitrogen-fixing *Rhizobia* represents another modern agricultural science success story (Hungria *et al.*, 2006). However, these drastic examples are the exception and the majority of advancements will be achieved by a gradual process. The greater understanding of plant and microbe genetics, determined by genomics and genetic modifications, now makes it possible to grow modified crops and also increases the speed at which new crop varieties can be developed by marker assisted-breeding. The collective understanding of the genomic and metabolic networks behind desired crop traits will enable the development of new crop varieties, which are better suited to individual microenvironments and are more resistant to pests or pathogens, matching the required demand for growth and through intellectual property rights stimulating economies.

1.2. The impact of fungal disease on cereal farming

The three cereal crops, wheat, rice and maize, provide the bulk of the worlds calorific intake and are all subject to infield and post-harvest diseases. Pathogens account for ~ 10 % of annual food production being lost, of which fungal incited diseases are a major contributor (Strange & Scott, 2005). Fungal diseases are particularly problematic due to their ability to sporulate profusely, where spores can be dispersed long distances in the wind or be delivered in high densities to the host in a water droplet and the relatively short time between the initiation of infection and the production of sporulation structures. Where airborne spores are lacking, vegetative propagules and / or highly resistant resting stages can lead to the contamination of the soil, often for decades. The genetic adaptability of fungal diseases can result in devastating consequences, as demonstrated by the Southern Corn Leaf Blight epidemic of the 1970s. Acquisition of a host selective toxin, the T-toxin, by *Cochliobolus heterostrophus* dramatically increased virulence and resulted in the worst agricultural epidemic in the history of the USA, with 15 % of the maize crop being lost (Inderbitzin *et al.*, 2010, Ullstrup, 1972). Stem rusts caused by *Puccinia graminis* have historically caused severe losses to wheat production. The worst rust epidemic in the USA, in 1935, resulted in 50 % of the wheat crop in North Dakota and Minnesota being lost (Leonard & Szabo, 2005). More recently, a new rust strain originating from Uganda in 1999, named Ug99, spread across Africa into Asia and overcame the majority of resistant wheat cultivars (Singh *et al.*, 2011). Variant strains of the Ug99 lineage that overcame different wheat resistance genes have also been identified and differ only in their avirulence / virulence profile (Singh *et al.*, 2011) demonstrating the pathogen's adaptive capability.

In the UK fungal disease pressure also has a dramatic impact on the productivity of the number one crop, wheat, for which 1,814,000 hectares were planted in 2009 (FAO, 2009). Problematic fungal disease for UK wheat production include: foliar diseases – Mildews (*Blumeria graminis*), Tan spot (*Pyrenophora tritici-repentis*), Septoria leaf blotch (*Mycosphaerella graminicola*), Yellow and Brown rusts (*Puccinia striiformis* and *P. triticina*), stem base diseases - Fusarium (*Fusarium spp.*) and Eye spot (*Tapesia yallundae*), ear diseases – Fusarium ear blight and glume spot, and finally root diseases - Take-All (*Gaeumannomyces graminis*)

and Fusarium root rot. In the 2009 / 2010 season, Septoria leaf blotch was the most prevalent foliar disease, despite severity dropping for four successive years, incidence remained high, affecting 52 % of samples (www.cropmonitor.org). Mildews and Tan spot represented the second and third most common foliar disease, while Yellow rust was detected at a low level and for the first time since records began, Brown rust was not detected at all (www.cropmonitor.org). The incidence of Fusarium and Eye spot stem infections, as well as Fusarium ear blight, remains above the 10 year mean (www.cropmonitor.org). The economically important diseases Fusarium ear blight, Septoria leaf blotch and Take-all individually attack the main three plant structures, but represent just a fraction of the threat. Together these three diseases cause annual losses to UK agriculture in excess of £90 million, despite farmers spending millions on fungicide applications. In severe disease epidemic years, great yield losses can be incurred, while lower grain quality and safety can also have major implications for the food, drink and feed supply chains. A greater understanding of the interactions between pathogenic species and host plants will enable the design of new approaches to minimise diseases now and permit the discovery of new compounds or protein targets for future advances in disease control.

The invention and advancement of genomic sequencing technologies continues to greatly advance the understanding of host pathogen interactions. This knowledge of the molecular determinants of host susceptibility / resistance, pathogen virulence and the understanding of what caused dramatic shifts in pathogenicity that resulted in disease epidemics over the decades will enable modern bioscience to adapt to the changing threat from fungal diseases. The analysis of historic natural species and strain collections will also play a major role in the discovery process. Histological and genetic studies of varying fungal modes of infection and concepts arising from the genomics era are discussed in turn.

1.3. Modes of infection across the spectrum of fungal lifestyles

Among plant pathogenic fungi a huge variability exists in the mode of infection and the method of obtaining nutrition. Fungal plant pathogens are generally sub-divided according to their nutritional strategy. Biotrophs acquire sustenance from live plant cells for extended periods, while necrotrophs rapidly kill the host

plant cells and live on the released nutrients. Not all fungal pathogens clearly fit into these two distinct categories. Pathogens that have an initial transient phase reminiscent of a biotroph, which precedes necrotrophy, are classified as hemibiotrophs (Agrios, 1997). However, pathogenicity has evolved many times and cannot easily be placed on a continuum between the two extremes (Oliver & Solomon, 2010), but for the purpose of this review, this has been attempted. Several economically and scientifically important examples of each fungal pathogen sub-division, biotrophs, hemibiotrophs and necrotrophs, are discussed. On occasions, the necrotrophs and hemibiotrophs are collectively referred to as the non-biotrophs. The differential mechanisms deployed by fungal pathogens to complete their lifecycle in association with a host plant have driven the evolution of different plant defence responses associated with the recognition of fungal pathogens with a specific lifestyle. Firstly, the implication of pathogen lifestyle on plant defence is introduced.

1.3.1. The differential response of plants to biotrophic and necrotrophic fungal infection

Constitutive plant defences require substantial resources and are difficult to mobilise. Constructing localised physical barriers in response to perceived infection through the production of callose or lignin and the synthesis of antimicrobial metabolites or proteins that contribute to resistance has a cost on plant fitness. Subsequently, many plant defence mechanisms are only induced upon pathogen attack (Smith *et al.*, 2010) and rely on the plant cell's innate immunity and emission of systemic defence signals. Such organisation of defence relies upon the successful recognition of infection and the induction of appropriate response to the presented threat. Plants utilise pathogen associated molecular patterns (PAMPs) that are often secreted, or on the surface of pathogen, or released as a result of the pathogens presence (modified self), such as chitin or cell wall fragments. PAMP recognition via transmembrane pattern recognition receptors (PRRs) causes an influx in calcium and the production of an oxidative burst, activating mitogen activated protein kinases (MAPK) and calcium-dependent protein kinases to induce defence gene expression (Smith *et al.*, 2010). Activation of plant basal defences leads to cell wall reinforcements, antimicrobial production and the induction of defence signalling components that collectively restrict infection and result in PAMP-triggered

immunity (PTI). PAMPs represent compounds that are difficult to modify or lose and as a result considerable selection pressure is exerted upon the pathogen by host PAMP recognition. Pathogens however, have evolved secreted effectors to interfere or suppress basal defences, resulting in effector-triggered susceptibility (ETS). In the constant arms race between pathogen and host, plants have acquired effector receptors, termed resistance (*R*) genes. *R* gene mediated effector recognition results in the activation of similar signal cascades as PRR triggered defences but the response is stronger and can result in host cell death. Highly localised cell death at the point of initial infection is frequently termed the hypersensitive response (HR) which limits water and nutrient availability to the pathogen and prevents the symplastic translocation of fungal toxins or effectors. Within the dead and surrounding plant cells antimicrobial concentration is also high. The induction of a strong *R* gene mediated defensive response and HR in effector-triggered immunity (ETI) is effective at restricting biotrophic and hemibiotrophic infections. Effectors that are recognised either directly or indirectly by *R* gene encoded receptors in this gene-for-gene interaction are termed avirulence (*Avr*) genes. Selection pressure exerted upon *Avr* genes can result in their mutation or loss. Alternatively, pathogens have also adapted to overcome ETI by secreting additional effectors that suppress ETI. The evolutionary view of plant immunity is summarised by the 'ZigZag' model first proposed by Jones and Dangl (2006) (Figure 1).

The activation of systemic acquired resistance (SAR) by two different mechanisms is somewhat slower. SAR induced by the salicylic acid (SA) mediated defence signalling pathway terminates with the production of pathogenicity-related (PR) proteins, which contribute to resistance (Smith *et al.*, 2010). While being effective against biotrophic pathogens, such a defensive response would be ineffective or only weakly effective at combating necrotrophic fungal infection and may actually assist necrotroph infection. SAR induced by the ethylene (ET) and jasmonic acid (JA) signalling pathways, which also plays a role in the wounding response, result in the production of antimicrobials such as phytoalexin and camalexin (Smith *et al.*, 2010). Indeed, blocking SA signalling in Arabidopsis via mutating the *npr1* (non expressor of PR1) gene causes an increase in susceptibility to

biotrophs, while blocking JA signalling via mutating *coi1* (coronatine-insensitive 1) increased susceptibility to necrotrophs (Spoel *et al.*, 2007).

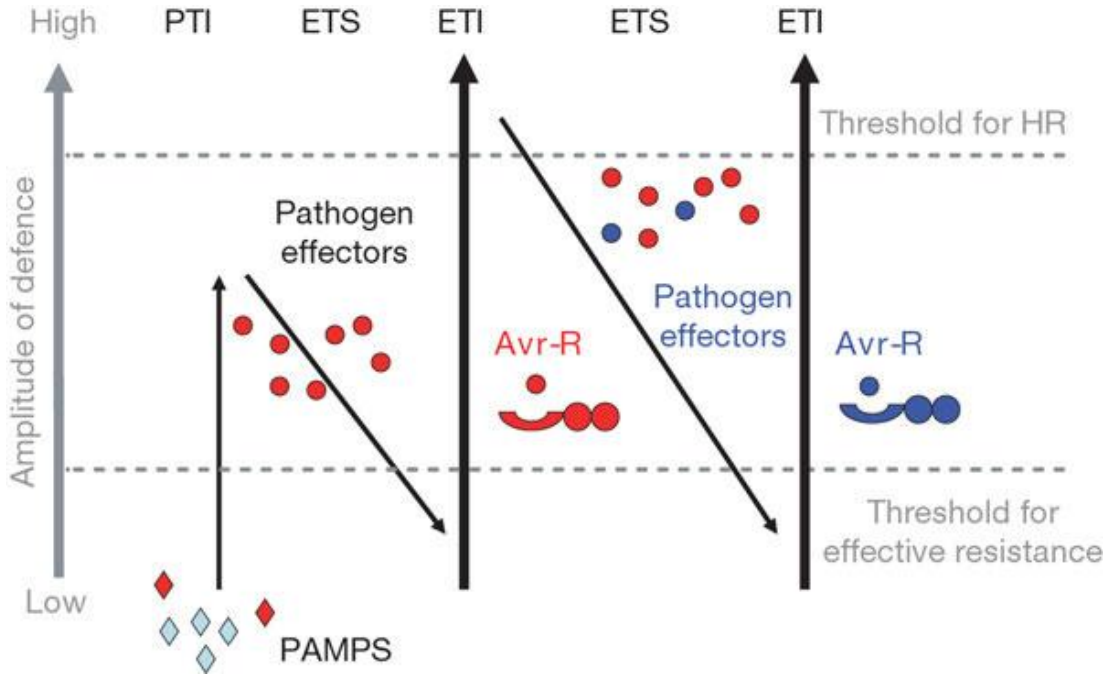

Figure 1 The four phased 'ZigZag' model of the plant immune system, taken from Jones and Dangl (2006).

1.3.2. Biotrophs

Biotrophic pathogens depend upon the integrity of the invaded plant cell(s) for supporting vegetative growth and reproduction. Therefore, the biotrophic lifestyle is intimately coordinated with, and specialised to, a particular host. For example, the seed transmitted endophyte *Epichlöe festucae* which tightly coordinates growth with ryegrass (*Lolium spp.*) leaf development. *E. festucae* initially colonises the seedling via invasive hyphal tip growth to establish a systemic colony that is followed by intercalary non-invasive hyphal growth during leaf extension. Other biotrophs, including the Ascomycetes *Blumeria graminis* f. sp. *hordei* and *tritici* and *Cladosporium fulvum* (*Passalora fulva*) and the Basidiomycetes *Puccinia spp.* and *Ustilago maydis* are not seed transmitted and must therefore invade the plant. For this purpose *B. graminis* and *U. maydis* form a specialised infection structure at the tip of the germ tube, called an appressorium which supports the development of a penetration peg that through mechanical pressure and enzymatic degradation punctures the plant cell wall (Deising *et al.*, 2000). Whilst other biotrophs, for

example *Puccinia spp.* and *C. fulvum* directly enter the plant via the open stomata and therefore, in the absence for a need to penetrate the plant cell wall, do not produce appressoria.

Beyond the cell wall, the invading hyphae of some species develop into specialised feeding structures called haustoria that are invaginated by the plant plasma membrane. The extrahaustorial space between the plant plasma membrane and haustoria is acidified to assist the uptake of amino acids and sugars (Voegele *et al.*, 2001). The haustoria are not only a site of nutrient exchange but also a mechanism of delivering secreted effectors to manipulate the host and maintain the interaction, as is the case for *B. graminis* (Panstruga, 2003). Fungal biotrophic pathogens that do not produce haustoria also secrete effector proteins to perturb host defences. The non haustorial producing intracellular *U. maydis* hyphae secrete an array of plant tissue specific effectors, in addition to Pep1 that is required for cell-to-cell passage, to permit infection of live host cells (Doehlemann *et al.*, 2009, Skibbe *et al.*, 2010). In comparison the non-haustorial producing extracellular biotroph, *C. fulvum*, adopts an alternative strategy and secretes an array of cysteine-rich apoplastic effectors that mask infection. The best characterised example, Avr4 binds chitin fragments, released from the fungal cell wall by the action of plant chitinases, preventing PTI (Stergiopoulos & de Wit, 2009). Another small secreted cysteine-rich protein called Ecp6 contains three LysM domains that also enable chitin scavenging and PTI prevention (de Jonge *et al.*, 2010). Plants have co-evolved a defensive strategy and in the case of *AVR4* the presence of the tomato *R* gene *CF-4* results in pathogen recognition, HR and ETI (Stergiopoulos *et al.*, 2010). *AVR4* has been demonstrated to be under diversifying selection, predominantly altering cysteine residues making the protein less stable and reducing fungal elicitor build-up in the apoplast and thereby reducing the likelihood of ETI (Van der Hoorn *et al.*, 2001).

Recently, several pathogen genome sequencing projects have greatly advanced the understanding of biotrophic infection and evolution (Cuomo *et al.*, 2007, Dean *et al.*, 2005, Kämper *et al.*, 2006, Spanu *et al.*, 2010). Comparative genomics between biotrophs and non-biotrophs revealed a reduction in plant cell wall degrading enzymes (PCWDEs) in biotrophs, where *U. maydis* is predicted to encode 33 compared with the 103 encoded by the non-biotroph *Magnaporthe oryzae*

(Soanes *et al.*, 2007). The plant tissues infected by biotrophic pathogens do not become macerated like tissue colonised by non-biotrophs. This suggests that the limited amount PCWDEs produced by biotrophs are restricted to particular infection phases, assisting cell-to-cell passage and not synthesised to obtain nutrition from plant polysaccharides. The release of cell wall fragments elicits host defences and HR, thus the wide scale secretion of PCWDEs would be counterproductive for a biotroph. Components of secondary metabolism, such as polyketide synthases, which are associated with antibiotics and mycotoxin synthesis are also dramatically reduced in *B. graminis* and *U. maydis* compared with the non-biotrophs *Fusarium graminearum* and *M. oryzae* (Soanes *et al.*, 2007). The reduction in virulence-associated and metabolic genes in biotrophic genomes has resulted in them encoding a far lower number of genes compared to non-biotrophs (Soanes *et al.*, 2007). However, this does not always result in a smaller genome. *B. graminis* f. sp. *hordei* has the largest ascomycete genome reported to date, of which 64 % is accounted for by transposable elements. This type of genome organisation is hypothesised to provide increased genetic variability in the presence of limited sexual recombination (Spanu *et al.*, 2010).

1.3.3. Hemibiotrophs

Not all non-biotrophs kill their host immediately and a growing list of pathogens, previously classified as necrotrophs keep the host alive for the initial phase of infection before switching to necrotrophy. These are the hemibiotrophs. *M. oryzae* was once thought to be a necrotroph, but live-cell imaging discovered that the intracellular hyphae, produced post appressorial penetration, are surrounded by the plant plasma membrane and these invaginated hypha have been shown to secrete fungal effectors that maintain the transitional biotrophic interaction (Kankanala *et al.*, 2007), similar to the appressoria and haustoria of biotrophs. The hemibiotrophs, *M. oryzae* and possibly *F. graminearum* possess a large number of G-coupled protein receptors, 61 and 84 genes respectively, reflecting the need to respond to environmental cues (Soanes *et al.*, 2007) and possibly play a role in the switch between biotrophy and necrotrophy. Similar to *C. fulvum*, the extracellular hemibiotroph, *Mycosphaerella graminicola* also penetrates the plant via stomatal openings and colonises the apoplast initially avoiding recognition through the

secretion of three LysM domain containing chitin-binding apoplastic effectors (de Jonge *et al.*, 2010, Marshall *et al.*, 2011). This lack of recognition permits *M. graminicola* hyphae to colonise by stealth, but to achieve this, the total amount of fungal biomass in the leaf remains very low. In rice, the existence of the two cooperating LysM containing receptors, CEBIP and OSCERK1 regulate chitin elicitor signalling (Shimizu *et al.*, 2010). Plant receptors of this type provided the selection pressure for fungal LysM effector evolution. After 10-14 days disease symptoms develop, which is proposed to occur after the pathogen is unmasked, widespread programmed cell death (PCD) is induced, the hyphae enter the host cells and asexual sporulation within pycnidia occurs (Deller *et al.*, 2011). The mechanisms controlling the switch between the two phases of the hemibiotrophic interactions are still not completely understood. During the necrotrophic phase of a hemibiotrophic interactions PCWDEs are synthesised to breakdown plant polysaccharides into ingestible carbon sources to support vegetative growth and reproduction. The maintenance of a large number of PCWDEs within the *M. oryzae* and *F. graminearum* genomes suggests that despite some enzymatic redundancy, such PCWDE diversity is required. By contrast, the genome of *M. graminicola* is predicted to encode a minimal number of PCWDEs (Goodwin *et al.*, 2011).

1.3.4. Necrotrophs

Necrotrophic pathogens attempt to kill the host plant via the production of reactive oxygen species (ROS), PCWDEs and toxic low molecular weight secondary metabolites or proteins. Many necrotrophic interactions do not conform genetically to the gene-for-gene type of interaction. These include *Botrytis cinerea* and *Sclerotinia sclerotiorum*. *B. cinerea* rapidly synthesises PCWDEs to obtain nutrients, while plant cell wall fragments and H_2O_2 released or produced by the pathogen induce host cell death (Govrin & Levine, 2000, von Tiedemann, 1997). Conversely, *E. festucae* also requires ROS but to maintain a mutualistic interaction with ryegrass. Disruption of ROS production in *E. festucae* results in proliferative pathogenic growth and a loss of mutualism (Tanaka *et al.*, 2008). Toxins are produced by some necrotrophic pathogen to kill plant cells and limit the production of antifungal compounds and ROS. *S. sclerotiorum* also secretes an array of PCWDEs that are transcriptionally controlled by nutrient availability and pH (Rollins, 2003, Rollins &

Dickman, 2001). The secretion of oxalic acid is also required for full pathogenicity as it inhibits the plant from producing the defence signalling and antimicrobial molecule H_2O_2, lowers the environmental pH weakening the plant cell and induces fungal PCWDEs production (Bolton *et al.*, 2006, Cessna *et al.*, 2000).

The production of a host selective toxin (HST) by some necrotrophic fungi represents an inverse gene-for-gene interaction, where both the plant target gene and a HST gene are required for infection. *Cochliobolus victoriae* produces the HST, victorin, which is a low molecular weight secondary metabolite that binds to the mitochondrial glycine decarboxylase inhibiting serine synthesis, but only if the host oat plant has the susceptibility *VB* gene (Navarre & Wolpert, 1999, Wolpert *et al.*, 2002). *Stagonospora nodorum* secretes a range of host selective proteinaceous toxins, ToxA, Tox1 Tox2 Tox3 and Tox4, recently termed necrotrophic effectors, which are recognised when the host wheat possesses the corresponding genes *TSN1*, *SNN1*, *SNN2*, *SNN3* and *SNN4* (Friesen *et al.*, 2007). The combined secretion of the range of Tox proteins has an additive effect, resulting in light induced damage of thylakoid membranes within chloroplasts and mesophyll cell death (Deller *et al.*, 2011). A *TOXA* homologue is also present in the taxonomically related species *Pyrenophora tritici repentis* genome. *TOXA* is hypothesised to have originated in *S. nodorum* and been transferred to *P. tritici repentis* via a horizontal gene transfer event (Friesen *et al.*, 2006). Similar to the biotrophic effectors of *C. fulvum*, *TOXA* has also been shown to be exposed to positive selection, encouraging rapid evolution, demonstrating the dynamic requirement for the generation of variation in the arms race between pathogen and host.

1.4. Fusaria

The genus *Fusarium* is large and contains both soil and plant associated filamentous species, some with sexual phases. The Fusaria include many destructive plant pathogenic species. In cereal and non-cereal agricultural crops, in horticultural production and in forestry, diseases caused by various *Fusarium* species are of growing concern and cause equivalent economic losses. For example, various *formae specialis* of *F. oxysporum* cause wilt diseases on a wide range of hosts, from banana to tomato (Michielse & Rep, 2009), *F. sambucinum* and *F. solani* cause dry rot of tubers (Delgado *et al.*, 2010), *F. circinatum* causes pine bark cankers (Wingfield *et*

al., 2008), while *F. culmorum, F. graminearum* and *F. verticillioides* cause ear blight disease on cereals (Leonard & Bushnell, 2003). The majority of Fusaria are harmless to human and animal health, however, some species, *F. oxysporum*, *F. solani* and *F. moniliforme*, have been associated with opportunistic animal infections, of which immunocompromised mammals are particularly susceptible (Dignani & Anaissie, 2004). Conversely, *F. venenatum* is used as an alternative to meat protein for human consumption and the commercial product, named Quorn, is popular among vegetarians.

1.4.1. Fusarium Ear Blight (FEB)

Reported outbreaks of FEB, alternatively known as head scab (www.scabusa.org), have been associated with 17 different *Fusarium* species, of which five are predominant; *F. avenaceum, F. culmorum, F graminearum, F. poae* and the non-mycotoxin producer *Microdochium nivale* (Parry *et al.*, 1995). The distribution of these pathogenic filamentous ascomycetes, throughout the cereal growing regions of the world, is temperature dependant. *F. graminearum stricto sensu* (teleomorph *Gibberella zeae*) globally is the most destructive and is generally associated with hotter regions such as the USA and Central Europe, whereas *F. culmorum* is prevalent in cooler regions such as Northern Europe (Xu *et al.*, 2008). The superior competitiveness of *F. graminearum* compared to *F. avenaceum, F. culmorum* and *F. poae* could help explain the global increase of this species. The thermo-geographic divide between different *Fusarium* species is becoming less defined and *Fusarium* species adapted to warmer environments are pushing north due to the direct and indirect effects of alterations to the global climate. Screening the long-term Broadbalk experiment at Rothamsted Research, in the UK, for the presence of *Fusarium* DNA revealed the historic predominance of *F. culmorum* (B. Fraaije, RRes, UK, pers. com.). However, since 2000, *F. graminearum* has increased in prevalence, which reflects the national situation where *F. graminearum* now accounts for 50 % of the contaminated grain in the UK (www.HGCA.co.uk). The increase in *F. graminearum* coincides with the banning of stubble burning in 1992, a rise in local temperature and the introduction of maize cultivation in rotation with wheat.

FEB disease has the potential to devastate wheat, barley, rye, oat or maize crops just weeks before harvest. In the UK, FEB epidemics arise after all inputs have been applied to the wheat crop and therefore are very costly. All major wheat producing countries have reported serious and repeated FEB outbreaks in the past decade making the impact of *Fusarium* infections a global issue. The international maize and wheat improvement centre (CIMMYT) describes FEB as a major limiting factor to wheat production across the world (Dublin *et al.*, 1997) (www.CIMMYT.org). Over the last 10 years the average incidence of the disease in wheat fields, in the England and Walse, is 39 % (www.cropmonitor.co.uk). Besides dramatically bleaching the ear and reducing yield, grain is also contaminated with various *Fusarium* trichothecene mycotoxins, such as deoxynivalenol (DON) and nivalenol (NIV), often making the grain unsuitable and / or unsafe for human consumption, animal feed or malting purposes (www.scabusa.org) (Kimura *et al.*, 2007, Wu & Munkvold, 2008) (Figure 2). In 2008, the last severe year in the UK, 11 % of the wheat crop was rejected due to *Fusarium* mycotoxin contamination. To protect consumers, there are now strict legal limits in the USA, EU and elsewhere as to the levels of the DON mycotoxin permitted to enter into the food chain via unprocessed or processed grain products (www.HGCA.co.uk, wwww.USDA.com) (Hook *et al.*, 2007). One fully infected wheat ear per square meter of crop is sufficient to exceed these thresholds. Co-products of the distilling and bioethanol industries, such as spent grain and dried solutes, are commonly used as feed for livestock. Mycotoxin levels within these co-products are higher than in the grain and therefore can result high mycotoxin exposure in animals (Wu & Munkvold, 2008).

In the northern Great Plains and the Central States of the USA between 1998 and 2000 direct economic losses due to FEB on wheat were estimated at $734 million (Nganje *et al.*, 2001). CIMMYT has now estimated that *Fusarium* infection of cereal crops worldwide and the contamination of the harvested grain with mycotoxins annually cause economic losses in excess of $300 million (www.CIMMYT.org). The brewing industry has a zero tolerance for *Fusarium* / DON infected grain. In South Africa and Zimbabwe, *Fusarium* infections are now so severe that irrigated wheat plantings have dropped to less than one-third of the annual area sown up to the late 1980s (T. Tsilo, Small Grain Institute, Bethlehem,

South Africa, pers. com.). This is now leading to a shortage of locally produced grain. Recent outbreaks of the disease have now reached as far afield as Asia and South America (Goswami & Kistler, 2004). Future socio-economic and climatic influences will alter the distribution of susceptible crops and FEB causing pathogens, changing regional risk. The dynamic situation therefore requires monitoring and fore planning by governmental agriculture departments worldwide.

Figure 2 A. Mist irrigation at anthesis of the wheat crop results in high incidence of FEB. **B.** The diagnostic FEB disease symptoms of a prematurely bleached wheat ear. **C.** Healthy grain and **D.** infected shrivelled grain appear pink.

1.4.2. Mycotoxins

Several toxic fungal metabolites, termed mycotoxins, have been associated with the *Fusarium* genus and toxicoses in humans or animals fed on contaminated food stocks, including the carcinogenic fumonisins and the non carcinogenic trichothecenes (including DON, NIV, T-2 and HT-2), and the not acutely toxic zearalenone (ZEA) which causes estrogenic syndrome (Desjardins, 2006) (Figure 3). Of the three main *Fusarium* mycotoxins, trichothecenes are most commonly associated with toxicoses in animals and humans.

Trichothecenes are non-volatile low molecular weight sesquiterpenoids with a C9,10 double bond and a C12,13 epoxide ring, which are classified into four types; type A (T-2, HT-2) and B (DON, NIV) are classified by the presence of a ketone at the C-8 position, while type C and D are not produced by *Fusarium* species and are therefore not discussed further (Kimura *et al.*, 2007). Type A trichothecenes have been shown to be more toxic to animals than type B (Thuvander *et al.*, 1999). T-2 and HT-2 produced by *F. sporotrichioides*, *F. poae*, *F. equiseti* and *F. acuminatum*

occur together in the infected cereals products. Type B trichothecenes are the predominant concern in wheat and barley growing regions, while NIV is also a concern in maize production. DON, commonly referred to as vomitoxin due to its effects, which result in feed refusal, is produced by *F. graminearum* and *F. culmorum* among other *Fusarium* species (Desjardins, 2006). *Fusarium cerealis* and *F. poae* are the main producers of NIV, but isolates of *F. culmorum* and *F. graminearum* are capable of producing NIV (Desjardins, 2006). Trichothecenes inhibit protein, DNA and RNA synthesis by binding to the 60S ribosomal subunit (Ueno, 1984).

Fumonisins are most commonly associated with *F. verticillioides* contamination of maize and animal diseases including, equine leukoencephalomalacia, fatal pulmonary edema of swine and cancer in rodents (Desjardins & Proctor, 2007). The chemical structure of fumonisins is similar to sphingolipids and can alter sphingolipid biosynthesis of the host (Yazar & Omurtag, 2008). The major fumonisin in cereals is FB_1. Zearalenones are non steroidal estrogenic mycotoxins that cause reproductive disorders in animals (Desjardins & Proctor, 2007). Zearalenones are produced by a wide range of *Fusarium* species and can be produced simultaneously with DON during cereal infection by *F. graminearum* and *F. culmorum* (Yazar & Omurtag, 2008).

1.4.3. The *Fusarium graminearum* life cycle

Post-harvest, the pathogen survives saprotrophically on crop debris, which acts as a reservoir of hyphal inoculum, asexual spores and for some *Fusarium* species sexual spore production. Epidemics on wheat occur when warm and moist weather conditions coincide with crop anthesis and sexual ascospores or asexual conidia are either rain splashed, or wind dispersed, onto the external anthers and outer glumes (Parry *et al.*, 1995). A combination of the correct environmental conditions, crop anthesis and the presence of spores will, after 20 days in the field, result in FEB disease symptoms (Figure 2 and Figure 4).

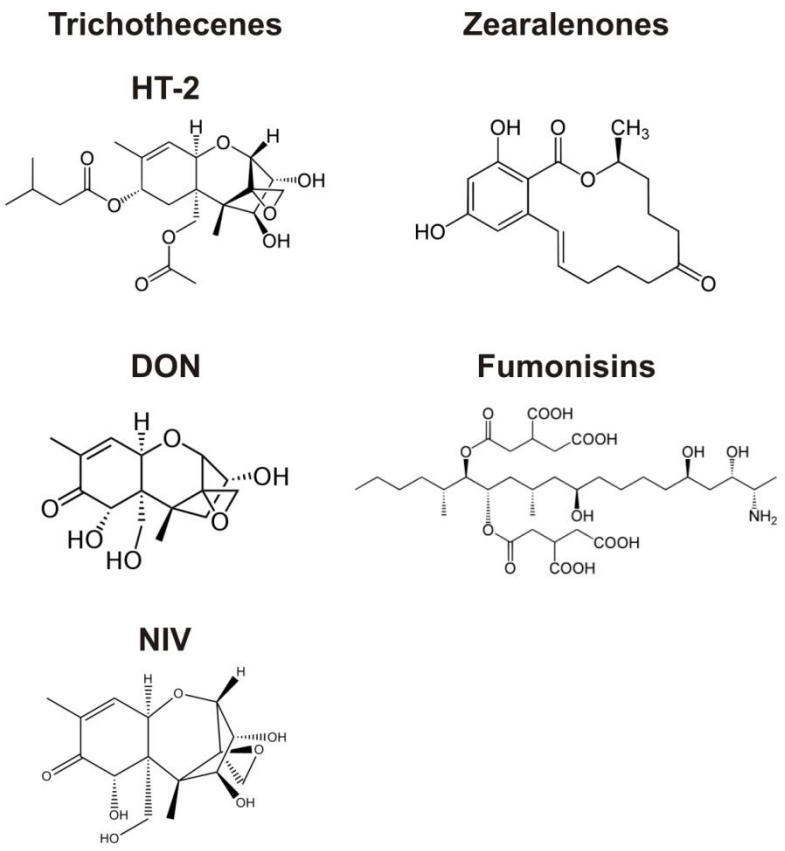

Figure 3 The chemical structure of the *Fusarium* mycotoxins. Images sourced from http://commons.wikimedia.org/.

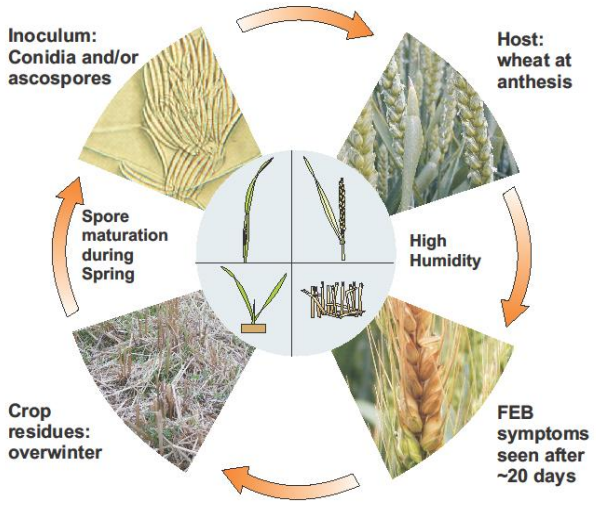

Figure 4 The disease cycle of FEB on wheat (Rothamsted Research Visual Communications Unit (2009), unpublished).

A review of the infection process carried out by Pugh (1933) was performed on a tall wheat genotype bred prior to the Green Revolution. In the presence of moisture the spores germinate, hyphae enter via the cracked anthers and grow down the anther filament into the host plant. Individual floral cavities open to permit anther extrusion and this allows spores to be deposited within the florets. The following investigations assessed the infection biology of *F. graminearum* on modern semi-dwarf hexaploid wheat. *Fusarium* spores germinate on the abaxial surface of the glumes and in the floral cavity within 12 hours post inoculation (hpi), giving rise to unbranched hyphae that frequently come in contact with stomata (Pritsch *et al.*, 2000, Wanjiru *et al.*, 2002). Despite not producing an appressorium, *F. graminearum* has been reported to penetrate the adaxial surface and the stomatal opening of the floral brackets such as the glume, lemma and palea (Pritsch *et al.*, 2000). The ovary and the floral brackets were invaded by 36 hpi, while the host cell walls and middle lamella in the vicinity of the hyphae demonstrated reduced cellulose, xylan and pectin (Wanjiru *et al.*, 2002). Thick, unbranched inter- and intracellular hyphae were present throughout the ovary and floral brackets by 76 hpi (Pritsch *et al.*, 2000, Wanjiru *et al.*, 2002).

Once the florets and spikelet have been colonised, infection proceeded further into the ear via the rachis. By 5 days post inoculation (dpi), inter- and intracellular hyphae spread down and to a lesser extent up the rachis in the vasculature and also the cortex (Jansen *et al.*, 2005, Miller *et al.*, 2004, Wanjiru *et al.*, 2002). Invaded phloem, chlorenchyma and occasionally parenchyma host cells collapsed (Guenther & Trail, 2005, Ribichich *et al.*, 2000). The culm and pith cavity were colonised by 12 dpi and lateral branching within the culm increased by 14 dpi (Guenther & Trail, 2005). Hyphae employed two mechanisms to traverse host cell walls, the production of penetration pegs and utilisation of pit fields (Guenther & Trail, 2005, Jansen *et al.*, 2005, Wanjiru *et al.*, 2002). Finally, sporulation occurs at the base of the infected florets and on the rachis node, represented by the salmon colour on the fully infected ears (Figure 2).

1.4.4. The wide host range of *F. graminearum*

Fusarium diseases exist in nearly all grown crops and this is reflected by the broad host range of *F. graminearum*. The establishment of *F. graminearum* infection on cereal hosts including wheat, barley, maize, oats and rye requires the same conditions (Bushnell *et al.*, 2003). The mode of infection has been most widely studied in wheat (as described above) and is believed to be similar in other cereals. Maize infection also commences with spore germination on the exposed silks, hyphae grow down into the ovary and rachis, subsequently throughout the cob (Miller *et al.*, 2007). No detailed cytological studies of how *Fusarium* infects barley have been carried. However, unlike FEB disease on wheat and maize, symptoms do not develop beyond an infected spikelet on barley ears, suggesting that infection is contained to the floret and spikelet tissues and that barley rachis tissue exhibits natural resistance (Bushnell *et al.*, 2003). *F. graminearum* infections of barley are therefore reminiscent of *F. avenaceum*, *F. poae* and *Microdochium* species on wheat.

F. graminearum is best known as a pathogen of small grain cereals. However, throughout the world reports implicate *F. graminearum* as causing multiple other plant diseases. Fusarium yellow of sugar beet, which can cause serious crop losses due to wilting and premature death, has been associated with 14 different Fusaria, predominately consisting of soil borne pathogens such as *F. oxysporum* and *F. solani* but also with mycotoxin producing FEB species. The *F. culmorum* strains isolated from sugar beet were of the 3A-DON, while the *F. graminearum* strains were of the 15A-DON, chemotypes (Schneider & Musters van Oorschot, 2008). Fusarium dry rot is one of the most important diseases of potato. *F. coeruleum, F. sambucinum, F. culmorum* and *F. avenaceum* account for 95 % of dry rot in the UK (Peters *et al.*, 2008a, Secor & Salas, 2001). However, *F. graminearum* has recently been identified as a potato dry rot pathogen (Estrada *et al.*, 2010, Peters *et al.*, 2008b). The *F. graminearum* strains isolated from sugar beet and potato have been proven to be capable of producing mycotoxins in wheat (Burlakoti *et al.*, 2007). Dry decay of sugar beet, soyabean and pea roots have now also being associated with *Fusarium* infections (Broders *et al.*, 2007, Estrada *et al.*, 2007, Feng *et al.*, 2010). Importantly, potatoes, sugar beet and soyabeans are commonly grown in rotation with cereals.

Therefore, this new epidemiological information must now be considered when designing an integrated control strategy with the aim of reducing inoculum build-up.

1.4.5. Development of an integrated control strategy for *F. graminearum*

Appropriate agronomy that incorporates all the influential variables is the most beneficial form of FEB control. As previously described, FEB causing species survive saprotrophically over winter on the crop debris. Therefore, cultural practices such as the burning of crop residues, increased tillaging, ploughing or crop rotation with a non gramineaceous species that is not a host, would decrease the source of inoculum. However, these practices are not economically beneficial to the farmer and can have an impact on the environment, such as increased soil erosion and release of CO_2. Maize is a highly susceptible host, its highly persistent stubble is a favourable environment for perithecia formation and is the most conductive cereal to *F. graminearum* infection (Maiorano *et al.*, 2008). As demonstrated by the correlation between the increased cultivation of maize and the rise in *F. graminearum* in the UK. Wheat cultivated in rotation with maize is therefore at the greatest risk of FEB infection and DON contamination (Maiorano *et al.*, 2008). In Austria, wheat crops are no longer grown in valleys where wide scale maize production is practiced. This has lead to a dramatic reduction in DON mycotoxin contaminated wheat grain samples (G. Adams, Boku, Austria, pers com.). Sugar beet preceding wheat has also been shown to be more conductive to DON contamination in the subsequent wheat crop than cultivating successive wheat crops (Clark *et al.*, 2009). Higher levels of nitrogen application can also increase FEB incidence and DON contamination (Lemmens *et al.*, 2004).

The application of fungicides as a seed treatment, at the T3 stage of wheat development or at the onset of anthesis can offer some protection to the crop. Applications at, or prior to, anthesis when the ear is most vulnerable to FEB infection would be the most beneficial, but within the crop canopy ears come into flower at different time (typically over a 14 day period), making it difficult to protect the crop with a single fungicide application. Fungicides with different modes of action affect individual species of the *Fusarium* complex differently. Triazoles have the highest efficacy against *Fusarium* mycotoxin producing species but less against *Microdochium* mycotoxin non-producing species, whereas strobilurins have low

efficacy against *Fusarium* species (Simpson *et al.*, 2001). *F. graminearum* is intrinsically less sensitive to triazoles than other fungi, which is hypothesised to be due to the presence of two additional *CYP51* genes, the target of the fungicide, in the genome (Liu *et al.*, 2011). Strobilurins increase grain filling by influencing the ethylene signalling pathway, delaying senescence and therefore possibly also suppressing FEB resistance mechanisms (S. Scofield, USDA Laboratory, Purdue University, USA, pers. com.). Other fungal species may also be affected differentially and could influence the risk of mycotoxin contamination. *Alternaria alternaria* and *Cladosporium herbarum* have been shown to produce inhibitors to *F. culmorum* infection (Liggitt *et al.*, 1997) but may be more susceptible to the fungicide treatment than the desired target organism. Choice of fungicide will subsequently affect the microbial community differentially and this should be considered when designing a chemical control programme. Environmental stresses including the application of a sub-lethal fungicide dose can increase DON production (Audenaert *et al.*, 2010), therefore the timing and dosage of a fungicide application is vital. At present commercially available fungicides are able to reduce disease incidence and the commercial product Prosaro (Bayer, 2006), which is a combination of tebucanozole and prothicanozole, is one of the most effective formulations (Yuen & Schoneweis, 2007). Nonetheless, the decline in disease symptoms does not significantly reduce DON contamination and subsequently may not be sufficient to limit the indirect losses cause by mycotoxin contamination of the grain.

The lack of an effective chemical strategy to limit the incidence and severity of FEB disease has enhanced the need for the improvement of crop resistance via breeding and / or genetic modification. Naturally large differences in wheat cultivar resistance to FEB exist. However, the combination of resistance and agronomically important traits, such as high yield, has been difficult to balance. For example, the ears of a taller wheat cultivar would be at a greater distance from the source of inoculum, but have a lower harvest index than a semi-dwarf wheat variety (Parry *et al.*, 1995). Similarly, a lax ear habit where the spikelets are spaced further apart are less susceptible to FEB than compact ears where the local relative humidity remain higher and favours infection and disease development (Parry *et al.*, 1995).

The genetic resistance of wheat germplasm to FEB predominantly comprises of two components, type I resistance against initial penetration and type II resistance against spread of infection within the ear (Schroeder & Christensen, 1963). Additional types of resistance have been proposed including; resistance to grain infection (type III), tolerance, an ability to produce marketable grain in the presence of infection (type IV) and resistance to mycotoxin accumulation (type V) (Mesterhazy *et al.*, 2005). The Brazilian cultivar Fontana and the Chinese cultivar Sumai-3 best represent type I and II wheat resistance. Fontana exhibits moderate type 1 resistance to FEB, which is believed to be due to morphological traits such as harder glumes and narrow flower opening (Buerstmayr *et al.*, 2009). The resistant Chinese wheat cultivar Sumai-3 and its derivatives combine both agronomic and resistance characteristics with the best effect. Resistance that originates from Sumai-3 is not *Fusarium* strain or species specific, hence it is not likely to be overcome by a new race of the pathogen (Bai & Shaner, 2004b). The major quantitative trait locus (QTL) on chromosome 3BS (now termed the *FHB1* gene) is responsible for the majority of the Sumai-3 resistance and is also thought capable of detoxifying DON by converting it into DON-3-O-glucoside. Two additional major QTLs have been associated with the Sumai-3 source of resistance, 5AS and 6BS. However, each accounts for less of the phenotypic variation. Conversely, conventional breeding can be used to remove QTLs associated with FEB susceptibility. A cross between Arina x Riband identified a susceptibility QTL on chromosome 4DS that was inherited with the semi-dwarfing allele *Rht-Db1*. This phenotype was not caused by the reduction in plant height and is due either to pleiotrophy or linkage to another gene(s) conferring disease susceptibility (Buerstmayr *et al.*, 2009). Currently, commercial breeders are attempting to incorporate type I resistance, against the initial infection, and type II resistance, against the spread of infection, into different agronomically important cereal cultivars. The development of marker-assisted QTLs should help breeders combine beneficial traits into commercial lines (Bai & Shaner, 2004b). At present marker-assisted selection is only available for a few of the major QTLs discovered.

Genome wide expression analyses and cytological studies that compared the resistant and susceptible interaction have pinpointed defence pathways that may be

critical to 3BS mediated FEB resistance. A cytological and immunological study revealed increased apposition and papillae formation was accompanied by plant cell wall reinforcement such as lignin, thionins and hydroxyproline-rich glycoproteins in the resistant interaction (Kang *et al.*, 2008). Increased plant β1,3-glucanases and chitinases and reduced DON labelling was also detected (Kang *et al.*, 2008). The key JA biosynthetic enzyme allene oxide synthase, which oxidises linolenic acid in the plant cell membrane phospholipids to release JA, was up regulated during Sumai-3 infection (Li & Yen, 2008). The cytochrome P450, *CYP709C1*, was induced by JA or DON application and was also expressed higher during Sumai-3 infection (Li *et al.*, 2010). Plant cytochrome P450s act as, antifungal compounds and can have a detoxification function. The a/b-chlorophyll binding proteins, which are up regulated by SA or down regulated by ET, act as molecular marker for the different defence signalling pathways and were decreased during Sumai-3 infection (Li & Yen, 2008). However, these transcription studies only correlate gene expression patterns to a specific host phenotype and do not provide direct evidence for a causal role in either resistance or susceptibility.

Following 1-methylcyclopropene (1-MCP) treatment, an inhibitor of ET perception, of the susceptible cultivar Bobwhite increases wheat susceptibility, while 1-aminocyclopropane-1-carboxylic acid, a precursor to ET, treatment increased resistance (S. Scofield, USDA Laboratory, Purdue University, USA, pers. com.). Using the Barley stripe mosaic virus vector system to mediate virus induced gene silencing (VIGS) of the ET biosynthetic enzyme gene, S-adenosyl-methionine synthase, reduced resistance in the genotype Ning7840, a Sumai-3 relative which harbours the *FHB1* gene on 3BS, has been repeatedly observed (S. Scofield, USDA Laboratory, Purdue University, USA, pers. com.). Ning7840 treated with DON demonstrated a mild response to the mycotoxin, while Ning7840 treated with DON and 1-MCP resulted in the whole ear becoming bleached, reminiscent of FEB symptoms (S. Scofield, USDA Laboratory, Purdue University, USA, pers. com.). ET signalling therefore appears to play a role in 3BS mediated FEB resistance and susceptibility to the DON mycotoxin.

In the absence of effective type I resistance, breeding cultivars with increased resistance post infection may never be able restrict the pathogen to such an extent

that the grain would be protected from mycotoxin contamination. Therefore genetic engineering solutions have focused on reducing or detoxifying DON content in infected grain. Identification of a gene that impedes mycotoxin production rather than the spread of the disease may be a greater advancement in crop protection. The *Fusarium* trichothecene biosynthetic gene, *TRI101*, transfers an acetyl group to the C_3 hydroxyl group of the trichothecene making the compound less volatile (Garvey *et al.*, 2008). The *Saccharomyces cerevisiae* ATP-binding cassette translocator, *PDR5*, exports DON from its cells (McCormick *et al.*, 1999). Transforming *TRI101* or *PDR5* into tobacco enhances the plant's tolerance of the mycotoxin, however, the result of *TRI101* or *PDR5* transformation into wheat and rice appears somewhat inconsistent and far less promising as a potential control strategy (Muhitch *et al.*, 2000, Ohsato *et al.*, 2007, Okubara *et al.*, 2002). A lactonohydrolase identified from endophytic Ascomycete *Clonostachys rosea* transformed into *E. coli* and *Schizosaccharomyces pombe* demonstrated a good ability to detoxify ZEA. The lactonohydrolase detoxification system has been transferred into maize where it can provide a simple solution on ZEA contamination caused by *F. verticillioides* infections (Igawa *et al.*, 2007, Takahashi-Ando *et al.*, 2002, Takahashi-Ando *et al.*, 2004). However, commercial application of these genetically engineered detoxification solutions have run into some regulatory issues, because the appropriate government authorities are concerned that the degradation products may themselves be toxic to humans and animals or are converted by the plants or *Fusarium* to other toxic compounds which then accumulate in the infected tissues.

Biological control methods have been considered as a mechanism of preventing fungal pathogens colonising the wheat ear, as until booting (growth stage GS41) the ear is covered by the flag sheath and lacks an established microflora. The use of microorganisms as nutritional or niche competitors, and as microparasites of the pathogen can have an impact on disease severity and mycotoxin production (Gilbert & Fernando, 2004, Khan *et al.*, 2001). For example, *Lysobacter enzymogenes* enhances host resistance and limits the *Fusarium* infection, while *Eubacterium* can detoxify trichothecenes (Binder, 2007, Jochum *et al.*, 2006). However, the success of biocontrol methods is dependent on the environmental conditions, the crop in question and the competitiveness of the agent in the required

environment. Targeting vulnerable traits of an individual component of FEB complex could provide opportunities to other FEB species. The uniform application of fungicides can also have a negative impact upon the populations of antagonistic microorganisms, making it more difficult to develop an integrated approach.

Current approaches to control the disease include fungicide treatment and the use of resistant plant varieties, but these are at best only 50-60 % effective. When used in isolation, cultural, chemical and biological control strategies are ineffective. If these practices are combined disease severity can be reduced but at a substantial cost to the producer. Hence, the need remains for the development of novel chemistries and identification of new resistance traits which can be incorporated into a more effective integrated control strategy. The generation of transgenic cereal cultivars that are either resistant to infection or accumulation of the mycotoxin are a real possibility. The production of the bacterial *Bacillus thuringiensis* (BT) toxin in genetically modified maize was designed to control the European corn borer, an insect pest. The incorporation of BT toxin into maize reduced insect wounding as well as FEB levels and fumonisin / zearalenone contamination (Bakan *et al.*, 2002, Dowd, 2001, Folcher *et al.*, 2010) while no reduction in trichothecenes contamination was found (Naef *et al.*, 2006). In Northern America commercially available BT maize is now marketed as a FEB control strategy. This demonstrates how genetically enhanced resistance to insect and fungal pests can be successful. However, until genetically modified crops are more widely accepted, this line of investigation, for commercial exploitation in Europe, will be futile.

Post-harvest stored, dry, cereal grain contains microbial contaminants including *Fusarium* species. The dry grain and microbes are still metabolically active and poor post-harvest conditions can result in the spoilage of the grain due to the microorganisms degrading carbohydrate, lipid and protein stores (Magan & Aldred, 2007). In the case of *Fusarium* infections this can also result in an increase in mycotoxin contamination. Post-harvest losses can amount to 50 % in the tropics (Hall, 1970). Reducing moisture content (<14 %), storing in elevated temperatures under reduced O_2 and inversely increased CO_2 levels can effectively control additional *Fusarium* growth and mycotoxin production (Magan *et al.*, 2010). While not evading the necessity for good pre-harvest control, minimizing the time between

grain harvest and drying, accompanied by good hygiene and management of storage and transport facilities, will reduce the risk of additional *Fusarium* contaminations.

1.4.6. The *F. graminearum* genome

Between 2002 and 2007 four *Fusarium* genomes were sequenced and have since been published, namely *F. graminearum*, *F. oxysporum*, *F. solani* and *F. verticillioides* (Coleman *et al.*, 2009, Cuomo *et al.*, 2007, Ma *et al.*, 2010). The sequenced *F. graminearum* PH-1 strain was from genetic lineage 7, which predominately causes FEB disease in the Northern hemisphere. The PH-1 strain possessed a 36.1 Mb genome that was aligned to 4 chromosomes and was predicted to encode 13,332 genes (Table 1). A close relative *F. culmorum* also has 4 chromosomes, whereas *F. oxysporum*, *F. solani* and *F. verticillioides* have between 9 and 17 chromosomes. The smaller size of the *F. graminearum* genome and the lack of repetitive sequences are hypothesised to be due to the homothallic nature of the fungus, which limits the opportunity to acquire repeats, and the presence of an active repeat-induced point mutation (RIP) system (Cuomo *et al.*, 2007). The very large 15 chromosome, 59.9 Mb, *F. oxysporum* f. sp. *lycopersici* genome only contains 17,735 genes but is 65 % larger than the *F. graminearum* genome, mainly due the presence of 16.83 Mb of repetitive sequence. Unlike *F. oxysporum*, the large size of the *F. solani* genome is not accounted for by repetitive DNA, but the presence of expanded gene families, with 77 % having more genes than the *F. graminearum* counterpart. A core set of approximately 9000 genes were conserved in all other Fusaria. Comparatively, *F. graminearum* possessed a greater number of transcription factors, hydrolytic enzymes and transmembrane transporters than the other Fusaria.

In the original genome sequencing project, a genomic comparison of the two *F. graminearum* strains of USA origin identified 10,495 single nucleotide polymorphisms (SNPs), of which 50 % resided in 13 % of genome, predominantly in the sub-telomeric regions. Several interstitial locations with a nigh SNP density were also identified that may represent ancestral telomeres incorporated by past chromosomal fusion events (Cuomo *et al.*, 2007). Highly conserved genes were underrepresented, while *F. graminearum* specific genes were overrepresented, in SNP dense regions. In contrast, *F. oxysporum* and *F. solani* do not have genomic islands of higher diversity, but possess additional large chromosomes as well as

smaller supernumerary chromosomes that contain lineage-specific sequences and are rich in repetitive DNA (Coleman *et al.*, 2009, Ma *et al.*, 2010). The lineage-specific chromosomes are enriched in secreted effectors, transcription factors and proteins involved in signal transduction, but encode no genes of housekeeping function. In *F. oxysporum* f. sp. *lycopersici* chromosomes 3, 6, 14 and 15 are of this type and account for 31.7 % of the genome. The highly diverse regions of the *F. graminearum* genome are also enriched in proteins exclusively expressed *in planta*, of which 31 % are predicted to be secreted, including known virulence factors and PCWDEs (Cuomo *et al.*, 2007). The *F. graminearum* genome resource is constantly evolving as the gene call is improved by manual annotation and experimental confirmation. The latest version of the genome (FG3) curated by the Munich Information Centre for Protein Sequences (MIPS) is now predicted to encode 13,826 genes (Wong *et al.*, 2011) (http://mips.gsf.de/genre/proj/FGDB/).

Table 1 The genome statistics of the four sequenced *Fusarium* species.

	F. graminearum	***F.oxysporum* f. sp. *lycopersici***	***F. solani***	***F. verticillioides***
Genome size (Mb)	36.1	59.9	54.43	41.7
No. chromosomes	4	15	17	11-12
No. genes	13,332*	17,735	15,707	14,179
Repetitive sequence (Mb)	0.24	16.83	2.78	0.36
% genome coding for genes	49.04	35.72	43	42.82
Supernumerary chromosomes	No	4, 19 Mb	3, Size not published	No

* Based upon the BROADs (http://www.broad.mit.edu/annotation/fungi/fusarium/) FG1 prediction.

All the proteins encoded by the *F. graminearum* genome have been functionally classified into 20 categories, while individual proteins can be included in various functional categories (Figure 5; http://mips.gsf.de/genre/proj/FGDB/). In the latest analysis, applied to the FG3 version of the *F. graminearum* genome, 9004 fungal proteins lacked functional annotation, representing 65.1 % of the gene space

and the gap in the understanding of the protein repertoire. The *F. graminearum* genome has also been mapped onto the Kyoto Encyclopedia of Genes and Genomes (KEGG) (http://www.genome.jp/kegg-bin/show_organism?org=fgr) linking the genome to enzymatic biosynthetic pathways. A *F. graminearum* Affymetrix array has been developed to study transcriptome alterations *in vitro* and *in planta* (Guldener *et al.*, 2006). All transcriptomic data-sets were generated using the sequenced strain PH-1 and are publically accessible from www.PLEXdb.org and represent a community resource. The significance of the various transcriptomic data-sets is discussed in chapter 7. To date only one proteomics study (Paper *et al.*, 2007) and one metabolomic triple fingerprinting study (Lowe *et al.*, 2010) are available for *F. graminearum*.

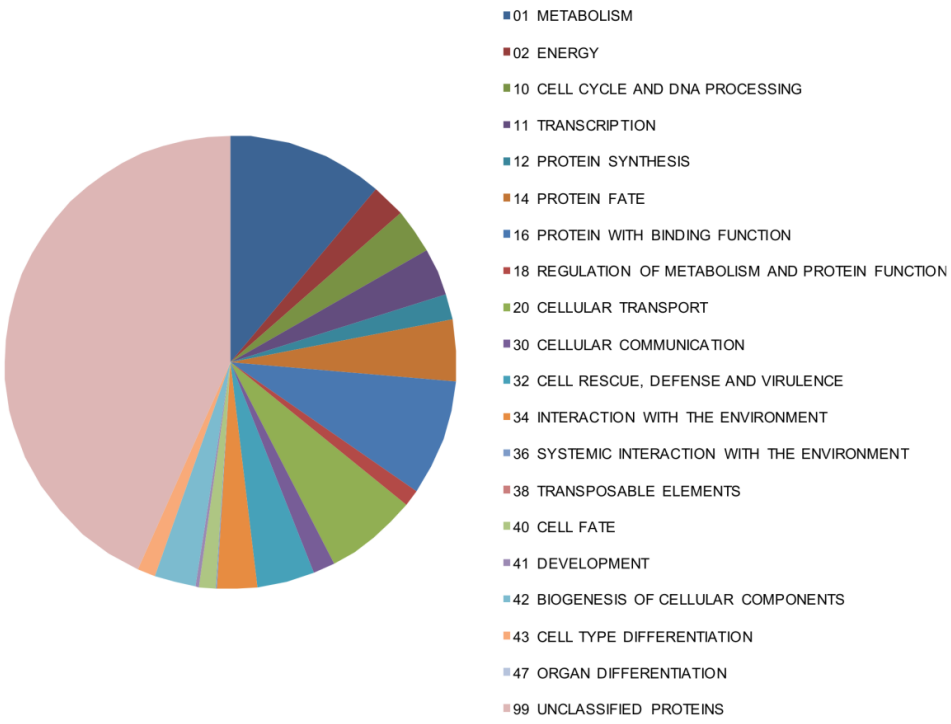

Figure 5 Proportional representation of the 20 MIPS functional categories including all the proteins predicted to be encoded by the *F. graminearum* FG3 genome. Number of gene = 13,826 genes. Number of MIPS functional category entries = 20818 (http://mips.gsf.de /genre/proj/FGDB/).

1.4.7. The molecular genetics of *F. graminearum* pathogenicity

F. graminearum produces a range of mycotoxins including butenolide, several type B trichothecenes and zearalenone. Butenolides and zearalenones are not phytotoxic and no evidence exists demonstrating they assist plant infection. Trichothecene synthesis however, is associated with pathogenicity. DON is required for full virulence on wheat ears but not for full virulence on barley ears, maize cobs or Arabidopsis floral tissue (Cuzick *et al.*, 2008b, Harris *et al.*, 1999, Maier *et al.*, 2006, Proctor *et al.*, 1995a, Proctor *et al.*, 1995b), while NIV is also required for full virulence on wheat ears and to a lesser extent on maize cobs, but is not required for barley infection (Maier *et al.*, 2006). Trichothecenes are widely associated with chronic and fatal toxicoses in humans and animals (Pestka, 2007). Trichothecenes originate from sesquiterpenes at the base of the isoprenoid or HMG-CoA reductase pathway (Kimura *et al.*, 2007). Trichothecene synthesis commences with the conversion of farnesyl pyrophosphate to trichodiene. Multiple oxygenation, isomerisation, cyclization and estification steps lead to the production of the mycotoxins. Post the calonectrin intermediate, the pathway branches into three resulting in the synthesis of either the T-2, NIV or DON chemotype (Desjardins, 2006) (Figure 3).

Another level of variation exists among *F. graminearum* strains of the DON chemotype. Deacetylation of differing position on DON molecule results in the production of 3A-DON and 15A-DON. *F. graminearum* DON chemotypes and its acetylated derivatives 3A-DON and 15A-DON provide a selective advantage on wheat over the ancestral NIV, which is being displaced by the more aggressive DON producers. While among the DON producing strains, 3A-DON chemotypes demonstrate higher fecundity and growth compared to 15A-DON producers (Ward *et al.*, 2008). The focus of this project is on *F. graminearum* infections of wheat and therefore, DON will be focused on henceforth. The biosynthetic pathway for DON production is present in figure 6.

DON inhibits protein synthesis in eukaryotes and prevents polypeptide chain initiation or elongation by binding to the 60S ribosomal subunit (Kimura *et al.*, 1998). The first committed step in the biosynthesis of trichothecenes is catalysed by the trichodiene synthase enzyme encoded by the *TRI5* gene. The role of DON in

pathogenicity was primarily examined via the construction and use of a non-DON producing *tri5*-deficient mutant. The absence of mycotoxin production during wheat ear infection results in an enhanced plant defence response in the form of plant cell wall thickening that impeded rachis colonisation (Jansen *et al.*, 2005). The *tri5* mutant infection is particularly intriguing as it creates an eye-shaped lesion on the glume of the inoculated floret that resembles either a *F. poae* or *M. nivale* infection (Cuzick *et al.*, 2008b). Interestingly, these two fungal pathogens differ from *F. graminearum* in their ability to produce DON mycotoxin, *M. nivale* does not produce DON, whilst different isolates of *F. poae* can produce a range of mycotoxins (Gutleb *et al.*, 2002). Clear evidence that trichothecenes are required for *F. graminearum* to be fully pathogenic was provided by targeted deletion of several trichothecene biosynthetic genes (*tri5*, and *tri14*) and a trichothecene transcription factor (*tri6*). Deletion of these *TRI* genes stopped *in vitro* mycotoxin production and caused a dramatic drop in virulence on wheat ears (Dyer *et al.*, 2005, McDonald *et al.*, 2005, Proctor *et al.*, 1995a). Immunolabelling studies demonstrated that DON accumulated at the infection front (Kang & Buchenauer, 1999). DON is then translocated by the host vascular system throughout the ear in advance of fungal infection and was found at a higher concentration in the rachis than the spikelets (Savard *et al.*, 2000). In the case of the wild-type interaction, the mycotoxin was localised over the cell walls, plasmalemma, cytoplasm, chloroplasts and vacuoles of the host cells (Kang *et al.*, 2008). However, DON has also been implicated in the activation of several wheat defence responses including, H_2O_2 production and PCD which may aid colonisation (Desmond *et al.*, 2008). Despite being a key virulence factor and the universal nature of the target molecule, the synthesis of phytotoxic DON was not essential for the infection of *F. graminearum* on Arabidopsis, maize, oat, and rye (PHI-base, www.phibase.org). DON therefore appears to play host-selective role in pathogenicity but is produced irrespective of the host species infected. Protection of the occupied host niche from infection by other microbial invaders is currently thought to be the most likely reason for DON production in a host species (N. Magan, Cranfield University, UK and K. Hammond-Kosack, RRes, UK, pers com.).

Similar to pathogenicity islands in bacteria, a cluster of 12 genes that are all up-regulated at the onset of trichothecene biosynthesis surrounds the *TRI5* gene on

chromosome 2. In the sequenced *F. graminearum* strain PH-1 which produces DON and 15A-DON, this cluster resides in a region with a normal GC content, contains no obvious border sequences and is ~ 25 Kb in length (Figure 6). *TRI1* and *TRI16* are situated together on chromosome 1 while *TRI101* is placed alone on chromosome 4 (BROAD; http://www.broad.mit.edu/annotation/fungi/fusarium/). The *TRI5* cluster contains two zinc finger transcription factors, Tri6 and Tri10. The *TRI6* binding motif, YNAGGCC, is present in the promoter region of several trichothecene biosynthetic genes and is also present in many isoprenoid biosynthetic gene promoters and other gene promoters (Seong *et al.*, 2009). Tri6 transcription factor positively regulates the *TRI5* cluster and disruption of *TRI6* results in a reduction in *TRI5* mRNA and a non-toxin-producing mutant (Proctor *et al.*, 1995b). Tri10 represents a novel regulatory protein and its over expression results in increased mycotoxin production via *TRI6* activation (Seong *et al.*, 2009). Interestingly, *TRI10* does not contain a *TRI6* binding domain in the promoter region but instead possesses a *TRI6* binding site within the coding region which may act as a negative feedback loop (Kimura *et al.*, 2007). Deletion of either the *TRI6* or *TRI10* transcription factors alters the expression of over 200 genes (Seong *et al.*, 2009). A third zinc finger trichothecene transcription factor, *TRI15*, resides outside the clusters on chromosome 3 and contains no *TRI6* binding site in the promoter sequence or coding region. Genetic deletion of *TRI15* creates a strain that produces more DON than the wild-type strain, while being hypervirulent on wheat and Arabidopsis (M. Jubault and K. Hammond-Kosack, RRes, UK, pers. com.). This demonstrates that *TRI15* is a negative regulator of DON production in *F. graminearum.*

The enzyme Tri4 carries out four consecutive oxygenation steps to convert trichodiene to isotrichotiol (Tokai *et al.*, 2007) (Figure 6). Tri7 and Tri13 are non-functional in DON producers due to a frame shift mutation and therefore determine whether the pathogen will produce DON or NIV (Lee *et al.*, 2002, Lee *et al.*, 2001). Deacetylation of different carbon positions on the DON intermediate, catalyzed by Tri8, determines if a strain produces 3A-DON or 15A-DON (Alexander *et al.*, 2011). The function of the two hypothetical proteins within the *TRI* cluster, Tri9 and Tri14, is unclear. However, Tri14 is required for high virulence on wheat ears and DON synthesis *in planta*¸ but is not required for DON production *in vitro* (Dyer *et al.*,

2005). The acetylation of C_3 acts as a self protection mechanism by reducing the toxicity of the intermediates during trichothecene biosynthesis. The final step in trichothecene biosynthesis, performed by Tri101, is to remove the C_3 acetyl group to create the toxic compound for secretion and is therefore a target for disrupting mycotoxin biosynthesis (Ohsato *et al.*, 2007). *TRI12* encodes an efflux pump of a major facilitator superfamily that is proposed to provide a self protection mechanism (Alexander *et al.*, 1999). Genome wide gene expression analysis of the *tri6*-deficient strain identified three genes of unknown function with *TRI6* binding sites. Genetic deletion of FGSG_00007 and FGSG_10397 created hypervirulent strains that produced more DON (Gardiner *et al.*, 2009a).

Biosynthetic genes clusters are believed to have evolved because the intermediate compounds in these pathways are highly toxic. Subsequently, the acquisition or loss of a cluster, in one swoop, will not result in the accumulation of harmful toxic intermediates (Rokas, 2011). The *TRI* cluster and the surrounding region also contain a very low level of single nucleotide polymorphism suggesting evolutionary stability. Interestingly, *TRI15*, FGSG_00007 and FGSG_10397, which negatively regulate DON production, all reside outside the *TRI* clusters. The latter two genes reside in sub-telomeric regions of chromosome 1 and 2, respectively that have a high frequency of SNPs (Cuomo *et al.*, 2007) and therefore possess a higher chance of mutation. Selection pressure exerted upon these negative regulators of DON may result in the loss of gene function, creating a more aggressive, hyper-DON producing strain with a competitive advantage over native strains and the pathogenic potential to spread throughout the cereal growing regions of the world.

Secondary metabolism is involved in maintaining cellular homeostasis, cell defence, development and promoting survival for nutrient starvation (Roze *et al.*, 2011). Fungal secondary metabolites are commonly produced during the transition between the active and stationary growth phases, when nutrients become limiting, as is the case for Aflatoxin production by *Aspergillus spp* (Brakhage & Schroeckh, 2011). A screen of trichothecene accumulation and *TRI* gene expression of *F. graminearum* grown on different carbon sources revealed that DON production was enhanced in sucrose-containing media, but was not repressed by the addition of glucose, and is therefore not control by catabolite repression (Jiao *et al.*, 2008).

Nitrogen source, pH and temperature also influence DON production. A large nutrient profiling study identified specific amines (Gardiner *et al.*, 2009b) which in combination with low pH were potent DON inducers (Gardiner *et al.*, 2009c). Therefore, nutrient availability appears not to influence DON mycotoxin production in a similar manner to other fungal secondary metabolites. Other abiotic stresses such as temperature and water potential have been demonstrated to influence DON production *in planta* (Ramirez *et al.*, 2006). The global regulators VelA and LaeA coordinate the expression of secondary metabolic gene clusters (Strauss & Reyes-Dominguez, 2011). As described above the *TRI* genes reside within a cluster on chromosome 2 (Cuomo *et al.*, 2007) and recent progress has demonstrated that the *VELA* homologue in *F. graminearum*, *VE1*, is required for DON production (Barreau *et al.*, 2011).

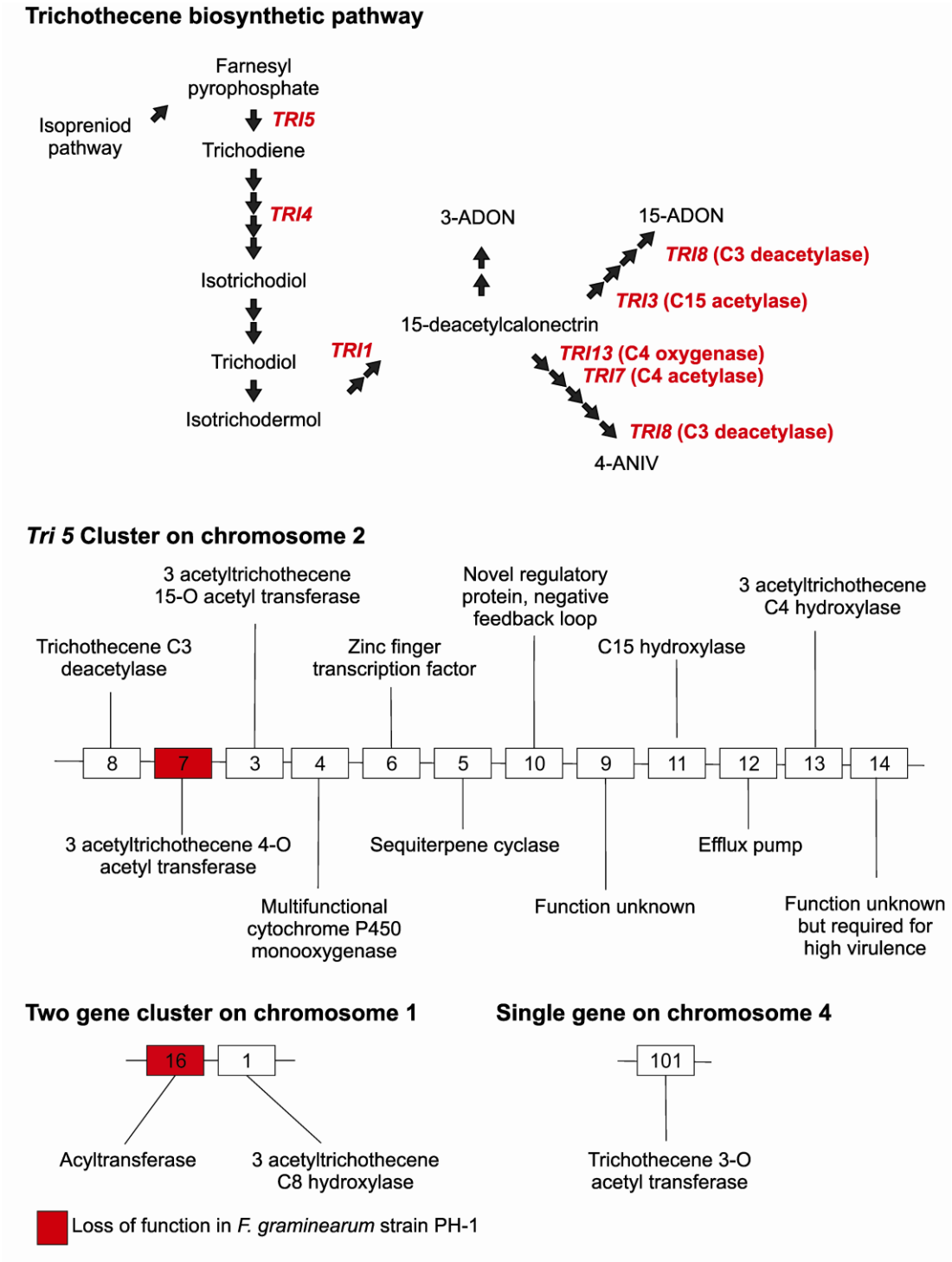

Figure 6 Trichothecene biosynthetic pathway, *TRI* gene function and organisation in *F. graminearum*.

Plant pathogens secrete extracellular enzymes to breakdown the plant cell wall to assist infection and to gain access to important sources of nutrition. Correlative evidence implies PCWDEs play a crucial role in the virulence of many phytopathogens (Agrios, 1997). In addition to the qualitative and quantitative difference in mycotoxin production, hydrolytic enzyme secretion may also contribute to fungal strains differing in virulence. Comparatively, *F. graminearum* has a greater number of hydrolytic enzymes and transmembrane transporters than the closely related pathogens and saprotrophs, *Neurospora crassa*, *M. oryzae* and *Aspergillus nidulans* (Cuomo *et al.*, 2007). In total, 408 *F. graminearum* genes were expressed solely during barley infection, of which 31 % were predicted to be secreted and 32 showed similarity to PCWDEs. Xylan is the major component of hemicelluloses in monocotyledonous cell walls. Therefore, xylanases and feruloyl esterases, which break the crosslinks between xylan and lignin, may assist the colonisation of cereals. Homology-based identification of PCWDEs are only predictive and require enzymatic confirmation. Only a limited number of xylanases from *F. graminearum* have been enzymatically characterised (Belien *et al.*, 2005, Carapito *et al.*, 2009b). The creation of fungal strains that lack particular PCWDEs would not necessarily reveal function, or result in a reduction in pathogenicity, due to the high possibility of genetic redundancy. The MAPK *map1*-deficient *F. graminearum* strain was non-pathogenic on wheat and demonstrated reduced glucanase, xylolytic and proteolytic activity (Jenczmionka & Schafer, 2005). Cytochemical evidence has demonstrated that PCWDEs produced by *F. graminearum* and *F. culmorum* are involved in the colonisation of the host tissue (Kang & Buchenauer, 2000b, Wanjiru *et al.*, 2002). Analysis of *F. graminearum* cultured in a liquid medium, where hop cell wall polysaccharides were the sole carbon source, revealed that the pathogen up regulates PCWDEs production in the presence of plant cell wall material (Carapito *et al.*, 2008). Evaluation of the exoproteome and genome suggested that the array of PCWDEs produced by *F. graminearum*, collectively, could digest the plant cell wall in its entirety (Cuomo *et al.*, 2007, Paper *et al.*, 2007, Phalip *et al.*, 2009). However, under field conditions even after heavy and prolonged infection, the sub-components of the ear remain macroscopically intact and rigid except for the developing grain (Figure 2).

PCWDE production in the exoproteome was repressed by the presence of glucose via catabolite repression (Phalip *et al.*, 2009). The F-box protein Frp1 is required for full virulence of *F. oxysporum* f. sp. *lycopersici* on tomato and for the expression of PCWDEs and isocitrate lyase (Duyvesteijn *et al.*, 2005). Alleviating catabolite repression via the mutation of the *CRE1* gene in the *frp1*-deficient strain restores a wild-type phenotype (Jonkers & Rep, 2009). The sucrose non-fermenting 1 (SNF1) protein kinase regulates the transcription of glucose-repressed genes in response to glucose starvation and plays a role in modulating CreA activity in *A. nidulans* (Strauss *et al.*, 1999). For *F. graminearum*, and other phytopathogens, *SNF1* disruption impedes PCWDE production and the utilisation of alternative carbon sources (Goodwin & Chen, 2002, Lee *et al.*, 2009b, Ospina-Giraldo *et al.*, 2003, Tonukari *et al.*, 2000). Therefore, carbon source, metabolism and the assimilation of sugars retrieved from the plant host influences the synthesis of virulence factors including PCWDEs.

In an attempt to understand the molecular processes underlying pathogenicity, the global scientific Fusarium community is constantly creating single gene disrupted / deleted strains via various forward and reverse genetic approaches. The success rate of identifying pathogenicity genes through reverse genetics was fairly successful, with approximately 70 % of the genes published via peer review reporting a defect in pathogenicity on at least one cereal host species. This could reflect the infrequent publication of genes that do not affect virulence or the fact that the majority of the 89 studied genes explored to date were not unique to *Fusarium* species (Table 2). These disrupted genes were involved in a wide range of processes from housekeeping and nutrition functions, to signal transduction, transport, transcription and virulence (Figure 7). Genes involved in highly conserved metabolic processes or signalling pathways, such as the MAPK cascades, which link external stimuli with gene expression, have attracted detailed attention.

The majority of genes explored in *F. graminearum* that were specific to *Fusarium* species were involved in mycotoxin biosynthesis. The exception was the identification of a *Fusarium* species specific virulence gene in *F. graminearum* that encodes an extracellular lipase, Fgl1 (Voigt *et al.*, 2005). Sequences homologous to *FGL1* are found in other fungi and this is bound to attract interest in determining its

role in pathogenicity in the plant pathogenic fungi. The *FGL1* gene deletion result is particularly intriguing because the reduced virulence strain triggered a massive defensive response in the wheat ear. The induction of this type of defensive reaction in rachis tissue has not been observed in any other strain recovered from either a forward or reverse genetic approach. Analysis of the mycotoxin biosynthetic genes accounted for all the other *Fusarium* species specific genes.

Table 2 The number of *Fusarium* species specific or non-specific genes and the impact of their genetic disruption on *F. graminearum* virulence. The values presented in this table represent a summary of the data collected in Appendix 1.

Virulence of single gene disruption strain	Unique to *Fusarium spp.*	Not unique to *Fusarium spp.*
Wild-type	3	22
Reduced	5	47

For this purpose of the project all the *F. graminearum* gene deficient strains have been reviewed and their functional categorisation determined using both the MIPS and BROAD gene annotations (Appendix 1). The percentage of single gene disrupted strains in each functional category, which did or did not influence virulence is summarised in Figure 7. The MIPS functional category that represented the highest proportion of gene disruptions was the metabolism group (MIPS code 1), where 27 / 62 genes disrupted reduced virulence. This would be expected due to the integral nature of their function in various life requiring processes. Cell rescue, defence and virulence (MIPS code 32) had the second highest representation of studied genes due to the disruption of many mycotoxin biosynthetic genes. The biosynthesis of the three mycotoxins attracted special attention in order to determine their roles in pathogenicity. Despite butenolide and trichothecenes being co-produced in wheat, of the two only trichothecenes were required for full pathogenicity on wheat ears (Gaffoor & Trail, 2006, Harris *et al.*, 2007) which accounts for why this category also shows a high representation in fungal mutants with wild-type virulence. The role of butenolide and zearalenone in the pathogen's life cycle remains unresolved. The proportion of genes with unknown function that had no influence on virulence was approximately three times greater than those which reduced virulence. This was

partly the result of a large reverse genetic screen of 15 genes predicted to encode different polyketide synthases (Gaffoor *et al.*, 2005). Overall, there appears to be an even spread of investigation across many functional categories over the past 16 years.

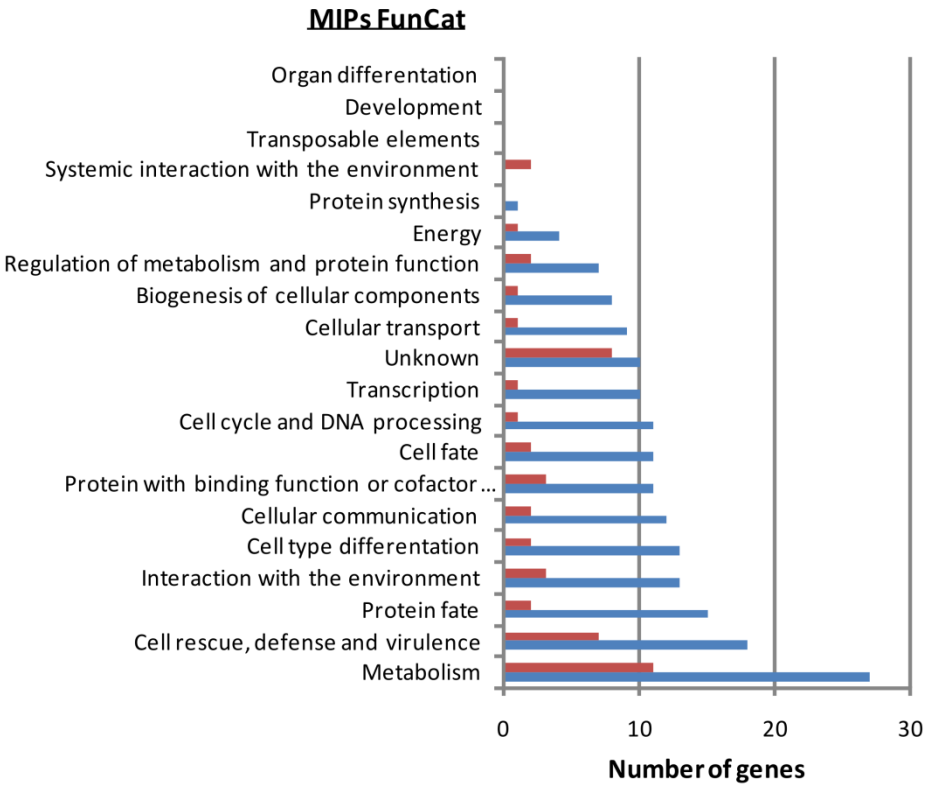

Figure 7 A diagrammatic representation of all the single gene disruption / deletion *F. graminearum* mutants created by the global scientific Fusarium community since 1995. The 89 genes were divided according to the impact of their disruption on the virulence of the mutant strain on a range of hosts (Arabidopsis, barley, maize, tomato and wheat). These groups were then sub-divided into MIPS functional categories (Appendix 2 for MIPS cats). The values presented in this figure represent a summary of the data collected in Appendix 1. Blue bar = genes required for virulence (n = 62). Red bar = genes not required for virulence (n = 27).

The cellular localisation of the protein products encoded by the disrupted genes was predicted via homology to the relevant gene products in *S. cerevisiae*. This was possible due to the conservation between many pathways, such as the MAPK signalling cascade. For gene sequences where the overall sequence similarity was low, the predicted protein structure of the disrupted gene was analysed for secretion signals (Signal P) or short domains similar to transmembrane helices. Gene products that remained unclassified were grouped as unknown. The localisation results are summarised in figure 8 and the information on individual genes are collected in Appendix 1. The unknown category represented a high proportion of the genes in question, demonstrating a gap in our knowledge. Two thirds of the gene products with unknown cellular location had no impact on virulence, thus it may be that they have not merited such a detailed analysis. The majority of protein products with known cellular localisation reside in the cytoplasm, followed by the nucleus and the plasma membrane. This result is explained by the focus of the Fusarium scientific community on the signalling cascades that start at the plasma membrane, pass via several intermediates before altering gene expression in the nucleus. It also highlights the importance of the link between the external environment and gene regulation in a pathogenic interaction. The mitochondrion was also highly represented due to the focus on metabolism and energy production, such as the tricarboxylic acid cycle.

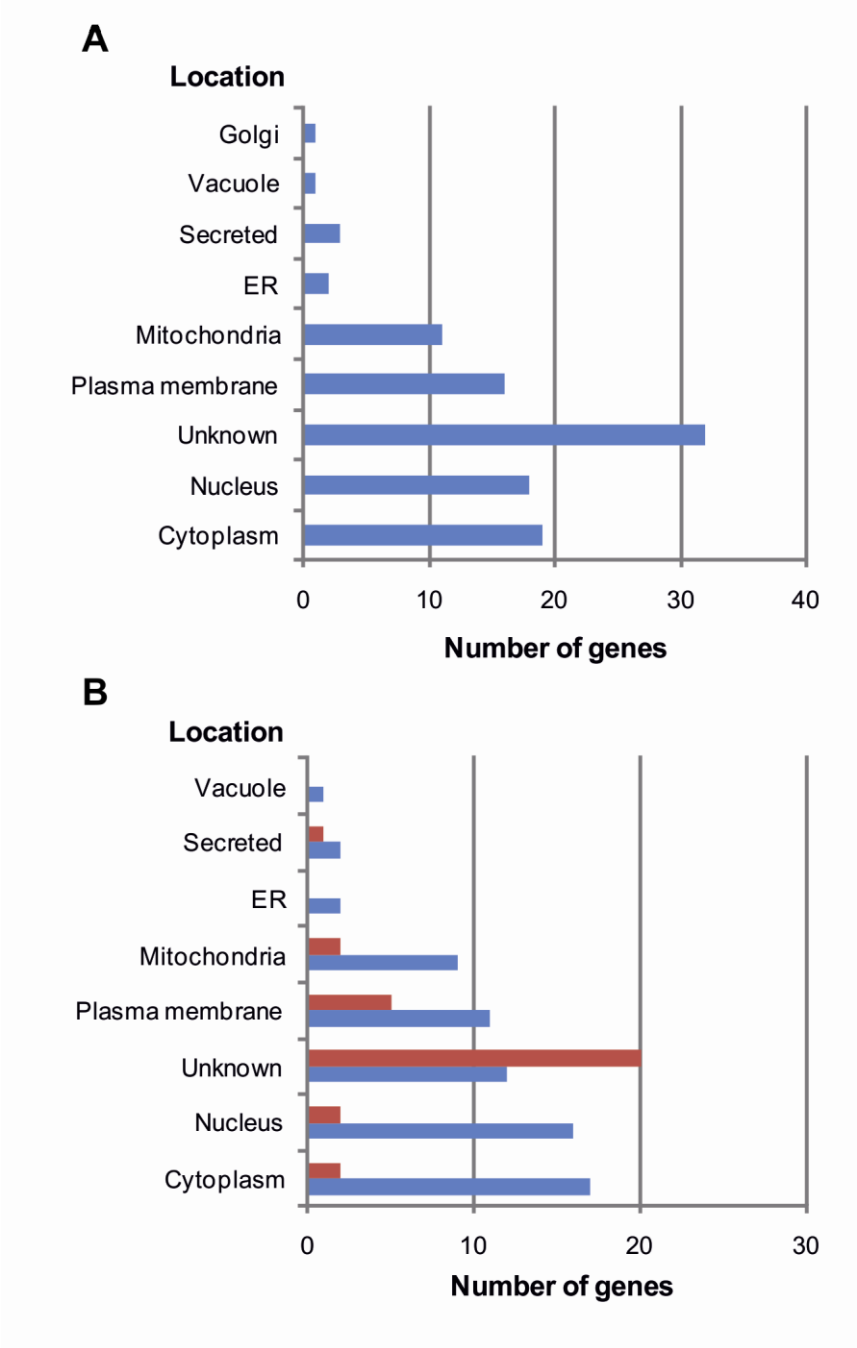

Figure 8 The hypothesised cellular location of the protein products encoded by all the disrupted *F. graminearum* genes (A). The impact of gene disruption on *F. graminearum* virulence sub-divided according to the hypothesised cellular location of the relevant protein product (B). Blue bar = virulence genes. Red bar = genes not required for virulence. The values presented in this table represent a summary of the data collected in Appendix 1.

1.4.8. The importance of signalling pathways in the coordination of pathogenicity in *F. graminearum*

The ability to perceive changes in the environment via monitoring external stimuli is essential for all organisms, especially for pathogens during host colonisation. The relay of activation from an extracellular receptor occurs via a diverse, complex and interlinked system of signal cascades. The accumulative result of such stimulation is the transcriptional and post-translational coordination of one or more intracellular processes.

MAPKs are of the serine / threonine protein kinase family and are highly conserved in eukaryotes (Chang & Karin, 2001). MAPK cascades start with the recognition of external signals and result in the regulation of growth and differentiation. Current understanding of these pathways predominantly comes from studies carried out on *S. cerevisiae* in which five MAPK cascades exist (Chen & Thorner, 2007). The phosphorylation of three protein kinases is central to each of these pathways, a MAP kinase kinase kinase (MAPKKK), a MAP kinase kinase (MAPKK) and terminating with the activation of a MAPK, which is translocated from the cytosol to the nucleus. Stimulation of the MAPK pathways starts either with an upstream kinase or small G-proteins, while phosphatases negatively regulate the MAPKs pathways via dephosphorylating both the MAPKK and the MAPK (serine / threonine) or solely the MAPK (tyrosine). These pathways separately control the cell's response to pheromone binding, nitrogen or carbon starvation, high temperature and changes in osmolarity, which results in the mating response, filamentous growth, the maintenance of cell integrity, the high osmolarity glycerol response and ascospore formation (Xu, 2000). The MAPK cascades have been studied in a variety of fungal pathogens. A homologue of the terminal MAPK involved in the mating response and filamentous growth (*FUS3 / KSS1* in *S. cerevisiae*) has been identified in *M. oryzae*, *PMK1*, *Colletotrichum lagenarium*, *CMK1*, *B. cinerea*, *BMP1* and *F. oxysporum*, *FMK1* (Di Pietro *et al.*, 2001, Takano *et al.*, 2000, Xu & Hamer, 1996, Zheng *et al.*, 2000) and *F. graminearum* (see below). *PMK1* and its homologues have been demonstrated to play a role in appressorium formation, hyphal growth, mating and conidiation. However, the roles

which they play appear to differ depending on the life cycle of the particular organism.

Disruption of the *F. graminearum PMK1* homologue known as *MAP1* or *GPMK1*, resulted in a non-pathogenic mutant that failed to invade host tissue, or colonise from a wounded surface, failed to develop perithecia and showed reduced DON production (Urban *et al.*, 2003). Other steps in the mating response and filamentous growth pathways have since been disrupted, which has enabled the partial construction of a combined cascade regulating sexual development and invasive growth (Figure 9). In *S. cerevisiae* the MAPK cascade for the mating response and cAMP-dependent pathway commences the cognate cell surface receptors Ste2 or Ste3 which release and activate the alpha subunit of a heterotrimeric G-protein, Gpa1 (Dohlman & Thorner, 2001). In *Cryptococcus neoformans* and *U. maydis*, Gpa1 and Gpa3 respectively, regulate mating and virulence (Alspaugh *et al.*, 2002, Lee *et al.*, 2003). The mucin-like Msb2 and the transmembrane Sho1 receptors initiate the *S. cerevisiae* Kss1 pathway in response to starvation, regulating the nitrogen starvation response, sporulation and filamentous growth. Disruption of the *F. oxysporum MSB2* homologue demonstrated that the glycosylated transmembrane protein is required for Fmk1 phosphorylation, promoting invasive growth, and also contributes to cell integrity (Perez-Nadales & Di Pietro, 2011). *F. graminearum* strain with the downstream GTPase *RAS2* disrupted demonstrated reduced virulence and DON production (Bluhm *et al.*, 2007). The signal relay that results in the Ste20/Ste50 activation of the kinase Ste11 has not been experimentally studied in *F. graminearum* but is highly conserved in filamentous fungi. The scaffold protein, essential for pheromone signalling in *S. cerevisiae*, Ste5 is poorly conserved among fungi and absent from *F. graminearum*, suggesting the existence of an alternative component. Ras2 and Gpa1 signal perception in *F. graminearum* may involve the scaffold protein Fsr1 (Shim *et al.*, 2006, Yu *et al.*, 2008). Based on the cascades similarity with the relative steps in *S. cerevisiae*, Fsr1 is predicted to bring together Ste11, Ste7 and Map1, thus permitting the relay of phosphorylation and activation. In *S. cerevisiae* Ras2 is also involved in the cAMP-dependent protein kinase A (PKA) pathway via a bound adenylate cyclase, Cyr1 (Santangelo, 2006). It appears that the cAMP-dependent and MAP

kinase pathways are closely linked in *S. cerevisiae*, as they converge on the regulation of similar genes, such as *FLO11*, which is a key glycoprotein required for adhesion and filamentation (Rupp *et al.*, 1999). Treatment of a *F. graminearum ras2* mutant with exogenous cAMP does not recover the wild-type phenotype, suggesting Ras2 plays a minor role in cAMP signalling in *F. graminearum* (Bluhm *et al.*, 2007). However, disruption of the PKA regulatory subunit altered hyphal morphology while reducing infection, DON production *in planta*, asexual and sexual reproduction (Beacham, 2010). In *S. cerevisiae* phosphorylated Map1 activates the Ste12 and Far1 transcription factors resulting in cell cycle arrest and polarised filamentous growth (Bardwell, 2005). Ste12 interacts with Tec1 to bind to filamentous responsive elements inducing transcription in *S. cerevisiae* (Gancedo, 2001), however a *F. graminearum TEC1* homologue does not exist.

Adaptation to osmotic stress (osmoadaption) in *S. cerevisiae* is controlled by the high osmolarity glycerol (HOG) response pathway. Osmotic stresses activate the Hog1 pathway by two mechanisms that converge on the MAPKK, Pbs2. Under severe osmotic stress, deactivation of a histidine kinase osmosensor Sln1 leads to enhanced levels of dephosphorylated Ssk1 which activates the Ssk2/22-Pbs2-Hog1 phosphorylation cascade (Hohmann, 2002). Alternatively, exposure to less severe hyperosmotic stress activates the plasma membrane protein Sho1, which recruits Ste11 and Pbs2, where Cdc42 and Sst50 activate two p21-activated kinases Ste20 and Cla4 which phosporylate Pbs2 (Hohmann, 2002). The Sln1 branch of the homologous MAPK cascade in *F. graminearum* is well characterised including the histidine kinase sensor (Os1) and the MAPKKK-MAPK cascade (Os4, Os5 and Os2, respectively, Figure 9) (Ochiai *et al.*, 2007). The transcription factors downstream of Hog1, with the exception of Hot1, are well conserved among fungi including the MADS-box Smp1, the leucine zipper Sko1, the transcriptional activators of stress responsive genes Msn2 or Msn4 and the cell-type specific, pheromone response transcription factor Mcm1 (Westfall *et al.*, 2004). In *S. cerevisiae* nuclear located Hog1 leads to the expression of ~ 600 genes (O'Rourke & Herskowitz, 2004), while the serine / threonine phosphatase Ptc1 deactivates the Hog1 pathway and is essential for the TOR pathway (Gonzalez *et al.*, 2009, Warmka *et al.*, 2001). Ptc1 is the only

the negative regulator of a MAPK cascade to be assessed in *F. graminearum* and is required for hyphal growth and virulence (Jiang *et al.*, 2010).

The cell integrity or PKC pathway controls cell morphology by regulating the expression of genes involved in cell wall synthesis and the reorganisation of the actin cytoskeleton. In *S. cerevisiae*, the integrin-like Wsc proteins and the O-glycosylated plasma membrane protein Mid2 interact with the guanine nucleotide exchange factors Rom1 or Rom2, which activate Rho1 and subsequently recruits pathway components to the site of polarised growth, activating the phosphorylation cascade from Pkc to Mpk1 (Levin, 2005). The cell integrity cascade is well conserved among fungi, except for the sensor Mid2 (Rispail *et al.*, 2009). Unlike the previous MAPK pathways, the cell integrity pathway resembles a network involving the TOR, pheromone and Cdc28-dependent cell-cycle pathways that can independently activate Pkc (Hohmann, 2002). While the HOG pathway acts synergistically to determine the correct cell wall strength and tugor pressure to support morphogenesis. The downstream targets of Mpk1 include Rlm1 that controls the expression of 20 genes involved in cell wall metabolism and the SBF complex (Swi4/Swi6/Mbp1) which is required for cell wall gene expression in the G1 phase of the cell cycle (Gustin *et al.*, 1998). The cell integrity pathway is the least well studied in *F. graminearum* (Figure 9), where only the *MPK1* homologue *MGV1* was demonstrated to be required for full virulence, DON production, perithecial development, hyphal fusion and heterokaryon formation (Hou *et al.*, 2002).

The nutrient limitation response in *S. cerevisiae*, in the form of sugar deprivation, is controlled by the cAMP-PKA, SNF1 and TOR pathways, while nitrogen or amino acid starvation is also regulated by the TOR pathway (Carlson, 1999, Lengeler *et al.*, 2000, Rohde *et al.*, 2001). Schematics of how cell metabolism is regulated by the nutritional environment are presented in figures 10 and 11. The presence of glucose represses the metabolism of alternate carbon sources in gluconeogenesis and respiration in both prokaryotes and eukaryotes. Glucose activates adenylate cyclase and cAMP synthesis via the G-coupled protein Gpa1, while acidification also activates adenylate cyclase cAMP production via Ras2 (Carlson, 1999). The SNF1 and TOR complexes monitor nutrient utilisation via the AMP:ATP ratio inside the cell (Hardie *et al.*, 1998, Rohde *et al.*, 2001). In *S.*

cerevisiae SNF1 acts as a broad regulator of the transcription of glucose-repressed genes in response to stress, such as genes involved in glycogen storage, thermotolerance, sporulation and pseudohyphal growth under nitrogen limiting conditions (Hardie *et al.*, 1998). SNF1 is a heterotrimeric protein complex consisting of a catalytic Snf1 α subunit, a stimulatory β subunit, Snf4 and the variable γ subunit, Sip1, Sip2 and Gal83 (Vincent *et al.*, 2001, Vyas *et al.*, 2003). Three isoforms of the SNF1 complex exist and, depending on which γ subunit is bound, the complex is targeted to different cellular localisation. The catalytic domain of SNF1 becomes active when the ratio of AMP:ATP increases and the Thr210 loop is phosphorylated (Hardie *et al.*, 1998). The TOR protein kinase pathway that signals nutrient availability negatively regulates phosphorylation of the Thr210 loop via TORC1 (Orlova *et al.*, 2006).

The general stress response is mediated by the partially redundant transcriptional activators Msn2/4. Under optimal, nutrient-rich conditions, inactive Msn2/4 are situated in the cytosol, while under stress conditions they are translocated to the nucleus where they bind to STREs elements in the promoter of stress-dependent genes, inducing transcription (MartinezPastor *et al.*, 1996). In response to nutrient availability, the TOR pathway controls cell growth via the 14-3-3 proteins Bmh1 and Bmh2 that act as cytosolic anchors for Msn2/4 (Beck & Hall, 1999), while PKA mediated dephosphorylation results in Msn2/4 being exported from the nucleus by Msn5 (Chi *et al.*, 2001). Bmh1/2 are also involved in the Ras2 mediated MAPK cascade (Bruckmann *et al.*, 2007). Glucose mediated repression of genes required to utilize alternative carbon sources and the flocculin glycoprotein essential for filamentous growth Flo11, is promoted by the nuclear localisation of Nrg1, Nrg2, Tup1, Cyc8 and Mig1. The SNF1 and cAMP-PKA pathways appear to be antagonistic in the control of glycogen synthesis as elements of the cAMP-PKA pathway are suppressed by SNF1 (Hardy *et al.*, 1994). Interesting, as was the case with the cAMP-PKA and MAP1 kinase pathways, the SNF1 complex is also involved in the regulation of *FLO11* via the action of Nrg1/2 (Kuchin *et al.*, 2002). Under nutrient-rich conditions, invasive filamentous growth, nitrogen scavenging, autophagocytosis and the retrograde or stress responses are all inhibited by TORC1 sequestering transcription factors in the cytosol (Rohde *et al.*, 2001). TORC1 also

promotes Tap42 and Sch9 inhibition of autophagocytosis (Noda & Ohsumi, 1998, Urban *et al.*, 2007, Yorimitsu *et al.*, 2007). The *S. cerevisiae* cyclin-dependent kinase (CDK) complex including Ume3 and Ume5 negatively regulates the transcription factors for filamentous growth Ste12, for amino acid biosynthesis Gcn4 and the stress response activators Msn2/4 (Nelson *et al.*, 2003). CDK mediated phosphorylation targets the transcription factors for ubiquitination. However, unlike the other proteins, Msn2/4 are not degraded but exported from the nucleus (Beck & Hall, 1999). So far, in *F. graminearum* the general stress response pathways have not been explored.

Exposure of *S. cerevisiae* to low glucose levels inactivates adenylate cyclase and the PKA/TOR/Bmh1/2 mediated localisation of Msn2/4 to the cytosol, while the activated SNF1, in response to the elevated AMP:ATP ratio, phosphorylates Msn2/4 promoting nuclear translocation and the transcription of the STREs genes, including neutral trehalase 1 (*NTH1*). Simultaneously, SNF1 inhibits the nuclear localisation of Nrg1/2 and phosphorylates Mig1 promoting Msn5 mediated nuclear export, thus alleviating Mig1 catabolite repression, resulting in the expression of genes involved in the utilisation of alternate carbon sources and *FLO11* (Carlson, 1999, Schuller, 2003). Under nutrient limiting conditions the Ume3 levels drop inactivating CDK inhibition, thus promoting Ste12, Gal4 and Gcn4 to translocate to the nucleus and induce invasive filamentous growth, the galactose response and amino acid biosynthesis, respectively (Nelson *et al.*, 2003). The removal of TORC1 inhibition also permits various transcription factors (Gln3, Gat1, Npr1) to promote nitrogen utilisation (Beck & Hall, 1999)and Rtg1/2 to stimulate the retrograde response (Dilova *et al.*, 2004). Alleviation of TORC1 mediated Tap42 and Sch9 inhibition permits Pp2A to promote autophagocytosis (Noda & Ohsumi, 1998, Yorimitsu *et al.*, 2007).

The highly conserved global regulator of nutrient availability, TOR, is essential to cell survival and subsequently difficult to investigate. However, experimental examination of downstream, highly conserved, components involved in modulating cell growth in response to nutrient availability, including SNF1, is possible. The AMP-activated kinase, *SNF1* has been identified in several plant pathogens. *SNF1* in *F. graminearum*, *F. oxysporum* and *Cochliobolus carbonum* is

involved in the regulation of PCWDEs and its disruption results in a reduction in virulence on their respective host (Lee *et al.*, 2009b, Ospina-Giraldo *et al.*, 2003, Tonukari *et al.*, 2000). Disruption of the *SNF1* gene in *F. graminearum* resulted in an interesting phenotype, where infection progressed from an inoculated single floret into the rachis but was unable to infect other spikelets of the wheat ear. In this mutant cellular AMP levels increased but DON production remained wild-type (M. Urban, RRes, UK, unpublished). SNF1 was also essential for normal sexual and asexual development and the utilisation of alternative carbon sources (Lee *et al.*, 2009b). The involvement of components of MAP1 and PKA cascades in *F. graminearum* virulence, such as Ras2 and Gpa1, have been described, but they also play a role in the nutrient availability response. In combination with TORC1, these signalling pathways modulate autophagocytosis, which has been demonstrated to be essential for pathogenicity in a range of plant pathogens including *M. oryzae* and *Colletotrichum orbiculare* (Asakura *et al.*, 2009, Liu *et al.*, 2007). In *F. graminearum* the transmembrane protein Atg15, which is essential in the final stages of autophagy (Teter *et al.*, 2001), was shown to have lipase activity and disrupted mutants exposed to starvation demonstrated reduced ability to degrade lipid stores (Long Nam *et al.*, 2011). Under normal *in vitro* conditions germination, hyphal growth and conidia production was also reduced. Wheat ear infection and DON mycotoxin production was severely reduced (Long Nam *et al.*, 2011). Mig1 mediated repression has not been assessed in *F. graminearum*, possibly due to the likelihood of it being essential for life, as was the case in *F. oxysporum* (Jonkers & Rep, 2009). However, disruption of the cyclin-like *UME3* homologue, *CID1*, which play a part in regulating catabolite repression resulted in reduced vegetative growth, DON production and was nearly non-pathogenic (Zhou *et al.*, 2010).

Trehalose is required for thermotolerance and resistance to desiccation in many species and it may also be involved in the survival of osmotic stress (Nwaka & Holzer, 1998). Resistance is not relative to the amount of trehalose present in *S. cerevisiae* (Nwaka *et al.*, 1995). Nth1 is a homodimeric cytoplasmic enzyme that breaks down trehalose into glucose and is required for recovery after exposure to heat shock. In *S. cerevisiae* disruption of *NTH1* increased trehalose and heat sensitivity (Zahringer *et al.*, 1997). Post-translational phosphorylation via a cAMP-

dependent PKA activates Nth1 and inhibits the nuclear localisation signal on Msn2/4. Thus the cAMP-dependent, the Ras2-mediated MAPK and the SNF1 pathways are all linked in the regulation of *NTH1*. Disruption of the *NTH1* homologue in *B. cinerea* and *Leptosphaeria maculans* had no affect on virulence, however, *M. oryzae* demonstrated reduced virulence (Doehlemann *et al.*, 2006, Foster *et al.*, 2003, Idnurm *et al.*, 2003). A *F. graminearum nth1* mutant demonstrated reduced virulence on wheat ears and was unable to cause crown rot symptoms at the stem base (Beacham, 2010). The link between the *NTH1* and *SNF1* pathways may explain the reduction in trehalose observed in the *F. graminearum snf1* mutant (M. Urban, RRes, UK, unpublished).

Unsurprisingly, the genetic assessments of individual signalling components involved in the regulation of filamentous growth, cell integrity, reproduction, and stress responses, often had an impact of *in vitro* growth and reproduction but were also essential for the full virulence of *F. graminearum* on wheat ears. Interestingly, the majority of these genetic manipulations also had a profound impact on DON mycotoxin synthesis, linking the MAPKs cascades and nutrient availability to DON production. The hostile environment within the plant host, the altering availability of nutrition and the involvement of hyphal fusion in reproduction and possibly during infection describes a situation where the pathogen is required to modulate growth, metabolism, virulence and cell fate in response to the conditions encountered. Therefore, in this dynamic situation environmental monitoring and cell signalling is paramount to the outcome of infection. A systems biology view of how *F. graminearum* modulates infection in response to the changing environmental conditions throughout infection is required and would provide new insights into how infection is established and identify novel targets for disease control.

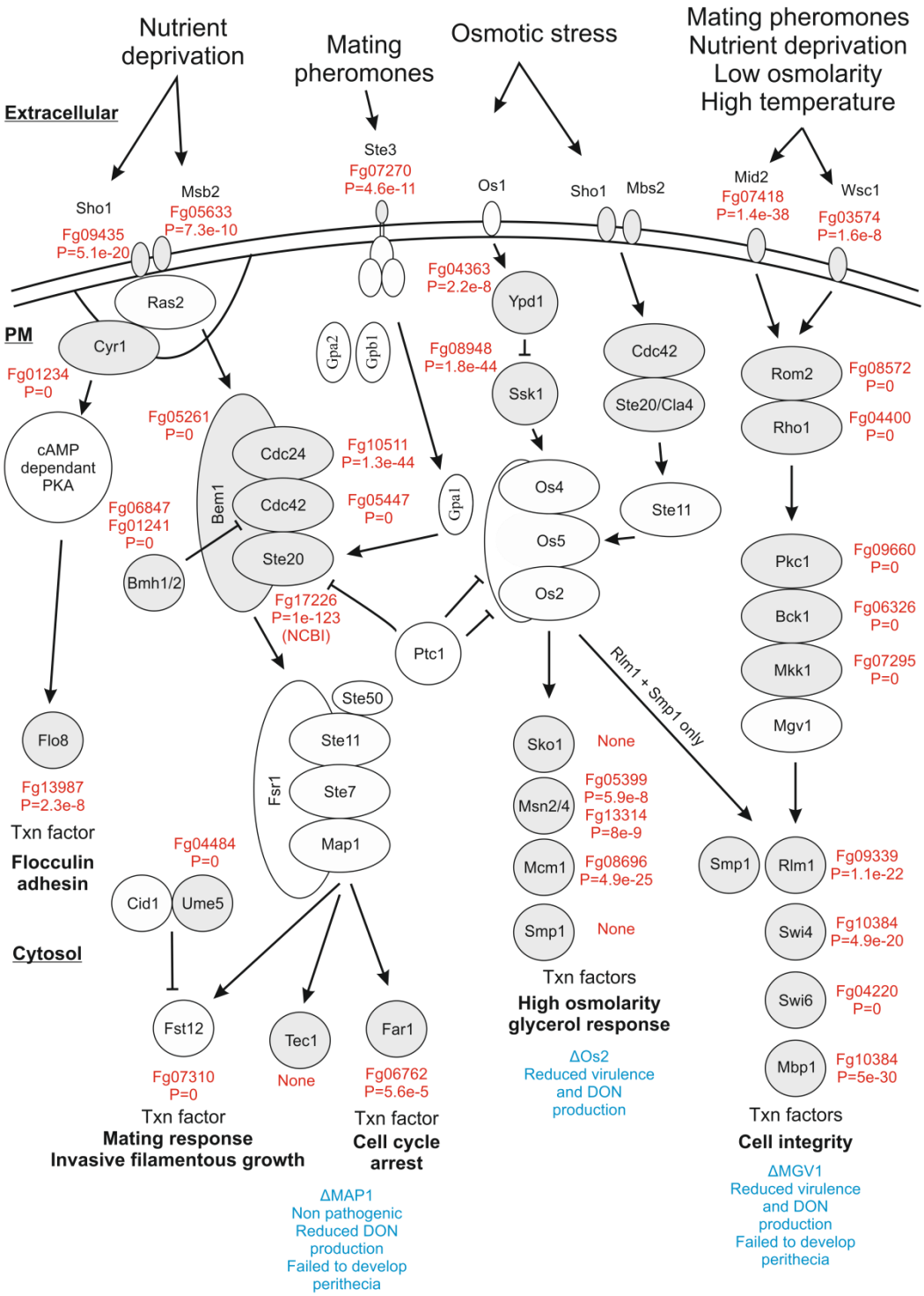

Figure 9 The three predicted MAPK cascades and the transcription factors (Txn) they regulate in *F. graminearum*. The genes coding for the proteins coloured white have been experimentally identified. Proteins in grey have been hypothesised due to their homology to the relevant step in the *S. cerevisiae* cascade and are labelled with their FGSG_ID and the P value for their similarity (BLASTP). The phenotypes of the three different MAPK deficient *F. graminearum* strains are presented in blue.

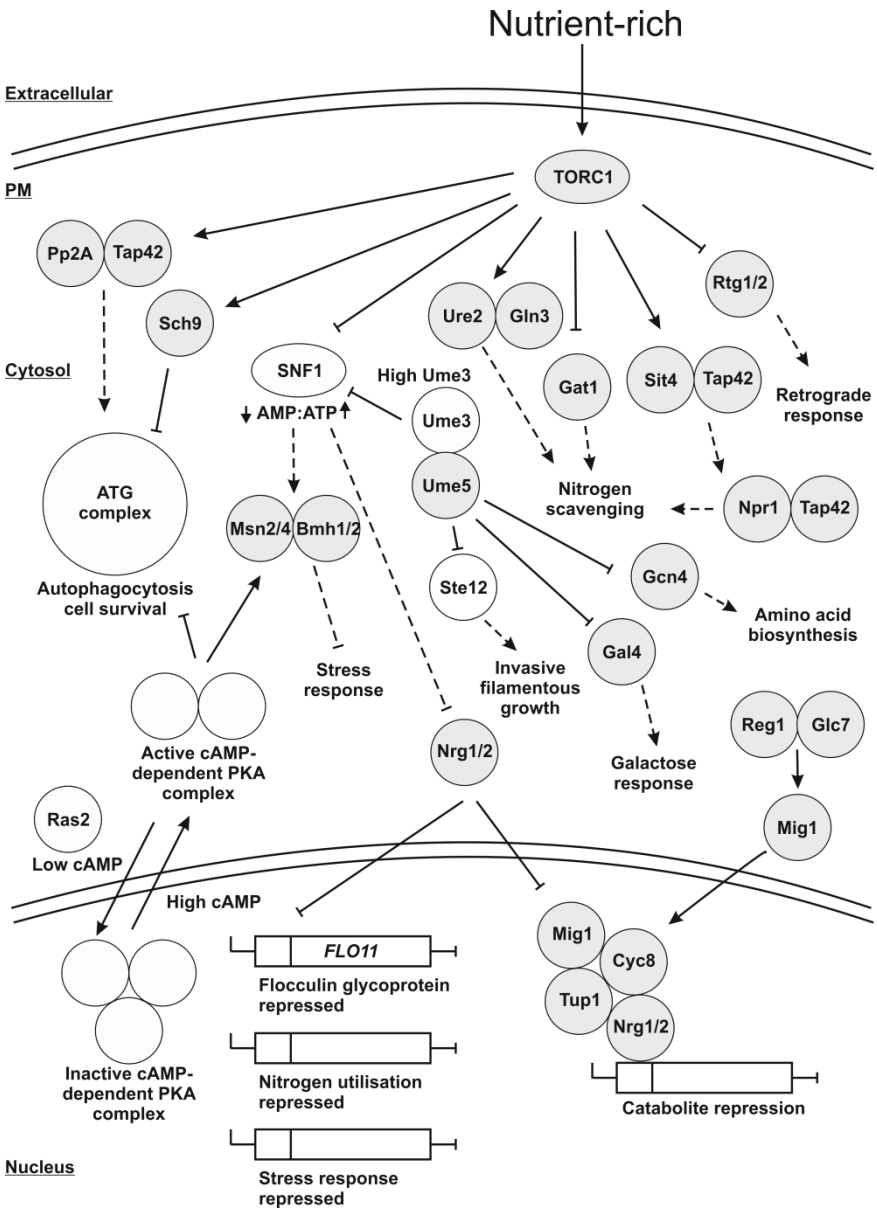

Figure 10 Under nutrient-rich conditions, invasive filamentous growth, nitrogen scavenging, amino acid biosynthesis and the retrograde, galactose or stress responses are all inhibited by the TORC1 complex sequestering transcription factors in the cytosol. TORC1 also promotes Tap42 and Sch9 inhibition of autophagocytosis. The genes coding for the proteins coloured white have been identified by sequence alignment analyses (BLASTP) with *S. cerevisiae* and have experimentally investigated in *F. graminearum*. Predicted proteins depicted in grey have been hypothesised due to their homology to the relevant step in the *S. cerevisiae*. Under nutrient-rich conditions the trichothecene mycotoxins are produced.

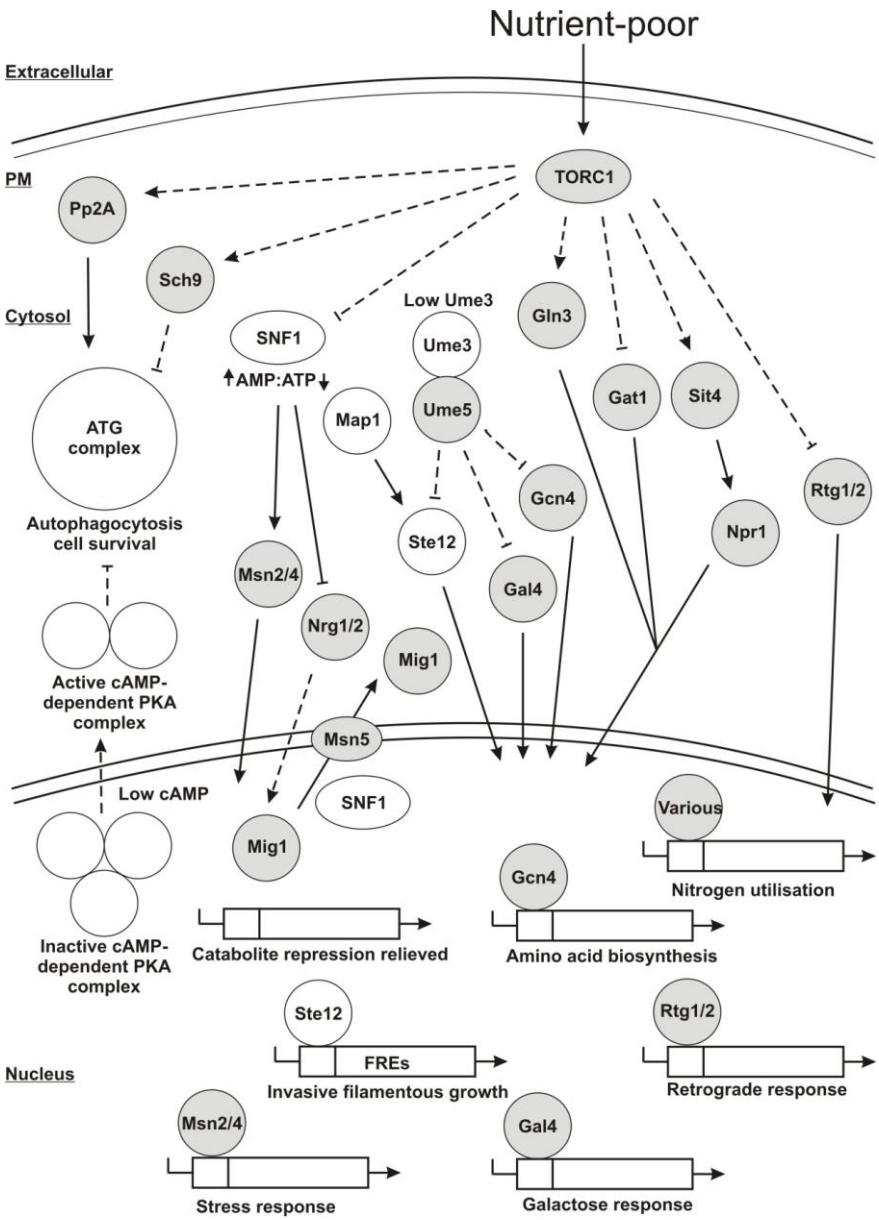

Figure 11 Nutrient limiting conditions inversely inactivates / activates the TOCR1 and SNF1 complexes, promoting the nuclear localisation of transcription factors that result in the expression of STREs genes, the utilisation of alternate carbon sources, invasive filamentous growth, amino acid biosynthesis, autophagocytosis and the galactose and retrograde responses. Genes coding for the proteins coloured white have been identified by sequence alignment analyses (BLASTP) with *S. cerevisiae* and have experimentally investigated in *F. graminearum*. Predicted proteins depicted in grey have been hypothesised due to their homology to the relevant step in the *S. cerevisiae.* Under nutrient-poor conditions the trichothecene mycotoxins are not produced.

1.5. Project objectives

The *F. graminearum* genome is sequenced and aligned to a genetic map, which has facilitated the generation of genetic mutations and transcriptomic data. Many of the single gene deficient *F. graminearum* strains are compromised in disease causing ability and have a post-invasion defect, but the exact point of fungal arrest at the cellular level is unclear. The lack of this detailed biological information hinders the ability to place each mutant within the context of the genomic understanding of host-pathogen interactions. A controversy also remains in the literature as to whether *F. graminearum* invades susceptible wheat floral tissue by a hemibiotrophic or necrotrophic mode of colonisation.

Therefore, the project aimed to carryout a precise assessment of how wild-type and / or mutant *F. graminearum* strains interact with the wheat ear. A transcriptomic and bioinformatic investigation was utlised to identify the molecular determinants of wild-type infection, while a laser capture microdissection procedure was developed to facilitate the generation of future cell-type specific information.

1.5.1. Hypothesis to be tested

- *F. graminearum* invades floral tissue by a hemibiotrophic mode of colonisation.
- The molecular mechanisms controlling spikelet-to-spikelet infection are distinct from the pathogenicity requirements for single floret invasion.
- The rachilla and rachis are the only floral tissues where host cells have the capacity to recognise compromised *F. graminearum* infection and activate plant defence responses.

Chapter 2. Experimental procedures

2.1. Fungal strains, plate cultures and conidia preparations

Fusarium graminearum wild-type strain PH-1 was used throughout this investigation. The wild-type fungus and the other modified strains (*tri5*, *top1*, *PH1:GUS*) used were routinely cultured on SNA (synthetic nutrient poor agar) plates containing 0.1 % KH_2PO_4, 0.1 % KNO_3, 0.1 % $MgSO_4$ x $7H_2O$, 0.05 % KCL, 0.02 % glucose, 0.02 % sucrose and 2 % agar. Plates were incubated at room temperature and under constant illumination from one near-UV tube (Phillips TLD 36W/08) and one white light tube (Phillips TLD 36W/830HF). To remove old conidia and induce fresh conidia formation, 10 day old SNA plates were washed with an overlay of sterile TB3 (0.3 % yeast extract, 0.3 % Bacto Peptone and 20 % sucrose) and placed back into the incubator. After 24 h a conidial suspension was harvested in sterile water, filtered through miracloth (Calbiochem) and then adjusted to a concentration of 4 x 10^4/ml or 2.5 x 10^5/ml with sterile water.

2.2. Fungal stocks

Fungal stocks were maintained either as a water solution of conidia freshly harvested from TB3 treated SNA plates, for short term storage (4 x 10^4/ml), or as soil stocks, for long term storage. For both procedures the stocks were frozen and stored at -80°C. Soil stocks were prepared from double-sterilised soil particles in 2 ml cryo-tubes (Nunc). An agar plug taken from the edge of hyphal growth on a SNA culture was placed into the tube and covered with 200 µl potato dextrose broth (PDB), incubated in the dark at 28°C for two weeks prior to storage at -80°C. To reactivate the stocks when required, a few soil particles were placed on SNA and cultured as described previously.

2.3. Fungal liquid cultures

A 5 cm^2 section of a SNA plate culture was added to 200 ml of PDB in a 500 ml conical flask which was incubated for 3 days in the dark at 28°C, shaking at 100 rpm. The liquid culture was filtered through Miracloth, flash frozen in liquid nitrogen, freeze-dried over night and then finally ground in liquid nitrogen using a sterile pestle and mortar prior to DNA / RNA extraction.

2.4. Wheat cultivar, growth of plants

The susceptible wheat (*Triticum aestivum*) cultivar, Bobwhite, bred by CIMMYT (Mexico) was used as the host plant throughout this investigation. Bobwhite carries the semi-dwarfing genes *Rht-B1b* (*RHT1*) on chromosome 4BS and the wild-type allele *Rht-D1a* on chromosome 4DS (Bayon, unpublished). Plants were grown in a glasshouse as previously described (Urban *et al.*, 2002). This cultivar was selected because each plant typically produces three or four tillers which come into anthesis and then mature at approximately the same rate.

2.5. Wheat ear inoculations

At the first appearance of anther extrusion 5 µl of a 4 x 10^4/ml conidial suspension was placed in the floral cavity between the palea and lemma of the first two florets of two spikelets in the middle of the ear. Control plants were inoculated with sterile water only. These are referred to as mocks throughout. Inoculated plants were incubated in a humid chamber for 72 h of which the first 24 h were in darkness. The plants were then kept in the glasshouse or controlled environment room at ambient humidity. A minimum of three inoculations per experimental treatment and three mock inoculations were sampled per study. The images presented throughout are representative of the biological replicates carried out for each experiment.

2.6. Stereomicroscopy and Photography

The macroscopic appearance of the selected wheat tissues was capture before sampling by stereomicroscopy on a Lecia MZFL11 under bright field light, or by photography on a Nikon D40X under natural light. All images were taken against a black background.

2.7. Preparation of individual wheat tissues for compound light microscopy

The excised tissue were fixed, individually, for 16 h with 4 % paraformaldehyde (Sigma), 2.5 % glutaraldehyde (Sigma) in 0.1 M Sorensen's phosphate buffer (NaH_2PO_4:Na_2HPO_4, pH 7.2), then washed 3x with 0.05 M Sorensen's buffer and once with sterile water. Samples were subsequently dehydrated in a graded ethanol series, embedded in hard grade LR White (TAAB) and polymerised at 60^{o}C for 24 h (Ruzin, 1999).

2.8. Compound light microscopy

Transverse semi-thin 1 μm sections of the LR White embedded samples were cut with a glass knife on an ultramicrotome (Reichert-Jung, Ultracut). Sections were collected on polysine coated glass slides (VWR International) and dried on a hot plate set at 40^{o}C. After staining with aqueous 0.1 % toluidine blue O (TBO) in 1 % sodium tetraborate (w/v) pH 9 (Ruzin, 1999), sections were mounted in DPX (Sigma), then examined and imaged using a Zeiss Axiophot light microscope.

2.9. Scanning electron microscopy (SEM)

Wheat tissues were excised using a sterile blade and forceps, mounted onto a cryo stub using OCT compound (Sakura FineTek) and plunge frozen in liquid nitrogen. Samples were transferred under vacuum to the Gatan Alto 2100 cryo chamber stage maintained at -180^{o}C. Samples were freeze fractured in the cryo chamber and then partially freeze dried for 1 min at -95^{o}C prior to gold coating. The samples were transferred to the cold stage of Jeol LV6360 scanning electron microscope maintained at -150^{o}C for examination.

2.10. DNA / RNA extraction, nucleic acid quantification and storage

Pure fungal nucleic acids were isolated from freeze dried mycelium prepared from *in vitro* cultures using either the NucleoSpin Plant XL (Macherey-Nagel) or the RNeasy Plant Mini (Qiagen) affinity columns, for DNA or RNA respectively, according to manufacturer's instructions. To isolate fungal and / or plant RNA from *in planta* experiments, various types of plant tissues were excised individually, then pooled and frozen in liquid nitrogen and freeze dried overnight. The freeze dried

samples were ground in liquid nitrogen with a sterile pestle and mortar. Total RNA was extracted using the TRIzol® reagent (Invitrogen) with minor modifications to the manufacturer's instructions. Total RNA was precipitated at -20°C for 16 h with 8 M lithium chloride. Total RNA was treated with a DNA-*free*™ kit (Ambion) to remove contaminating DNA. Purified DNA / RNA was quantified on a Nanodrop ND-1000 spectrophotometer (NanoDrop Technologies) by absorbance at 260 nm and the purity evaluated by determining the 260 / 280 nm absorbance ratio. All nucleic acids were placed at -20°C or -80°C for short and long term storage, respectively.

2.11. Electrophoresis and visualisation of nucleic acids

Nucleic acids were separated by electrophoresis on a 1 or 2 % agarose gel (w/v), in 1x TAE buffer (40 mM tris(hydroymethyl) aminomethane-HCl (Tris-HCl), 1 mM EDTA pH 8 and 0.1142 % (v/v) glacial acetic acid) containing 5 µl ethidium bromide (Bio-Rad, 10µg/ml) per 100 ml solution. The agarose solution was heated in a microwave until completely dissolved and cooled to 50°C before adding the ethidium bromide. The gels were cast with a comb that made sufficient wells for the experiment. Once the gel was firm, the comb was removed, the gel placed into the electrophoresis tank and bathed in 1x TAE. The nucleic acids were mixed with loading buffer (25 % bromophenol blue, 40 % (w/v) sucrose in water) at a 4:1 ratio prior to loading into the wells alongside a 100 base pair (bp), a 1 kilobase pair (kb) DNA ladder (GeneRuler, Fermentas) or a Lambda_BstEII_DNA ladder (New England Biolabs) according to the predicted size of the nucleic acids. Electrophoresis was performed at 80V for 40 – 60 mins and then the nucleic acids were visualised under ultraviolet (UV) light on a Gene Genius imager with GeneSnap software (Syngene). Electrophoresis was utilised to confirm nucleic acid integrity and to determine the size or number of amplicons generated by a polymerase chain reaction.

2.12. DNA primer design and Polymerase chain reaction (PCR)

All DNA primers were designed on the Vector NTI software (Invitrogen) using the following setting: Tm 55 or 62°C, GC content 30-65 %, primer length 18-25 bp, less than 4°C or 4 % difference in Tm or GC content, a Vector NTI primer score of 171 and contains a GC clamp at the 3' end. DNA primers were purchased from Sigma-Aldrich as dry samples and subsequently diluted with dH_2O to 100 µM

(Table 3). An aliquot at 10 µM was prepared and used of PCR investigation. Primers were stored at -20^{o}C. A single PCR reaction consisted of 12.5 µl of HotStarTaq master mix (5 U /µl HotStarTaq DNA Polymerase, 1.5 mM $MgCl_2$ and 200 µM of each dNTP) (Qiagen) plus 0.4 µM of each primer, and 25 ng nucleic acid template in a final volume of 25 µl. Thermal cycling conditions [95^{o}C 15 min, (95^{o}C 30 sec, 55-62^{o}C 30 sec, 72^{o}C 2 min) x 35] were performed on a G-Storm GS4 (AlphaMetrix Biotech). The annealing temperature varied according to the requirements of the primers used. Specific primer details are presented within the relevant sections.

Table 3 Fungal genes selected for expression analysis by RT-qPCR, their FGSG locus ID, MIPS function (www.mips.helmholtz-muenchen.de) and their primer sequence. Intergenic primers used to confirm absence of gDNA contamination of RNA samples.

Fungal gene	FGSG locus ID	MIPS function	Primer sequence (5'-3')	
			Sense	Antisense
Intergenic	Region between *TRI6*& *TRI4*		TGAAGTTGTCCTCAGTATCG	TCCTGTGTGAAATTGTTATCCGCTGGGTAGTCAAAATAGATGTTC
FgActin	07335.3	Probable Actin	ATGGTGTCACTCACGTTGTCC	CAGTGGTGGAGAAGGTGTAACC
FgTubulin	09530.3	Beta-tubulin	TCAACATGGTGCCCTTCC	TTGGGGTCGAACATCTGC
FgTri4	03535.3	Trichodiene oxygenase	AGACTACTTCAAGGACACTGGCC	GGTAAGGGAGATTCTCTAGGGTAGC
FgTri5	03537.3	Trichodiene synthase	GATGAGCGGAAGCATTTCC	CGCTCATCGTCGAATTCC
FgTri6	03536.3	Trichothecene biosynthesis positive transcription factor	TGTCGCTACTCAGAATGCC	CCCTGCTAAAGACCCTCA
FgTri9	03539.3	Hypothetical protein	TATCCACTCAAACACTCACCCC	TGGTAGCGCATAAAGCAGC
FgTri14	03543.3	Putative trichothecene biosynthesis gene	CTGATAAGCTTGAACCACCTCG	TTGATCACAACGGGAGTTCC

Chapter 3. The infection biology of *Fusarium graminearum*

3.1. Introduction

The establishment of *F. graminearum* infection in a single spikelet is well documented (Parry *et al.*, 1995)(Reviewed in Chapter 1). However, how this pathogen spreads from spikelet to spikelet and ultimately colonises the entire wheat ear is unclear. There is controversy over whether *F. graminearum* invades wheat floral tissue using a necrotrophic or a non-necrotrophic mode of nutrition (Leonard & Bushnell, 2003). The multiple investigations described in chapter 1 focused on different aspects of fungal pathogenicity, in specific tissues of the ear, mainly a single floret (Pritsch *et al.*, 2000, Pugh, 1933, Ribichich *et al.*, 2000, Wanjiru *et al.*, 2002) or the spread of infection from the peduncle into the stem and culm tissue below the ear (Guenther & Trail, 2005). A few studies using a GFP labelled *F. graminearum* strain described the early infection process and documented colonisation of excised caryopsis and not the intact ear (Jansen *et al.*, 2005). These excised tissues over time do not truly represent the normal source-sink relationships in the ear. Other studies have documented the early ear infection pathway of the related asexual *Fusarium* species, *F. culmorum* (Kang & Buchenauer, 2000a, 2000b, 2000c) and these studies are commonly referred to in the *F. graminearum* literature. However, active trichothecene mycotoxin production in *F. culmorum* occurs over a wider range of permissive conditions than *F. graminearum* (Hope & Magan, 2003) and so care must be exercised when extrapolating the findings from other cereal ear infecting *Fusarium* species. Finally, in none of the previous cytological and histological studies has the advancing front of hyphal infection been accurately located and described in different tissues over the course of infection.

In this study, I have addressed each of these omissions and described a detailed microscopy investigation of the entire colonisation of a susceptible wheat ear by the wild-type *F. graminearum* strain PH-1. This study, tracked the infection pathways and hyphal networks generated by *F. graminearum* from the initially inoculated floret into the rachis nodes and internodes and beyond into the neighbouring spikelets revealing: (1) the wide variety of inter- and intracellular colonisation routes successfully employed, (2) the dramatic changes in hyphal

diameter, density and appearance in the different host tissue types, (3) the appearance of the host cells in advance of the hyphal front, at the hyphal front and further behind the hyphal front and (4) a novel way in which *Fusarium* hyphae degraded sclerenchyma cell walls during the late phases of infection. Overall this study supports a non-necrotrophic mode of colonisation occurring at the advancing hyphal front. The text and figures that forms the basis of this chapter were published in Fungal Biology (2010), DOI: 10.1016/j.funbio.2010.04.006.

3.2. Experimental Procedures

3.2.1. Preparation of individual tissues of the wheat ear for light microscopy

The selected inoculated wheat ears were photographed at 2, 5, and 12 dpi before sampling. The rachilla of the inoculated spikelet and palea of the inoculated florets were excised. The rachis node of the inoculated spikelet along with the successive rachis internodes and nodes, above and below, were individually dissected. Tissue samples were individually fixed, dehydrated, embedded and polymerised as described previously. Transverse semi-thin 1 μm sections stained with aqueous 0.1 % TBO in 1 % sodium tetraborate pH 9, mounted in DPX (Sigma), were imaged using a Zeiss Axiophot light microscope. The images presented are representative of the three biological replicates from the PH-1 infected and the mock control.

3.2.2. Calculation of hyphal colonisation patterns

Images of the PH-1 infected rachis were analysed using the colour thresholding software provided by MetaMorph version 7.5.5 (Molecular Devices). Different cell-types were selected in order to generate data on the cellular colonisation patterns.

3.2.3. Scanning electron microscopy (SEM)

The entire inoculated spikelet and rachis node or the first rachis internode below the inoculated spikelet were excised, mounted, frozen and transferred into the Gatan Alto 2100 cryo chamber. Rachis internodes were freeze fractured and all samples partially freeze dried prior to gold coating. The samples were imaged on the cold stage of Jeol LV6360 scanning electron microscope maintained at -150^{o}C for examination.

3.3. Results

To aid interpretation of the results described below, a schematic illustration of the anatomy of a hexaploid wheat ear (*Triticum aestivum*) is given in Figure 12. Typically the wheat ear consists of two rows of spikelets which are successively positioned on alternate sides of the rachis. Each spikelet is supported by a rachilla arising from a rachis node. Individual spikelets are protected by a pair of glumes which encase a minimum of four florets. Florets consist of two floral brackets, the lemma and palea, and within the floral cavity a single grain develops. For the modern hexaploid wheat cultivar used in this study, Bobwhite, each floret has a long awn attached to the lemma while short rachis internode segments connect neighbouring spikelets. A typical ear is 10 cm long and contains 13-17 spikelets. Anthesis commences from the middle of the ear and was the point of inoculation.

Macroscopic disease symptoms were carefully monitored following the inoculation of two florets within the two middle spikelets of each ear with either a spore droplet or a water-only droplet. Key time points were selected and dissected to determine the extent of the visible symptoms. The symptoms identified at 2, 5 and 12 dpi, and for which in depth microscopy images are presented below, are given in Figure 13. After two days the inoculated florets remained mainly green and were indistinguishable from the water-only inoculated spikelets. However, in the *Fusarium*-inoculated spikelets some aerial mycelium associated with extruding anthers was visible. By 5 dpi, the *Fusarium*-inoculated spikelets, and florets within, were fully bleached while the water-only inoculated florets, rachis and rachis node connected remained green. Subsequently, the symptoms of infection were macroscopically visible within successive rachis internodes, rachis node and spikelets, as they bleached both above and below the point of *Fusarium* inoculation.

Within such ears, uninoculated spikelets bleached once the rachis node to which they were attached became discoloured. By 12 dpi the majority of the ear was bleached and the grain, which had not developed post *Fusarium* infection, remained in the floral cavity of the inoculated florets. The mock inoculated ears remained green and the grain developed throughout this time course reached approximately 7.5 mm in length by 12 dpi.

Schematic illustrations that describe each stage of the infection process at the cellular level have been included in the appendix. These illustrations will assist the interpretation of the results (Appendix 3, 5-7).

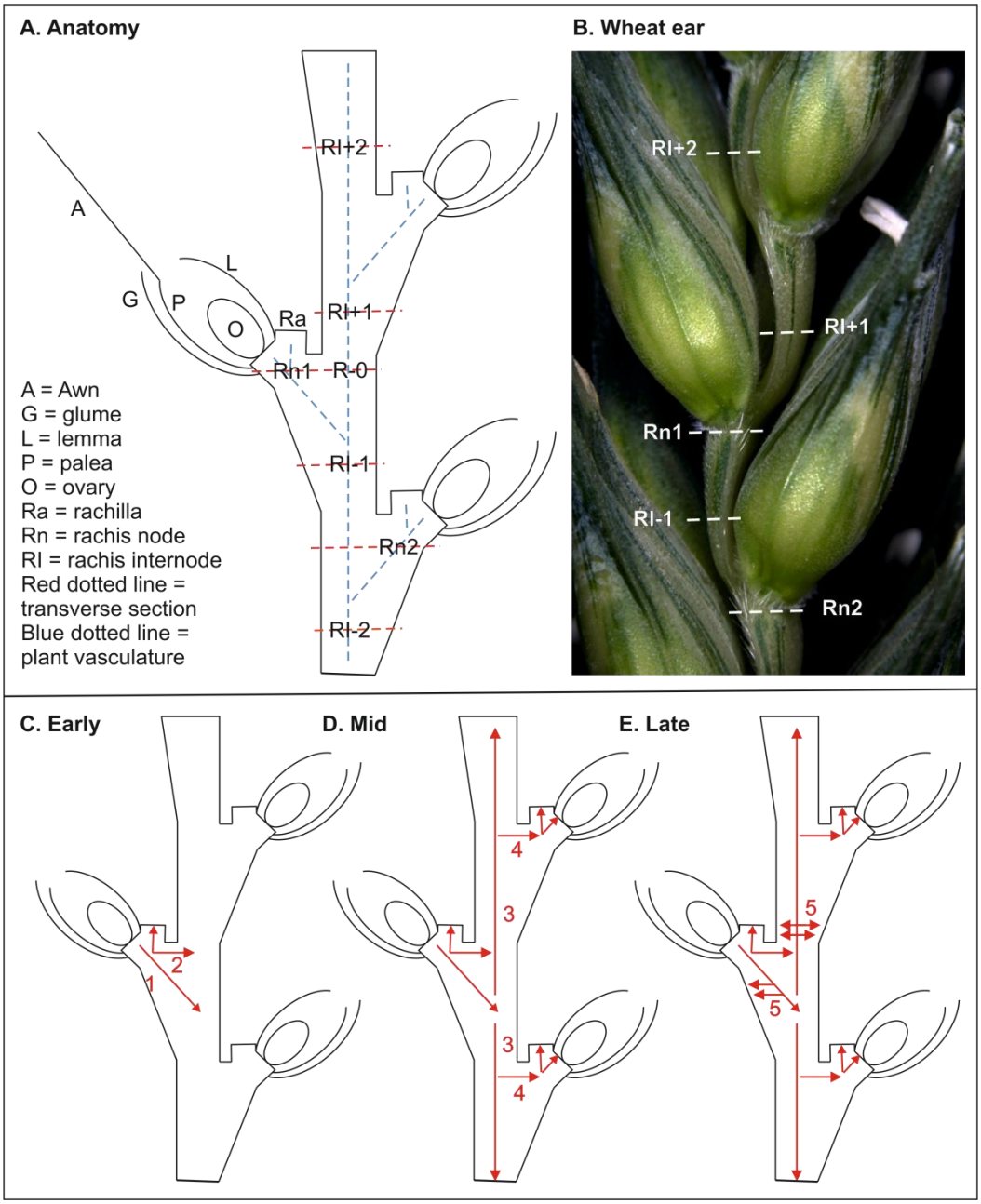

Figure 12 A schematic illustration of the anatomy of the wheat ear and the vascular connections between neighbouring spikelets, for simplicity only one floret per spikelet is shown **(A)**. Image of a wheat ear, cultivar Bobwhite, showing the positions of the transverse sections taken. Note that the awn is only depicted in this panel. **(B)**. A schematic illustration of the path of *F. graminearum* infection, from the inoculated spikelet to the neighbouring spikelets (above and below), at the early **(C)**, mid **(D)**, and late **(E)** time points. Legend: blue dotted lines = plant vasculature, red / white dotted lines = positions of transverse sections illustrated respectively in figures 14 – 20, red arrow = overall direction of fungal infection, red number = stage of fungal infection described in this study. **1**, vertical inter- and intracellular hyphal growth in the cortex and vasculature, down from the inoculated spikelet into the rachis. **2**, lateral intracellular hyphal growth through the sclerenchyma into the rachis. **3**, vertical hyphal growth up and down the rachis, intercellular colonisation of the cortex followed by intracellular colonisation of the cortex and vasculature. **4**, lateral intercellular hyphal growth below the sclerenchyma tissue into the uninoculated rachis node. **5**, increased lateral hyphal growth, accumulation under the surface, rupture of the epidermis and production of an aerial mycelium.

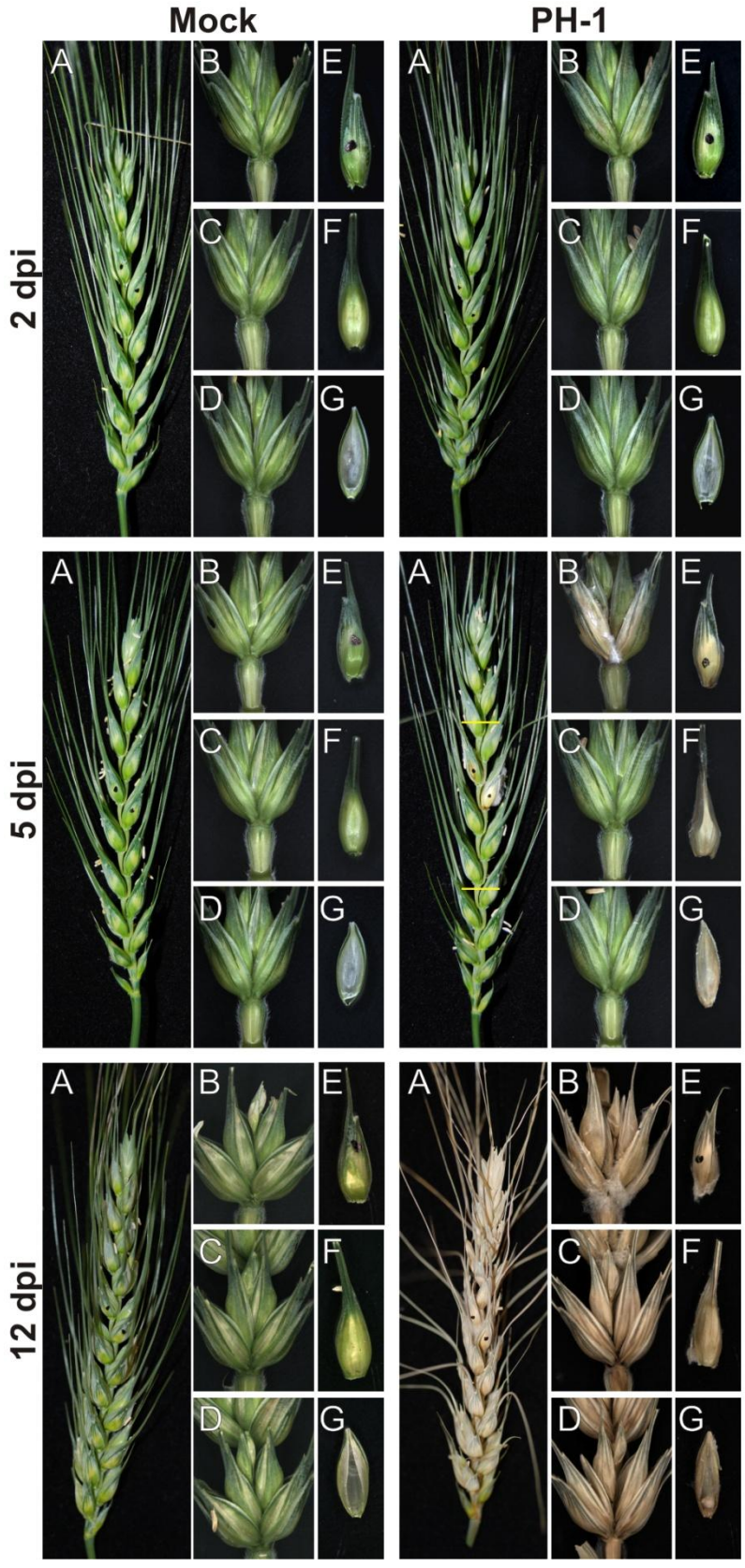
Mock
PH-1
2 dpi
5 dpi
12 dpi
A
B
C
D
E
F
G

Figure 13 The macroscopic symptoms of *F. graminearum* infection at 2, 5 and 12 dpi following the addition of conidia into two adjacent spikelets in the middle of the ear. The column of panels on the left are the water-only inoculated controls (Mock). The column of panels on the right depicts the progression of macroscopic symptoms of infection at 2 dpi (top row), 5 dpi (middle row) and 12 dpi (bottom row). Generic legend for each of the panels: **(A)** An entire ear with a black dot marking each of the two inoculated spikelets. The two yellow horizontal lines superimposed on the inoculated PH-1 ear at 5 dpi indicate the extent of symptomless *Fusarium* colonisation identified by the microscopy analyses. **(B)** The inoculated spikelet and adjoining rachis node and rachis segment (overall height 12 mm). **(C)** and **(D)** Successive spikelets below the inoculated spikelet. The individually excised tissues of the inoculated spikelet, glume **(E)**, lemma **(F)**, palea **(G)**. In the mock inoculated ears, the developing grains were approximately 3.5, 4.8 and 7.5 mm in length at 2, 5 and 12 dpi respectively (data not shown). In the PH-1 infected ear the grain remained in the floral cavity but had not developed post inoculation and appeared shrivelled at 12 dpi.

3.3.1. The establishment of infection in the inoculated spikelet

Many aspects of the infection process of a single spikelet have been described previously (Chapter 1) and therefore only the salient points will be briefly described here. The first microscopic sign of fungal colonisation in the palea at 2 dpi was limited to sub-cuticular and intercellular hyphal growth. Rapidly, by 5 dpi all cell-types of the palea were colonised and the non-lignified lower parenchyma had lost cell integrity. By 12 dpi the parenchyma layer had collapsed (Figure 14). This pattern of colonisation in the palea correlates well with that presented in a previous study of *F. graminearum* infection through the anatomically similar lemma (Wanjiru *et al*., 2002). At 2 dpi, within the inoculated ears, hyphae were absent from the adjacent rachilla and rachis node. By 5 dpi intercellular hyphae had colonised just the cortex of the rachilla and were already abundant. Intracellular lateral hyphal growth then penetrated the sclerenchyma, ruptured the epidermis and grew on the surface, while the previously colonised cortex and phloem collapsed by 12 dpi (Figure 14).

3.3.2. Initial hyphal colonisation of the rachis occurred via two different paths, vertical intercellular and lateral intracellular hyphal growth

The rachis node provides structural support and nutrition to the developing spikelet. The node differentiates from the rachis and eventually the two tissues are separated by a thick layer of sclerenchyma cells (Figure 15). Both the node and the rachis consist of a ring of vascular bundles embedded in cortical cells, surrounded by sclerenchyma cells and ultimately encased by the epidermis (Whingwiri *et al.*, 1981). For spikelet to spikelet spread, the pathogen has to colonise the node and subsequently the rachis. From the rachilla of the inoculated spikelet, intercellular hyphae entered the cortex of the node (Figure 14) and colonised the vasculature by 5 dpi. Vertically growing hyphae progressed down the node to the point where this tissue differentiated from the rachis, thereby granting the hyphae entry into the cortex and vasculature of the rachis. The pattern of colonisation in the node and rachis was similar with inter- and intracellular colonisation of the cortex and heavy colonisation of the vasculature. In the latter, hyphae accumulated in the collapsed non-lignified cells, namely the phloem and / or vascular parenchyma (Figure 15; Appendix 3). An alternate route of colonisation from the node to the rachis was also commonly observed. Intracellular hyphae grew laterally, constricting in diameter in order to pass through the pit fields of the sclerenchyma cells separating the rachis node and rachis. Successful hyphal growth via pit fields was observed to have occurred sequentially through the thick walled sclerenchyma cells. There was minimal evidence of enlargement of the pit field diameter once colonised. Upon entry into the rachis, hyphal growth reverted back to a mixture of intercellular and intracellular colonisation and became solely vertical again (Figure 15; Appendix 3).

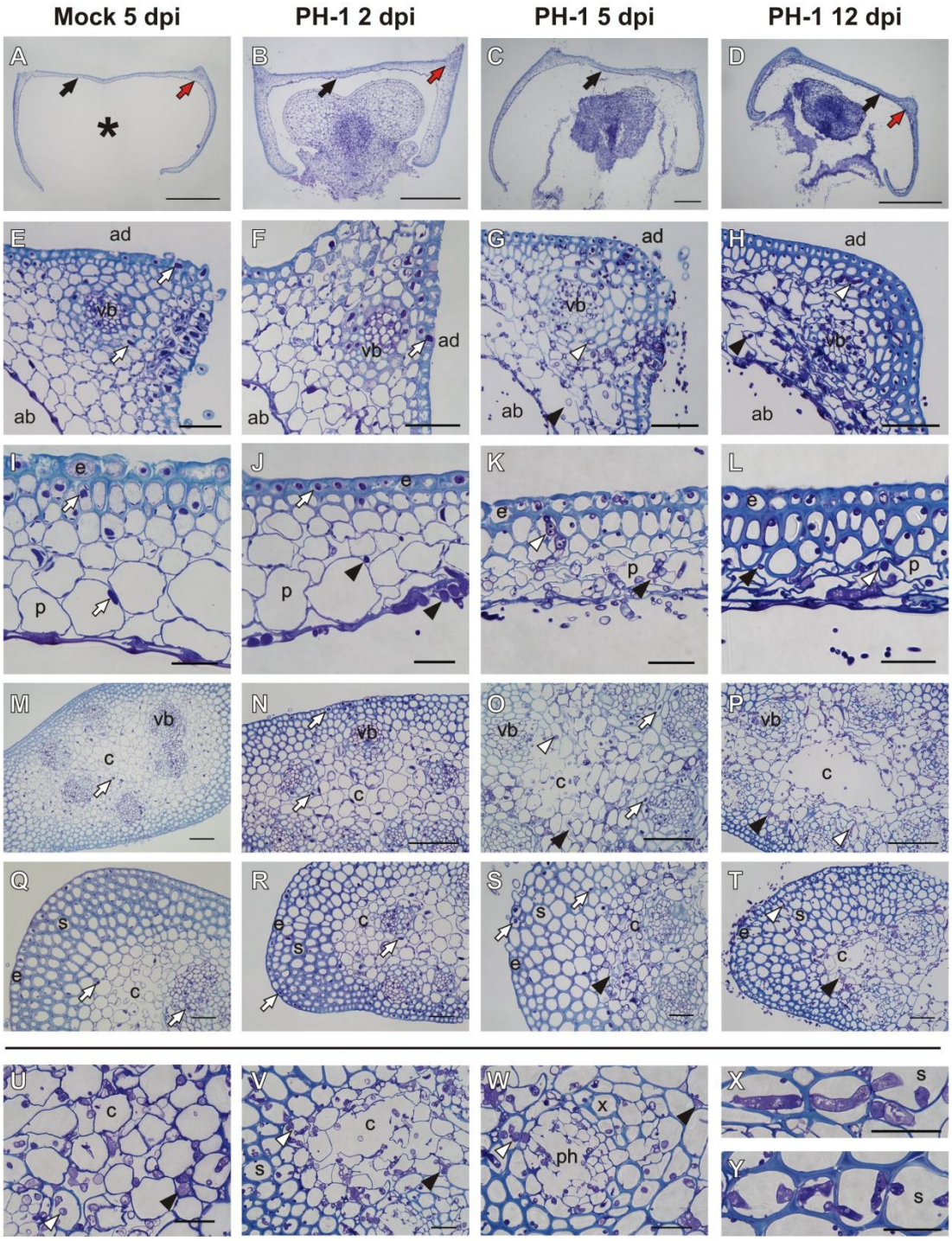
Mock 5 dpi
PH-1 2 dpi
PH-1 5 dpi
PH-1 12 dpi
A
B
C
D
E
ad
vb
ab
F
vb
ad
ab
G
ad
vb
ab
H
ad
vb
ab
I
e
p
J
e
p
K
e
p
L
e
p
M
vb
c
N
vb
c
O
vb
c
P
vb
c
Q
s
e
c
R
e
c
s
S
s
c
e
T
s
e
c
U
c
V
c
s
W
x
ph
X
s
Y
s

Figure 14 Colonisation of wheat spikelets by *F. graminearum* over a 12 day time-course. The extreme left column of panels (A, E, I, M and Q) describes the anatomy of the water-only inoculated controls (Mock) at day 5, whilst the three columns of panels to the right depict the successive phases of infection by the wild-type strain PH-1 at 2, 5 and 12 days post inoculation (dpi) with water droplets containing conidia. All images in this figure are transverse 1 µm LR white sections stained with 0.1 % toluidine blue O, buffered to pH 9. Generic legend: ab = abaxial surface, ad = adaxial surface, black arrowhead = intercellular fungal hyphae, white arrowhead = intracellular fungal hyphae, white arrow = host nuclei, c = cortex, e = epidermis, p = parenchyma, ph = phloem, s = sclerenchyma, vb = vascular bundle, x = xylem. **(A)** through **(D)** Low magnification images of the anatomy of the palea and developing grain. (A) Healthy, asterix (*) denotes developing grain is missing, (B) through (D) the progressive shrivelling of the developing grain. The full arrows indicate the vascular region (red) and central palea region (black) explored at a higher magnification, depicted in the other panels. Bar = 500 µm. **(E)** through **(H)** Anatomy of a vascular bundle residing at the corner of the palea, marked in the panel immediately above. (E) Healthy, (F) no hyphae detected within the vasculature, (G) inter- and intracellular hyphae present in all cell types and some colonised parenchyma cells have ruptured, (H) abundant inter- and intracellular hyphae present in all cell types, some of the colonised parenchyma on the abaxial side have collapsed. Numerous extracellular hyphae were present on both palea surfaces at 5 and 12 dpi. Bar = 50 µm. **(I)** through **(L)** Anatomy of the central palea region, marked in the corresponding panels A, B, C and D. (I) Healthy, (J) intercellular hyphae present just below the abaxial cuticle and in the lower parenchyma layer, (K) inter and intracellular hyphae present in all cell types, some host cells ruptured particularly in the lower parenchyma, (L) inter- and intracellular hyphae present in all cell types and the parenchyma layer has fully collapsed. Numerous extracellular hyphae were on the palea surface at 5 and 12 dpi. Bar = 25 µm. **(M)** through **(T)** Anatomy of the spikelet rachilla at two different magnifications. (M) and (Q) Healthy, (N) and (R) no hyphae present, (O) and (S) intercellular mycelium present in the cortex and the host cells in this region have ruptured, (P) and (T) inter- and intracellular hyphae present in all cell type and large numbers of host cortical cells

have been destroyed. Specifically in (T) the number of laterally growing hyphae has substantially increased in the sclerenchyma layer, also in places the epidermis has been ruptured and numerous hyphae were present on the surface. Bar = 50 µm. **(U)** through **(Y)** Higher magnification images of infected rachilla at 12 dpi. (U) Abundant inter- and intracellular hyphae in cortex and epidermis but host cell destruction is only observed in the cortex, (V) Many hyphae in the cortex have an enlarged diameter, (W) hyphal colonisation of the phloem has resulted in the destruction of many host cells, whereas the colonised xylem vessel were still intact, (X) and (Y) lateral intracellular hyphal growth through sclerenchyma cells and hyphal constriction at the points where thick host cell walls have been successively traversed. Bar = 25 µm.

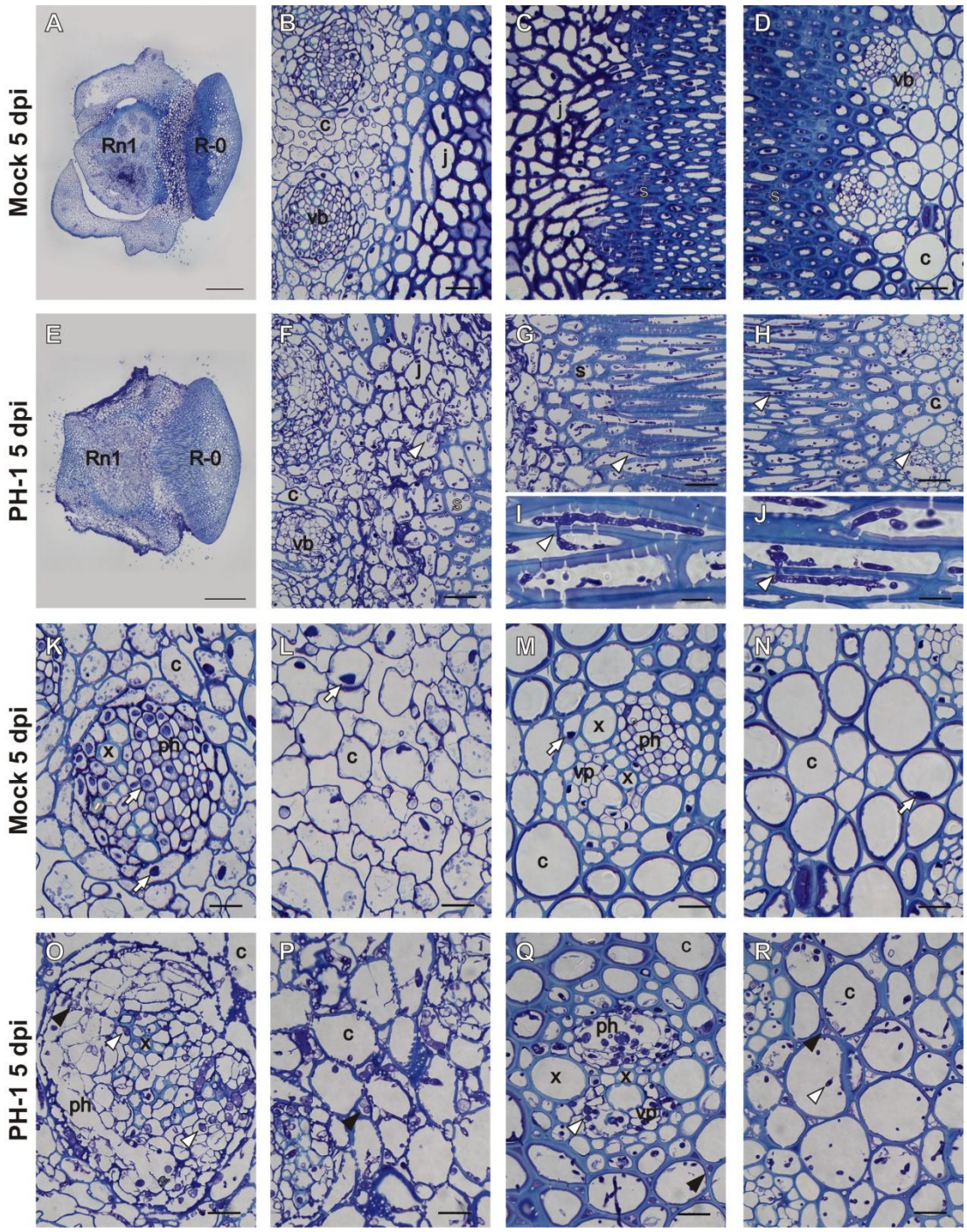
Mock 5 dpi
PH-1 5 dpi
Mock 5 dpi
PH-1 5 dpi
A
B
C
D
E
F
G
H
I
J
K
L
M
N
O
P
Q
R
Rn1
R-0
c
j
vb
s
x
ph
vp

Figure 15 Growth of *F. graminearum* from the inoculated wheat spikelet into the rachis by 5 dpi. The first and third row of panels describes the anatomy of the water-only inoculated control (Mock), whilst the second and fourth row of panels depicts the spread of wild-type PH-1 infection. **(A)** The healthy rachis node and connected rachis. Bar = 500 µm. **(B)** through **(D)** Illustrate how the healthy plant cell structure alters between the rachis node, junction and the rachis. Bar = 50 µm. **(E)** through **(J)** Colonisation from the rachis node to the rachis by lateral hyphal growth. (E) Bar = 500 µm. (F) through (H) Bar = 50 µm. (I) and (J) Bar = 15 µm. **(K)** Vascular bundle and **(L)** the cortex in the healthy rachis node, **(M)** vascular bundle and **(N)** the cortex in the healthy rachis. Bar = 25 µm. **(O)** through **(R)** Vertical hyphal growth in the vascular bundles and cortex of the rachis node and rachis. Bar = 25 µm. All images in this figure are transverse 1 µm LR white sections taken through both the rachis node and rachis, stained with 0.1 % TBO, pH 9. Legend: Rn1 = rachis node attached to the inoculated spikelet, R-0 = rachis parallel to the rachis node of the inoculated spikelet, c = cortex, j = junction between the rachis node and rachis, s = sclerenchyma, ph = phloem, vb = vascular bundle, vp = vascular parenchyma, x = xylem, black arrowhead = intercellular fungal hyphae, white arrowhead = intracellular fungal hyphae, white arrow = host nuclei.

Table 4 Comparison of the average hyphal number and maximum size of a single hypha within different cell-types of the rachis vasculature

Host cell-type[a]	Hyphal number	Hyphal area (pixels)
Xylem	7 (2)[b]	58 (36)
Phloem	30 (3)	138 (70)
Vascular parenchyma	19 (6)	178 (81)

[a] Numerical data was obtained via thresholding images of the first rachis internode below the inoculated spikelet at 5 dpi.

[b] Means of hyphal number and the maximum size of a single hypha are presented with standard deviation in brackets.

3.3.3. Systemic colonisation of the rachis occurred via intercellular hyphal growth in the cortex and intracellular hyphal growth in the vasculature

Hyphae predominantly grew along the vertical axis within the rachis at 5dpi. Immediately below the inoculated spikelet, inter- and intracellular hyphae were abundant. All cell-types of the vasculature were heavily colonised, hyphae with a large diameter remained in the collapsed phloem and vascular parenchyma, while hyphae with a significantly smaller diameter resided within the xylem vessels (Table 4). Simultaneously, inter- and intracellular hyphae colonised the cortex and no host nuclei were present in any cell-type possessing intracellular hyphae (Figure 16). Within the second rachis internode below the inoculated spikelet, colonisation of the cortex was solely intercellular. Nuclei were present in these cortical cells but appeared round and enlarged (Figure 16; Appendix 4 and 5). No hyphae were present in the third rachis internode below the inoculated spikelet and host cells appeared normal (Figure 16; Appendix 5). Sequential sections between rachis internodes were viewed in order to determine the sequence of events. Intercellular colonisation of the cortex represented the advancing hyphal front, followed by colonisation of the vasculature, and then intracellular colonisation of the cortex.

Infection of the rachis above the inoculated spikelet followed the same pattern, with intercellular colonisation of the cortical cells always occurring in advance of intracellular colonisation. However, colonisation of the vasculature was slower than progress down the ear. This difference between the lower and upper ear regions was primarily caused by the lack of a direct connection between the vascular bundle of the inoculated spikelet and the rachis above the point of inoculation (Figure 16).

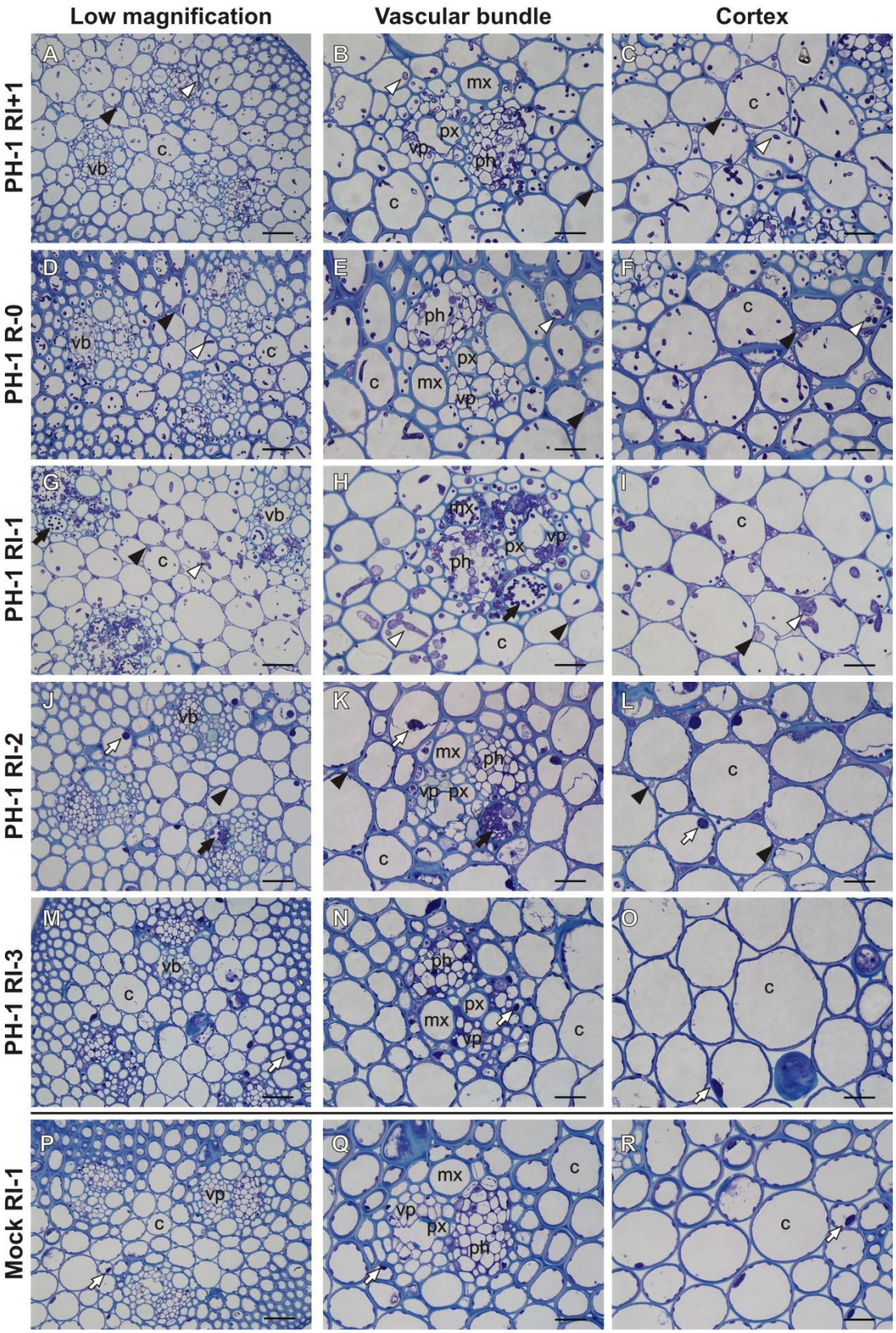
Low magnification
Vascular bundle
Cortex
PH-1 RI+1
PH-1 R-0
PH-1 RI-1
PH-1 RI-2
PH-1 RI-3
Mock RI-1
A
B
C
D
E
F
G
H
I
J
K
L
M
N
O
P
Q
R
vb
c
mx
px
vp
ph

Figure 16 Systemic colonisation of the wheat rachis by *F. graminearum* at 5 dpi. The column of panels on the left (low magnification) illustrates the location examined in sequential rachis internodes (RI+1 to RI-3). The columns of panels in the middle (vascular bundles) and on the right (cortex) depict the extent of hyphal infection in each rachis internode. The bottom row of panels (Mock RI-1) represents the anatomy of a healthy rachis internode from a representative water-only inoculated control. **A**, **D**, **G**, **J**, **M** and **P**, bar = 50 µm. **B**, **E**, **H**, **K**, **N**, **Q** and **C**, **F**, **I**, **L**, **O**, **R**, bar = 25 µm. All images in this figure are transverse 1 µm LR white sections stained with 0.1 % TBO, pH 9. Legend: c = cortex, mx = metaxylem, px = protoxylem, ph= phloem, vb = vascular bundle, vp = vascular parenchyma, black arrowhead = intercellular fungal hyphae, white arrowhead = intracellular fungal hyphae, white arrow = host nuclei, black arrow = colonisation of the metaxylem.

3.3.4. Secondary colonisation of uninoculated spikelets occurred via intercellular lateral growth beyond the sclerenchyma separating the rachis and the rachis node

By day 5, infection had progressed down the ear into the rachis, the adjacent spikelet, and extended into the node supporting the third uninoculated spikelet below the point of inoculation. When approached from above, the node and rachis are separated by a thick inner layer of sclerenchyma cells that lack intercellular spaces. Sixty microns lower down, in the central region of the node, the thick walled sclerenchyma cells are replaced by thin-walled cells with intercellular spaces (Figure 17). No lateral intracellular hyphae were present in the sclerenchyma. However, beyond the sclerenchyma, numerous intercellular hyphae passed from the cortex of the rachis into the connecting region between the thin walled host cells. These intercellular hyphae subsequently colonised the cortex of the node and progressed into the uninoculated spikelet (Figure 17; Appendix 6). Interestingly, hyphal infection was entirely absent from the vasculature of the node at this time point. Macroscopically, the rachis and rachis node were green at this time point and appeared identical to those present in the mock-inoculated ears (Figure 13).

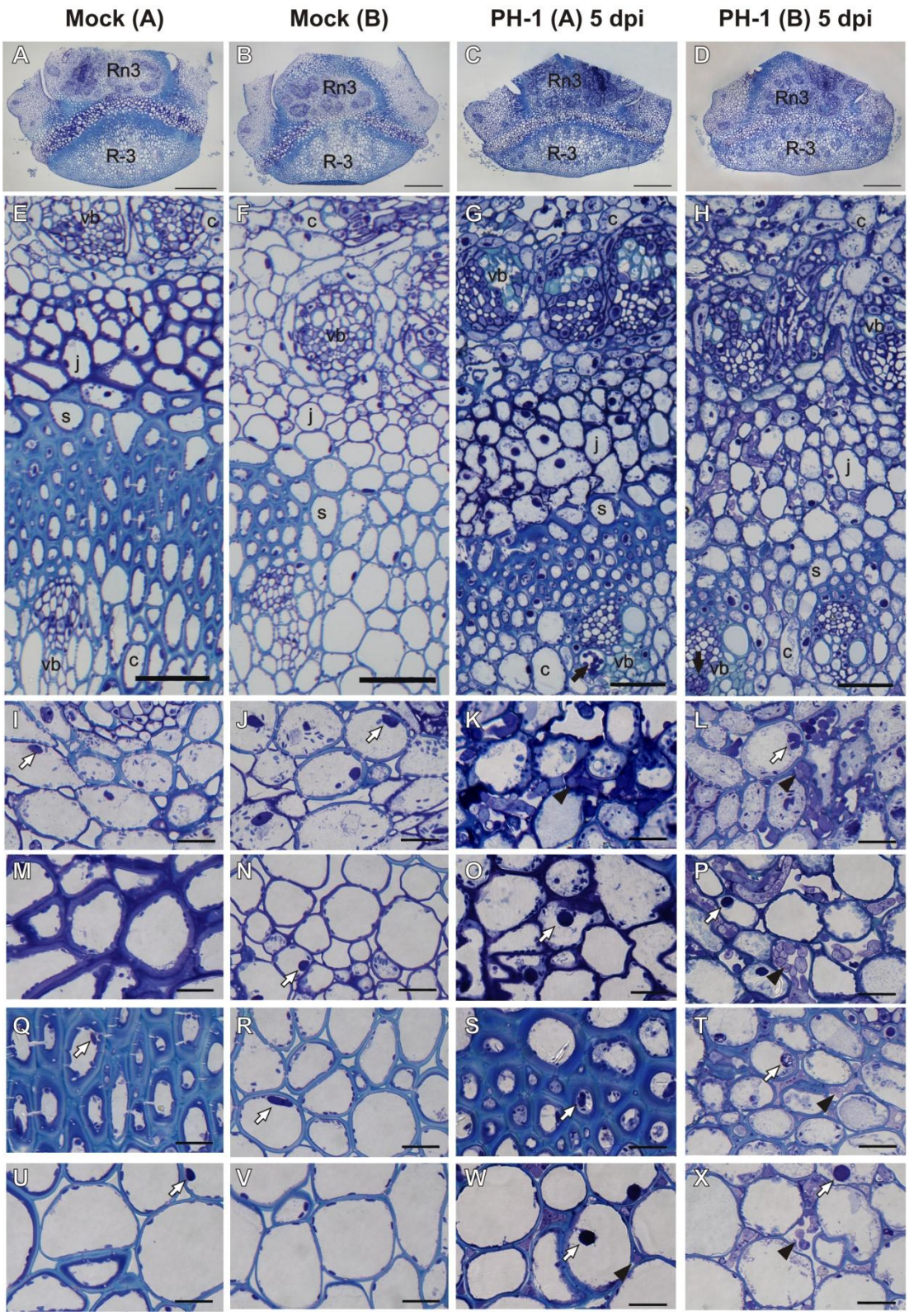
Mock (A)
Mock (B)
PH-1 (A) 5 dpi
PH-1 (B) 5 dpi
A
Rn3
R-3
B
Rn3
R-3
C
Rn3
R-3
D
Rn3
R-3
E
vb
c
j
s
vb
c
F
c
vb
j
s
G
c
vb
j
s
c
vb
H
c
vb
j
s
vb
c
I
J
K
L
M
N
O
P
Q
R
S
T
U
V
W
X

Figure 17 Colonisation of the third rachis node below the original point of inoculation by *F. graminearum* at 5 dpi. The first two columns from the left describe the anatomy of the healthy rachis node at two different positions. Mock A illustrates the anatomy at the top of the rachis node, whilst Mock B illustrates the anatomy 60 µm below. The two columns on the right describe the spread of infection from the rachis to the rachis node and into the adjacent spikelet. PH-1 A illustrates fungal colonisation at the top of the rachis node, whilst PH-1 B illustrates fungal colonisation 60 µm below. **(A)** through **(D)** The entire section through the rachis and rachis node demonstrating how the two tissues were connected. Bar = 500 µm. **(E)** through **(H)** The region connecting the rachis and rachis node. Bar = 100 µm. Note, at the top of the node the two tissues are separated by a layer of thick walled sclerenchyma which is not present lower down the node. **(I)** through **(L)** The cortex of the rachis node. **(M)** through **(P)** The region connecting the rachis and rachis node. **(Q)** through **(T)** The layer of sclerenchyma separating the rachis and rachis node. **(U)** through **(X)** The cortex of the rachis. Bar = 25 µm. All images in this figure are transverse 1 µm LR white sections stained with 0.1 % TBO, pH 9. Legend: Rn3 = third rachis node below the inoculated spikelet, R-3 = rachis parallel to the third rachis node, c = cortex, j = junction, s = sclerenchyma, vb = vascular bundle, black arrowhead = intercellular fungal hyphae, white arrow = host nuclei.

3.3.5. The advancing front of infection appeared macroscopically symptomless, while at the cellular level the consequences of the internal infection were clearly visible

A very rapid phase of colonisation occurred between 2 and 5 dpi. Besides hyphae entering the adjacent spikelets, the advancing fronts of hyphal infection were already located in the third rachis node, approximately 25 mm below the inoculated spikelet by 5 dpi. Two thirds of the colonised tissue, including the rachis and spikelets, macroscopically appeared symptomless. The characteristic symptoms of the disease, such as bleaching and necrosis of the chlorenchyma bands, were confined to the inoculated spikelet and node, while the second and third rachis node appeared normal (Figure 18). Hyphae were absent from the chlorenchyma cells of the second and third rachis node. However, samples cleared prior to embedding showed internal browning of the cortex and vasculature of the second and third rachis nodes (data not shown). Microscopy analysis revealed that host cell content had changed dramatically and the cells of the infected rachis node stained a darker purple with toluidine blue O (TBO) compared to the mock (Figure 18). In the third rachis node, the advancing front of infection in the vasculature was confined to the metaxylem of the single vascular bundle, which the serial sectioning had revealed to be connected to one of the initially inoculated spikelets. This infected metaxylem was occluded by a dense deposition and no hyphae were present beyond this point. Numerous hyphae filled the intercellular spaces of the neighbouring cortex, but no intracellular hyphae were present. The internal contents of the cortical cells of the third rachis node appeared to be condensed and a dense intercellular deposition was also found throughout this colonised tissue (Figure 18). In the region where the third rachis node underwent transition into an internode there was no intercellular depositions visible and intercellular hyphae were low in number. At 5 dpi colonisation of the cortex was approximately 400 µm ahead of vascular colonisation.

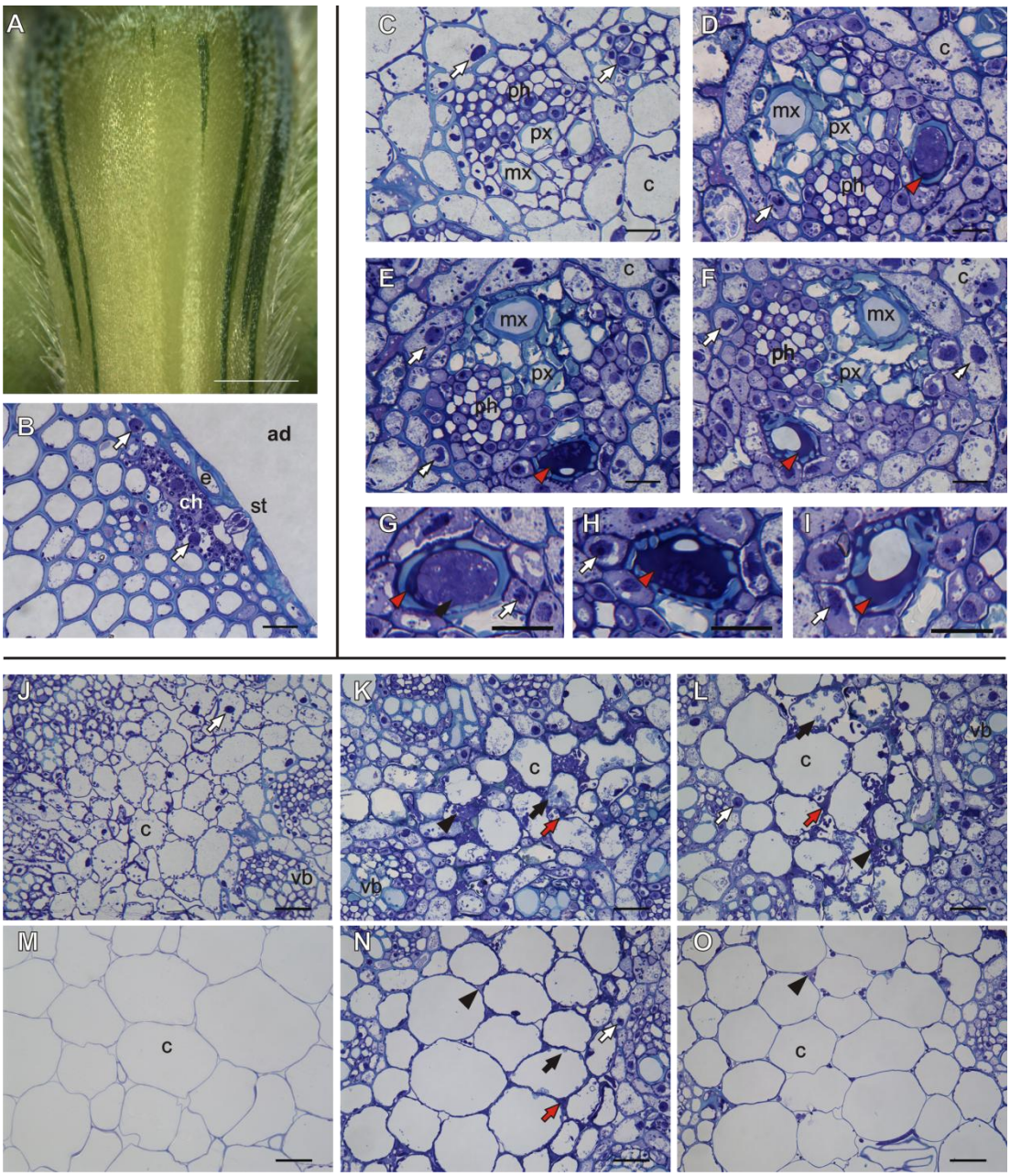
A
B
ad
e
ch
st
C
ph
px
mx
c
D
c
mx
px
ph
E
c
mx
px
ph
F
c
mx
ph
px
G
H
I
J
c
vb
K
c
vb
L
vb
c
M
c
N
O
c

Figure 18 The advancing front of *F. graminearum* infection, progressing down the wheat ear in the third rachis node below the inoculated spikelet at 5 dpi, demonstrating the subtle spread of infection beyond the macroscopically visible symptoms. Panels **(A)** PH-1 infected third rachis node, bar = 2 mm, and **(B)** the non colonised chlorenchyma band of the infected node, bar = 25 µm, demonstrate the lack of macroscopic symptoms. **(C)** through **(I)** depict the advancing front of hyphal infection in the plant vasculature approximately 400 µm into the rachis node. (C) Healthy, (D) and (G) PH-1 infected metaxylem full of hyphae, (E) and (H) a further 15 µm below, the metaxylem was completely occluded, (F) and (I) a further 5 µm below, hyphae were absent from the metaxylem. Bar = 25 µm. **(J)** through **(O)** illustrate the advancing front of hyphal infection in the cortex, 380 µm below the last hyphae identified in the vasculature. (J) Healthy, anatomically similar to panels L and M, (K) 400 µm and (L) 480 µm into the PH-1 infected rachis node, (M) healthy cortex in the region where the rachis node undergoes transition into an internode, anatomically similar to panels O and P, (N) 550 µm and (O) 780 µm into the PH-1 infected rachis node. Bar = 50 µm. All images in this figure (except A) are transverse 1 µm LR white sections stained with 0.1 % TBO, pH 9. Legend: ad = adaxial surface, c = cortex, ch = chlorenchyma, e = epidermis, st = stomata, mx = metaxylem, px = protoxylem, ph = phloem, vb = vascular bundle, black arrowhead = intercellular fungal hyphae, red arrowhead = occlusion of the metaxylem, white arrow = host nuclei, black arrow = alteration of host cell contents, red arrow = dense intercellular deposition.

3.3.6. General patterns observed in fungal growth over the course of infection in the rachis

Irrespective of the location in the rachis internode or rachis node several general patterns of *F. graminearum* hyphal growth and colonisation were observed. The first appearance of infection in any cell-type commenced with thin, densely stained hyphae. After substantial colonisation and the collapse of non-lignified cells, hyphae were larger in diameter and stained less intensely. Hyphae located far behind the advancing front of infection lost their contents, staining only at the cell wall and some had also collapsed (Figure 19).

In the vasculature, the phloem was predominantly the first cell-type to be colonised, followed by the vascular parenchyma and finally the xylem. Colonisation of non-lignified cell-types, such as the phloem and vascular parenchyma, resulted in their collapse. SEM analysis of the colonisation of the rachis revealed that initially the infected phloem contained a fluid content, however as colonisation progressed and the phloem elements collapsed, this content was lost. Hyphae within the xylem were shown to be covered by extracellular mucilage. At later stages of infection only a few hyphae remained far behind the hyphal front in the vasculature (Figure 19). In the cortex, hyphae initially colonised the intercellular spaces and these host cells which were surrounded by hyphae contained organelles and enlarged, rounded nuclei. Hyphae often became triangular in appearance as they adopted the form of the available intercellular space. Intracellular hyphae only became prevalent as disease progressed and were restricted to well behind the advancing hyphal front. Once a wheat cell was intracellularly colonised host organelles and nuclei were lost. This was confirmed by the SEM analysis of the rachis cortex, revealing the penetrative hyphae entering a dead host cell devoid of any content (Figure 19).

Behind the advancing front of infection in the rachis, hyphae colonised the periphery, which included small vascular bundles, sclerenchyma, chlorenchyma and epidermal cells. As previously described, initial colonisation occurred in the central cortex and vasculature. However, prior to hyphal colonisation of the rachis periphery the chlorenchyma cells died. Upon colonisation of this region the chlorenchyma and sub-stomatal cavities were colonised. The chlorenchyma cells were the only cell-type that died ahead of infection without hyphal contact.

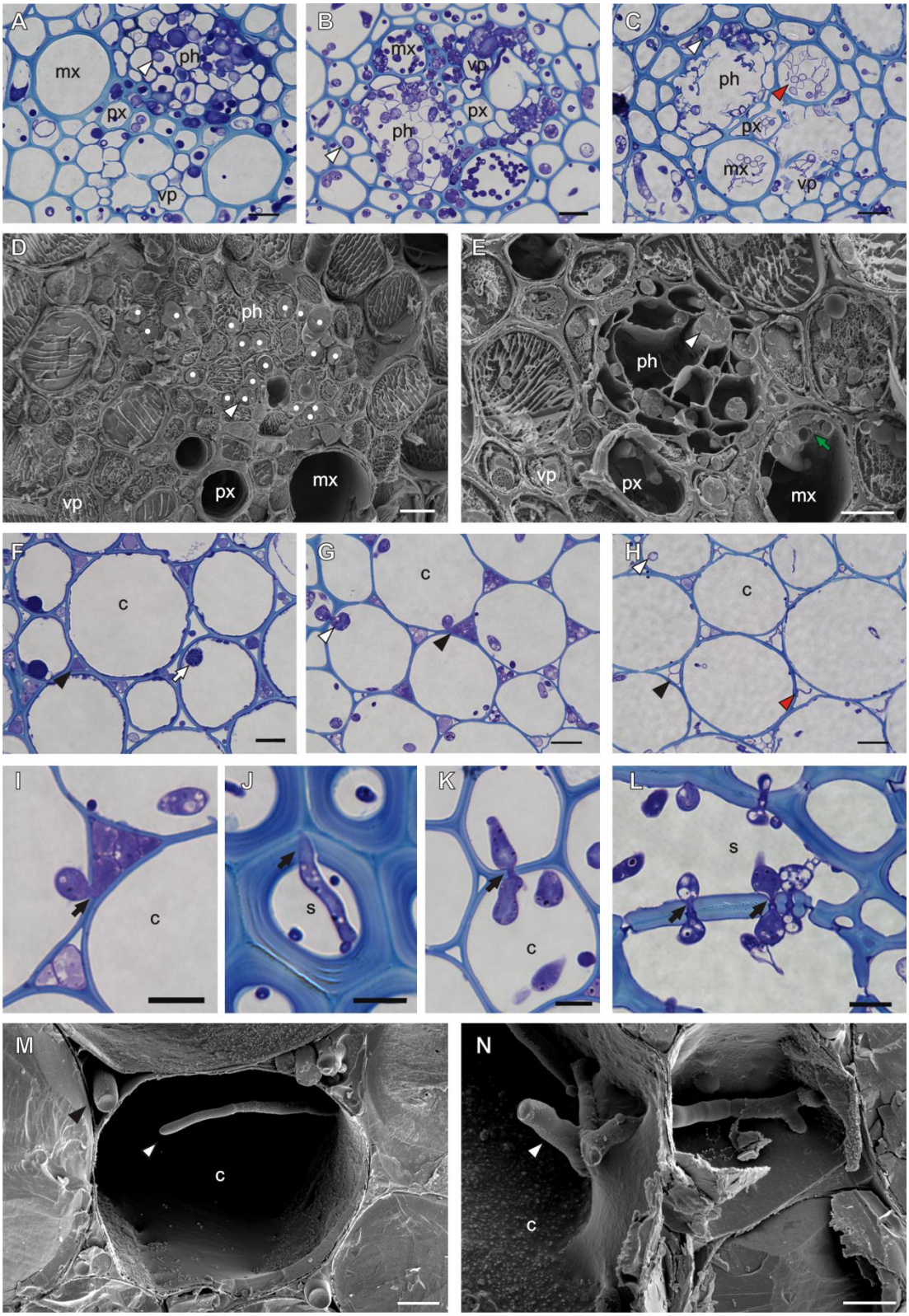
A
mx
ph
px
vp
B
mx
vp
px
ph
C
ph
px
mx
vp
D
ph
vp
px
mx
E
ph
vp
px
mx
F
c
G
c
H
c
I
c
J
s
K
c
L
s
M
c
N
c

Figure 19 The general pattern of fungal growth in the centre of the rachis internodes over the course of *F. graminearum* infection. **(A)** through **(E)** illustrate the sequential, (A) and (D) early, (B) and (E) mid and (C) late, development of infection in the vascular bundles. (A) through (C) Bar = 25 µm. (D) and (E) Bar = 10 µm. **(F)** through **(H)** demonstrate the sequential, (F) early, (G) mid and (H) late, development of infection in the cortex. Bar = 25 µm. **(I)** through **(N)** describe how fungal hyphae traverse host cell walls. The penetration of a dead host cells (I) and (M), the penetration of a thickened cell walls (J), the constriction of intracellular hyphae to pass between host cells via pit fields (K) and (L), the passage between host cells without utilising a pit (N). Bar = 10 µm. All images in this figure (excluding panels D, E, M and N) are transverse 1 µm LR white sections stained with 0.1 % TBO, pH 9. Panels D, E, M and N are scanning electron micrographs. Legend: c = cortex, s = sclerenchyma, mx = metaxylem, px = protoxylem, ph = phloem, vp = vascular parenchyma, black arrowhead = intercellular fungal hyphae, white arrowhead = intracellular fungal hyphae, red arrowhead = empty or collapsed hyphae, white arrow = host nuclei, black arrow = fungal hyphae traversing host cell walls, white dots = intracellular hyphae in the phloem (Panel D only), green arrow = extracellular mucilage.

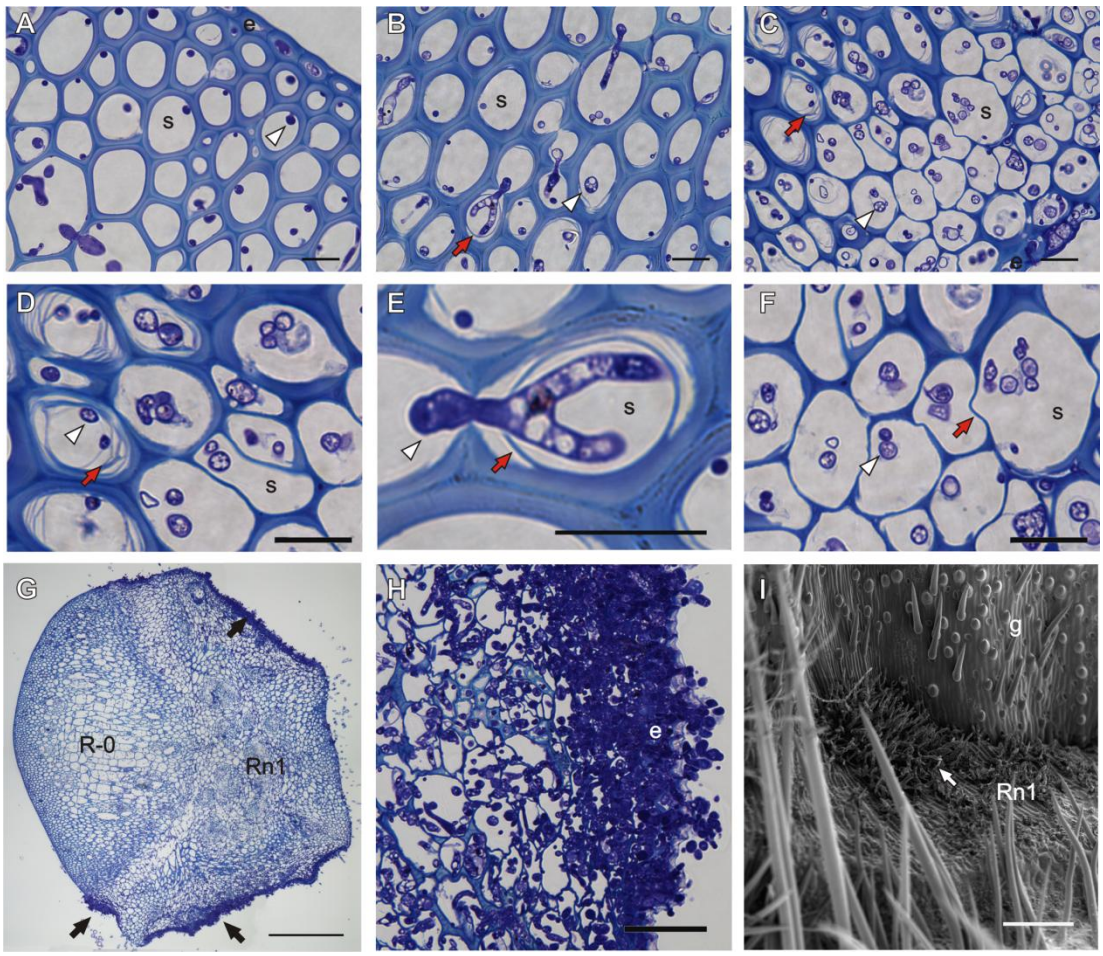

Figure 20 The general pattern of fungal growth in the outer host cell layers of the rachis internodes and nodes over the course of *F. graminearum* infection. **(A)** through **(C)** depict the sequential, (A) early, (B) mid and (C) late, development of infection in the sclerenchyma and epidermis. Bar = 25 µm. **(D)** through **(F)** illustrate fungal degradation of the host cell wall. Bar = 25 µm. **(G)** through **(I)** describe the accumulation of hyphae in the rachis node and the rupturing of the epidermis. (G) Bar = 500 µm. (H) Bar = 50 µm. (I) Bar = 100 µm. Images A through H in this figure are transverse 1 µm LR white sections stained with 0.1 % TBO, pH 9. Image I is a scanning electron micrograph. Legend: Rn1 = rachis node of the inoculated spikelet, R-0 = rachis parallel to the node of the inoculated spikelet, e = epidermis, s = sclerenchyma, g = glume, white arrowhead = intracellular fungal hyphae, red arrow = thinning of the host cell wall, black arrow = accumulation of hyphae, white arrow = aerial mycelium.

In the sclerenchyma and epidermis, hyphal growth followed a different colonisation pattern to the cortex and vasculature. Initially only a few hyphae of small diameter were present and all were intracellular because no natural intercellular spaces existed between these two cell-types. At later stages of infection, there was an increase in lateral hyphal growth, hyphae accumulated near the surface and their density in each host cell increased. Simultaneously, individual layers of the heavily lignified sclerenchyma cell walls were observed to have 'peeled off' from within the cell lumen, resulting in the dramatically thinner cell walls and an accompanied increase in hyphal diameter. Host cell wall digestion was not associated with hyphal contact and no cell wall debris remained in the cell lumen of the thin walled cells (Figure 20; Appendix 7). Epidermal cells were forcibly ruptured from within and hyphae subsequently grew on the surface.

The increased lateral hyphal growth at the later stages of the ear infection resulted in the accumulation of thick hyphae near the surface and the loss of host cell integrity. This was most prominent in the region of non-lignified cells in the rachis node at the base of the glumes. When maintained at ambient humidity, this hyphal mass below the surface ruptured the epidermis and gave rise to an aerial mycelium on the rachis node by 12 dpi (Figure 20; Appendix 7).

Two different mechanisms were employed by hyphae to traverse host cell walls. Intercellular hyphae possessed the ability to penetrate host cells, while intracellular hyphae were able to produce penetration pegs that could traverse the thickest of host cell walls. Frequently, intracellular hyphae also became dramatically reduced in diameter and passed between host cells via pit fields and afterwards the original hyphal diameter was restored (Figure 19).

3.4. Discussion

A spring wheat cultivar possessing the *RHT1* semi-dwarfing gene that along with a second semi-dwarfing gene *RHT2* drove the Green Revolution in global wheat production over the last 50 years was used (Peng *et al.*, 1999). Recently, the chromosome segment harbouring this dwarfing gene, *RHT1*, has been associated with increased susceptibility to FEB disease (Srinivasachary *et al.*, 2008). In light of these new findings, a comprehensive histological study of the infection process in a modern wheat cultivar possessing a semi-dwarfing gene was required. This

investigation explored the infection processes deployed by *F. graminearum* to colonise susceptible wheat ears and has linked the macroscopic appearance of disease symptoms with the underlying cellular colonisation pathways. This is the first comprehensive study to track infection by the sequenced wild-type PH-1 strain from the point of inoculation throughout the ear. It establishes the events occurring at the advancing hyphal front in all host tissues, defines the spikelet to spikelet spread of infection and adds to the debate concerning the mode of fungal nutrition.

Post floral invasion intercellular hyphae spread throughout the spikelet, down into the rachis node and subsequently up and down the ear in the rachis. This entire infection route is summarised schematically in Figure 12 C-E. The advancing front of infection in the rachis was found to be solely in the apoplast of the cortex and not the vasculature as previously described (Miller *et al.*, 2004, Ribichich *et al.*, 2000, Tu, 1950). At the infection front, the parenchyma cells of the cortex surrounded by intercellular hyphae had not plasmolysed and still contained organelles. Also, the hyphae adopted the form of the intercellular spaces, often at the junctions of neighbouring cortical cells, taking on a triangular shape rather than disrupting the surrounding host cells. This mode of colonisation is reminiscent of that of the closely related endophyte *E. festucae* (Christensen *et al.*, 2008). Closely behind the advancing front of infection the nuclei of the host cortical cells became enlarged and round. Subsequently, the cytoplasm appeared granulated and the host cell plasmolysed. Whether this host cell death was programmed or was the result of necrosis remains unclear. In other studies, the infiltration of the apoplast of wheat stems with varying concentrations (1-100 mg/L) of DON mycotoxin elicited hydrogen peroxide production, PCD and the activation of various defence responses (Desmond *et al.*, 2008). DON may initiate PCD of the wheat host cells once a certain concentration or length of exposure has been reached. The earlier study by Savard *et al.* (2000) identified a greater accumulation of DON in rachis tissue than the actual spikelets, indicating that within the ear the host cells residing in the different tissue types are experiencing different DON concentrations. In the present study, intracellular hyphae were never seen within host cells that possessed organelles. After host cell death, numerous intracellular hyphae grew within the cell lumen. Non-lignified cell-types without secondary cell walls, such as the parenchyma of the

palea and rachilla, as well as the phloem and vascular parenchyma of the rachis, rapidly collapsed after intracellular colonisation. The *F. graminearum* hyphae may have rapidly degraded these host primary cell walls through the localised secretion of PCWDE and this could have lead to the initiation of host cell death behind the hyphal front. The chlorenchyma cells present in narrow bands just below the surface were the only cell-type to exhibit cell death, without any hyphal contact, in advance of infection. Whether this is due to increased sensitivity to the mycotoxin or related to their higher photosynthetic activity is not known.

The mode of *F. graminearum* nutrition described in this study, in part, resembles all three classical definitions, namely, biotroph, hemibiotroph or necrotroph (Agrios, 1997). Macroscopically, wheat ear *F. graminearum* infections have a considerable symptomless phase. At the cellular level, the intercellular hyphae always advanced through living host tissue. This latent growth period, although sustained in each tissue colonised throughout the ear, was only for a limited duration and was always followed by the onset of host cell alterations. No specialised feeding structures were observed, either at the hyphal front or within the zones containing dead host cells, while no intracellular hyphae were found within live host cells. Chlorenchyma cells were the only cell-type that died ahead of infection. This colonisation pattern indicates that the *Fusarium* hyphae are initially feeding solely off the extracellular exudates in the apoplast, but once host cell death is initiated, this is accompanied by necrotrophic intracellular colonisation of the cell lumen and survival off the dead host cells which lack cellular contents. Thus over time, as the percentage of the ear tissue colonised by *F. graminearum* hyphae gradually increases, so the proportion of the fungal infection in association with living host cells gradually decreases, but remains present. Therefore, it would appear that *F. graminearum* exists towards the non-necrotrophic end of the continuum during the initial infection phase and at the advancing hyphal front, but very much at the necrotrophic end of the continuum in the infection centre and where the macroscopic symptoms are observed.

Serial sections revealed that the appearance of the fungal hyphae changed dramatically throughout the colony. At the advancing front of infection, hyphae were small in diameter, possess few vesicles and stained a uniform dark purple with TBO,

suggesting the presence of a high number of ribosomes indicating a high level of translation. Once infection was established, all host cells within the colonised plant tissue possessed hyphae and every host cell at the centre of the infection network contained multiple hyphae. Such an extremely high density of hyphae throughout all the infected plant tissue is uncommon in pathogenic fungi of wheat ears. As hyphae matured they increased in diameter, stained a light purple with TBO and possessed vesicles that did not stain. The change in appearance of the fungal hyphae may be linked to the source and / or amount of nutrition available at the relevant stage in the infection process.

Far behind the advancing front of fungal infection, the lignified host cells remained as 'skeletons' that retained the overall structure of the tissue. This probably accounts for why the ear remains stiff to the touch even when heavily colonised by *Fusarium*. The hyphae in this region had lost their contents and only the fungal cell walls were stained positively. The process(es) responsible for the lack of contents in fungal cells is unknown, but this could have been caused by cell death or nutrient cycling via autophagocytosis. In a recent proteomics study, a high percentage of fungal housekeeping proteins without signal peptides were detected in the apoplast of the infected ear, which the investigators suggested was due to fungal cell lysis or leakage (Paper *et al.*, 2007). The loss of fungal cell contents was unlikely to be the result of recently induced plant defences as the entire ear was colonised by 12 dpi and all host cells would have been dead for at least six days. However, induced antimicrobial compounds produced by plants can subsequently accumulate to high concentrations in dead host cells (Ingham *et al.*, 1982). An alternative and potentially the more plausible explanation for the lack of viable fungal cells in the centre of the *Fusarium* infection may be the lack of readily available nutrition and / or water. Deletion of the *ATG8* and *ATG15* genes responsible for the production of autophagosomes in the PH-1 strain gave rise to a transformant which showed reduced pathogenicity on susceptible wheat ears and was restricted to the point of inoculation, demonstrating the importance of nutrient cycling for full virulence (Josefsen *et al.*, 2008, Long Nam *et al.*, 2011). The *ATG8* and homologue in *M. oryzae* is also required for rice infection and colonisation (Veneault-Fourrey *et al.*, 2006). Therefore, autophagocytosis plays an important role in plant pathogenicity

and may provide the best explanation for the appearance of empty *Fusarium* hyphae in the infection centre.

At the later stages of infection, the axis of hyphal growth altered with a marked increase in lateral spread towards the outer surface. At the base of the glume, on the rachis node exists a region where all host cells, including those forming the epidermis, are non lignified. This region has in the past attracted attention as a possible route of entry (Tu, 1950). In the present study, the accumulation of hyphae was found always to be at its highest in this region, with hyphae rupturing the epidermis and producing extracellular aerial mycelium. In this region an orange colouration and sporulation has been observed on plants grown in the field (Beacham *et al.*, 2009).

Also at the later stages of the infection, hyphae accumulated *en masse* in the heavily lignified epidermis and sclerenchyma of the rachis internodes, which initially were sparsely colonised compared to the cortex and vasculature. The lignified host cell walls of intracellularly colonised rachis sclerenchyma were degraded layer by layer from the inside of the cell lumen. Similarities can be drawn with the white rots of hardwoods which progressively attack the host cell wall from within the cell lumen, where degradation occurs via diffusion of PCWDE and not hyphal contact (Schwarze *et al.*, 2000). Lignified secondary cell walls largely consist of three polymers cellulose, hemicelluloses and lignin. These three polymers differ in their complexity and mode of breakdown. In the secondary cell walls, lignin and hemicelluloses form an amorphous matrix in which the cellulose fibrils are embedded. Lignin degradation is a multi enzymatic process that involves peroxidases, oxidases and laccases. However these enzymes are too large to penetrate the wall (Martinez *et al.*, 2005). Therefore, it may be that small chemicals such as oxidizers and activated oxygen species are involved in the initial steps, providing entry for the sequential degradation of intermediate non-lignified layers. The lignin component of the wall was ultimately digested as no debris was left in the lumen of host cells that demonstrated extreme cell wall thinning. The *F. graminearum* genome is predicted to possess 103 PCWDEs including xylanase and pectate lyases (Cuomo *et al.*, 2007) which is far more than many other fungal plant pathogens (Soanes *et al.*, 2007). Therefore, *F. graminearum* is probably able to

sustain hyphal growth via cell wall digestion. Interestingly, cell wall degradation appears to occur in a sequential manner and this secondary cell wall degradation occurred only in specific cellular locations.

A considerable difference between the host cell response to infection in the rachis internodes and rachis nodes was noted. Dense intercellular depositions between parenchyma cells and within the metaxylem were identified in the rachis nodes but not the internodes. Recently, the trichodiene synthase gene *TRI5* was demonstrated to be expressed at a higher level in the rachis nodes compared to the internodes (Ilgen *et al.*, 2009). This coincides with the increase in extracellular depositions that appear to be a host defensive response. The DON mycotoxin is known to inhibit protein synthesis (Kimura *et al.*, 1998) and the increased amount of DON may play a role in limiting the host's defensive response in this region. Interestingly, the wheat ear infection of *TRI5* deficient fungal mutant strain was blocked at the rachis node and confined to the inoculated spikelet (Proctor *et al.*, 1995a).

This investigation has revealed the various pathways developed by *Fusarium* hyphae to successfully colonise a susceptible wheat ear. The intricate hyphal network which forms is maintained over many centimetres of ear tissue and appears to be very dynamic. Both hyphal physiology and mode of colonisation change throughout this network. These spatial and temporal changes to the nature of the *Fusarium* and wheat cell interaction indicate that the *F. graminearum* transcriptome, proteome, secretome and metabolome are also likely to change dramatically in the different regions of the hyphal network. This idea is already supported by the identification of the differential expression of essential pathogenicity genes in different host tissue types (Ilgen *et al.*, 2009). Recent works on *M. oryzae* and *B. graminis* f. sp. *hordei* have revealed dynamic changes in transcription and metabolism during fungal development in specific host tissues over time (Both *et al.*, 2005, Mosquera *et al.*, 2009).

Chapter 4. Molecular characterisation of the *Fusarium graminearum* – wheat floral interaction

4.1. Introduction

In the early phase of *F. graminearum* wheat ear infection, macroscopically the colonised tissue appears healthy and this symptomless growth represents the majority of the infection. The plant cells then die prior to the onset of intracellular colonisation and this plant cell death coincides with the onset of externally visible disease symptoms on the wheat ears (Brown *et al.*, 2010). At the later phases of infection, ascogenous hyphae form just below the wheat cell surface layers in preparation for perithecial formation (Guenther & Trail, 2005). The identification and evaluation of symptomless infection in wheat ears via light and electron microscopy is time consuming and costly. In this study the infection biology of a transgenic *F. graminearum* reporter strain (*PH1:GUS*) that expresses the β-glucuronidase enzyme (GUS), driven by the constitutive glyceraldehyde 3 phosphate dehydrogenase promoter from *A. nidulans* (*gpdA*) (Roberts *et al.*, 1989), was evaluated. This reporter strain enabled the rapid evaluation of symptomless infection throughout the fungal colony in the ear.

The early events that control the establishment of infection could have a more profound effect on the outcome of an interaction. Trichothecenes are reported to be cytotoxic and immunosuppressive, assisting microbial infections (Rotter *et al.*, 1996). Their phytotoxic effect is the result of inhibiting DNA, RNA and protein synthesis, lipid peroxidation and mitochondrial function, which can accumulate in apoptosis (Shifrin & Anderson, 1999). DON and NIV are the two major trichothecenes produced by *F. graminearum* (Desjardins, 2006). Trichothecene chemotype is determined by the presence of functional *TRI7* and *TRI13* genes within the *F. graminearum* strain (Lee *et al.*, 2002). DON is required for full virulence on wheat ears, but not for full virulence on barley ears, maize cobs or Arabidopsis floral tissue (Cuzick *et al.*, 2008b, Harris *et al.*, 1999, Maier *et al.*, 2006, Proctor *et al.*, 1995a, Proctor *et al.*, 1995b). NIV is also required for full virulence on wheat ears and to a lesser extent maize cobs, but is not required for barley infection (Maier *et al.*, 2006). In barley DON production is detectable as early as 36 hpi (Evans *et al.*,

2000). DON inhibits protein synthesis in eukaryotes by preventing polypeptide chain initiation or elongation by binding to the 60S ribosomal subunit (Kimura *et al.*, 1998). This ribotoxic stress activates MAPKs involved in the immune response and apoptosis (Pestka, 2008, Pestka *et al.*, 2004). Despite the universal nature of the target molecule, DON appears to play a host-selective role in pathogenicity but is produced irrespective of the host species. Wheat ear infection by a non-DON producing *tri5* gene deficient mutant results in an enhanced defence response in the form of plant cell wall thickening which impedes rachis colonisation (Jansen *et al.*, 2005). DON has also been implicated in the activation of several wheat defence responses including, hydrogen peroxide production and programmed cell death which may aid colonisation (Desmond *et al.*, 2008).

This study utilised the wild-type *F. graminearum* PH-1 strain that has non-functional *TRI7* and *TRI13* genes and is therefore a DON chemotype. Biochemical analyses have confirmed that the PH-1 strain produces DON and 15A-DON (Lowe *et al.*, 2010). In order to further elucidate the role that DON plays during the establishment of the different phases of infection, the expression of various *Fusarium TRI* genes was explored. Two trichothecene biosynthetic enzymes, conserved in both the NIV and DON chemotypes, two *TRI* gene regulators and a hypothetical protein, were selected for investigation. These *TRI* genes were chosen due to their known involvement in pathogenesis and mycotoxin production (Dyer *et al.*, 2005, Kimura *et al.*, 2007, Proctor *et al.*, 1995a, Proctor *et al.*, 1995b, Seong *et al.*, 2009, Tokai *et al.*, 2007). The trichodiene synthase enzyme, encoded by the *TRI5* gene, is the catalysis for the first committed step in the biosynthesis of trichothecenes, the conversion of farnesyl pyrophosphate to trichodiene (Hohn & Vanmiddlesworth, 1986). The multifunctional trichodiene oxygenase encoded by *TRI4* is responsible for three of the following 9 steps that result in the synthesis of calonectrin (Tokai *et al.*, 2007). The zinc finger transcription factor encoded by *TRI6* enhances the expression of genes in the isoprenoid and *TRI* pathways (Seong *et al.*, 2009). *TRI14* encodes a specific regulator of *TRI* genes that has no effect on DON production *in vitro*. However, deletion of the *TRI14* gene results in a loss of DON production *in planta* and a reduction in pathogenicity (Dyer *et al.*, 2005). *TRI9* encodes a hypothetical protein that resides within the core *TRI* gene cluster (Brown *et al.*, 2001) and

demonstrates a similar expression pattern as *TRI4* and *TRI5* during infections of susceptible barley ears (www.PLEXdb.org).

This investigation of the infection of a susceptible wheat genotype by *F. graminearum* has: (1) correlated the presence of fungal RNA with observed fungal colonisation at the cellular level, (2) compared fungal gene expression at the advancing front of symptomless infection with the origin of infection in the rachis, (3) revealed that the expression of several *TRI* genes is maximal at the advancing front and (4) has shown that the centre of the *Fusarium* colony within the wheat ear has only minimal physiologically active hyphae. Overall this study has shown that there are distinct phases to the *Fusarium* infection within the developing wheat ears and that these phases are maintained as infection proceeds. The text and figures presented in this chapter formed the basis of an article published in a special issue of the Journal of Pathogens on Molecular and Biochemical Interactions between Plants and Phytopathogenic Fungi and Oomycetes DOI:10.4061/2011/626345 (Brown *et al.*, 2011).

4.2. Experimental Procedures

4.2.1. The evaluation of wheat ear infection by the *PH1:GUS* reporter strain via X-gluc histochemical staining and the MUG fluorometric assay

The creation of the transformed constitutive GUS strain, confirmation of wild-type traits (growth under various nutritional states, DON production *in vitro / in planta* and sexual / asexual sporulation) was undertaken by previous group members, namely Dr Chris Bass and Dr Thomas Baldwin. The same two individuals evaluated the accumulation of fungal biomass throughout infection using both X-gluc (5-bromo-4-chloro-3-indolyl-β-D-glucuronic acid) histochemical GUS staining and the fluorometric MUG (4-methylumbelliferyl-b-D-glucuronide) assay. For a detailed description of these experimental procedures refer to Baldwin (2007).

4.2.2. Extraction of RNA from rachis internodes

The four or seven rachis internodes (relative to the dpi when harvested) below the inoculated spikelet of each ear were individually excised and frozen in liquid nitrogen at 5 dpi and 7 dpi. In total 15 wheat ears were dissected for each treatment, mock-inoculated or *F. graminearum*-infected, and the individual internode segments from each ear / treatment were collected starting from those nearest the point of inoculation and pooled. Freeze dried samples were ground in liquid nitrogen with a pestle and mortar. Total RNA was extracted using the TRIzol® reagent (Invitrogen) with minor modifications to manufacturer's instructions. Total RNA was precipitated at -20°C for 16 h with 8 M lithium chloride. Purified RNA was quantified by absorbance at 260 nm.

4.2.3. Gene expression analysis

The absence of genomic DNA (gDNA) in the RNA samples was confirmed by PCR using intergenic primers. The complementary DNA (cDNA) was synthesised from 1 µg of RNA using 500 ng of OligodT primers and 200 U Superscript III (Invitrogen) according to manufacturer's instructions. Reverse transcriptase-PCR (RT-PCR) with the fungal γ-actin primers was used to confirm fungal infection. Quantitative RT-PCR (RT-qPCR) was performed on a Real Time PCR System 7500 (Applied Biosystems). All sense and antisense primers used are presented in Chapter 2, table 3. A standard curve of gDNA, from an *in vitro* culture, with known concentrations ranging from 25 ng to 0.025 ng was created for each primer pair. Synthesised cDNA was diluted 1/50 in sterile H_2O. The PCR analysis was performed in a final volume of 20 µl and consisted of 10 µl of Jumpstart Taq Ready mix plus ROX (Invitrogen), 5 µl of 1.2 µM of each primer, and 5 µl of the relevant nucleic acid template. Thermal cycling conditions were as follows: [95°C 2 min, (95°C 15 sec, 62°C 20 sec, 72°C 45 sec) x40]. The dissociation curves were as follows: [95°C 15 sec, 60°C 1 min, 95°C 15 sec] x1. The average cycle threshold value for each sample was calculated from triplicate technical replicates. Fungal housekeeping genes γ-actin and β-tubulin were used to normalise the RT-qPCR data for fungal biomass.

4.3. Results

The results presented in some of the sections below represent the work carried out by two former group members (T. Baldwin / C. Bass) and myself. Data produced by these former group members and co-authors of the Brown *et al.*, (2011) publication is referenced accordingly throughout this chapter and in the figure legends. The results of others are included as they provided the foundation on which my study was based. For clarity, I explored the GUS staining at the cellular level (Figure 21 and Figure 24), devised the linear rachis infection assay and completed the entire RT-qPCR analysis.

4.3.1. The *F. graminearum* constitutive GUS expressing strain exhibits a wild-type phenotype

The *PH1:GUS* reporter strain was selected post fungal transformation using an *in vitro* growth assay and a colormetric GUS assay. The quantitative MUG assay demonstrated that the selected transformant had a stable, high level, of GUS activity when grown on nutrient rich potato dextrose agar (PDA). The *PH1:GUS* strain produced 1153 nM MU min^{-1} mg $protein^{-1}$ StD ± 165 nM min^{-1}. This strain also showed wild-type growth rates on minimal SNA and rich PDA media. Asexual and sexual sporulation after growth under near UV / white light on either SNA or carrot agar, respectively, was wild-type. DON concentration, measured by ELISA, after growth on DON-inducing corn meal agar showed DON production was unaltered, (PH-1 (1.6 ppm), *PH1:GUS* (1.5 ppm), analysis of variance (ANOVA) and Fisher F-test ($p>0.05$)). The *in vitro* characterisation of the initial population of primary transformants generated and the selection of the representative *PH1:GUS* strain was carried out by Baldwin and Bass.

4.3.2. The constitutive GUS expressing strain shows wild-type pathogenicity

The high levels of GUS produced by the *PH1:GUS* strain allowed the infection process to be followed by dissection and histochemical staining at 8 and 12 dpi. The specificity of macroscopic GUS staining was confirmed to localise to the fungal hyphae (Figure 21). Staining at 8 dpi revealed hyphae had colonised beyond the visible disease symptoms (Figure 22). By 12 dpi hyphae had grown throughout the entire rachis below the inoculated spikelet and down into the peduncle (Figure 22).

The fluorescent MUG assay is a more sensitive method to quantify fungal infection. The extent of infection varied significantly between individual wheat ears, typically by 2 spikelets by day 8 and 4 spikelets by day 16. Subsequently, representative ears were evaluated separately and these results are presented. All spikelets on wheat ears were individually assessed at 8 and 16 dpi (Figure 23). Combined with the histochemical staining, substantial symptomless colonisation continually advanced the infection throughout the wheat ear, relative to the progression of visible disease in that ear. The MUG assay also confirmed that some of the severely bleached spikelets towards the tip of the ear late in infection commonly lacked GUS activity and therefore remained non-infected. Interestingly, on occasions individual spikelets on fully disease ears appeared healthy. For example, at 16 dpi one spikelet (no. 12) in an otherwise heavily diseased ear had developed no macroscopic disease symptoms. The MUG assay confirmed spikelet 12 to be free of fungal infection and demonstrated the reliability of the system to monitor accurately the progression of infection. Disease free spikelets were identified on many of the inoculated ears and could be located at any position in the ear. It was also noted that overall there was a 15-fold reduction in total GUS activity between 8 and 16 dpi throughout the spikelets of the ear (Table 5). To determine if this was caused by a reduction in active fungal biomass and a re-distribution of resources to the actively growing region of the colony as infection progresses, a detailed microscopy analysis of infected ears was carried out. This revealed that hyphae had indeed lost their cell content at the late time point, 12 dpi (Figure 24) which would account for this reduction in GUS activity.

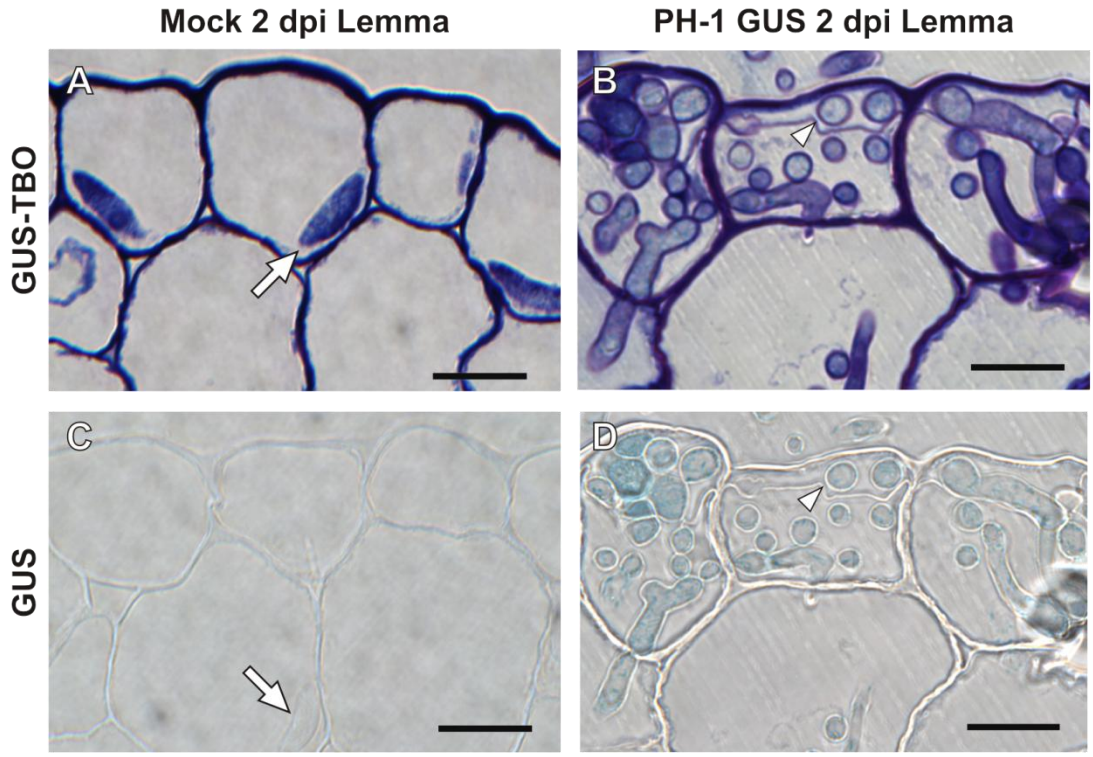

Figure 21 Confirmation that X-gluc specifically stains the hyphae of constitutive GUS expressing strain. All images in this figure are of the lemma from the inoculated floret at 2 dpi, which was stained with X-gluc prior to fixation. All images are of sequential transverse 3 µm LR white sections; panels **(A)** and **(B)** are stained with 0.1 % TBO, pH 9, while panels **(C)** and **(D)** are not. White arrow = host nuclei, white arrowhead = intercellular fungal hyphae. Bar = 15 µm.

Figure 22 X-gluc stained susceptible Bobwhite wheat ear at 8 days **(A)** and 12 days **(B)** post point inoculation with the constitutive GUS expressing strain. The four ears displayed from left to right in each panel were either photographed before and then after staining of the same intact ear, or before and after staining of an ear longitudinally sliced through the mid-point. The white brackets surrounding a portion of each ear pair indicates the two spikelets which received the original *F. graminearum* inoculum. Note: Mock inoculated ear demonstrated no non-specific GUS staining (data not shown). (This data was generated by T. Baldwin)

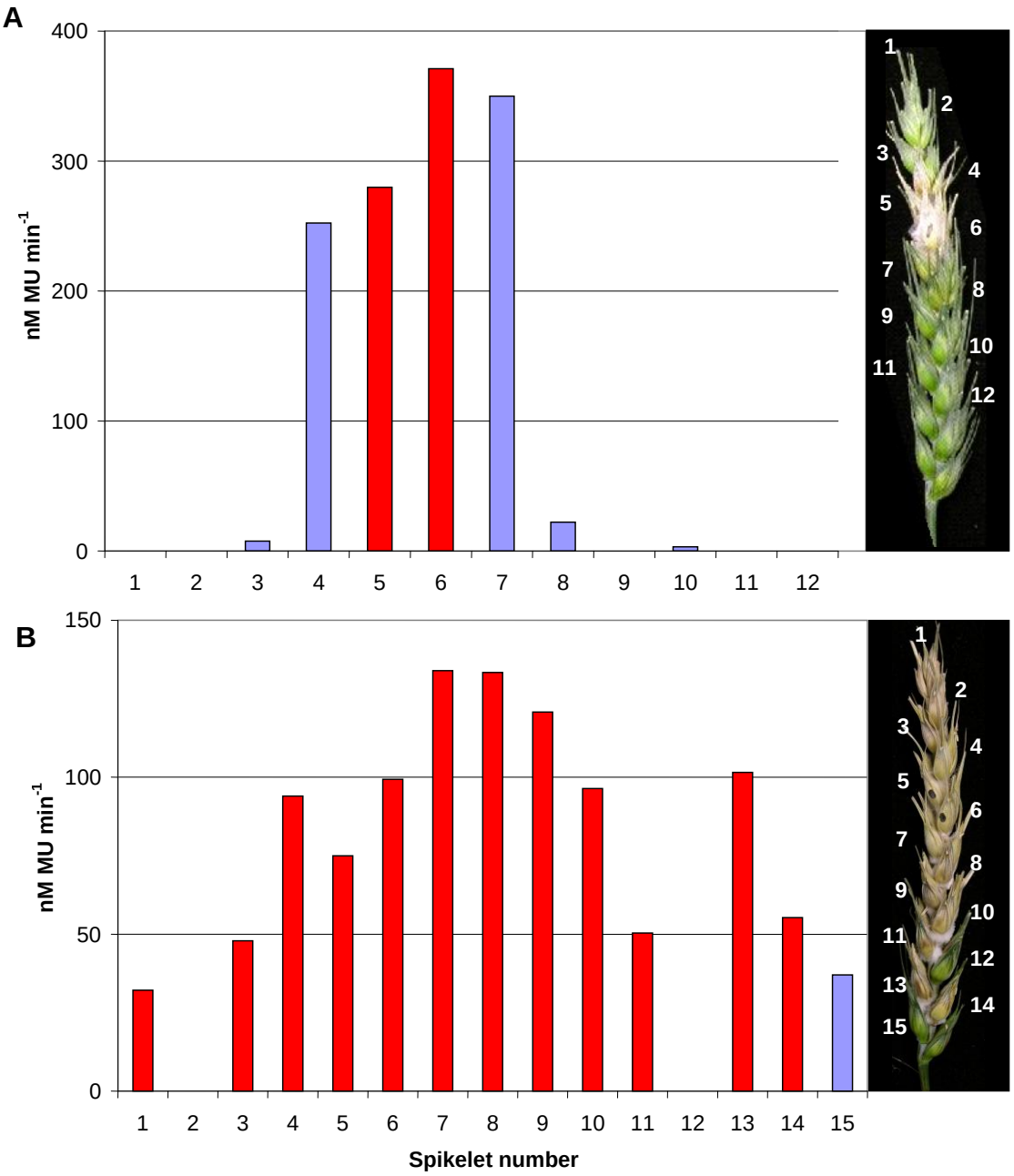

Figure 23 GUS activity (nM MU minute^{-1}) of individual spikelets in a single wheat ears (susceptible cv. Bobwhite) inoculated with constitutive GUS expressing *Fusarium* strains at 8 dpi **(A)** and at 16 dpi **(B)**. Selected ears were representative of the norm. The right portion of each panel is a photograph showing the macroscopic disease symptoms on the ear immediately prior to all the spikelets being sampled. The bars in red represent symptomatic infection whilst the bars in blue represent symptomless infection. In technical replicates, the values obtained never varied more than 5 % from each other. (This data was generated by T. Baldwin)

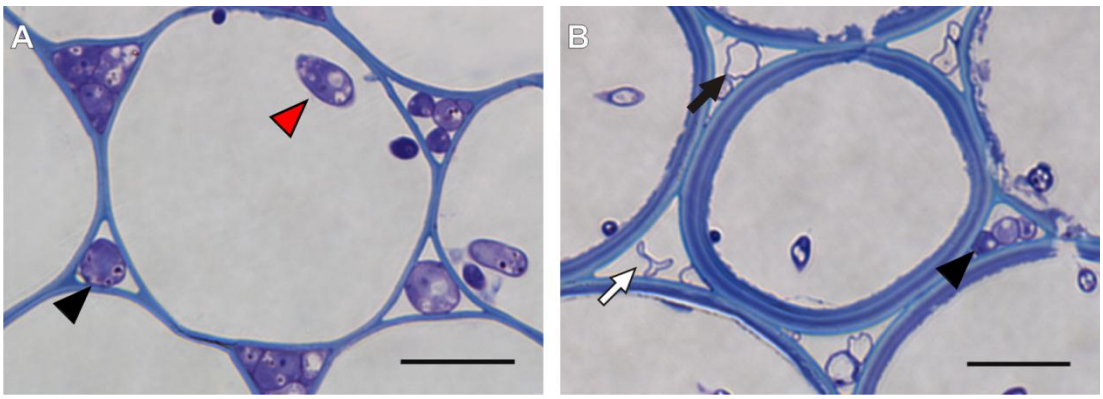

Figure 24 The reduction in fungal biomass at the centre of the colony as infection progressed throughout the wheat ear by 12 dpi. Images of transverse 1 µm LR white sections of cortical cells within various rachis internodes stained with 0.1% TBO pH 9. The first rachis internode below the point of inoculation at 5 dpi **(A)** and at 12 dpi **(B)**. Generic legend: black arrowhead = intercellular hyphae, red arrowhead = intracellular hyphae, black arrow = hyphae devoid of content, white arrow= collapsed hyphae. Bar = 15 µm.

Table 5 GUS activity within the individual wheat spikelets at 8 and 16 dpi, as determined by the MUG assay, demonstrates a dramatic drop in MUG activity and therefore active fungal biomass at 16 dpi. In technical replicates, the values obtained never varied more than 5 % from each other. This data is from a representative ear from the six explored in detail. (This data was generated by T. Baldwin)

Spikelet	**MUG (nmol/min)**	
	8 dpi	**16 dpi**
1	8.8	8.9
2	0.0	0.0
3	43.2	10.0
4	1397.5	41.7
5	1517.4	47.9
6	1863.3	51.6
7	1732.7	63.1
8	129.4	44.3
9	0.0	34.1
10	12.5	30.5
11	0.0	34.3
12	0.0	0.0
13	0.0	34.9
14	0.0	25.5
15	0.0	9.1
Sum	6704.8	435.8
Fold drop in MUG activity		**15.3847**

4.3.3. The identification of fungal hyphae at the cellular level correlates with the detection of *F. graminearum* RNA

Colonisation of the rachis represented a simplified linear system for monitoring and quantifying the development of infection which leads to sequential spikelets becoming colonised. Within the rachis internodes hyphae predominantly grow in one direction, enabling the accurate isolation of the advancing front of infection. The four rachis internodes below the inoculated spikelet were excised and separately pooled at 5 dpi to determine the extent of the macroscopically visible symptoms (Figure 25). The appearance of disease symptoms, in the excised rachis internodes (RI), was also evaluated at the cellular level (Figure 26). No hyphae were detected in RI-4, the internode the furthest from the point of inoculation. The active front of infection was identified in RI-3 and consisted of a low number of intercellular hyphae in association with live cortical cells. RI-2 possessed a higher number of intercellular hyphae, than RI-3, surrounding live plant cells. The internode closest to the point of inoculation, RI-1, where the rachis infection had begun contained both inter- and intracellular hyphae. Plant cortical cells and vascular elements in the centre of this rachis internode were intracellularly colonised and dead. However, the infected cell-types were surrounded by live sclerenchyma and epidermal cells, accounting for the slight appearance of macroscopically visible disease symptoms on this internode at 5 dpi.

Total RNA was extracted from pooled rachis internodes (Figure 27) and post DNAase treatment, a PCR analysis was done using intergenic primers designed to amplify only genomic DNA. These checks confirmed the absence of DNA contamination (Figure 28). In the first three rachis internodes below the point of inoculation, fungal RNA was identified via RT-PCR using primers to the fungal housekeeping gene γ-actin (Figure 25). This result correlated well with the observation of hyphal infection at the cellular level.

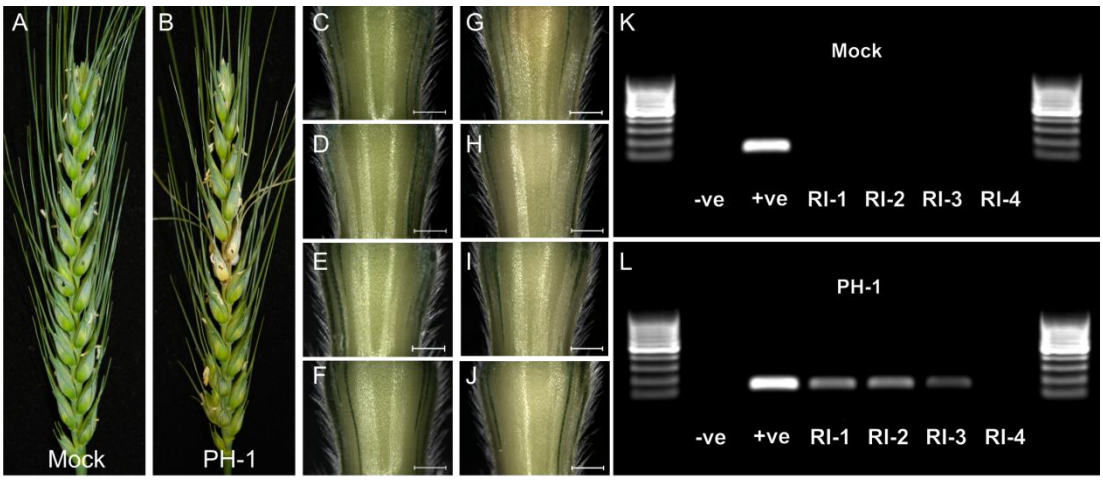

Figure 25 Detection of fungal RNA within the relevant rachis internode correlated with the identification of fungal hyphae at the cellular level (presented in Figure 15). Panel **(A)** and **(B)** are photographs of the mock and the PH-1 infected ears at 5 dpi. The four sequential rachis internodes below the inoculated spikelet from the mock control **(C through F)** and PH-1 infected **(G through J)** ears, bar = 1 mm. RT-PCR of the RNA extracted from the rachis internodes of the mock control **(K)** and the PH-1 infected **(L)** using primers for *F. graminearum* gamma actin (141 bp) separated on a 2 % agarose gel alongside a 100 bp DNA ladder (Generuler, Fermentas). Legend: RI-1 to RI-4 = the sequential rachis internodes below the inoculated spikelet, –ve = the non template negative control, +ve = the *F. graminearum* gDNA positive control.

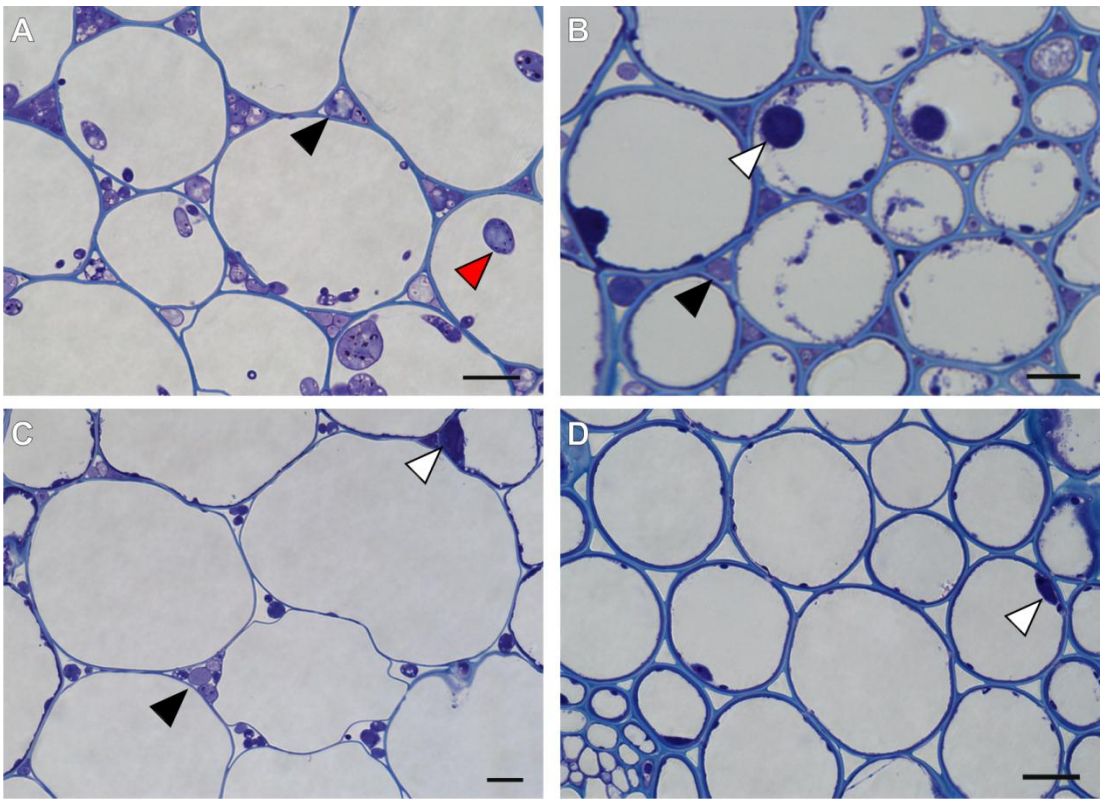

Figure 26 The identification of fungal infection in the first three rachis internodes at 5 dpi. Images of transverse 1 µm LR white sections of cortical cells within various rachis internodes stained with 0.1% TBO pH 9. The first **(A)**, second **(B)**, third **(C)** and fourth **(D)** rachis internode below the point of inoculation at 5 dpi. Generic legend: black arrowhead = intercellular hyphae, red arrowhead = intracellular hyphae, white arrowhead = host nuclei. Bar = 15 µm.

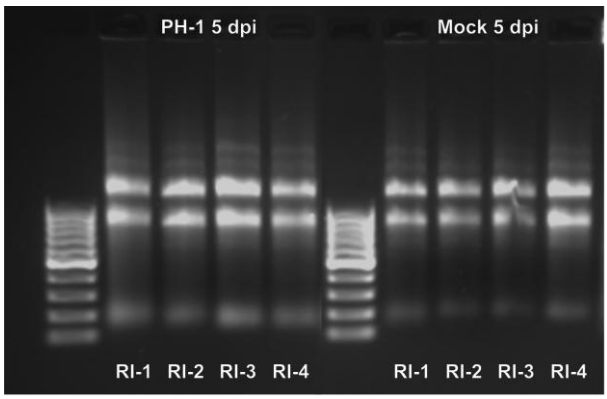

Figure 27 The extracted RNA from the rachis internodes of the PH-1 infected and the mock control at 5 dpi. One µg of total RNA was separated on a 1 % agarose gel alongside a 100 bp DNA ladder (Generuler, Fermentas). Legend: RI-1 to RI-4 = the sequential rachis internodes below the inoculated spikelet.

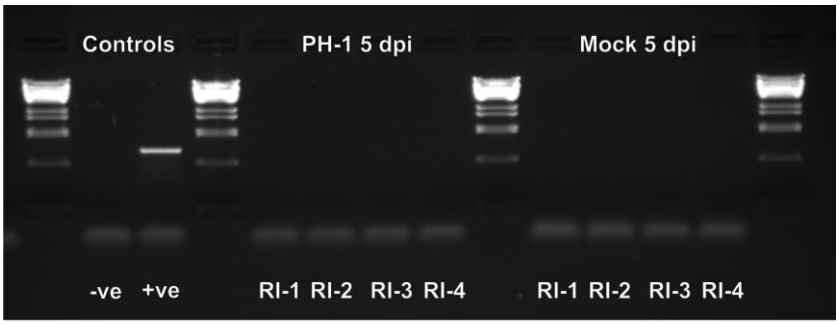

Figure 28 The extracted RNA from the rachis internodes of the PH-1 infected and the mock control at 5 dpi is free of gDNA contamination. Intergenic primers that only amplify gDNA were used. The presence of an amplicon (902 bp) on the 1 % agarose gel, separated alongside a lambda_DNA_BstE II ladder, represents the presence of gDNA. Legend: RI-1 to RI-4 = the sequential rachis internodes below the inoculated spikelet, –ve = the non template negative control, +ve = the gDNA positive control.

4.3.4. *TRI* gene expression is up regulated at the active hyphal front of symptomless infection

Five *Fusarium* genes from the *TRI* cluster, namely *TRI4*, *TRI5*, *TRI6*, *TRI9* and *TRI14*, along with two housekeeping genes, γ-actin and β-tubulin were selected for analysis. Each *TRI* gene was normalised for fungal biomass and screened by RT-qPCR for changes in transcript abundance within the three colonised rachis

internodes at 5 dpi. For the 7 dpi, six colonised rachis internodes were separately sampled from each wheat ear, and then pooled. At 7 dpi the analysis focussed only on the expression of *TRI4* / *TRI5* genes and the two housekeeping genes.

The initial analysis of 15 pooled ears revealed that at 5 dpi, the transcripts of all five *TRI* genes were detected at their highest level at the active hyphal front of infection and decreased as the distance from the advancing front of infection increased (Figure 29A). All the *TRI* genes showed a greater than two fold change in abundance in RI-3 (symptomless infection front) compared to RI-1 (the onset of disease symptoms, origin of rachis infection). *TRI5* expression was very low in RI-1 and exhibited a dramatic 11.90 fold increase in abundance between the RI-1 and the advancing hyphal front in the RI-3 tissue, reaching a modest expression level (Table 6). *TRI4*, *TRI9* and *TRI14* expression was substantially higher than *TRI5* in RI-1, whilst their increase in expression level was more modest in RI-3. Interestingly, the relative level of expression of *TRI6* was considerably lower than the four other *TRI* genes, namely, *TRI4*, *TRI5 TRI9* and *TRI14* throughout all rachis internodes.

The later 7 dpi time point was studied in more detail and included 45 ears (3 pools of 15 ears). This time-point was chosen to determine whether elevated *TRI* gene expression at the advancing front of infection was retained throughout the progression of infection. At 7 dpi the first two rachis internodes (RI-1 and RI-2) represented fully symptomatic infection, the following two (RI-3 and RI-4) harbour the onset of macroscopically visible disease symptom formation, while the final two colonised internodes (RI-5 and RI-6) represented symptomless infection. The *TRI* genes that had shown the highest level and the greatest change in expression, at 5 dpi, were chosen for further analysis. The expression of *TRI4* and *TRI5*, relative to fungal biomass, again was higher during symptomless infection (Table 6). Within the fully symptomatic plant tissue *TRI* gene expression was very low. The amount of fungal biomass demonstrated an inverse relationship to *TRI* gene expression (Figure 29B; Appendix 8).

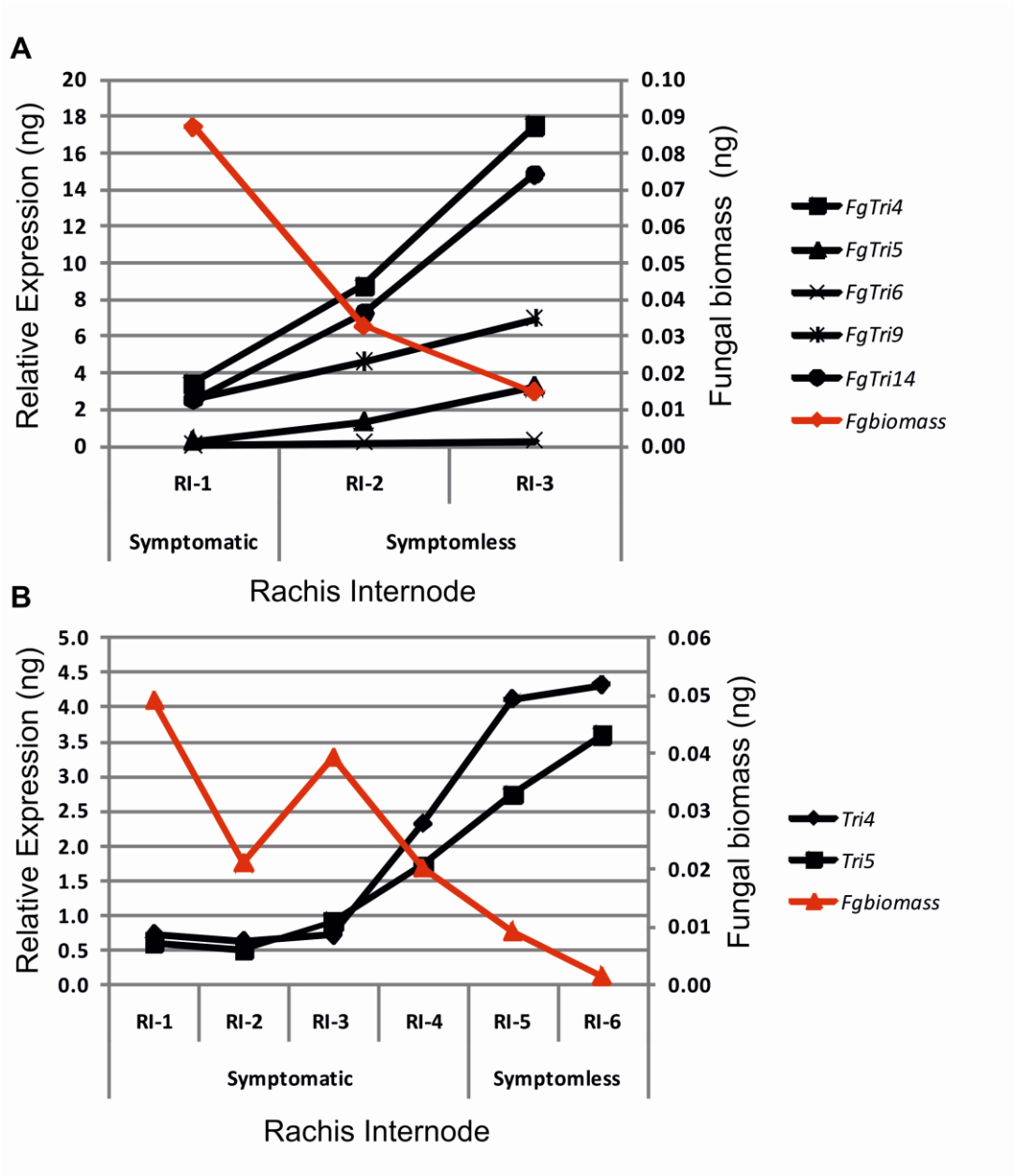

Figure 29 Fungal *TRI* gene in the infected rachis internodes in which *F. graminearum* was detected at 5 dpi **(A)** and 7 dpi **(B)**. Relative expression was measured by RT-qPCR and values normalised for fungal biomass using the expression of *F. graminearum* γ-actin and β-tubulin. **(A)** Represents a single biological replicate of 15 pooled wheat ears. **(B)** Represents three biological replicates of 15 pooled wheat ears. Error bars are presented on the individual graphs in Appendix 8.

Table 6 Fold change in normalised fungal gene expression between the symptomless (RI-3) and the microscopically symptomatic (RI-1) at 5 dpi. Fold change in fungal gene expression between the symptomless (RI-6) and the microscopically symptomatic (RI-1) at 7 dpi. Each gene showed a greater than two fold changes in expression. Standard errors for the three biological replicates at the 7 dpi are given in brackets.

Fungal gene	Fold change in gene expression	
	5 dpi	7 dpi
FgTri4	5.14	5.92 (0.32)
FgTri5	11.90	6.03 (0.49)
FgTri6	4.31	-
FgTri9	2.68	-
FgTri14	5.96	-

4.4. Discussion

4.4.1. The effectiveness of the reporter strain to track *F. graminearum* infection

The original objective of this study was to create a *F. graminearum* reporter strain that would simplify the quantification of the progression of infection throughout the ear. The GUS reporter strain had wild-type growth rates, pathogenicity and mycotoxin production. *In planta* experiments confirmed that the constitutive GUS expressing strain can be used to quantify fungal biomass within both the symptomatic and symptomless infected wheat tissue. Histochemical and biochemical analyses verified the presence of a substantial phase of symptomless growth ahead of disease symptoms, as previously noted by Brown *et al.*, (2010). Therefore in this interaction there is a considerable latent period between the tissue becoming infected and the development of macroscopically visible symptoms. These studies also showed that a spikelet at the tip or in other locations of the ear can fail to become infected even though the ear is otherwise heavily diseased (Figure 23). The histochemical and microscopy analyses of sectioned tissues confirmed that GUS activity was detected only within the *Fusarium* hyphae. Analysis of the *Fusarium* infection process using the constitutive GUS expressing strain revealed a considerable reduction in GUS activity at late time points in infection, which is believed to be caused, in part, by the reduction in physiologically active hyphae. It is currently unknown what triggers the increase in abundance of ‘ghost’ hyphae in the

later stages of infection of a susceptible wheat genotype. In various other host–pathogen interactions when compatible interactions have been quantitatively analysed using fungal transformants that contained the *gpdA*:*GUS* reporter construct, a steady increase in the levels of detectable MUG activity over the time-course has usually been reported. For example, in the interaction between tomato leaves and the intercellularly growing biotroph *C. fulvum*, an 100 fold increase in detectable MUG activity was observed over the 12 day time course prior to the onset of sporulation (Oliver *et al.*, 1993). The final developmental stage in the *Fusarium*-wheat ear infection process is sporulation and the re-distribution of resources to areas of sporulation may concentrate activity to these regions of the colony.

4.4.2. Mycotoxin production during the early phases of infection

The early infection process was explored further using the simplified linear rachis internode system and RT-qPCR to determine the expression of various *Fusarium* genes required for mycotoxin production. *TRI* gene expression was found to be maximal at the hyphal front at both 5 and 7 days post spikelet inoculation. This indicates that the mycotoxin induction pattern is maintained as the hyphae advance symptomlessly through newly colonised wheat tissue. In addition to the up regulation of trichothecene biosynthetic genes (*TRI4*, *TRI5* and *TRI9*), these quantitative analyses also revealed the elevated transcription of *TRI* gene regulators *TRI6* and *TRI14*, at the advancing front of infection. Deletion of the *TRI6* gene, which encodes a transcription factor, down regulates more than 200 genes, including most *TRI* genes and many genes from the preceding isoprenoid pathway, resulting in a reduction in DON production and pathogenicity (Seong *et al.*, 2009). Interestingly, a *F. graminearum TRI14* deletion strain demonstrated wild-type DON production *in vitro* while losing the ability to produce DON *in planta* resulting in a reduction in pathogenicity (Dyer *et al.*, 2005). The combination of these results implies that *TRI6* and *TRI14* regulation of the *TRI* genes is essential for DON production and pathogenesis during establishment of symptomless wheat ear infections. Expression of all of the *TRI* genes was minimal in the symptomatic wheat tissue within which an abundance of *Fusarium* hyphae are associated with dead plant cells. This suggests that for this phase of the infection process DON production is either not required or the tissue already contains considerable DON because of the earlier colonisation.

The mycotoxin, DON and its acetylated derivatives, produced by *F. graminearum* during infection of susceptible wheat have been demonstrated to be essential for the spread of infection beyond the inoculated spikelet (Proctor *et al.*, 1995a). For wheat cultivar Bobwhite and the sequenced *F. graminearum* strain PH-1 (Cuomo *et al.*, 2007) this result has been verified (Cuzick *et al.*, 2008b). In the absence of DON production, symptomless infection is lost and the wheat plant is able to lay down a defensive barrier which appears as a brown ring around the lesion (Cuzick *et al.*, 2008b). The production of DON may therefore inhibit the defensive response of plant cells in the vicinity of invading hyphae, minimising the onset of various cell wall reinforcement processes (Jansen *et al.*, 2005) by preventing protein synthesis (Kimura *et al.*, 1998). This strategy would assist *Fusarium* infection. Indeed, previous detailed microscopy analyses revealed minimal changes to the appearance of wheat cortical cells surrounding the advancing DON-producing *Fusarium* hyphae (Brown *et al.*, 2010). For DON production to be relatively uniform throughout the plant tissue at an early stage in the infection, the limited number of intercellular hyphae at the actively advancing front of symptomless infection would need to produce a higher amount of DON per fungal cell compared to fungal cells further into the colony where the ratio of fungal cells to live plant cells is consistently higher. Accordingly, once the plant cells have died DON production would no longer be required.

The analysis of the expression of individual genes via RT-qPCR is a time consuming and costly process. The validity of the infection model created from the study of a limited number of genes depends on the genes selected for evaluation. The small number of genes ultimately analysed, although informative and accurate, may give an unbalanced picture of the true situation. For example, potentially there are multiple enzymes attacking each plant cell wall component and these enzymes may exhibit a different expression pattern to those presented previously. To create a more robust model of the symptomless and symptomatic phases of the infection, genome wide transcriptomics is required.

Chapter 5. Characterisation of *Fusarium graminearum* single gene deletion mutants

5.1. Introduction

The *F. graminearum* wild-type PH-1 strain was selected for study for two reasons. Firstly, considerable genomic sequence information is now available for this strain and this has been aligned to the four *F. graminearum* chromosomes (Cuomo *et al.*, 2007). Secondly, an increasing number of laboratories are using PH-1 in forward and reverse genetic experiments aimed at identifying pathogenicity and virulence genes (Ramamoorthy *et al.*, 2007b, Seong *et al.*, 2005). The characterisation of genes and pathways confirmed to be involved in pathogenicity by forward and reverse genetic investigations provides an enhanced understanding of how infection is established and how tissue colonisation occurs. This new knowledge then enables the identification of targets for chemical intervention. However, characterisation of sub-cellular infection by single gene deletion strains is commonly overlooked and generally efforts are focused on the impact on visible disease symptoms and / or mycotoxin production. Histological studies of infection would give a greater understanding of how the interaction between pathogen and host is altered by the absence of a specific gene or pathway, providing clues to the role it plays during infection.

A reverse genetics approach identified the *TRI5* gene as being essential for the production of the *F. graminearum* mycotoxin, DON, and for full virulence on wheat ears, but not for full virulence on barley ears, maize cobs or Arabidopsis floral tissue (Cuzick *et al.*, 2008b, Harris *et al.*, 1999, Maier *et al.*, 2006, Proctor *et al.*, 1995a, Proctor *et al.*, 1995b). The trichodiene synthase enzyme encoded by the *TRI5* gene is the catalysis for the first committed step in the biosynthesis of trichothecenes (Hohn & Vanmiddlesworth, 1986). Spray inoculation of a susceptible wheat ear with the *tri5*-deficient, DON-minus, strain resulted in the production of eye-shaped lesions surrounded by a brown ring on the glumes of the wheat florets (Cuzick *et al.*, 2008b). Wheat point inoculations resulted in cell wall thickening in the rachis node (Jansen *et al.*, 2005). Both infection assays revealed an enhanced host defensive response that restricted infection to the spikelet. Expression of the several *TRI* genes,

including *TRI5*, was previously demonstrated to be maximal during symptomless infection (Brown *et al.*, 2011)(Chapter 4). Subsequently, the confirmation of the presence or absence of symptomless colonisation during DON-minus *tri5* infection was required.

A forward genetic screen of a transformant library, generated by random insertion of a linearised plasmid, identified a mutant with reduced virulence on susceptible wheat ears. Plasmid rescue identified the disrupted gene as being topoisomerase I (*TOP1*), which had not previously been linked with plant, but was known to be required for animal, pathogenicity. Targeted gene deletion, in *F. graminearum*, revealed that *TOP1* played a role in pathogenicity and asexual sporulation but not mycotoxin production (Baldwin *et al.*, 2010). Type I topoisomerases modify the topological state of the DNA helix by creating single stranded breaks in the helix, whereas type II topoisomerases make double stranded breaks. This allows the DNA strands to be unwound, which is required for transcription, recombination and replication (Champoux, 2001). Single and double mutations of the topoisomerases in *Candida albicans* reduced virulence on mice (Jiang *et al.*, 1997). In pathogenic bacteria, DNA relaxation and supercoiling modulates the expression of many virulence genes during the different phases of the host-pathogen interaction (Dorman & Corcoran, 2009). *Salmonella enterica* serovar *typhimurium* has two type III secretion systems with separate sets of effector proteins located on different pathogenicity islands (Galan & Collmer, 1999, Hensel, 2000). One set is up regulated by DNA relaxation and the other by DNA supercoiling. The environmental conditions influence DNA topology, up regulating and repressing the different gene sets (O Croinin *et al.*, 2006). Therefore, in fungi, DNA topology may also play a role in gene regulation (Lotito *et al.*, 2008) possibly including virulence genes and secreted effectors.

Several different methods to assess FEB development on wheat exist, including ear, detached leaf and seedling assays (Bai & Shaner, 2004a, Mesterházy, 2003). An alternative, quick assay to screen wheat genotypes for disease resistance and to test *F. graminearum* wild-type or gene deficient strains for their disease-causing ability, is highly desirable. Under field conditions leaf lesions caused by *F. graminearum* are very rare and an attached wheat leaf lesion assay for a mycotoxin

producing Fusaria does not exist (Browne & Cooke, 2004). The identification of the prolonged latent phase of symptomless infection in the wheat ear, where the fungal hyphae are in association with live plant cells for several days, implies that a detached leaf assay would not reflect the true situation. Therefore, an attached, wounded, leaf assay has been developed at Rothamsted which could provide a fast method for screening resistance or pathogenicity. The capabilities of the wounded leaf assay to reflect wheat ear resistance has been confirmed (K. Hammond-Kosack, RRes, UK, pers. com.). However, the ability of the leaf assay to identify *F. graminearum* strains with attenuated virulence remains unknown.

The detailed microscopy analysis of the infection biology of the two different single gene deficient strains has demonstrated how histology aids in the generation of hypothesis concerning the mode of wild-type infection. The leaf infection assay successfully portrayed the different characteristics of wild-type and *tri5* infection as seen in the wheat ear assay, but can be completed in a fraction of the time. Consequently, the leaf assay represents a useful method for identifying fungal strains with attenuated virulence. The study of leaf infection in the absence of DON mycotoxin production revealed an enhanced host response to infection and the formation of an intercellular deposition in advance of infection. This implicates DON mycotoxin as playing a role in inhibiting the plant's ability to respond to infection and thus promoting symptomless colonisation. The *TOP1* investigation exposed the inability of the *top1* deficient strain to mask fungal infection despite having the ability to produce the DON mycotoxin, suggesting that additional mechanism(s) are required to inhibit the plant's capacity to respond and promote symptomless infection. The text and figures concerning the *TOP1* investigation are published in MPMI (2010), DOI:10.1094/MPMI-23-5-0566, while the *TRI5* data will be included in a manuscript on the leaf assay.

5.2. Experimental procedures

5.2.1. Juvenile wheat leaf – *F. graminearum* infection assay

The second leaf of two week old wheat plants cv. Bobwhite, were fixed horizontally and wounded with a sterile needle. A 7.5 µl spore suspension of either the wild-type PH-1 or the *F. graminearum tri5* at 2.5 x 10^5 conidia/ml and a sterile

water control, was placed onto the wound and covered with sterile Biofolie, hydrophilic side down. The juvenile plants were kept at high humidity throughout the experiment of which the first 24 h are dark. At least ten wheat leaves were assessed on two separate occasions. Representative wheat leaves were assessed by photography and sampled for fixation at 4 dpi.

5.2.2. Hand sectioning and stereomicroscopy of the wheat ear

Wheat ears inoculated with either wild-type PH-1 or the *F. graminearum top1* strains and mock controls were sampled regularly until 14 dpi. Freehand longitudinal sections that cut through the centre of all spikelets dividing the ear in two were prepared using a clean scalpel. Sectioned ears were observed under bright field and UV light (excitation 360 nm / barrier filter 420 nm) on a Leica MZFL11 stereomicroscope. A minimum of three wheat ears were assessed per treatment.

5.2.3. Preparation of the wheat tissues for light microscopy

The inoculated wheat ears were sampled at 5 dpi. The rachis node of the inoculated spikelet and palea of the inoculated floret were collected. Portions of the leaf lesion were excised at 4 dpi. A minimum of three wheat ear or leaf tissues were assessed per treatment. All samples were fixed, dehydrated, embedded and polymerised as described previously. Transverse semi-thin 1 µm sections, stained with aqueous 0.1 % TBO in 1 % sodium tetraborate pH 9 were imaged using a Zeiss Axiophot.

For histochemical analyses, the palea of the inoculated floret was excised then fixed with a cold solution of 75 % ethanol (v/v) and 25 % acetic acid (v/v). The fixed tissues were infiltrated with a 15 % sucrose (w/v) solution, individually embedded in Tissue Tek OCT (Sakura Finetek, USA) and frozen in liquid nitrogen. The embedded tissues were subsequently transferred to a Leica Cryostat CM1850 set at -15^{o}C. The frozen tissues were cut into 10 µm thick sections by the cryostat, collected on glass slides and dried on a hot plate set at 40^{o}C. Sections were stained to detect lignin polymers with aqueous 1 % Safranin O for 2 min, washed with deionised water, counterstained with aqueous 1 % Alcian blue for 2 min and then finally washed with deionised water. Stained sections were examined and imaged using a Zeiss Axiophot.

5.2.4. Cryo-SEM analyses

The palea of the inoculated two florets were excised using a sterile blade and forceps, mounted, frozen and transferred to the Gatan Alto 2100 cryo chamber maintained at -180^{o}C, where fracturing, sublimation and gold coating was performed. The samples were transferred to the Jeol LV6360 scanning electron microscope chamber maintained at -150^{o}C for examination. Three wheat ears were examined.

5.3. Results

5.3.1. Detailed microscopy analysis of wheat leaf infection by the *F. graminearum* wild-type PH-1 strain and the *tri5* deficient strains

After 4 days there was little difference in the average lesion size between the wild-type and the *tri5* strains (Table 7). However, the difference in appearance between the two lesion types was striking. Macroscopically, the *tri5* lesion was surrounded by a brown ring that was constantly absent from the wild-type lesion (Figure 30). The *tri5* lesion expanded throughout the time course, as did the brown front bordering the lesion. At the microscopic level, no host response to wild-type infection was observed. Sub-cellular colonisation of the wheat leaf by the *tri5* strain, in the absence of DON synthesis, appeared similar to wild-type. However, ahead of infection plant cells responded to colonisation by laying down a defensive barrier in the form of intercellular depositions and cell wall thickening (Figure 30). However, the defensive barrier was unable to significantly impede the progression of infection as the lesion expanded at a similar rate as the wild-type.

Table 7 The average lesion length for infection by the *F. graminearum* PH-1 or *tri5* strains at 4 days post inoculation.

Treatment	Average lesion length (mm)	Standard error
Water control	0	0
PH-1 wild-type strain	11.0	1.34
Tri5-deficient strain	9.1	0.51

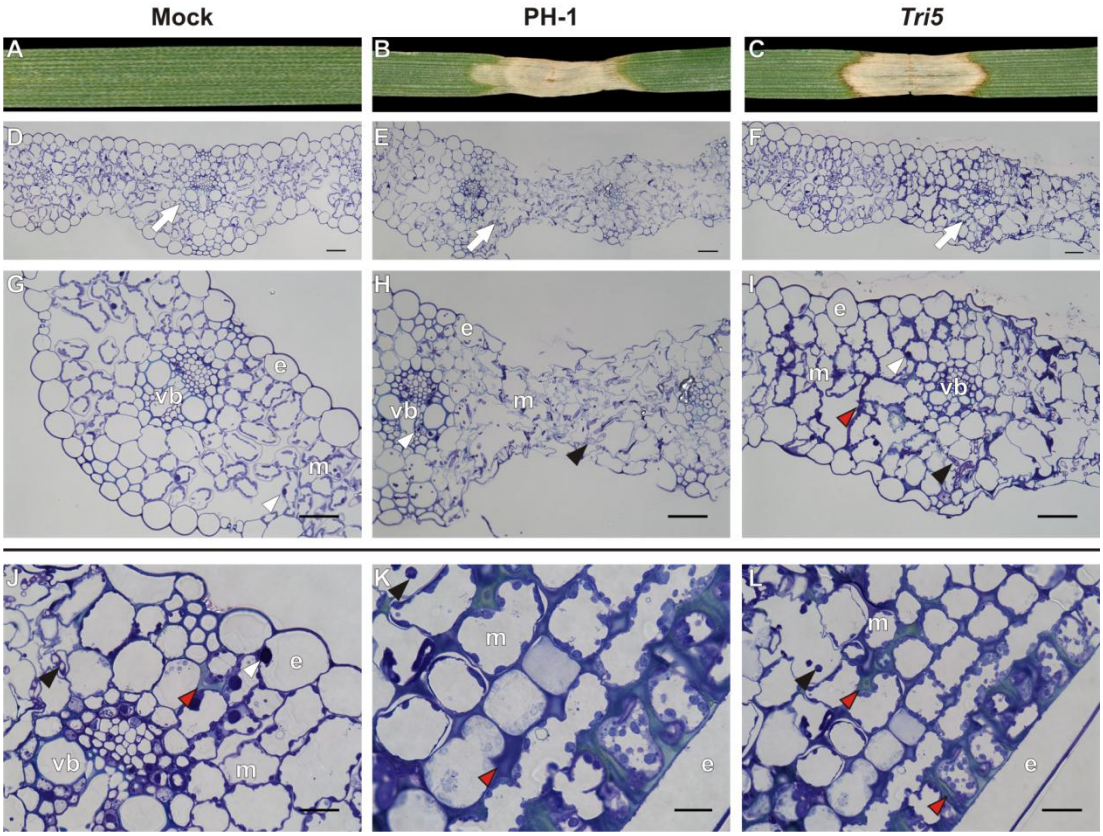

Figure 30 Colonisation of a juvenile leaf by the wild-type and *Tri5* deficient *F. graminearum* strains at 4 dpi. The first row of panels (**A, B, C**) depicts the macroscopic appearance of the leaf. The second and third row (**E, F, G** and **H, I, J**) describe the anatomy of the water inoculated control (mock), and the appearance of the lesion edge at the cellular level, bar = 50 µm. The forth row illustrates the intercellular deposition that surrounds the *Tri5* lesion, bar = 25 µm (**J** and **K**), 50 µm (**L**). All images in this figure are transverse 1 µm LR white sections, stained with 0.1 % TBO, pH 9. Generic legend: e = epidermis, m = mesophyll, vb = vascular bundle, white arrowhead = host nuclei, black arrowhead = fungal hyphae, red arrowhead = intercellular depositions and cell wall reinforcements, white arrow = region presented subsequently at a higher magnification (G through I).

5.3.2. Detailed microscopy analysis of the infection biology of the *F. graminearum top1* mutant in wheat ears

The progress of fungal infection was monitored regularly until 14 dpi by taking longitudinal sections of the ear (Figure 31 A through F). By 9 dpi the wild-type infection had spread beyond the inoculated florets into the neighbouring spikelets and the desiccated tissue lacked red autofluorescence suggesting the absence of chlorophyll. Over the identical time period and inoculation conditions the *F. graminearum top1* mutant infection was limited to the inoculated florets, which showed only discrete patches of browning on the floral brackets. However, the rachis node of the *top1* mutant infected spikelet had turned brown and emitted a pale blue–yellow autofluorescence, indicative of the accumulation of phenolic compounds.

Within each floret, the palea is one of the floral brackets within which the developing wheat grain resides. This structure consists of a thick-walled abaxial surface and a very thin-walled adaxial surface (Figure 31 G & J). By 5 dpi, the wild-type PH-1 hyphae were present throughout the palea in all cell types (Figure 31 H & K). By contrast, the *top1* mutant hyphae were restricted to the lower parenchyma cells on the adaxial surface and were absent from the vascular bundles (Figure 31 I & L). In response to the *top1* mutant infection, many of the nearby plant cells appeared misshapen and collapsed. There was also substantial cell wall deposition. Cryostat sections of mock inoculated and *top1* mutant infected palea stained with safranin O / alcian blue gave a strong red colouration solely in the abaxial epidermal cell layer. This stain is indicative of the presence of lignin polymers (Figure 32A and B). CryoSEM analysis revealed that the *top1* mutant infected palea tissue had lost considerable cellular integrity compared to the mock inoculated control (Figure 32C and D).

The development of the necrotic region in the rachis node of the *top1* mutant infected floret by 7 dpi led to the hypothesis that the progress of the *top1* mutant hyphae into the rachis was blocked via a host response in this region. Five dpi was the time point chosen for further study because this coincided with the onset of visible autofluorescence at the rachis node. In contrast to the wild-type infection where abundant intra- and inter-cellular hyphae were present throughout the tissue examined, no *top1* mutant hyphae were identified in the serial sections of the entire rachis or rachis node. Despite the absence of *top1* mutant hyphae, cellular depositions were present throughout the vascular tissue of the rachis node. These were absent from the healthy and wild-type infected rachis node (Figure 31 M through R). The host response in the rachis node was approximately 1000 μm ahead of the *top1* mutant hyphal front which remained confined to the floral brackets. By 9 dpi, numerous dead host cells were present within the tissue surrounding the rachis node but still no *top1* mutant hyphae were identified in the rachis or rachis node (Figure 33).

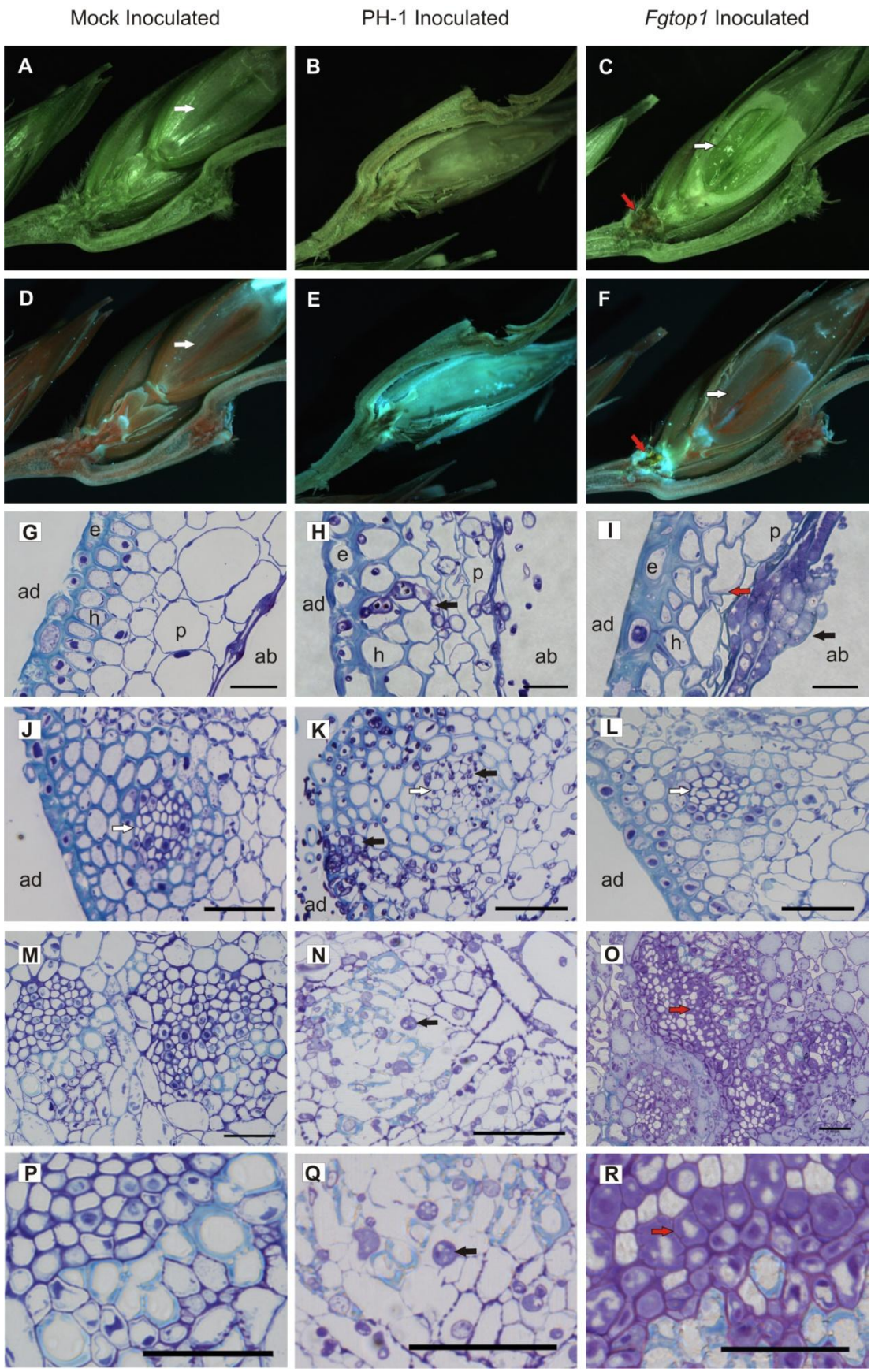
Mock Inoculated
PH-1 Inoculated
Fgtop1 Inoculated
A
B
C
D
E
F
G
H
I
J
K
L
M
N
O
P
Q
R
e
ad
h
p
ab

Figure 31 Detailed microscopy analysis of the infection biology of the *F. graminearum top1* mutant in wheat ears. **(A)** and **(D)** Mock inoculated healthy spikelet 9 dpi showing developing grain with crease (white arrow) under brightfield light **(A)**. Plant tissue emits a red autofluorescence (white arrow) under ultraviolet light **(D)** representative of chlorophyll. **(B)** and **(E)** Wild-type infection has spread beyond the inoculated spikelet and by 9 dpi the host tissue has become desiccated, brightfield **(B)**. Plant tissue lacks red autofluorescence under ultraviolet light **(E)**. **(C)** and **(F)** *top1* infection 9 dpi is confined to the inoculated floret where a necrotic region has formed at the rachis node (red arrow), the uninoculated floret appeared healthy and contained a developing grain (white arrow) under brightfield **(C)**. The necrotic region emits a pale blue-yellow autofluorescence ultraviolet light **(F)** representative of phenolic compounds. **(G)** through **(R)** Transverse 1 μm sections stained with toluidine blue O and observed on a Zesis Axiophot; ab = abaxial surface, ad = adaxial surface, e = epidermis, h = hypoepidermis, p = parenchyma, white arrow = vascular bundle, black arrow = hypha, red arrow = host response. **(G)** and **(J)** Palea of the mock inoculated floret at 5 dpi. **(G)** Bar = 25 μm. **(J)** Bar = 50 μm. **(H)** and **(K)** Palea of the PH-1 inoculated floret at 5 dpi. **(H)** Bar = 15 μm. **(K)** Bar = 50 μm. Hyphae penetrated the adaxial surface, colonised the all cell types and extruded from the abaxial surface. **(I)** and **(L)** Palea of the *top1* inoculated floret at 5 dpi. **(I)** Bar = 50 μm. **(K)** Bar = 50 μm. Hyphae confined to the lower parenchyma and absent from the vascular bundles. The host response to infection is cell wall deposition in the epidermis and hypodermis beyond the hyphal front. **(M)** and **(P)** The rachis node of the mock inoculated spikelet at 5 dpi. Bars = 25 μm. **(N)** and **(Q)** The rachis node of the PH-1 inoculated spikelet at 5 dpi, showing the destruction of host cellular organisation. Bars = 50 μm. **(O)** and **(R)** The rachis node of the *top1* inoculated spikelet at 5 dpi. The host response to infection is primary cell wall thickening of the phloem elements in the vascular bundle approximately 1000 μm ahead of the hyphal front. Bars = 50 μm.

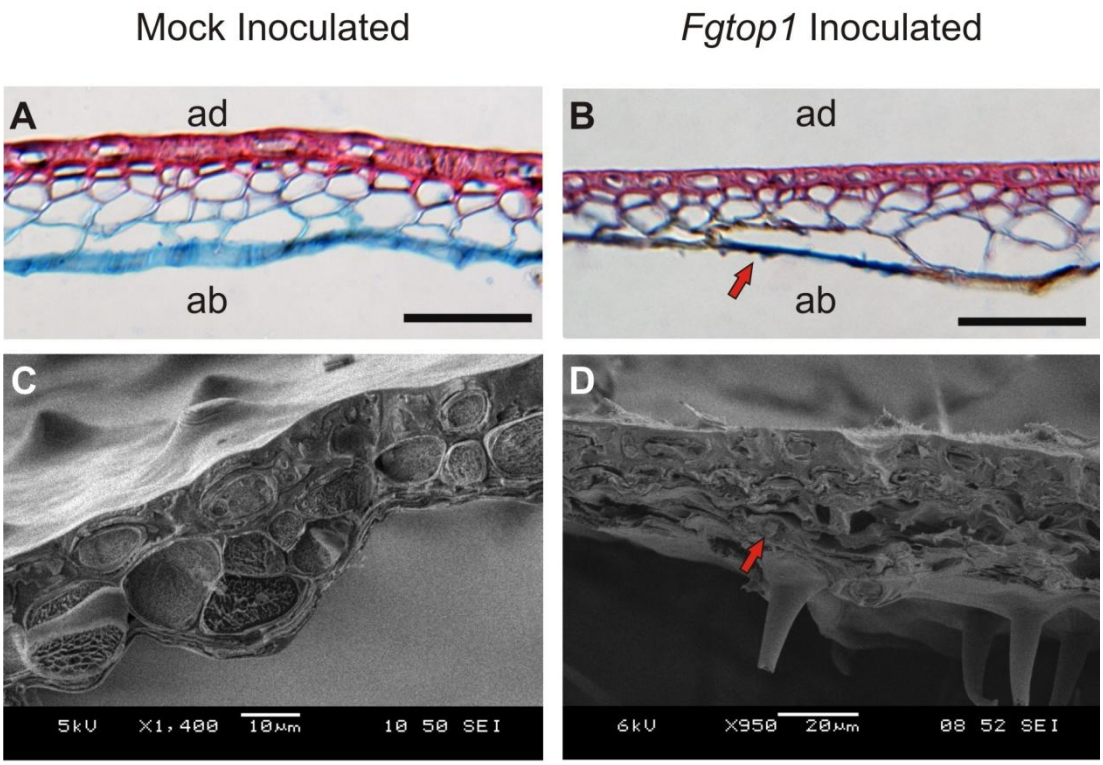

Figure 32 The *F. graminearum top1* mutant inoculated palea tissue. Cryostat sections of mock inoculated **(A)** and *top1* infected palea tissues **(B)** stained with safranin O / alcian blue. Bar = 50 µm. CryoSEM images of mock inoculated (**C**, bar 10 µm) and *Fgtop1* infected palea tissues (**D**, bar 20 µm). Red arrow = collapse of the mesophyll cells.

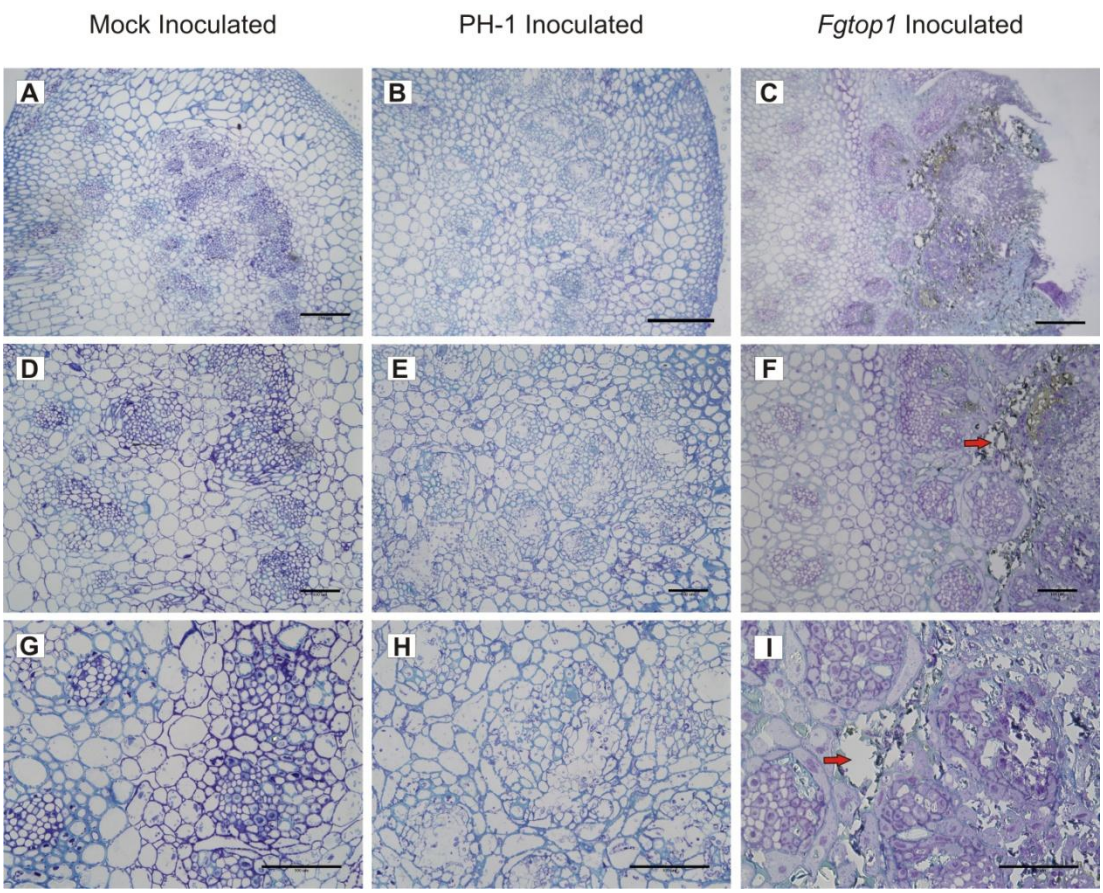

Figure 33 The rachis and rachis node 9 days post inoculation with the *F. graminearum top1* mutant. **(A, D and G)** The rachis node of the mock inoculated spikelet. **(B, E and H)** The rachis node of the wild-type PH-1 infected spikelet. **(C, F and I)** The rachis node of the *top1* infected spikelet, demonstrating cell death (red arrow) surrounding the rachis node. Transverse 1 µm sections through the rachis node, stained with toluidine blue O and observed on a Zesis Axiophot. **(A, B, C)** Bar = 250 µm; **(D)** through **(I)** Bar = 100 µm.

5.4. Discussion

The wounded wheat leaf assay was developed to assess disease caused by *Fusarium* strains, to measure mycotoxin accumulation and to distinguish resistant genotypes such as Sumai-3. The wounded leaf assay can be completed within three weeks. In comparison to the wheat ear assay can take longer than twelve weeks. DON mycotoxin production in wheat leaves has been confirmed (Holdgate, 2009). Wild-type fungal hyphae were identified not only in the necrotic region but also within green leaf tissue between intact mesophyll cells of a susceptible wheat genotype, demonstrating that *F. graminearum* also forms symptomless infection in wheat leaves (Holdgate, 2009).

Plant pathogens need to circumvent or suppress the plants defensive response in order to prevail. For *F. graminearum* to infect and cause disease throughout the wheat floral tissue, the key metabolite produced is the β-type trichothecene, DON (Trail, 2009). In the absence of DON synthesis, cell walls thicken ahead of *tri5* infection in the wheat rachis node (Jansen *et al.*, 2005). In this study, the epidermal and mesophyll cells of the wheat leaves infected by the DON-minus strain responded by reinforcing cell walls and intercellular spaces to impede hyphal progression. It is probable that the phenotypic brown ring encircling leaf and glume lesions is of a similar composition. Histochemical staining the plant derived polymers, surrounding the leaf and glume lesions, confirmed that the defensive response is the same in both systems. In both the ear and leaf assays symptomless infection by the pathogen was lost in the absence of DON synthesis. However, DON production is not required for the successful colonisation of barley ears, maize cobs or Arabidopsis floral tissue (Cuzick *et al.*, 2008b, Maier *et al.*, 2006). Although the target of DON, the 60S ribosomal subunit, is universal, the contribution of DON production to disease formation is somehow host plant species selective. A substantial phase of symptomless infection does not appear to occur in wild-type Arabidopsis floral tissues (H. Kinns, RRes, unpublished) and is yet to be confirmed in maize.

Molecular genetic studies in pathogenic bacteria implicated that topoisomerases play a key role in virulence (Dorman & Corcoran, 2009, O Croinin *et al.*, 2006). The *F. graminearum* investigation was the first to demonstrate that *TOP1* was involved in fungal pathogenicity on a host plant (Baldwin *et al.*, 2010). Analyses

in *S. cerevisiae* have shown that cell cycle status and Top1 modulate transcription (Hirschman *et al.*, 2006). During the exponential growth phase Top1 is localised to telomeres and is required for normal expression of the highly expressed genes (Lotito *et al.*, 2008). In pathogenic bacteria, changes in the environment influence DNA topology and control virulence gene transcription (Dorman, 1991, Galan & Curtiss, 1990, O Croinin *et al.*, 2006, Ye *et al.*, 2007). In fungi, nutritional status and the MAP kinase signalling pathways influence the cell cycle to promote or inhibit polarised fungal growth controlling pathogenicity (Perez-Martin *et al.*, 2006). Although the *F. graminearum top1* deficient mutant had reduced virulence on wheat ears, this mutant had wild-type *in vitro* growth and DON production, but reduced pigmentation (aurofusarin, not required for virulence), reduced asexual sporulation, but normal sexual sporulation (Baldwin *et al.*, 2010). Therefore the *top1* mutant has an unusual combination of phenotypes compared to other *F. graminearum* mutants with reduced virulence on wheat ears. Typically reduced virulence is accompanied by reduced DON mycotoxin production and little or no sexual reproduction (Reviewed by M. Urban and K. Hammond-Kosack, RRes, UK, 2012, In press). The reduction in invasive growth by the *top1* mutant was accompanied by an enhanced plant defensive response to infection. This host reaction may partly explain the novel combination of phenotypes exhibited the *top1* mutant.

Within the sub-telomeric regions of the four *F. graminearum* chromosomes exists higher proportion of genes that encode secreted proteins and many genes that are solely expressed *in planta* (Cuomo *et al.*, 2007). Localisation of the Top1 protein to this region and relaxation of DNA supercoil could lead to increased transcription of unidentified virulence factors. Possibly, the *top1* deficient strain failed to respond to the changing internal conditions associated with the different tissue types encountered. Alternatively, the lack of production of the correct repertoire of secreted effectors and / or the altered timing of their production may have lead to the confinement of the infection to the floral brackets and the elicitation of a systemic defensive response(s) which the debilitated pathogen could not overcome. It is noteworthy that the *in vitro* growth tests failed to find a dramatic reduction in *top1* growth under either nutrient-rich or nutrient-poor conditions (Baldwin *et al.*, 2010).

These findings support the notion that host defence responses are contributing to the virulence defect observed in wheat ears.

In the absence of the DON mycotoxin the wheat plant is able to respond to infection and forms a rolling defensive barrier that limits infection. In the presence of the DON mycotoxin, but the absence of Top1 modification of DNA topology, the wheat plant again restricts infection by forming a defensive barrier. Unlike the wild-type interaction, in both situations the susceptible wheat plant is able to detect the presence of the debilitated pathogen and respond to curtail invasive growth. DON is hypothesised to inhibit the plant's ability to respond to infection via interfering with protein synthesis (Kimura *et al.*, 2007). However, it would appear that DON alone is not sufficient to mask infection. The reduced capacity to change to environmental conditions and the possible reduction in secreted proteins by the *top1* deficient strain suggests the presence of additional fungal effectors. The secretion of effector proteins that prevent, manipulate or utilise the plant's defensive response to the benefit of the pathogen appears conserved across many fungal lifestyles. In some pathosystems, pathogens have also evolved the ability to produce non-proteinaceous secondary metabolites that aid infection, such as tabtoxin produced by bacteria (Kimura *et al.*, 2001) and oxalic acid produced by *S. sclerotiorum* (Bolton *et al.*, 2006). It is highly likely that *F. graminearum* uses a combination of DON mycotoxin production and the secretion of an array of effectors to establish and maintain the advancing front of hyphal growth through the apoplast between living wheat cells. In effect, the hyphae use a dual approach to successfully perturb and / or suppress basal wheat defences in floral tissue. The combination of the DON mycotoxin and the secretion of unknown fungal effector(s) permit symptomless infection of wheat and the progression of the disease into the wheat rachis.

A transcriptomic approach that assessed both plant and fungal gene expression during infection by the two debilitated fungal strains in comparison to the wild-type interaction would be informative. The plant transcriptome during infection by the *tri5* strain would assist the identification of the plant pathways that are influenced by the mycotoxin and how the inhibition of protein synthesis impacts plant transcription. An analysis of the fungal / plant gene expression during infection by the *top1* strain may reveal which genes, in particular the secreted protein and

those located in the sub-telomeric regions, are modulated but Top1 relaxation of the DNA helix. While the analysis of the plant transcriptome would also show which pathways are differentially activated or repressed in the *top1* interaction. These two relatively simple experiments could prove particularly informative, create new hypothesis concerning how *F. graminearum* circumvents plant defences and assist in the design of further investigations. Currently, the most cost effective way to explore simultaneously the changes to the fungal and wheat transcriptome would be to use a next generation sequencing approach. This point will be returned to in the general discussion (Chapter 9).

Chapter 6. Analysis of the predicted *Fusarium graminearum* secretome

6.1. Introduction

Comparative genomics enables distinct and orthologous gene sets to be defined and related to observed difference in lifestyle or phenotype between fungal species or strains. The number of sequenced fungal genomes is increasing at an ever faster rate due to the technical advances made in next generation sequencing, providing a wealth of genomic resources for comparative analyses. The intimacy of the association between a microbe and host plant is represented by viable foreign cells growing within plant tissue or even within living plant cells. Communication through the secretion of proteins and metabolites which are either taken up by the host or detected at the cell surface plays a pivotal role in determining the outcome of the interaction.

The secretome is defined as being all the proteins that are secreted outside the fungal cell. Secreted proteins from animal infecting malaria parasites and plant infecting oomycete pathogens possess a conserved RxLR secretion motif. This motif facilitates the uptake of secreted proteins into host cells and subsequently modulate host transcription (Bhattacharjee *et al.*, 2006, Kale *et al.*, 2010, Tyler, 2009). Fungi and oomycetes have convergently evolved a range of mechanisms to acquire nutrition from various habitats, including mutualistic, biotrophic, hemibiotrophic, necrotrophic and non-pathogenic saprotrophic lifestyles. In fungi however, no conserved translocation motif has been discovered, yet many small secreted proteins and metabolites are proven virulence factors (Deller *et al.*, 2011). Experimentally, secreted proteins termed 'effectors' that modulate the interaction between pathogenic microbe and host have been identified from all lifestyles. Examples include; the Avr and Ecp proteins from the tomato leaf mold fungus *C. fulvum* (Stergiopoulos & de Wit, 2009), the Tox proteins from the wheat glume blotch fungus *S. nodorum* (Tan *et al.*, 2010), Avra10 and Avrk1 from the barley powdery mildew fungus *B. graminis* f. sp. *hordei* (Ridout *et al.*, 2006), the SIX proteins from vascular wilt fungus *F. oxysporum* f. sp. *lycopersici* (Lievens *et al.*, 2009), the Avr-Pita and Pwl proteins from the rice blast fungus *M. oryzae* (Valent & Khang, 2010), Pep1 and Pit1/2 from

the corn smut fungus *U. maydis* (Doehlemann *et al.*, 2009), 3LysM from the wheat leaf blotch fungus *M. graminicola* (Marshall *et al.*, 2011) and Sp7 from the tomato mutualist *Glomus intraradices* (Kloppholz *et al.*, 2011). Several apoplastic effectors contain several LysM domains which bind fungal chitin fragments. For example, *C. fulvum* Ecp6 and *M. graminicola* 3LysM are now known to mask infection by inhibiting PAMP-triggered immunity (PTI) and thereby prevent the induction of PTI mediated basal defence (de Jonge *et al.*, 2010, Marshall *et al.*, 2011). Several intracellular effectors contribute to virulence in a different way. For example, Sp7 and Pwl2 are translocated to the host nucleus where they influence host transcription (Khang *et al.*, 2010, Kloppholz *et al.*, 2011). Alternatively in *U. maydis*, Pep1 accumulates at the site of cell-to-cell passage and is essential to the establishment of infection (Doehlemann *et al.*, 2009), while clusters of effectors contribute to organ specificity (Skibbe *et al.*, 2010). Different again are the small necrotrophic effectors (Tox proteins) that induce host programmed cell death to assist infection (Tan *et al.*, 2010). These examples are from fungi with different *in planta* lifestyles, includes mutualistic non-pathogens as well as biotrophic, hemibiotrophic and necrotrophic pathogens. Their recent discovery demonstrates how different types of secreted fungal proteins define the outcome of an interaction between a microbe and its host.

F. graminearum was one of the first plant pathogens to be selected for full genome sequencing due to the growing global importance of the disease, the large number of cereal species infected and the health concerns posed because of the mycotoxins produced during floral infections. The latest version of *F. graminearum* genome available from MIPS (version FG3.2) has a considerable amount of manual annotation incorporated and is predicted to encode 13,718 genes (Wong *et al.*, 2011). In the original genome analysis (Cuomo *et al.*, 2007), the Signal P defined secretome was predicted to account for approximately one tenth of the predicted genes ~ 1,369. Low level sequence coverage of a second *F. graminearum* strain, GZ3639, demonstrated the non random distribution of nucleotide polymorphism in the genome, with hot spots of sequence variation occurring in sub-telomeric and central regions (Cuomo *et al.*, 2007). These highly variable 'hot' regions of the genome were found to be enriched for genes coding for predicted secreted proteins. An analysis of the genomic location of experimentally proven *F. graminearum*

pathogenicity / virulence genes, and homologues of verified pathogenicity / virulence genes from other species, (www.PHIbase.org) has revealed that most genes with this function resided in regions of low level recombination. Their location in the 'cooler' parts of the genome has been suggested to protect them from gene loss (Beacham, 2010). The majority of these genes encode conserved intracellular proteins involved in signal transduction, such as MAPKs, and represent ancient conserved signalling pathways recruited by pathogens to coordinate infection (Xu, 2000). Within *F. graminearum* genomic regions found to exhibit high recombination frequencies (Cuomo *et al.*, 2007) reside genes that encode small and large sized secreted proteins. For instance, an abundance of PCWDEs were identified. This type of genome positioning is hypothesised to assist the evolution of the pathogen in the rapidly changing arms race with its host. By contrast, in the oomycete *Phytophthora infestans* the vast majority of the predicted secretome, which is evolving rapidly, is located in regions of the genome where an abundance of transposon sequences reside (Haas *et al.*, 2009).

Production of the water soluble, secreted mycotoxin, DON, is required by *F. graminearum* for full virulence on wheat ears, but not for full virulence on barley ears, maize cobs or Arabidopsis floral tissue (Cuzick *et al.*, 2008b, Harris *et al.*, 1999, Maier *et al.*, 2006, Proctor *et al.*, 1995a, Proctor *et al.*, 1995b). DON inhibits protein synthesis in eukaryotes and prevents polypeptide chain initiation or elongation by binding to the 60S ribosomal subunit (Kimura *et al.*, 1998). In *F. graminearum* infections of wheat, the trichothecene mycotoxin genes of the *Tri* cluster are maximally expressed during symptomless infection (Brown *et al.*, 2011). Wheat ear infection by the non-DON producing *tri5* gene deficient mutant results in an enhanced defence response in the form of plant cell wall thickening adjacent to the invading *Fusarium* hyphae (Jansen *et al.*, 2005). In the absence of DON production, the interaction between the two organisms at the infection front is altered. A brown ring forms around the slowly expanding lesion on the glumes of wheat ears sprayed with *F. graminearum* (Cuzick *et al.*, 2008b). The symptomless latent phase of infection is lost and unlike the wild-type interaction, advancing hyphae are confronted by a defensive barrier produced by plant cells responding in advance of infection (Jansen *et al.*, 2005). Topoisomerase modulation of DNA

topology has been demonstrated to regulate virulence gene expression, especially secreted proteins (Dorman & Corcoran, 2009, O Croinin *et al.*, 2006). The *top1* deficient *F. graminearum* strain was unable to colonise the wheat ear despite producing wild-type DON levels, infections were restricted to just below the surface of the glumes, lemma and palea (Baldwin *et al.*, 2010). While the secreted lipase *fgl1*-deficient strain produced enhanced DON *in planta*, yet in wheat ears an extensive host cell browning reaction becomes evident in the tissue immediately beyond the confined *Fusarium* hyphae. Collectively this implies that additional virulence factors, in combination with the secreted DON mycotoxin, promote symptomless infection and implicates a role for secreted proteins in *F. graminearum* pathogenicity.

In view of the recently identified symptomless phase of wheat ear infection where the *F. graminearum* hyphae advance exclusively extracellularly between the wheat cells (Brown *et al.*, 2010), we decided to explore in detail the predicted secretome. This new study of the secretome could potentially give the first clues to what proteins are involved in the establishment / maintenance of symptomless infection, as well as the transition from extracellular to intracellular growth. Bioinformatic tools that assist the prediction of fungal secretomes are available which utilise different but highly complementary analytical approaches, namely prediction of the presence of a signal peptide (Signal P / Target P) and predicting the eventual cellular location of the mature protein (WoLFPSORT). Used individually these approaches often predict non-secreted proteins as secreted, but when used in combination an increased accuracy of the prediction was anticipated. In this study we describe, in detail, a refined prediction of the *F. graminearum* secretome. Finally a genomic comparison of the *F. graminearum* secretome with 57 similarly predicted fungal and oomycete secretomes, including other Fusaria and many pathogenic / non-pathogenic species, has been used to partition this predicted secretome into species specific, genera specific and highly conserved gene sets.

6.2. Experimental Procedures

6.2.1. Bioinformatic analyses of the secretome

The FG3 version of the genome was downloaded from MIPS (http://mips.helmholtz-muenchen.de/genre/proj/FGDB/) in October 2009. The prediction of the refined *F. graminearum* secretome was based on the procedure described by Muller and colleagues (2008) for *U. maydis*. We developed an automated secretome prediction pipeline based on this procedure using bash shell, AWK and Python scripts on a PC running Red Hat Linux 5.2. Initially all proteins with a Target P Loc = S (TargetP v1.1; http://www.cbs.dtu.dk/cgi-bin/nph-sw_request?targetp) or a Signal P D-score = Y (SignalP v3.0; http://www.cbs.dtu.dk/cgi-bin/nph-sw_request?signalp) were combined (Emanuelsson *et al.*, 2007, Emanuelsson *et al.*, 2000). These were then scanned for transmembrane spanning regions using TMHMM (TMHMM v2.0; http://www.cbs.dtu.dk/cgi-bin/nph-sw_request?tmhmm) and all proteins with 0 TMs or 1 TM, if located in the predicted N-terminal signal peptide, were kept. GPI-anchor proteins were predicted by big-PI (http://mendel.imp.ac.at/gpi/cgi-bin/gpi_pred_fungi.cgi) (Eisenhaber *et al.*, 2004). ProtComp was also used to predict localization of the remaining proteins using the LocDB and PotLocDB databases (ProtComp v8.0; http://www.softberry.com). WolfPSort analysis was done using "runWolfPsortSummary fungi" in the WoLFPSORT v0.2 package (Horton *et al.*, 2006). All proteins predicted as extracellular or unknown were kept in the final secretome dataset. Pfam analysis was done using the Pfam database (ftp://ftp.ncbi.nih.gov/pub/mmdb/cdd/) and the rpsblast program in the NCBI blast+ software package (ftp://ftp.ncbi.nlm.nih.gov/blast/executables/blast+/). The number of cysteine residues within the mature peptide was computed using a custom Python script. The number of internal amino acid repeats was predicted using RADAR (http://www.ebi.ac.uk/Tools/Radar/) (Heger & Holm, 2000). The detection of RNA transcripts for the 574 *F. graminearum* genes of interest was explored using Affymetrix gene expression data generated in several published *in planta* and *in vitro* investigations (Experiments FG1, FG2, FG15 and FG16) downloaded from www.PLEXdb.org.

For the detailed follow up analyses, only proteins with a predicted signal peptide sequence and a value of 18 or greater from the WolfPSort analysis were used. The *F. graminearum* secretome was compared with 57 other fungal and oomycete genomes of pathogens varying in host range, tissue specificity and lifestyle as well as several exclusively saprotrophic species (Appendix 9). The fungal and oomycete genomes and their predicted gene repertoires were downloaded from either the BROAD or JGI websites or from species specific websites maintained by various research communities. For the comparative analyses, the conservation, absence or expansion of the genes coding for the *F. graminearum* secreted proteins was explored by BLASTP analysis, determined at two levels of confidence, $p < e^{-5}$ and $p < e^{-40}$.

6.2.2. Analysis of chromosome location alongside other key features of the *F. graminearum* genome

To inspect the position of individual or clusters of genes on the four *F. graminearum* chromosomes, the Fgra3Map tool was downloaded from www.Omnimapfree.org which displays a map of the complete *F. graminearum* genome (MIPS version 3.1). The Fgra3Map was used according to methods described (Antoniw *et al.*, 2011).

6.3. Results

6.3.1. The secretome of *F. graminearum*

In the original genome paper (Cuomo *et al.*, 2007), the secretome was predicted from the FG1 gene call using only the TargetP software. In the current study we analysed an updated, refined FG3 gene call (13,937 proteins) of the *F. graminearum* genome in two phases. In the first phase (Figure 34A), designed to predict all possible secreted proteins, SignalP and TargetP were used to identify secreted proteins with signal peptides (1,853 proteins) and those predicted to contain GPI anchors (120 proteins) were identified. After removal of the signal peptide, any mature proteins that contained a transmembrane domain were excluded. An initial screen used ProtComp software to exclude proteins that were probably not located in the extracellular space. This produced a set of 1,369 secreted proteins (including those with GPI anchors). Phase 2 (Figure 34B), designed to identify proteins with a

high probability of being secreted, contained more stringent conditions to further refine this set of proteins, discarding both those that did not begin with a methionine and small proteins where the mature proteins were shorter than 20 amino acids. At this stage, the 41 proteins with a TM domain predicted within the signal peptide sequence were also excluded. Similarly, all proteins predicted to contain a GPI-anchor were removed. A second software package (WolfPSort) that predicts the eventual location of proteins was used to identify only those proteins secreted to the extracellular spaces (extracellular score > 17). This resulted in a reduced set of 574 secreted proteins. In total 99 % of the refined *F. graminearum* is supported by transcriptional evidence from published *in vitro* and *in planta* investigations. Five of the fungal genes included within the refined secretome have not been assigned Affymetrix probe-sets and are therefore not supported by transcriptional evidence.

The MIPS annotation and functional classification was determined for the 574 secreted proteins present in the FG3 gene call (http://mips.helmholtz-muenchen.de/genre/proj/FGDB/). Of these, 278 proteins possessed information on protein function whilst 296 proteins were described as hypothetical or conserved hypothetical.

The chromosomal location of the genes encoding the 574 secreted proteins was compared to the recombination frequency across the four chromosomes using Fgra3Map software (Antoniw *et al.*, 2011). Genes coding for secreted proteins were identified on all four chromosomes and were found to be preferentially located within sub-telomeric regions and regions with a high recombination frequency (Figure 35). A similar distribution pattern had been noted in the original FG1 analysis (Cuomo *et al.*, 2007). Annotated and unannotated genes of the secretome were equally represented within the high and low recombination regions of the genome. To inspect whether any *F. graminearum* genes that encode secreted proteins were organised in clusters the secretome was divided into genes that reside in regions of low or high frequency recombination and displayed on the genome. A few small clusters that demonstrated no clear conservation in function were identified in regions of low and high recombination (Figure 35). In total, 51.6 % of these genes were annotated as either hypothetical or conserved hypothetical. Secretome clusters were small in size, containing three to nine genes and were coded for by either DNA

stand. The clusters within areas of high recombination were sub-telomerically located on chromosomes 1 and 3 as well as an interstitial hot spot on chromosome 2. Eight clusters resided in regions of low recombination and were closely located within a 97 and 495 Kb region of chromosomes 2 and 3, respectively. The 9th cluster was located in a 'cool' sub-telomeric region on chromosome 1. No clusters were found on chromosome 4.

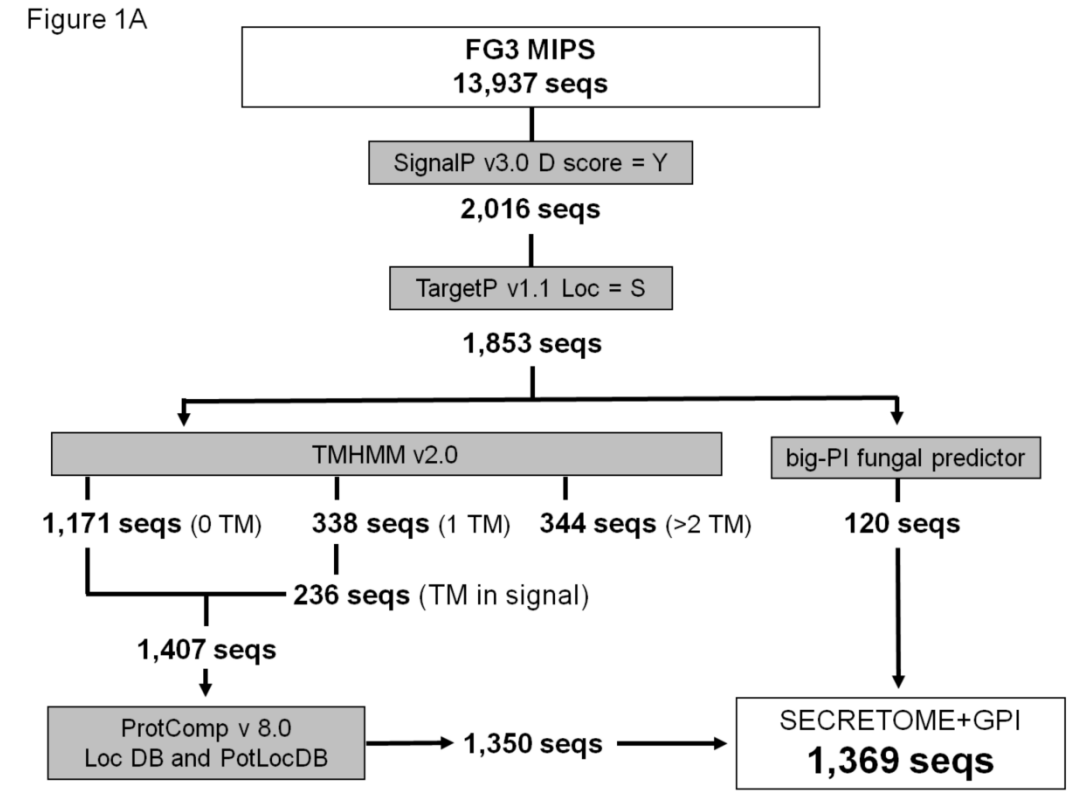

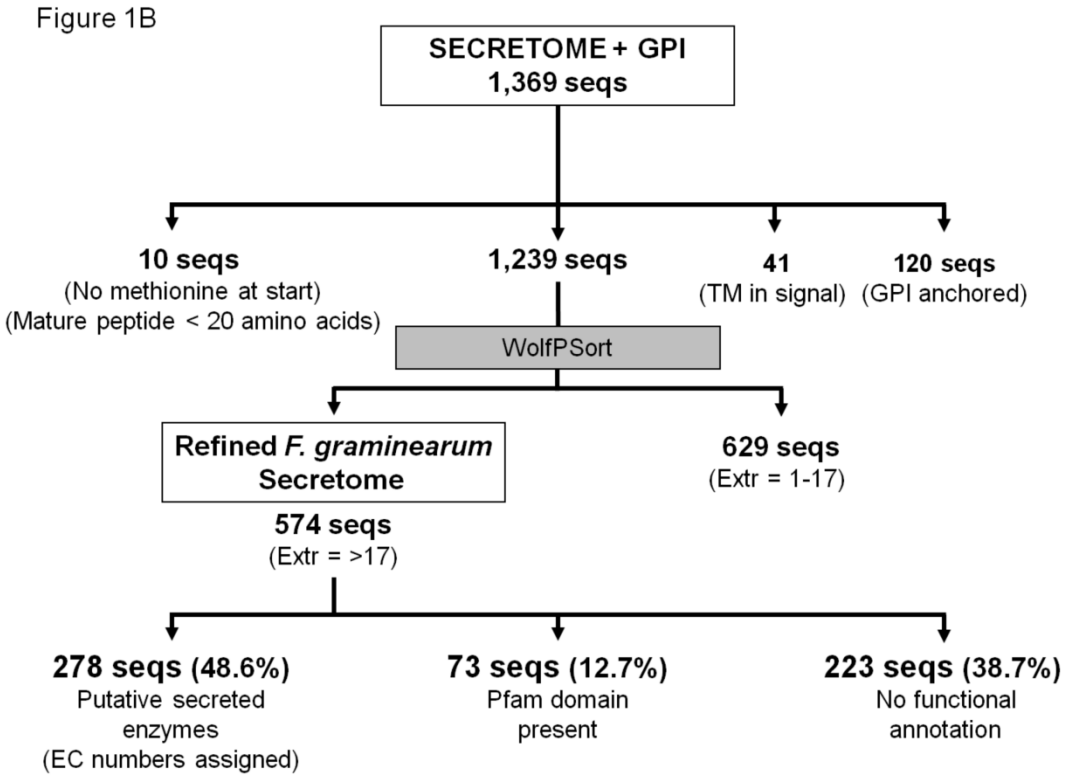

Figure 34 The bioinformatics pipelines used to predict **(A)** the *F. graminearum* secretome and **(B)** to refine the predicted *F. graminearum* secretome.

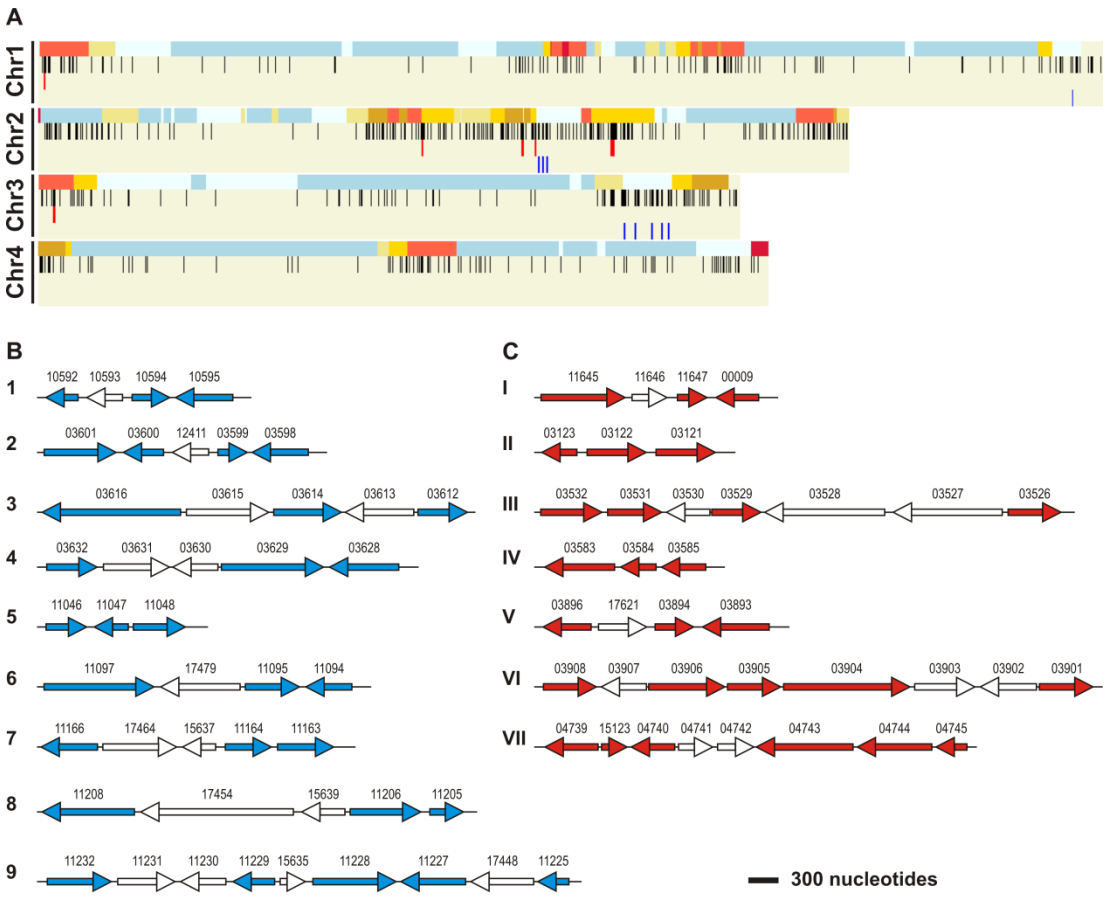

Figure 35 A) The distribution of the genes coding for the predicted *F. graminearum* secretome (black vertical bars, n = 574) across the four chromosome (Chr 1-4) aligned next to a heat map for genetic recombination (red = high to blue = low, recombination frequency - upper row of each chromosome) displayed on Fgra3Map. Some *F. graminearum* genes that encode secreted proteins were organised in clusters. The secretome was divided into genes that reside in regions of low (blue bars) or high frequency recombination (red bars) and displayed on Fgra3Map. Details of the gene clusters coding for secreted proteins in low **(B)** and **(C)** high recombination regions. Clusters are presented in chromosome order, while the coloured arrows (secreted proteins) or white arrows (non secreted proteins) represent gene orientation. Arrow length is proportional to gene length with the length of the scale bar representing 300 nucleotides. Genes are labelled with their respective FGSG_identifiers.

6.3.2. Analysis of the proteins with a predicted function

Closer inspection of the 278 proteins possessing information on protein function revealed that 243 contained at least one Pfam domain. A sub-set of 171 proteins was predicted to be involved in the degradation of plant derived compounds. These were divided according to substrate specificity (Table 8, Appendix 10 and 11). After excluding five fungal chitinases, the remaining 102 annotated proteins considered not to be involved in plant substrate degradation were organised according to their MIPS functional category. Each sub-set is described in turn.

Almost all host plant surfaces are coated by a waxy cuticle, which represents the first barrier to plant infection. The plant cell wall beneath consists of cellulose microfibrils cross- linked by an amorphous matrix of hemicellulose and pectin, often encased in lignin polymers as the plant matures. The *F. graminearum* secretome possesses an arsenal of secreted proteins and enzymes that target the plant cuticle and each of the cell wall components. This arsenal potentially involving up to 109 secreted proteins (Table 8 and Appendix 10). Thirty secreted proteins involved in the degradation of cellulose were identified, four of which were predicted to bind cellulose, fourteen were predicted to target β-1,4 glucans and twelve to target the breakdown product cellobiose. Enzymes that modify the different polysaccharides which make up hemicellulose represent the largest group of secreted cell wall modifying proteins and this reflects the diversity in hemicellulose composition. The two major components of hemicelluloses, arabinose and xylan, were targeted by the greatest number of secreted proteins. Nine secreted enzymes were detected that degrade the phenolic polymer lignin and its cross links to hemicellulose, including laccases, peroxidases and ferulic acid esterases. Multiple pectate lyases and pectin esterases, which breakdown pectin in the middle lamella and cell wall of the plant, were found. Callose is a polysaccharide of β-1,3 glucan that exists in plasmodesmata, phloem sieve plates and is laid down in response to wounding or imminent pathogen attack. Nine enzymes that target callose were identified, including endo- and exo- β-1,3 glucosidases.

Beyond the plant surface and the cell wall, the rest of the plant cell consists of proteins, lipid, sugars and nucleic acids. In total, 37 protein digesting enzymes were identified (Table 8 and Appendix 11), and included multiple alkaline / neutral and

serine / aspartyl proteinases as well as amino, carboxy and endo peptidase. In contrast, only three enzymes were identified that were predicted to breakdown starch into sugars suitable for uptake by the fungal cell. These were two amylases and a glucose dehydrogenase. A high number of secreted enzymes that target lipids were identified, including 15 triacylglycerol lipases. Therefore, *F. graminearum* secretes an array of proteins that possess the ability to degrade and utilise the plant cell in its entirety. In a comparative analysis performed in 2006, before the *F. graminearum* genome was published (Cuomo *et al.*, 2007), 103 plant cell wall degrading enzymes were predicted (Kämper *et al.*, 2006).

Table 8 The number of secreted *F. graminearum* proteins possibly involved in the degradation of the different components of the wheat host cell.

Plant cell component	**Target for degradation**	**Number of secreted proteins**
Waxy cuticle	Cuticle	2
Plant cell wall	Cellulose	30
	Hemicellulose	46
	Lignin	9
	Callose	9
Plant cell wall and the middle lamella	Pectin	13
Plasma membranes and fat bodies	Lipids	19
Starch bodies	Starch	3
Situated throughout the cell, e.g. wall, membrane and protein bodies	Proteins	37
Plasma membranes	Choline	3
Total		**171**

The sub-set of 102 MIPS annotated secreted proteins not predicted to function in the degradation of plant cells were organised according to their MIPS functional category and scrutinised further (Appendix 12). Within this diverse selection of proteins, those involved in metabolism accounted for the greatest proportion (43 %; Figure 36). These included acid / alkaline phosphatases, alcohol oxidases, a salicylate hydroxylase and four extracellular nucleases (Table 9).

The other MIPS functional categories that were highly represented within the annotated sub-set were proteins with binding functions or cofactor requirements and cell rescue, defence and virulence. Two fungal proteins similar to plant pathogenesis related (PR) proteins PR1 in *Nicotiana tabacum* and PR5K pathogenesis-related thaumatin family protein in *A. thaliana* were identified. The only protein to possess both nuclear export and location signals was FGSG_04685 and this protein contained a dioxygenase domain that incorporates O_2 into an unknown substrate. Two *F. graminearum* secreted proteins were predicted to be phytotoxic and were highly related ($6e^{-40}$ and $9e^{-47}$) to the *S. nodorum* phytotoxin, Snodprot1 (Hane *et al.*, 2007). Four other *F. graminearum* secreted proteins were predicted to possess antifungal properties and three of these were related to the KP4 killer toxin from *U. maydis* (Koltin & Day, 1976). Two detoxifying lactonohydrolases were identified.

Despite the stringency of the requisites of the predicted *F. graminearum* several proteins believed to be intracellular were present. Two orthologs of *GEGH16* from the powdery mildew fungi *B. graminis* f. sp. *hordei* and Gas1 and Gas2 from *M. oryzae* that function in pathogenicity and penetration (Xue *et al.*, 2002) were predicted to be secreted. However, fluorescently labelled Gas proteins localised to the cytosol of *M. oryzae* appressoria implying that the two *F. graminearum GEGH16* homologues may not be secreted (Xue *et al.*, 2002). The trichothecene 3-O esterase code by *TRI8* (FGSG_03532), was also predicted to be secreted, but this biosynthetic enzyme is not detected in culture filtrates of *F. sporotrichioides* (McCormick & Alexander, 2002) suggesting that it is also not extracellular in *F. graminearum*.

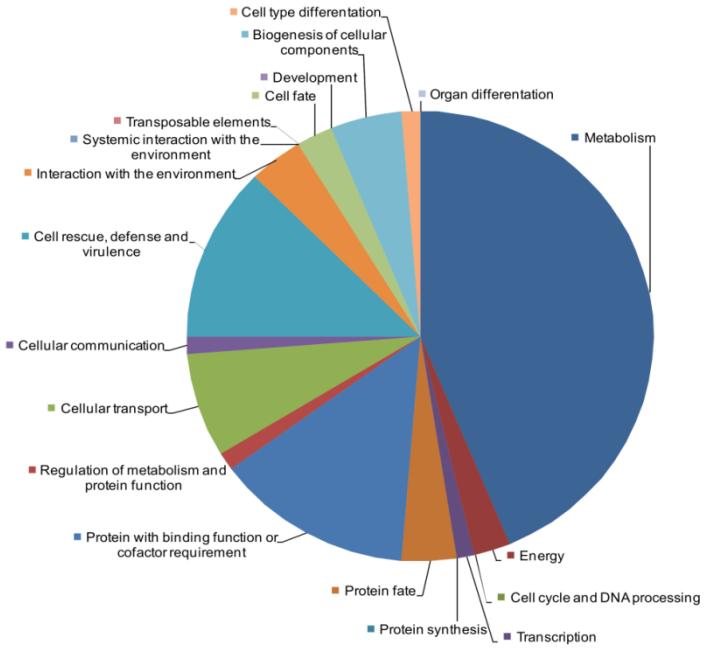

Figure 36 The sub-set of MIPS annotated secreted *F. graminearum* proteins, which are not involved in the degradation of plant cells, organised according to their MIPS functional category (http://mips.helmholtz-muenchen.de/genre/proj/FGDB/). N = 102.

Table 9 A selection of MIPS annotated secreted *F. graminearum* proteins, which are not involved in the degradation of plant cells, but are associated with metabolism or pathogenicity.

Function	FGSG_ID	MIPs Annotation
Acid / alkaline phosphatases	FGSG_04504	Related to acid phosphatase precursor
	FGSG_05933	Related to acid phosphatase precursor
	FGSG_06610	Related to alkaline phosphatase D precursor
	FGSG_07608	Related to acid phosphatase precursor
	FGSG_07678	Related to acid phosphatase Pho610
Alcohol oxidases	FGSG_03307	Related to isoamyl alcohol oxidase
	FGSG_03616	Related to isoamyl alcohol oxidase
	FGSG_03972	Related to isoamyl alcohol oxidase
	FGSG_06438	Related to isoamyl alcohol oxidase
	FGSG_07838	Probable isoamyl alcohol oxidase
	FGSG_10986	Related to alcohol oxidase
	FGSG_12127	Probable isoamyl alcohol oxidase
	FGSG_12390	Related to alcohol oxidase
	FGSG_13450	Related to isoamyl alcohol oxidase
	FGSG_13840	Probable isoamyl alcohol oxidase
Salicylate hydroxylase	FGSG_08116	Related to salicylate hydroxylase
Extracellular nucleases	FGSG_02686	Related to ribonucleases
	FGSG_03379	Related to ribonucleases
	FGSG_11190	Probable ribonuclease T1
	FGSG_15003	Related to dnase1 protein
Phospholipases	FGSG_08150	Related to PLB1 - phospholipase B (lysophospholipase)
	FGSG_11236	Related to non-hemolytic phospholipase C precursor
PR-like proteins	FGSG_03109	Related to plant PR-1 class of pathogen related proteins
	FGSG_08549	Related to pathogenesis-related protein PR5K (thaumatin family)
Antifungal proteins	FGSG_00060	Related to KP4 killer toxin
	FGSG_00061	Related to KP4 killer toxin
	FGSG_00062	Related to KP4 killer toxin
	FGSG_04745	Related to antifungal protein
Pathogenicity related	FGSG_00006	Related to gEgh 16 protein
	FGSG_09353	Related to gEgh 16 protein
Phytotoxin	FGSG_10212	Probable SnodProt1 precursor
	FGSG_11205	Probable SnodProt1 precursor
Detoxification	FGSG_03816	Probable lactonohydrolase
	FGSG_10675	Related to lactonohydrolase

6.3.3. Analysis of the proteins with no predicted function

The remaining 295 predicted secreted proteins that lacked annotation were analysed for internal amino acid repeats, high cysteine content and Pfam domains. The majority of these proteins, 190, are conserved. Protein functional domains can be predicted by sequence similarity. Using the Pfam database (http://pfam.sanger.ac.uk/) a total of 82 functional protein domains were found to be present within 73 secreted proteins, including 11 proteins with multiple Pfam domains (Appendix 13). The most abundant domain is Pfam04616 that belongs to the glycoside hydrolase 43 family (n=5), which have been reported to have arabinofuranosidases, arabinanase and xylosidase activity. Other common domains included; a GDSL-like lipase domain (Pfam00657) involved in lipid metabolism (n=4), a beta-lactamase domain (Pfam00144) associated with antibiotic resistance (n=4), a nuclease / phosphatase family domain (Pfam03372) involved in intracellular signalling (n=3), a necrosis inducing protein domain (Pfam05630) similar to the NPP1 protein from *P. infestans* (Fellbrich *et al.*, 2002) (n=3), and a carbohydrate-binding domain (Pfam10528) found in fungal adhesins (n=3).

The unannotated *F. graminearum* secreted proteins were screened at two thresholds, where the total number of cysteine residues represented greater than 5 or 10 % of the mature protein. The majority (80 %) of these predicted proteins had an even number of cysteine residues (Cys). At the > 5% Cys threshold, 61 proteins were identified (31 conserved and 30 hypothetical proteins) (Appendix 14), whilst at the > 10 % Cys threshold, 11 proteins were identified (7 conserved and 4 hypothetical proteins) (Table 10). Four of these FGSG genes were not identified in the other *Fusarium* species. Orthologs of the 29 *F. graminearum* proteins with 4, 6 or 8 cysteine residues were determined using BLASTP. Of these *F. graminearum* proteins 20 were conserved amongst the Fusaria while seven had no strong hits. Eight, five and three proteins were conserved in other saprotroph (*Aspergillus* species and *Neurospora crassa*), necrotrophs (*Botrytis cinerea*, *Cochliobolus heterostrophus*, *Sclerotinia sclerotiorum*, *S. nodorum* and *Pyrenophora tritici-repentis*) and hemibiotrophs (*M. oryzae*, *P. infestans* and *Verticillium albo-atrum*), respectively. The locus FGSG_03969 was atypical, coding for a somewhat larger

mature protein at 482 amino acids in length of which 58 (12 %) were cysteine residues and also contained 13 internal amino acid repeats.

All 574 sequences were inspected for the presence of the degenerative RxLR-dEER motifs (Tyler, 2009) in close proximity to the predicted signal peptide sequence. However, no exact matches were found within the refined *F. graminearum* secretome. The unannotated portion of the predicted secreted proteins were screened for the presence of both perfect and imperfect internal repeats using the RADAR software (Heger & Holm, 2000). This analysis identified 28 proteins ranging from 297-1862 amino acids in length of which five were also cysteine-rich (>5%). Multiple copies of nine of these proteins were found by BLASTP at two different thresholds, four at e^{-100} and nine at e^{-40} (Table 10). The 28 secreted proteins of *F. graminearum*, which were predicted to contain internal repeats, were highly conserved. For example; *F. oxysporum* f. sp. *lycopersici* possessed 19, *F. solani* 21, *F. verticillioides* 22 and *M. graminicola* 22 orthologous proteins (Table 10).

Gene family size for each *F. graminearum* encoded secreted protein of unknown function was determined by BLASTP. As anticipated, the majority of the *F. graminearum* gene families were larger in the other *Fusarium* species (*F. oxysporum* f. sp. *lycopersici*, *F. solani* and *F. verticillioides*). A limited number of proteins including four conserved hypothetical and six hypothetical proteins demonstrated gene expansion within the Fusaria (Table 10). The function of these secreted proteins is unclear as they possess no Pfam domains. The *F. graminearum* secreted proteins were also screened for the expansion of gene families in other fungal organisms. A single gene, FGSG_08958, was expanded in *F. oxysporum* (43 copies) and *F. solani* (23 copies) as well as other saprotrophic and soil dwelling organisms including 26 to 52 copies in *Trichoderma spp.*, 30 copies in *A. nidulans*, and 22 copies in *Chaetomium globosum*. The conserved hypothetical, FGSG_08958, contained a nucleoside phosphorylase domain. Four genes were dramatically expanded in *Phytophthora* species with up to 19 copies identified ($p < e^{-40}$). Ten copies of a single gene FGSG_ 03708 were detected in *M. graminicola* and *M. fijiensis* ($p < e^{-40}$).

Table 10 The *F. graminearum* genes predicted to encode secreted proteins of unknown function that are cysteine-rich (> 10 % mature protein) (A), possess internal amino acid repeats (B) or are encoded by an expanded gene families in *F. graminearum* (C). Fol = *F. oxysporum* f. sp. *lycopersici*, Fs = *F. solani*, Fv = *F. verticillioides* and Mg = *M. graminicola.*

Analysis	Locus_ID	Mature peptide length	Cysteine residues		Radar repeats	Pfam domain	Twin e-40	Conservation			
			Number	Percentage of mature peptide				*Fv*	*Fol*	*Fs*	*Mg*
A	FGSG_00260	60	6	10	-	-	0	1.11e-28	-	5.32e-23	9.8e-20
	FGSG_03969	482	58	12.03	13	-	0	4.14e-141	5.25e-158	8.65e-106	2.31e-97
	FGSG_03599	77	10	12.99	3	-	0	3.93e-21	5.20e-27	-	-
	FGSG_06712	129	16	12.4	3	-	0	1.12e-27	3.01e-27	5.56e-28	6.08e-14
	FGSG_09066	64	8	12.5	2	-	0	4.00e-14	6.05e-15	1.56e-12	1.07e-22
	FGSG_12214	79	10	12.66	2	-	0	5.23e-47	2.37e-47	-	-
	FGSG_15142	71	8	11.27	-	-	0	-	-	-	-
	FGSG_15437	53	8	15.09	-	-	0	-	-	-	-
	FGSG_15448	71	8	11.27	-	-	0	-	-	-	0.00022
	FGSG_15251	47	6	12.77	-	-	0	-	-	-	-
	FGSG_15661	77	10	12.99	-	-	0	1.04e-21	-	-	-
B	FGSG_00002	714	70	9.8	15	-	1	9.94e-46	2.01e-129	8.05e-83	4.47e-95
	FGSG_00031	1349	25	1.85	12	05109	1	-	-	1.22e-10	-
	FGSG_00411	518	3	0.58	8	-	0	1.07e-85	2.08e-115	3.20e-46	6.03e-50
	FGSG_00987	321	0	0	5	-	0	4.32e-40	3.22e-44	3.75e-12	-
	FGSG_01570	363	4	1.1	6	-	0	2.68e-86	6.27e-92	5.31e-64	1.35e-60
	FGSG_01588	708	18	2.54	5	09770	0	4.81e-59	2.12e-70	1.64e-34	2.88e-33
	FGSG_02448	588	5	0.85	6	05109	0	3.69e-41	1.03e-50	1.35e-23	4.54e-22
	FGSG_02888	997	41	4.11	5	05109	1	6.68e-78	1.14e-80	1.14e-41	5.87e-40
	FGSG_02898	1195	98	8.2	10	-	0	1.50e-77	1.54e-47	-	6.52e-28
	FGSG_03054	365	2	0.55	6	-	0	-	-	2.33e-165	7.02e-163
	FGSG_03274	861	16	1.86	6	-	1	9.78e-143	2.73e-169	8.83e-07	8.26e-15
	FGSG_04429	974	52	5.34	6	-	0	-	-	3.43e-28	5.26e-21
	FGSG_04563	297	0	0	5	-	0	5.22e-10	-	-	-
	FGSG_04824	682	9	1.32	9	09770	0	4.10e-23	3.39e-06	1.73e-06	1.45e-05

Table 10 continued The *F. graminearum* genes predicted to encode secreted proteins of unknown function that are cysteine-rich (> 10 % mature protein) (A), possess internal amino acid repeats (B) or are encoded by an expanded gene families in *F. graminearum* (C).

Analysis	Locus_ID	Mature peptide length	Cysteine residues		Radar repeats	Pfam domain	Twin e-40	Conservation			
			Number	Percentage of mature peptide				*Fv*	*Fol*	*Fs*	*Mg*
B	FGSG_04900	428	9	2.1	6	-	0	2.95e-45	2.86e-07	1.13e-32	1.38e-22
	FGSG_05719	1136	20	1.76	6	-	1	-	-	-	3.79e-51
	FGSG_06479	745	32	4.3	7	-	3	1.55e-164	1.75e-137	1.07e-80	4.51e-67
	FGSG_09142	328	0	0	6	-	0	1.03e-164	1.11e-165	6.35e-131	6.76e-126
	FGSG_10435	1746	40	2.29	9	Multiple*	0	-	-	-	-
	FGSG_10676	995	4	0.4	17	05792/10528	2	9.35e-159	-	1e-45	1.53e-46
	FGSG_10972	355	5	1.41	6	-	0	3.13e-08	9.90e-33	-	-
	FGSG_11238	578	25	4.33	5	-	2	8.73e-60	7.18e-47	2.13e-111	1.54e-118
	FGSG_11379	442	9	2.04	8	-	0	8.15e-52	9.56e-52	9.43e-52	8.44e-50
	FGSG_12918	499	24	4.81	6	-	2	3.25e-106	5.08e-130	1.27e-70	9.21e-88
	FGSG_12439	638	58	9.09	12	-	0	5.03e-58	4.75e-174	4.89e-95	6.05e-88
	FGSG_13583	1862	0	0	25	-	0	-	-	-	2.49e-12
C	FGSG_00111	113	5	4.42	-	-	0	-	1.53e-52	-	-
	FGSG_07755	86	6	6.98	-	-	0	1.43e-36	2.17e-49	2.76e-24	1.30e-21
	FGSG_08026	754	14	1.86	4	-	2	3.39e-63	1.01e-60	2.64e-38	1.99e-47
	FGSG_08213	328	10	3.05	2	-	1	-	9.73e-31	7.80e-11	3.93e-08
	FGSG_09071	359	10	2.79	3	-	0	2.28e-06	3.48e-09	-	-
	FGSG_11276	618	9	1.46	4	-	1	2.05e-47	1.28e-48	6.21e-21	5.66e-21
	FGSG_11675	259	3	1.16	3	-	0	5.69e-48	2.79e-49	-	-
	FGSG_12434	564	24	4.26	4	-	0	4.47e-54	1.44e-118	7.50e-158	2.28e-144
	FGSG_12622	275	7	2.55	3	-	0	-	-	1.68e-08	4.35e-06
	FGSG_13443	114	4	3.51	-	-	0	-	7.13e-43	-	-

* FGSG_10435 Pfams: 01034, 01822, 03154, 03935, 03999, 04415, 04484, 04683, 05109, 05110, 05539, 05642, 05792, 05955, 06075, 06933, 07010, 07218, 07263, 08550, 08580, 08601, 08639, 08702, 08729, 09319, 09595, 09726, 09786 and 10033.

6.3.4. Comparison of the predicted *F. graminearum* secretome with a broad range of fungal and oomycete species

A total of 57 genomes covering animal / plant pathogens, saprotrophs and free living eukaryotic microbes were assembled. This list included 44 fungal and oomycete species (Appendix 9). The objective of this part of the study was to identify the *F. graminearum* specific secreted proteins, and the level of gene sequence conservation between species with a range of lifestyles or tissue specificities. Each genome was screened for the presence of *F. graminearum* secretome homologues (Table 11). The results from this BLASTP analysis are reported at two levels of stringency, however for clarity the results obtained at a p value < e^{-5} are focused upon below.

The majority of the *F. graminearum* secretome was detected in all four *Fusarium* species assessed (78.05 %), while 5.4 % of the *F. graminearum* secretome was unique to these four *Fusarium* species and not detected in other the fungi or oomycetes (Appendix 15) including, 22 hypothetical proteins, eight conserved hypothetical proteins and a related cell wall mannoprotein. An additional 3.31 % of the secretome was only found in *F. graminearum* (Appendix 16). These 19 genes that all encoded hypothetical proteins therefore represent either the species specific and / or strain specific secreted gene repertoire.

Among the four Fusaria assessed, *F. solani* was the most dissimilar to the *F. graminearum* secretome, showing 82.75 % conservation, while *F. oxysporum* f. sp. *lycopersici* and the *F. verticillioides* demonstrated 88.5 % and 88 % conservation, respectively. The *F. graminearum* secretome was well conserved beyond these four Fusaria, with a total of 83.97 % being conserved in at least one additional species. Of the other fungal genomes analysed, the predicted ascomycete secretomes of the rice infecting pathogen *M. oryzae* and the wheat infecting pathogen *S. nodorum* showed the most similarity to the *F. graminearum* secretome, with 66.38 % and 66.03 % of genes conserved, while only 56.97 % of the secretome was conserved in the closely related saprotroph *Trichoderma reesei.* The basidomycete biotroph *U. maydis* demonstrated 38.85 % conservation, more than the ascomycete obligate biotroph *B. graminis* f. sp. *hordei* at 30.14 %. The oomycete hemibiotroph *P. infestans* demonstrated 32.4 % conservation. The yeast secretomes, including the animal

pathogen *Candida albicans* at 17.07 %, and non-pathogen *Saccharomyces cerevisiae* at 14.81 %, were less well conserved.

Conservation of the *F. graminearum* secretome was subsequently determined for the different sub-sets of species depending on host tissue specificity including, animal, plant and cereal ear or cereal leaf infecting pathogens (Appendix 9). The other Fusaria genomes were excluded from these analyses. Conservation of the *F. graminearum* secretome among 13 animal pathogens was surprisingly high at 68.64 %, however this was still lower than the conservation with plant and cereal ear or cereal leaf infecting pathogens at 80.14 %, 73 % and 76.13 %, respectively.

The genomes of plant interacting organisms were divided according to their mode of colonisation. The *F. graminearum* secretome was most well conserved within the nine saprotrophic species that obtain nutrition from dead plant material (78.05%). Conservation of the *F. graminearum* secretome among the seven hemibiotrophs, and seven necrotrophs was also high at 76.13 % and 73.52 %, respectively. The only class of plant pathogens within which the *F. graminearum* secretome was poorly conserved was the seven biotrophs (54.53 %). This figure is substantially less than the level of conservation with the 13 animal pathogens. This result we consider to be somewhat artifactual and has been caused by the underrepresentation of ascomycete species within the biotroph sub-set. The only genome that is currently available for an ascomycete species that has a biotroph lifestyle is *B. graminis* f. sp. *hordei.* This species forms abundant intracellular haustoria. The other six species of biotrophs were either basidiomycetes or oomycetes, whereas in the animal pathogens examined there were 10 ascomycetes. The two non-pathogens, *S. cerevisiae* and *Schizosaccharomyces pombe*, demonstrated a very poor level of conservation (22.13 %) with *F. graminearum*.

When this comparative analysis was repeated using a higher confidence level ($p < e^{-40}$) a similar pattern of conservation and species ranking was revealed (Table 11). However, the number of *F. graminearum* specific, and Fusaria unique, proteins increased substantially. At this p value 103 genes were still considered to be *F. graminearum* specific and 179 genes were considered to be *Fusarium* specific.

Table 11 Conservation of the *F. graminearum* (*Fg*) genes, predicted to encode secreted proteins, among the 57 fungal genomes assessed and the analysis of individual sub-sets of species depending host range and lifestyle. Conservation was determined at two confidence levels, $p < e^{-5}$ and $p < e^{-40}$. Sub-sets including all secreted proteins, only the hypothetical proteins or only the conserved hypothetical proteins were assessed in turn. Analyses: A) determined the *Fg* and *Fusarium* (*Fus*) specific gene sets, B) compared gene conservation relative to tissue specificity, C) examined conservation between different microbial lifestyles. Apart from *Fg*, the three other *Fus* species were excluded from analyses B and C.

		All secreted proteins	
Analyses	**Sub-sets**	**e-5**	**e-40**
	Total gene number	**574**	
A	*Fg* specific	**19 (3.31 %)**	**103 (17.94 %)**
	All *Fus*	448 (78.05 %)	365 (63.59 %)
	Unique to all *Fus*	**31 (5.4 %)**	**179 (31.19 %)**
	Fg + other non *Fus*	482 (83.97 %)	395 (68.82 %)
B	Animal pathogen	**394 (68.64 %)**	**289 (50.35 %)**
	Plant pathogen	460 (80.14 %)	372 (64.81 %)
	Cereal ear pathogen	419 (73 %)	337 (58.71 %)
	Cereal leaf pathogen	437 (76.13 %)	344 (59.93 %)
C	Budding yeast	**127 (22.13 %)**	**35 (6.1 %)**
	Biotroph	313 (54.53 %)	156 (27.18 %)
	Hemibiotroph	437 (76.13 %)	361 (62.89 %)
	Necrotroph	422 (73.52 %)	330 (57.49 %)
	Saprotroph	448 (78.05 %)	354 (61.67 %)

6.3.5. Comparison of the predicted secretome with published *F. graminearum* proteomic data sets

A proteomic comparison of the secretome from *F. graminearum* grown *in vitro* and *in planta*, identified 122 extracellular proteins and according to Paper and colleagues (2007), 68 of these proteins possessed a signal peptide. Only 14 of the 68 proteins identified were detected exclusively *in planta*, and these included a metallopeptidase, a KP4 killer toxin, a pectin lyase and an endoglucanase. A total of 68 % of the proteins found in the proteomic study were also identified in our predicted secretome, which was designed to be extra stringent. In the proteomic study, nine proteins detected and found to have a signal peptide, were excluded from the predicted secretome generated by this study due to the stringency of the combined SignalP, TargetP and WolfPSort analysis. The majority of the 68 proteins not detected in the predicted secretome were excluded during the WolfPSort analysis. A cut off score of 18 had been used. For all 68 proteins to have been included a far lower WolfPSort cut off score would have needed to have been used, and this would have raised considerably the potential number of false positives included within these analyses. Even when the WolfPSort score was lowered to 17, this included three proteins where the probability scores from SignalP were only modest. The other 46 proteins detected in the proteomic study, which lacked signal peptides were all excluded from this detailed analysis by the WolfPSort analysis. The authors of the proteomic study (Paper *et al.*, 2007) concluded that the detection of these proteins may have arisen, because the *Fusarium* cell ruptured during sample preparation. For example, NADP-dependent oxidoreductase and elongation factor 1 are not known in other species to be extracellularly located.

6.4. Discussion

Communication through the secretion of proteins and metabolites frequently defines the outcome of the interaction between a host and a fungal symbiont, irrespective of their lifestyle (Gan *et al.*, 2010, Howlett, 2006, Tan *et al.*, 2010). During the formation of Fusarium Ear Blight disease an intimate host-pathogen association develops and an extended growth phase occurs in the apoplast, which is extracellular to the living wheat cells (Brown *et al.*, 2010). In the original analysis of the newly sequenced *F. graminearum* genome, only TargetP was used to predict the secretome (Cuomo et al., 2007). Since this time, the gene call for *F. graminearum* has been considerably changed through the combined efforts of the BROAD and MIPS. In the current study, a refined *F. graminearum* secretome was predicted by the combination of multiple bioinformatic approaches. This strategy increased the probability of identifying truly secreted proteins. A secretome size of 574 proteins is predicted for *F. graminearum*, representing 4.2 % of the predicted total gene repertoire. The cell biology of the different phases of wheat ear infection depicts a situation where *Fusarium* hyphae are exposed to different environments / distinct substrates, thereby causing transcriptional, proteinaceous and metabolic changes. *Fusarium* hyphae in the symptomless phase of infection are in close contact with live plant cells for two to three days (Brown *et al.*, 2010). During this prolonged latent period, communication between pathogen and host must occur. After several days the wheat cells die and are intracellularly colonised by the pathogen resulting in the development of visible disease symptoms and asexual sporulation. Transcriptional differences between the two phases of infection have been confirmed for the biosynthetic genes responsible for the virulence factor DON, which showed maximal *TRI* gene expression during symptomless infection (Brown *et al.*, 2011). The secretion of DON is hypothesised to inhibit the plant's ability to respond to infection by impeding protein synthesis (Ueno, 1984). Mechanisms in addition to DON mycotoxin may also be required to promote infection, implicating a role for the *F. graminearum* secretome (Cuomo *et al.*, 2007). Therefore, an in depth re-analysis of the secretome's capabilities was undertaken.

The comparative genomics analysis of 57 fungal and oomycete genomes revealed a high level of secretome conservation among filamentous ascomycetes,

irrespective of their mode of obtaining nutrition from plant or animal hosts or during a free living lifestyle. This high level of secretome conservation may reflect the ability of *F. graminearum* to survive both as a pathogen and as a saprotroph. The identification of 31 *Fusarium* specific and 25 *F. graminearum* specific secreted proteins, of which all were functionally unannotated proteins, may represent the conserved and unique protein-protein interactions that assist *Fusarium* pathogenicity. The predicted *F. graminearum* secretome, with a size of 1,369 from the initial analysis and 574 from the refined selection (Figure 34) appears larger than the *U. maydis* (426) secretomes, but possibly slightly smaller than that of *M. graminicola* (1,020, J. Antoniw, J. Rudd and K. Hammond-Kosack, Unpublished) and *M. oryzae* (739) (Dean *et al.*, 2005, Kämper *et al.*, 2006, Spanu *et al.*, 2010). However, the size of these fungal secretomes was predicted using slightly different approaches, with the exception of *M. graminicola*. Despite representing a large fungal secretome, the refined set of *F. graminearum* secreted proteins demonstrated less species specificity than the biotrophic pathogens *B. graminis* and in particular *U. maydis* where two thirds of the secreted proteins are species specific.

As previously noted, the *F. graminearum* secretome predominantly localises to hot spots of chromosomal recombination and sub-telomeric regions (Cuomo *et al.*, 2007) facilitating alterations to the secretome that could enable the pathogen to cope with changes in the host plant response. However, some genes predicted to encode a secreted protein were located in the intervening low or no recombination regions found on each of the four chromosomes. In addition, several small clusters of secreted proteins (ranging from 3 – 6 genes) were identified in regions of the genome located with either a low or a high level of recombination and in both sub-telomeric and more central locations. Unlike *U. maydis* (Kämper *et al.*, 2006) these *F. graminearum* clusters did not contain genes of similar function and did not represent gene duplication events.

In total 99 % of the refined bioinformatic prediction of the *F. graminearum* secretome was supported by transcriptional evidence. During early *F. graminearum* infection *TRI* gene expression is up-regulated at the advancing hyphal front in the florets (Boenisch & Schäfer, 2011) and the rachis tissue (Brown *et al.*, 2011). Along with the array of secreted proteins, DON may inhibit the plant cells ability to detect

or respond to infection. The small cysteine-rich secreted proteins, of which many contained internal amino acid repeats, and the additional protein related to a circumsporozoite that has been shown to inhibit protein synthesis in cells infected by malaria *Plasmodium* parasites (Menard *et al.*, 1997) may also play a role in establishing wheat infection. An ability to obtain nutrition from the apoplast and possibly inhibit, or circumvent, plant defences is in agreement with the observed lack of physiological changes to the plant cells during this initial phase of infection (Brown *et al.*, 2010).

After a latent period of infection wheat host cells die prior to, or at the same time as, *F. graminearum* hyphae penetrate host cells *en masse* (Brown *et al.*, 2010). Whether host cell death is induced by the plant in an attempt to limit infection, or by the fungus to obtain nutrition, remains unknown. The two small secreted proteins, related to Snodprot1 from *S. nodorum* that has proven phytotoxin activity (Hall *et al.*, 1999) also contain the cerato-platanin Pfam07249 domain. In *Ceratocystis fimbriata,* the Snodprot1 protein exists in the fungal cell wall and has been shown to induce host cell phytoalexin synthesis as well as necrosis (Pazzagli *et al.*, 1999). In *M. oryzae* the Snodprot1 homologue is required for full virulence (Jeong *et al.*, 2007). Several *F. graminearum SNODPROT1* homologues were identified in the secretome that have been demonstrated to be transcribed during wheat ear infection (Lysoe *et al.*, 2011). From the extracellular location, the possible phytotoxic activity of these two small *F. graminearum* secreted proteins may play a role in the induction of host cell death. In wheat, infiltration of high concentrations of DON mycotoxin into healthy leaves has been shown to elicit hydrogen peroxide production and programmed cell death (Desmond *et al.*, 2008). Therefore, the level or length of exposure to the mycotoxin could also be involved in the induction of host cell death. Interestingly, several lactonohydrolases were predicted in the secretome. A novel lactonohydrolase cloned from *Clonostachys rosea* into *S. pombe* or *Escherichia coli* was able to detoxify the trichothecene mycotoxin, zearalenone (Takahashi-Ando *et al.*, 2002, Takahashi-Ando *et al.*, 2004). The localised secretion of a lactonohydrolase by *F. graminearum*, may therefore act as a self defence mechanism, in addition to the experimentally proven Tri101 protein (McCormick *et al.*, 1999).

Once within dead plant tissue *F. graminearum* is predicted to secrete an array of PCWDEs and other enzymes, far more than many other fungal pathogens (Cuomo *et al.*, 2007, Soanes *et al.*, 2007). *F. graminearum* also appears to possesses the capacity to utilise the plant cell in its entirety, which is in agreement of the observed phenotype of wheat rachis infection (Brown *et al.*, 2010). This ability of the secretome to breakdown the plant cell is probably essential for *F. graminearum* pathogenesis, but will be difficult to test experimentally because of the problem of genetic redundancy. The extensive repertoire of PCWDEs would also assist in the saprotrophic phase of the *F. graminearum* lifecycle, which occurs post-harvest (Parry *et al.*, 1995).

F. graminearum may be able to produce a range of antifungal proteins, including FGSG_04745 and four KP4 killer toxins. Their production could prevent additional colonisation by fungal competitors and protect the niche the *F. graminearum* hyphae have occupied. The trichothecene mycotoxins may also have some antifungal activity (Lutz *et al.*, 2003). The *U. maydis* KP4 killer toxins provide antifungal activity by blocking calcium uptake thereby interfering with calcium signalling (Gage et al 2001). The increased production of antifungal proteins may be essential during late infection, reflecting the vulnerability of the dead plant tissue to further microbial colonisation.

The functional analysis of the secretome revealed the presence of a large set of extracellular proteins with a function in metabolism. This suggests *Fusarium* hyphae can manipulate or directly interfere with the plant's metabolism. Acid and alkaline phosphatases are responsible for protein dephosphorylation, which is pivotal to cell signalling. Alcohol oxidases catalyse the reaction between alcohol and O_2 releasing an aldehyde and H_2O_2, which is an important plant signalling molecule. Salicylate hydroxylase is capable of degrading the plant defence signalling molecule, salicylic acid, which has been shown to be required for maintaining basal defence against *Fusarium* in the floral tissues of Arabidopsis (Cuzick *et al.*, 2008a, Makandar *et al.*, 2010) while a delay in salicylic acid signalling has also been associated with increased *Fusarium* susceptibility in wheat ears (Ding *et al.*, 2011). The extracellular nucleases indicate the potential to degrade DNA / RNA or interfere with nucleic acid

function. Extracellular proteins involved in protein-binding were also highly represented.

Plant PR proteins are rapidly expressed upon the perception of pathogen attack (Sels *et al.*, 2008). The secretion by *Fusarium* of related PR proteins, such as PR1 and PR5K is intriguing. The *F. graminearum* PR1-like protein is conserved in *F. oxysporum*, *F. verticillioides*, *F. solani* and *M. oryzae*, while the PR5K-like protein in addition to the aforementioned species is widely conserved in *S. nodorum*, *S. sclerotiorum*, *P. tritici repentis*, *Leptosphaeria maculans*, *T. reesei* and *N. crassa.* The role of PR proteins in fungal pathogenesis has so far not been reported for any interaction.

Approximately half of the predicted secretome encoded for proteins of unknown function (n = 296). These proteins of unknown function could include key effectors that control host species or tissue specificity. To provide some annotation, these sequences were surveyed for functional domains and characteristics for high cysteine content, internal amino acid repeats and the presence of the consensus and / or degenerative RxLR motif. These additional analyses have provided sequence based annotation for the majority of the predicted secreted proteins of unknown function. A frequent functional domain present in the proteins of unknown function was the NPP1 domain, which has been associated with inducing plant necrosis during *P. infestans* infection (Fellbrich *et al.*, 2002) and is specifically expressed during the transition between biotrophic-necrotrophic *P. sojae* infection (Qutob *et al.*, 2002). However, in the *M. graminicola* wheat leaf interaction, which also switches from symptomless to symptomatic infection, a NPP1 homologue was not required for full virulence (Motteram *et al.*, 2009). Neither the consensus nor degenerative RxLR motif situated in the N terminus of the predicted protein was identified in the refined secretome studied here.

This study has greatly increased our understanding of the *F. graminearum* secretome and identified genes coding for secreted proteins that can be considered to be *Fusarium* conserved and *F. graminearum* specific. Once the genomic sequences of additional Fusaria species and strains and other fungal species are published, these secretome predictions can be further refined. In order to achieve a greater understanding of the transcriptional differences between the different phases of *in*

planta infection in different plant host species and different tissues, genome wide investigations coupled with a synchronised biological assay that accurately separates the different phases of infection will be required. The use of the *Fusarium* Affymetrix array (Guldener *et al.*, 2006) and / or a next generation deep-RNA sequencing approach would be ideal. The latter would also give considerable information, in parallel, on the nature of the induced host responses. The gene models for *F. graminearum* continue to evolve through the increased use of manual sequence corrections (Wong *et al.*, 2011). This activity is likely to lead to further refinements to the predicted *F. graminearum* secretome.

Chapter 7. Transcriptome analysis of the *Fusarium graminearum* - wheat ear interaction

7.1. Introduction

The discovery of different phases of *F. graminearum* wheat ear infection reignited the interest in transcriptome investigations. The prolonged latent phase of symptomless infection is accompanied by maximal *TRI* gene expression (Brown *et al.*, 2011)(Chapter 4). These intercellular hyphae are in association with live wheat cells for two to three days. Late symptomatic infection, in which *TRI* gene expression is reduced, is accompanied by autophagocytosis and the dramatic production of PCWDEs that culminates in asexual sporulation at the plant surface. These later inter- and intracellular hyphae are in association with dead wheat cells. The different characteristics of colonisation and the change in *TRI* gene expression suggest that *F. graminearum* modulates its transcriptome during the different phases of wheat ear infection (Brown *et al.*, 2011)(Chapter 4). The comparative evaluation of wheat infection by the *tri5* and *top1* deficient *F. graminearum* strains demonstrated the failure of DON alone to promote infection and implicated the requirement for additional secreted virulence factors (Chapter 5). A bioinformatic analysis of the *F. graminearum* secretome revealed many conserved hypothetical and taxon specific hypothetical proteins. Some of these proteins had characteristics of fungal effectors (Chapter 6). A transcriptome analysis of the two phases of infection will assist in the identification of highly expressed secreted proteins during symptomless colonisation, which may include unidentified *F. graminearum* effectors. The late symptomatic phase that includes perithecial formation and asexual sporulation is well studied in *F. graminearum* (Hallen & Trail, 2008). However, to identify the function of autophagocytosis and plant cell wall degradation, which occur in discrete locations within the plant tissue, cell-type specific transcriptome analyses would be required (Chapter 8).

Two independent gene predictions of the *F. graminearum* genome, by the BROAD and MIPS, were used in the construction of the *Fusarium* Affymetrix array (Guldener *et al.*, 2006). This *Fusarium* array was initially tested on three *in vitro* cultures, namely complete media (CM), CM minus carbon and CM minus nitrogen,

alongside the early infection of susceptible barley ears. No enrichment of the fungal transcripts from the *in planta* studies was required. Subsequently, multiple *in vitro* studies of sexual development, conidial and ascospore germination and DON induction were done (Gardiner *et al.*, 2009a, Guenther *et al.*, 2009, Seong *et al.*, 2008). These studies have already aided the identification of some genes directly involved in the production of the relevant phenotype. For example, a comparison of the transcriptome during growth on DON-induction and non-induction media identified two novel genes (FGSG_00007 and FGSG_10397). Genetic disruption of either gene enhanced DON production and virulence (Gardiner *et al.*, 2009a). Transcriptome analysis of single gene deletion *F. graminearum* strains has also proven informative. The regulation of DON production was investigated further using the *tri6* / *tri10* deficient strains and demonstrated that these regulators controlled the expression of over 200 genes (Seong *et al.*, 2009). The response of mycelial cultures to trichodiene intermediates, or end products, up regulated 153 genes enriched in cellular transport functions (Seong *et al.*, 2009) demonstrating that a metabolic feedback loop may enhance mycotoxin export.

Multiple wild-type infection time courses have been carried out, including the aforementioned barley ear blight study along with the wheat crown rot and wheat ear blight investigations (Guldener *et al.*, 2006, Lysoe *et al.*, 2011b, Stephens *et al.*, 2008). The wheat stem analysis of sexual development did not use a time course but was defined by perithecial developmental stage (Guenther *et al.*, 2009). Limited *in planta* transcriptome evaluations of single gene deletion strains exists. The developmental regulator StuA, involved in metabolism, secreted enzymes, cAMP signalling and virulence has been shown to control the expression of thousands of *F. graminearum* genes during wheat infection with their primary function being cell-cycle. The *stuA* strain exhibited reduced virulence, spore production and secondary metabolite synthesis (Lysoe *et al.*, 2011a). The absence of the Cch1 calcium channel, involved in ascospore discharge, was shown to influence the expression of 2449 genes, while having an effect on growth and development. The *cch1* strain was unable to infect wheat stalks and prevented colonisation by other saprotrophs (Hallen & Trail, 2008). Symptomless infection has not been explored in wheat crown rot, while is unexpected in barley as infection is confined to individual spikelets. The

previous transcriptome study of wheat ear infection (Lysoe *et al.*, 2011b) was completed prior to the discovery and publication of the symptomless phase, and therefore is an amalgamation of the two phases of infection. The investigation of sexual development in wheat stems however provides the most applicable data-set to symptomless infection (Guenther *et al.*, 2009). The infection front data-set from the sexual development analysis will prove a useful comparative tool.

Advancements in sequencing technologies have drastically reduced the procedure length and cost, enabling the rapid sequencing of entire transcriptomes. The *F. graminearum* Affymetrix array has proven very useful. However the array only acquires information on one organism in the interaction. A wheat Affymetrix array does exist, however this does not represent the complete genome and has been made predominantly from cDNA libraries of wheat plants that were not exposed to either biotic or abiotic stresses. Therefore, many essential wheat transcripts, important to the interaction with a pathogenic organism, may be missing. With the sequencing of the wheat genome nearing completion (Hall, Edwards and Bevan; www.cerealsdb.uk.net), RNA-sequencing can simultaneously provide transcript abundance data for both *F. graminearum* and wheat. The sensitivity of RNA-sequencing on the *Fusarium* – wheat interaction is untested. A recent RNA-sequencing time course study of *M. graminicola* infections of wheat leaves resulted in 5 to 10 % of total transcripts being of fungal origin (J. Rudd, RRes, UK, 2010, pers. com.). The application of RNA-sequencing to study symptomless *F. graminearum* – wheat ear infection, where live fungal and plant cells are in association, will prove the most informative. However, during symptomless infection the ratio of fungal to plant biomass will be at its lowest and therefore, a pilot study is required.

This investigation demonstrates that genome wide transcriptome alterations occur between the different phases of infection and depicts a situation where the symptomless infection front is the most distinct, especially in terms of the expression of genes that encode secreted proteins. The Affymetrix analysis of the transcriptome revealed the up regulation of various pathogenicity-related genes in combination with *TRI* genes during symptomless infection, including several genes already proven to be required for fully virulence on wheat. Genes predicted to encode

secreted proteins involved in plant cell degradation and proteins related to a phytotoxin were up regulated during the onset of cell death and disease symptoms. The pilot RNA-sequencing study revealed that this technique can be used successfully to study the *Fusarium* wheat interaction and provide informative data without enriching the ratio of fungal to plant transcripts. The transcriptome profiles generated via RNA-sequencing also demonstrated that substantial transcriptional alterations occur during symptomless infection and that the profile of the absolute infection front is distinct. In addition to information on the pathogen, the RNA-sequencing investigation generated the first full genome data-sets on the transcriptome alterations of the susceptible wheat plant to infection. In combination these studies provide a unique comparative resource for future transcriptome studies and identified many fungal and plant genes of interest for future molecular genetics and genetic evaluation of function.

7.2. Experimental Procedures

7.2.1. Use of the rachis internode assay to isolate the different phases of infection and RNA preparations

The four or seven rachis internodes (relative to the dpi when harvested) below the inoculated spikelet of each ear were individually excised and frozen in liquid nitrogen at 5 dpi and 7 dpi. In total 15 wheat ears were dissected for each treatment, mock-inoculated or *F. graminearum*-infected, and the corresponding internode segments and the inoculated spikelet collected and pooled. Tissues were harvested during the last two hours of the 16 h photoperiod. For the 7 dpi time point, the tissues from two additional experiments were prepared in the same way. Freeze dried samples were ground in liquid nitrogen with a pestle and mortar. Total RNA was extracted using the TRIzol® reagent (Invitrogen) with minor modifications to manufacturer's instructions. Total RNA was precipitated at -20^{o}C for 16 h with 8 M lithium chloride. Purified RNA was quantified by absorbance at 260 nm. Total RNA was treated with a DNA-*free*™ kit (Ambion) to remove contaminating DNA and the absence of genomic DNA confirmed by PCR using intergenic primers (Chapter 2, Table 3).

7.2.2. *F. graminearum* Affymetrix arrays

The RNA isolated from pairs of rachis internodes that appeared symptomatically the same was combined to reduced sample number; the symptomless advancing front of infection (RI5 + RI6), the onset of disease symptoms (RI3 + RI4) and the fully symptomatic tissue (RI1 + RI2). The RNA from the inoculated spikelet (SP1) was not combined. Three biological replicates for each tissue per treatment at 7 dpi were analysed. The RNA extracted from a single mock rachis internode (RI4) from the three biological replicates, was combined to form the mock non-infected wheat control. Similarly, the inoculated spikelet samples from the three biological replicates were combined to form a single spikelet infected control. Purified total RNA (> 10 µg) was *in vitro* transcribed, labelled using the BioArray high yield RNA transcript labelling kit (T7) according to manufacturer's instructions (Enzo Life Science), fragmented using 200 mM tris-acetate, pH 8.2, 500 mM MgOAc and mixed with the BioArray Eurkaryotic hydridization controls (Enzo Life Science) that included 3 nM control oligo B2, 20x control cRNA cocktail, herring sperma (10 mg / ml), acetylated BSA (50 mg / ml) 2x MES hybridization buffer and water. A final aRNA concentration of 10 µg in 200 µl was hybridized to the *F. graminearum* Affymetrix arrays (Guldener *et al.*, 2006). Hybridization of the Affymetrix arrays was carried out by Jane Coghill at the University of Bristol, UK in the laboratory of Prof Keith Edwards.

7.2.3. High throughput RNA-sequencing

Purified RNA (> 10 µg) from the second and third rachis internode below the point of inoculation, at 5 dpi, from both the mock and *Fusarium* infected sample were sent to Syngenta Biotechnology, USA for RNA-sequencing. For the four samples, 72 cycles of single end reads were ran on a Solexa sequencer. Sequences were aligned to the *F. graminearum* and the wheat reference genomes using the software programme Tophat and Bowtie to generate read counts per kilobase of sequence. Genes were subdivided according to whether they were predicted to reside within the fungal cell or were predicted to be secreted. The MIPS functional categories for the highly expressed genes were determined. The location of the highly expressed gene set was displayed on the four *F. graminearum* chromosomes

using the FGRAM3Map software (http://www.omnimapfree.org/)(Antoniw *et al.*, 2011).

7.2.4. Bioinformatic and statistical analyses

The degree of correlation between treatments within, and between the two techniques for assessing the transcriptome, was determined using GeneStat 12 (VSN International). Genome wide scatter plots were generated on SigmaPlot 11 (Systat Software Inc.). Only probes with a greater than two fold change between infection front (RI5-6) and the origin of rachis infection (RI1-2), or probes with a presence or absence score, were considered differentially expressed. The MIPS functional categories for the 100 most highly, or differentially, expressed genes were determined (http://mips.helmholtz-muenchen.de /genre/proj/FGDB/). An equivalent analysis was performed solely on genes that are predicted to encode secreted proteins (Chapter 6). The expression patterns of individual genes involved in pathogenicity, DON production and plant cell degradation were inspected individually. Due to the late arrival of this data, in the last month of the project, further statistical analyses will be perform at a later date to confirm the significance of the trends observed.

7.3. Results

The results arising from the wheat ear infection time course (Appendix 17), the macroscopic study of rachis infection (Appendix 18) and the *TRI* gene expression data (Chapter 4) were used to select the time points for transcriptome investigation. The RNA isolated from three independent 7 dpi experiments that covered the change from symptomless to fully symptomatic rachis infection and the inoculated spikelet, were used for the complete *Fusarium* Affymetrix array investigation. The RNA isolated from the single 5 dpi experiment, previously used to monitor *TRI* gene expression, was sent for RNA-sequencing. The 5 dpi time point was chosen as it represented early symptomless colonisation. The rachis internodes that contain both live fungal and host cells were selected, which due to low fungal biomass also tested the depth of sequencing possible (Figure 37). A comparison with the mock inoculated control will enable the identification of transcriptional changes of wheat gene expression in response to infection.

7.3.1. Confirmation of RNA integrity, absence of fungal DNA and presence of fungal infection

The integrity, purity and presence / absence of fungal infection had previously been confirmed for the relevant rachis internodes at 5 dpi, as required for the RNA-sequencing project (Chapter 4). The integrity of the RNA extracted from the 7 rachis internodes below the point of infection and the inoculated spikelet, at 7 dpi (Figure 38) as required for the Affymetrix study, was confirmed by gel electrophoresis (Figure 39). The absence of fungal DNA and the presence of fungal RNA were confirmed by intergenic PCR (Figure 40) and RT-PCR (Figure 41), respectively. The infection front was isolated in the sixth rachis internode (RI-6) for two of the three biological replicates (Rep 1 and 3) and in the seventh internode in Rep 2. Minimal differences between sequential pairs of rachis internodes in the appearance of infection and *TRI* gene expression were observed (Chapter 4). Subsequently, the RNA from these pairs was combined to reduce sample number. Combined RNA samples were labelled, fragmented (Figure 42) and hybridized to the *F. graminearum* Affymetrix arrays. A total of 14 arrays were used.

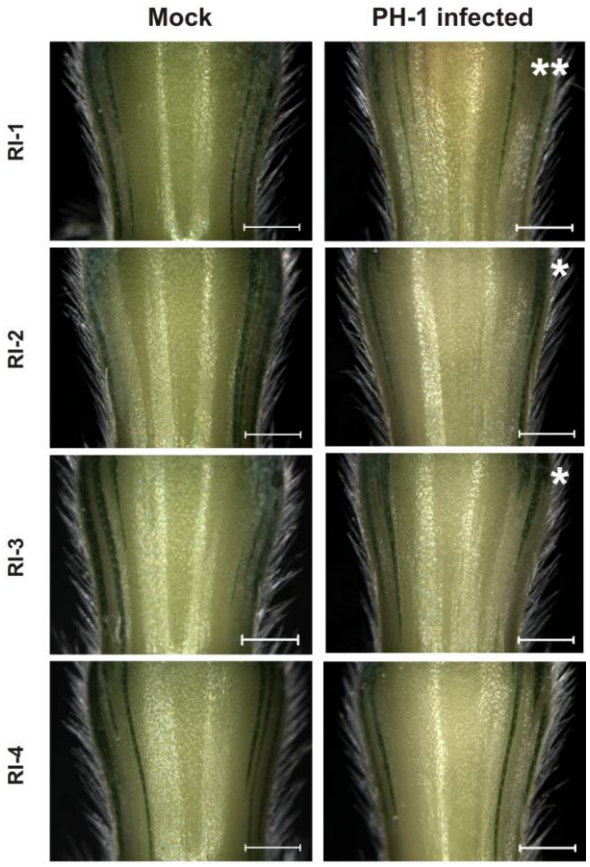

Figure 37 The second (RI-2) and third (RI-3) rachis internodes below the inoculated spikelet of the mock-inoculated and the *F. graminearum*-infected wheat ears at 5 dpi were selected for RNA-sequencing. This captured the interaction between live plant and fungal cells (single asterix) during symptomless infection before the onset of plant cell death (double asterix) in the PH-1 infected wheat ear. Bar = 1 mm.

Figure 38 The mock inoculated (left panel) and the *F. graminearum* PH-1 infected (right panel) wheat ears **(A)** at 7 dpi alongside seven sequential rachis internodes below the inoculated spikelets (**B** through **I**). The inoculated spikelets are marked with a black dot. Bar = 1 mm.

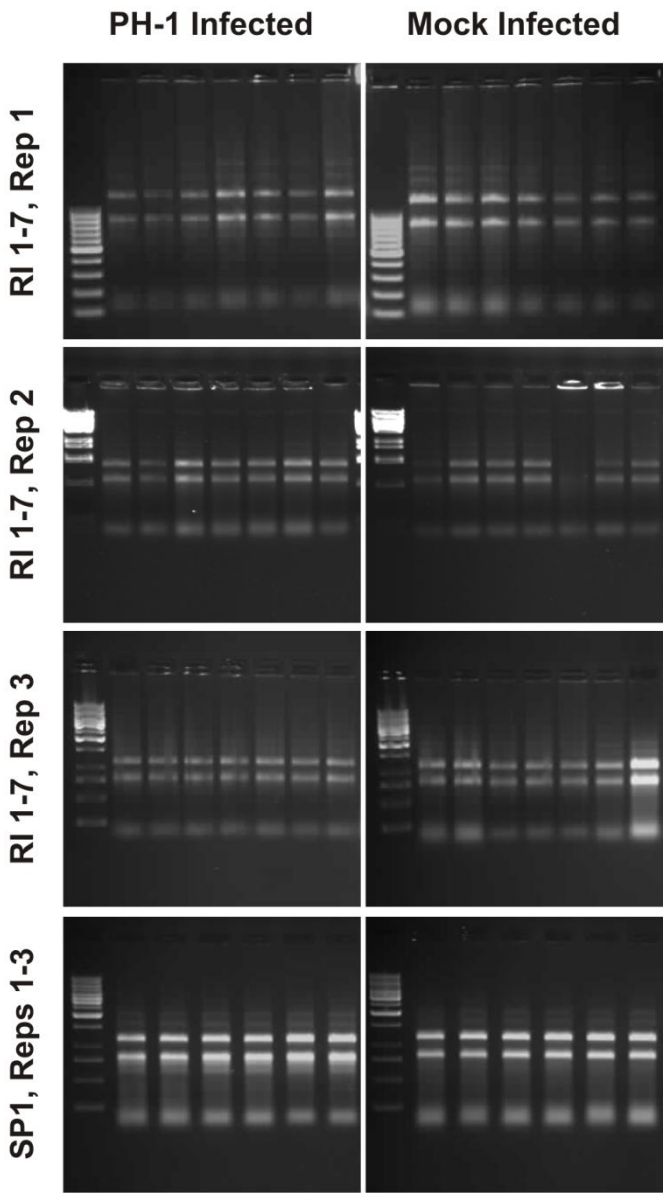

Figure 39 The RNA extracted from the *F. graminearum* PH-1 infected and the mock controls at 7 dpi. The RNA from the seven sequential rachis internodes below the inoculated spikelet (RI 1-7 and the RNA from the inoculated spikelet, SP1), which also contains two technical replicates, are presented separately. The samples were loaded in numerical order from left to right. Between 500-1000 ng of RNA was separated on a 1 % agarose gel alongside different DNA ladders. Rep1 = a 100 bp ladder (Generuler, Fermentas), Rep 2 = lambda_DNA_BstE II ladder, Rep 3 and SP1 = 1 kb ladder (Generuler, Fermentas).

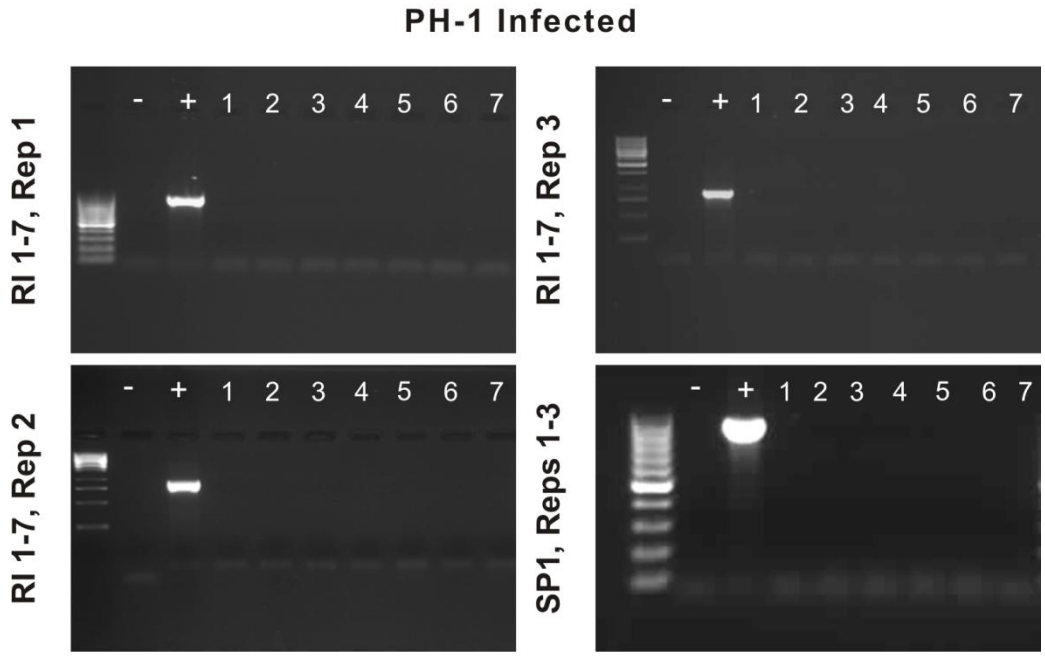

Figure 40 The extracted RNA from the PH-1 infected rachis internodes and the inoculated spikelet at 7 dpi is free of gDNA contamination. Intergenic primers that only amplified a gDNA region between *TRI6* and *TRI4* were used. The presence of an amplicon (902 bp) on the 1 % agarose gel, separated alongside a 100 bp (Rep 1 and SP1) or a 1 kb (Rep 2 and Rep 3) DNA ladder, represents the presence of gDNA. Amplicon only present in the positive controls. Legend: –ve = the non template negative control, +ve = the PH-1 gDNA positive control, 1 – 7 = the sequential rachis internodes below the inoculated spikelet, RI-1 to RI-7.

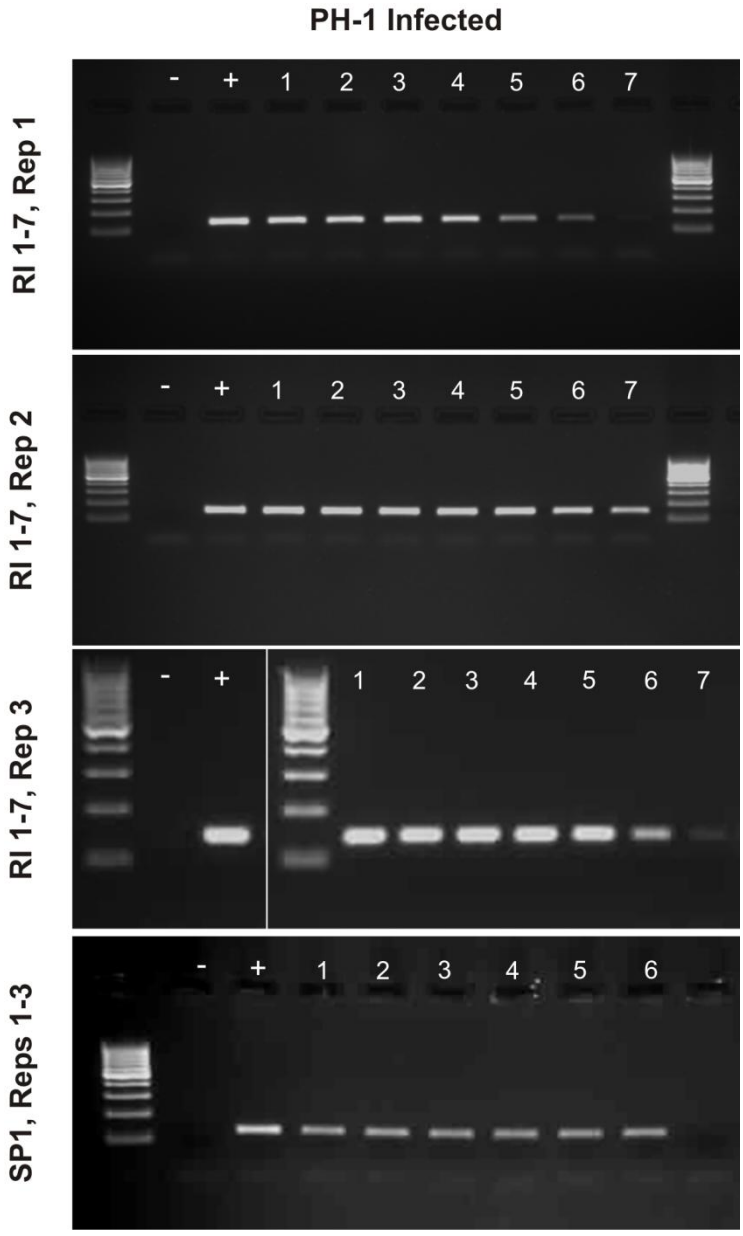

Figure 41 Detection of fungal RNA within the relevant rachis internodes at 7 dpi. The seven sequential rachis internodes below the point of inoculation (RI 1-7) and the inoculated spikelet (SP1) from the *F. graminearum* PH-1 infected ears. RT-PCR using primers for the *F. graminearum* γ-actin gene (141 bp) separated on a 2 % agarose gel alongside a 100 bp DNA ladder (Generuler, Fermentas). Legend: –ve = the non template negative control, +ve = the gDNA positive control, 1 – 7 = the sequential rachis internodes below the inoculated spikelet, RI-1 to RI-7. SP1 specific legend: lanes 1-2 = technical repetitions from Rep 1, lanes 3-4 = technical repetitions from Rep 2, lanes 5-6 = technical repetitions from Rep 3.

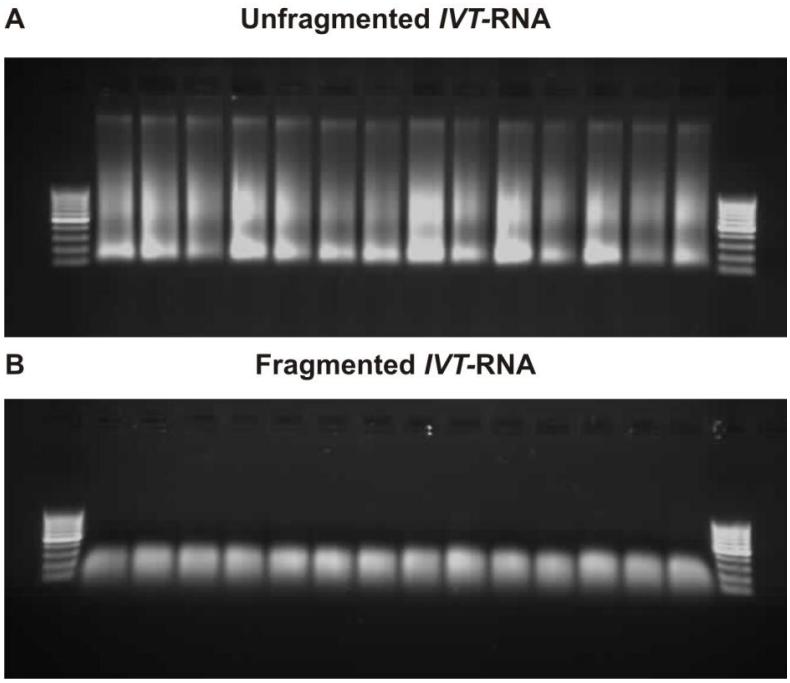

Figure 42 The unfragmented **(A)** and the fragmented **(B)** *in vitro* transcribed labelled RNA, prepared for hybridization to the *Fusarium* Affymetrix arrays, separated on a 1 % agarose gel alongside a 100 bp DNA ladder (Generuler, Fermentas).

7.3.2. *F. graminearum* Affymetrix arrays

In total 13,250 *F. graminearum* specific probe sets, of the 17,830 present on the Affymetrix array, were detected. Overall the genome wide correlation in gene expression across the different samples at 5 dpi was high (Figure 43). Significant p values (<0.001) were obtained for each correlation however, this is due to the large sample size. The correlation improved between samples exhibiting macroscopically similar infection phenotypes (Table 12). The Affymetrix analysis revealed that 48.6 % of the *F. graminearum* genes (6,440/13,250) were differentially expressed between the two infection phases within the rachis. The number of genes up regulated during symptomless infection (5,347) was far greater than the number down regulated (1,093). The *Fusarium* wheat specific genes, identified in the whole wheat ear study were assessed. Of the 369 *F. graminearum* genes described as being specifically expressed during wheat infection by Lysoe (2011b), 61 % were differentially regulated between symptomless and symptomatic infection, with 46.9 % and 14.1 % being up and down regulated respectively. Genes with a hybridisation value greater than 10,000 represented approximately the top 1 % of the most highly

expressed genes. The number of genes in common between the top 100 most highly expressed fungal genes during symptomless and symptomatic infection was 68 %, while those in common between the symptomatic infection of the spikelet and rachis was 51 %. *F. graminearum* genes differentially expressed between rachis and spikelet infection represented 27.2 % (3,584/13,158) of the transcriptome, with 1,331 and 2,253 genes being up and down regulated, respectively.

Table 12 The correlation coefficients for genome wide gene expression between the different pooled tissue samples assessed at 7 dpi via Affymetrix arrays. RI5-6 = rachis internodes symptomless infection. RI3-4 = rachis internodes onset of disease symptoms. RI1-2 = rachis internodes fully symptomatic. SP1 = fully symptomatic spikelet. Mock-RI = Non infected rachis internodes. Mock-SP = Non infected spikelet. P = <0.001 for each correlation.

	RI1-2	RI3-4	RI5-6
SP1	0.8530	0.8076	0.6787
RI1-2	n/a	0.9499	0.8204
RI3-4	n/a	n/a	0.9068

The MIPS functional category for the top 100 most highly expressed genes detected in the three rachis segments and the inoculated spikelet was determined along with the top 100 genes that demonstrated the greatest degree of differential expression between the advancing front and origin of rachis infection (Figure 44). The sub-set of fungal genes that are predicted to encode secreted proteins (Chapter 6) were independently analysed in the same manner. Overall, for all genes or for the genes coding for the secreted protein sub-set, the functional profile of the top100 most highly expressed genes did not alter to a large extent between tissues. Genes that encoded proteins with binding function or cofactor requirement and proteins involved in protein synthesis where highly represented. The proportion of differentially expressed genes, which were up or down regulated at the advancing front of infection that encode proteins of unknown function, increased substantially. Similarly, the proportion of genes that encode secreted proteins which were up regulated at the advancing front of infection also increased. Therefore, proteins of

unknown function are dramatically up regulated at the advancing front of infection, including numerous secreted proteins.

Subsequently, genes involved or suspected to be involved in pathogenicity were assessed. All the *TRI* genes required for DON mycotoxin production, excluding the negative regulator *TRI15*, were up regulated at the advancing front of infection (Figure 45). Conversely, *TRI15* was up regulated in the spikelet where infection began and *TRI* gene expression was at its lowest. The expression level of the known transcriptional regulators of *TRI* gene expression was substantially lower than the biosynthetic enzymes. The two genes of unknown function that are proposed negative regulators of DON production (Gardiner *et al.*, 2009a) are expressed at a high level, unlike the transcriptional regulators, and are dramatically up regulated at the advancing front of infection. A lactonohydrolase (FGSG_10675) possibly involved in DON detoxification (Takahashi-Ando *et al.*, 2002, Takahashi-Ando *et al.*, 2004) was also up regulated at the advancing front, while another was not (FGSG_03816). Beside the low level expression of the *VELA* homologue in *F. graminearum*, which forms part of the light sensitive velvet complex (Duran *et al.*, 2007), transcription was also up regulated during symptomless infection.

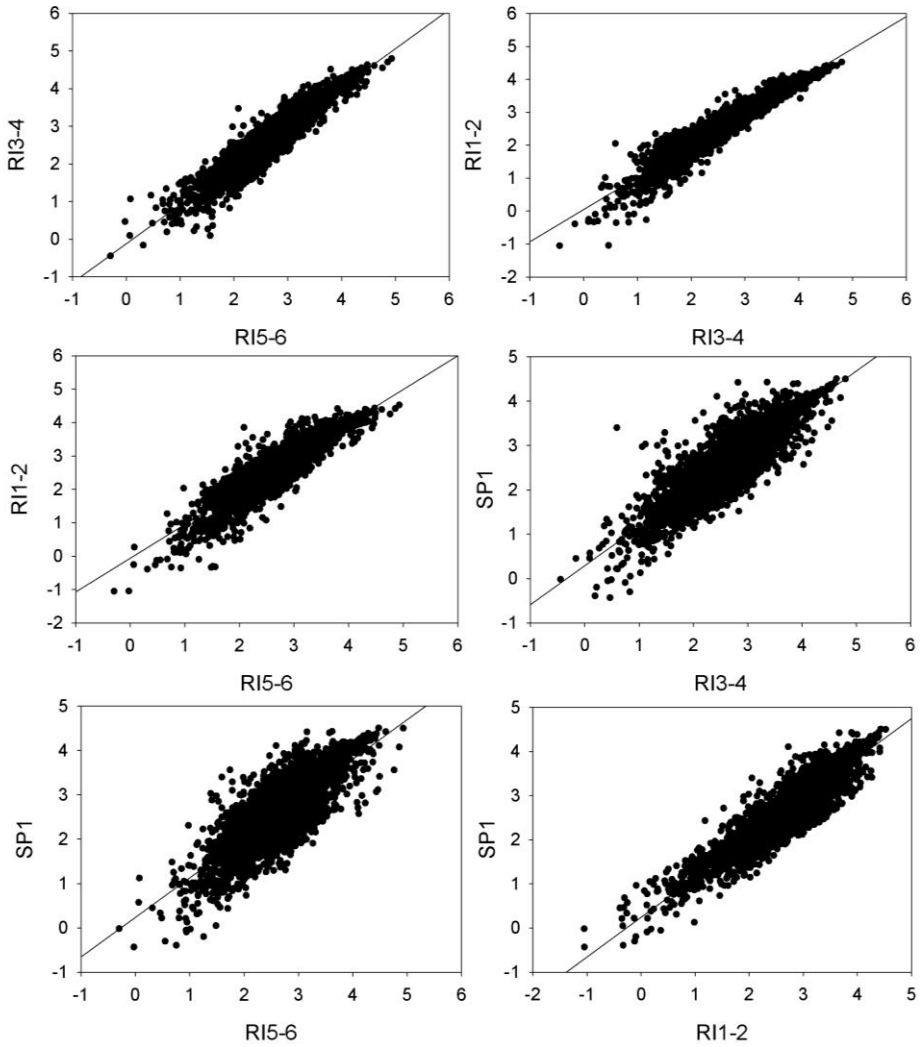

Figure 43 Scatter plot representation of the transcriptome of the symptomless (RI5-6), the onset of disease symptoms (RI3-4) and fully symptomatic (RI1-2) rachis internodes and the inoculated spikelet (SP1) at 7 dpi, assessed by Affymetrix arrays. Log_{10} expression values are present.

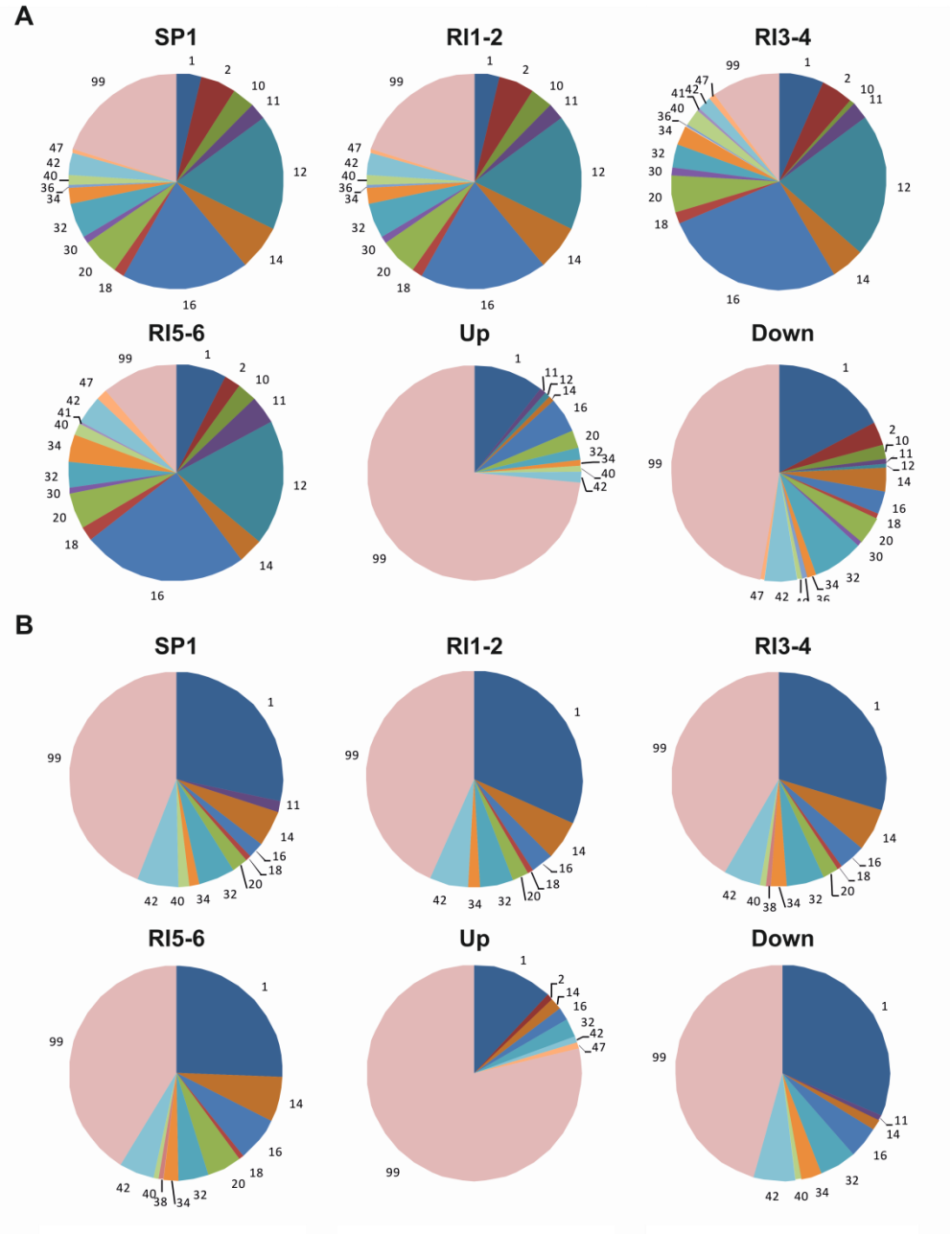

Figure 44 The MIPS functional categories of the top 100 most highly expressed genes detected in the three rachis internode samples (RI1-2, RI3-4, RI5-6) and the inoculated spikelet (SP-1) was determined along with the top 100 genes that demonstrated the greatest degree of differential expression (up regulated or down regulated) between the advancing front, and origin, of rachis infection **(A)**. The equivalent analysis of the sub-set of fungal genes predicted to encode secreted proteins is presented separately **(B)**. The infection front alone represents symptomless infection. The MIPS code is described in Appendix 2.

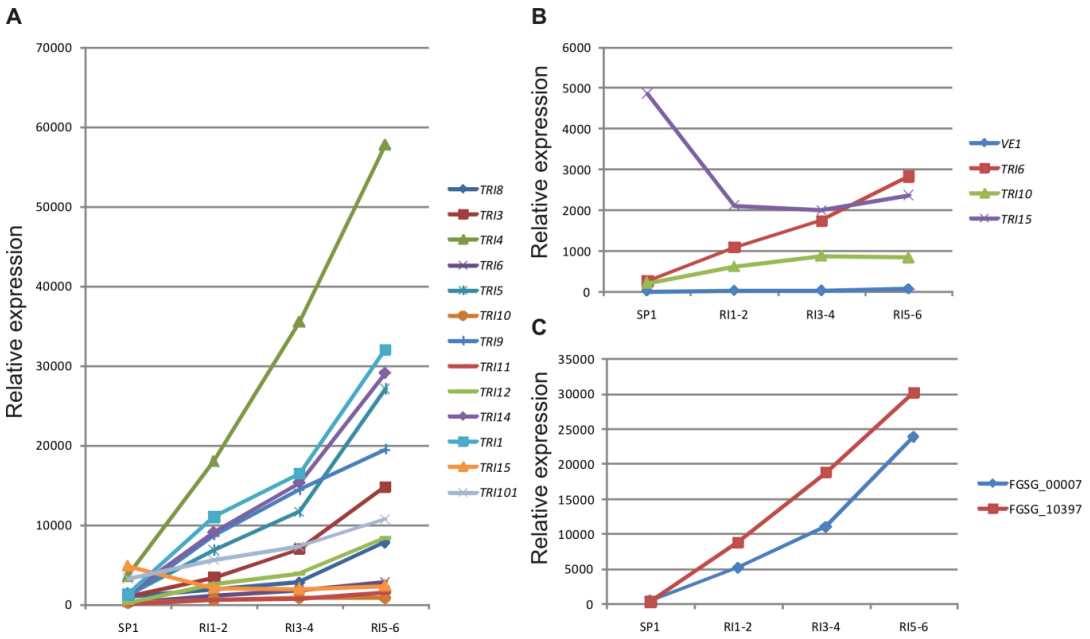

Figure 45 The expression pattern of genes involved in DON mycotoxin production from the point of inoculation (SP-1) through the rachis (RI1-2, RI3-4) to the advancing front of infection (RI5-6). The infection front alone represents symptomless infection. All of the *TRI* genes **(A)**, the transcriptional regulators of DON production **(B)** and the two genes of unknown function which are hypothesised to be negative regulators **(C)** are presented. Relative expression is representative of the mean Affymetrix hybridisation values across the three biological replicates.

A homologue of gEgh16 from powdery mildew fungi *B. graminis* f. sp. *hordei* and Gas proteins from *M. oryzae* that are required for successful penetration of the host (Xue *et al.*, 2002) was highly expressed by *F. graminearum* during the phases of active colonisation, but was expressed at a minimal level in the fully colonised spikelet (Figure 46). A gene that encodes a circumsporozoite related protein (FGSG_09390), which is produced by *Plasmodium* malaria parasites to inhibit protein synthesis in their host (Menard *et al.*, 1997), was also up regulated at the advancing front of *F. graminearum* infection (Figure 46). The genes that encode Snodprot1 related proteins (FGSG_10212, FGSG_11205), which is a known phytotoxin from *S. nodorum* (Hall *et al.*, 1999), where most highly expressed during the symptomatic phase of rachis infection (RI1-4) coinciding with host cell death (Figure 46, Chapter 3). The only secreted *F. graminearum* protein so far to be proven

to be essential for fully virulence, the lipase *FGL1* (Voigt *et al.*, 2005) was expressed at low level and was only up regulated within RI1-2 in association with wide scale intracellular colonisation (Figure 46). Interestingly, a gene predicted to encode a secreted protein of unknown function (FGSG_00379), which possesses an RxLR in the N terminus of the protein but no dEER motif, was substantially up regulated at the advancing front of infection (Figure 46).

Four genes that encode antifungal proteins, including three *KP4* homologues from *U. maydis*, were identified in the bioinformatic analysis of the secretome (Chapter 6). The antifungal protein (FGSG_04745) was most highly expressed during the symptomatic phase of rachis infection (RI1-4) in association with host cell death (Chapter 3), while the *KP4* homologues (FGSG_00060, FGSG_00061, FGSG_00062) were only expressed in the spikelet, during the last phase of infection (Figure 46).

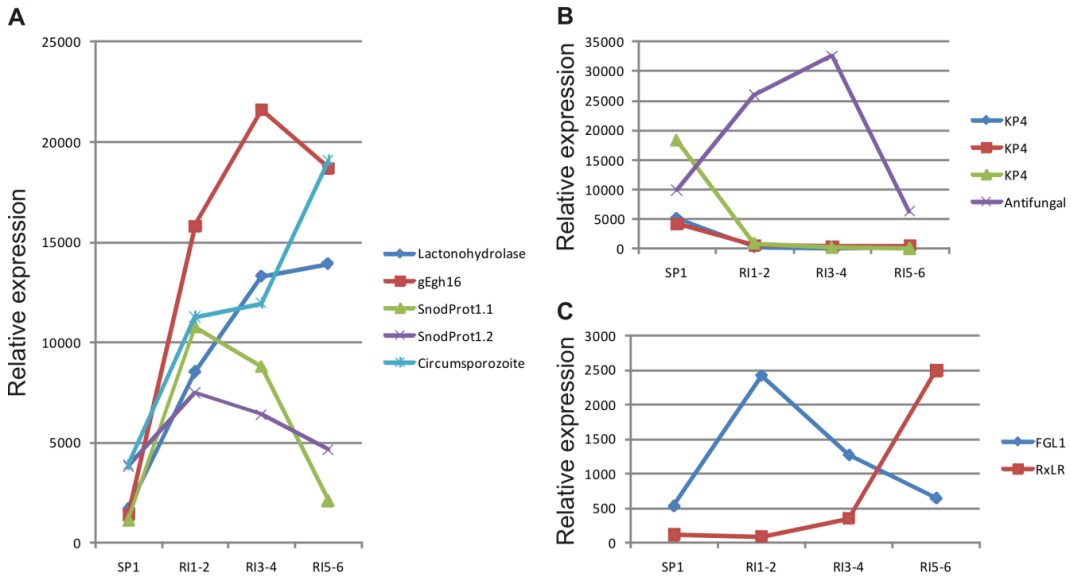

Figure 46 The expression pattern of pathogenicity related genes from the point of inoculation (SP-1) through the rachis (RI1-2, RI3-4) to the advancing front of infection (RI5-6). The infection front alone represents symptomless infection. **(A)** Highly expressed pathogenicity genes. **(B)** Antifungal proteins. **(C)** Pathogenicity genes expressed at a low level. Relative expression is representative of the mean Affymetrix hybridisation values across the three biological replicates.

All the genes that were predicted to encode secreted proteins involved in degradation of the plant cell and cell wall (Chapter 6) were sub-divided according to the target compound and expression pattern determined. The 134 genes were divided into those which target cellulose / cellobiose (n = 30), hemicellulose (n = 45), protein (n = 37), lipids (n = 19) and starch (n = 3) (Figure 47). The highly expressed plant cell and plant cell wall degrading proteins were up regulated during the middle phase of infection (RI1-4) in association with host cell death and intracellular colonisation (Chapter 3). Alternatively, a glucoamylase (FGSG_04704) was up regulated in the spikelet where the aborted grain resides. The majority, 42.7 %, of PCWDEs were down regulated at the advancing front of infection (RI5-6) compared to the origin of rachis infection (RI1-2). Not all PCWDEs were differentially expressed throughout infection (42.7 %) and some were up regulated (14.7 %). These genes however were expressed at a far lower level than the genes which were down regulated at the infection front (Table 13). Genes encoding secreted proteins involved in plant lipid, protein and starch degradation showed a similar expression pattern but were not down regulated to such a wide extent.

Table 13 The mean expression values of the genes predicted to encode proteins involved in plant cell and cell wall degradation, sub-divided according to whether they are differentially regulated throughout the infection colony. The overall mean for all genes within each sub-group is presented, with the number of genes in each group in brackets. Differential regulation was determined by a greater than two fold change in mean expression between symptomless (RI1-2) and fully symptomatic (RI5-6) rachis infection.

Target	Expression pattern	Mean expression				
		SP1	RI1-2	RI3-4	RI5-6	Overall
Plant cell wall	Down (32)	2679	5438	3661	1288	3267
	Up (11)	143	144	237	430	**239**
	No dif. (32)	727	1956	1854	1562	1525
Plant cell	Down (18)	1088	3235	2325	829	1869
	Up (7)	99	163	272	518	**263**
	No dif. (34)	1056	1597	1598	1475	1431

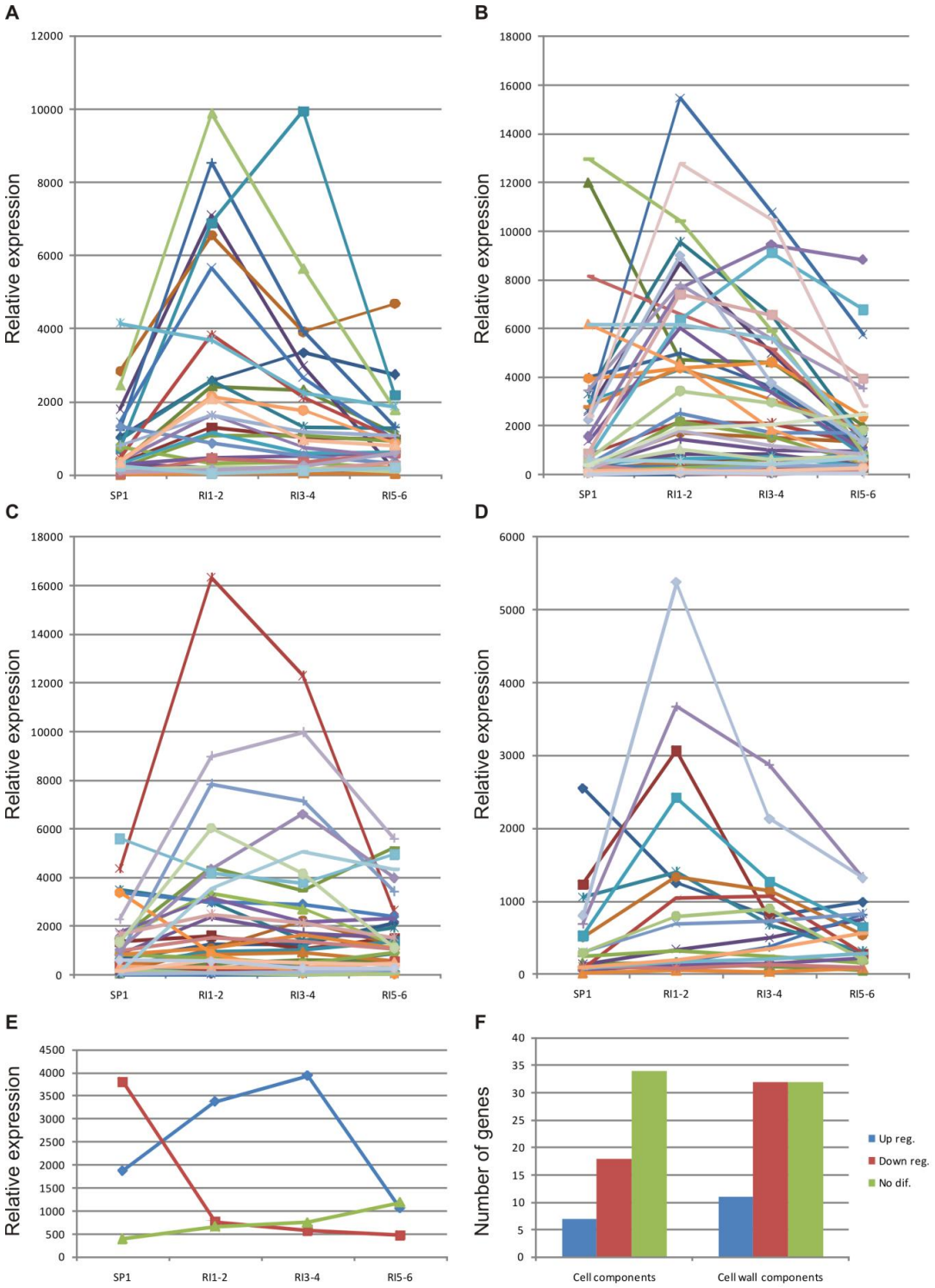
A
Relative expression
12000
10000
8000
6000
4000
2000
0
SP1
RI1-2
RI3-4
RI5-6
B
Relative expression
18000
16000
14000
12000
10000
8000
6000
4000
2000
0
SP1
RI1-2
RI3-4
RI5-6
C
Relative expression
18000
16000
14000
12000
10000
8000
6000
4000
2000
0
SP1
RI1-2
RI3-4
RI5-6
D
Relative expression
6000
5000
4000
3000
2000
1000
0
SP1
RI1-2
RI3-4
RI5-6
E
Relative expression
4500
4000
3500
3000
2500
2000
1500
1000
500
0
SP1
RI1-2
RI3-4
RI5-6
F
Number of genes
40
35
30
25
20
15
10
5
0
Cell components
Cell wall components
Up reg.
Down reg.
No dif.

Figure 47 The expression pattern of genes predicted to encode secreted proteins involved in plant cell degradation, from the point of inoculation (SP-1) through the rachis (RI1-2, RI3-4) to the advancing front of infection (RI5-6). The infection front alone represents symptomless infection. The expression patterns of genes involved in cellulose **(A)**, hemicellulose **(B)**, protein **(C)**, lipid **(D)** and starch **(E)** degradation are presented separately. Relative expression is representative of the mean Affymetrix hybridisation values across the three biological replicates. The number of differentially expressed genes, with a greater than two fold up or down regulation, at the advancing front of infection is presented **(F)**.

As a consequence of the high representation of genes that encode proteins of unknown function (Figure 44) these genes were studied in more detail. The most highly expressed and differentially regulated genes were identified (Figure 48) and the analysis repeated for the genes predicted to encode secreted proteins (Figure 49). The characteristics of the 16 genes identified are presented in table 14. The secreted proteins identified to be up regulated during colonisation of live wheat tissue were small peptides (< 200 amino acids) with the majority being cysteine-rich and possessed internal amino acid repeats, characteristic of fungal effectors. Two of these small up regulated secreted proteins, FGSG_12504 and FGSG_10622, are specific to *F. graminearum*. FGSG_03960 contained a hydrophobin domain (Pfam01185), while FGSG_10622 contained a Cyano virin-N sugar-binding antiviral protein domain (Pfam08881) which may both be involved in adhesion and attachment. The secreted proteins that were down regulated were not cysteine-rich but did contain internal amino acids repeats. FGSG_08825 contain a dienelactone hydrolase domain (Pfam01738) involved in aromatic compound degradation, such as phenolic substrates including lignin. No coordinated gene expression was found for the secreted protein gene clusters identified in chapter 6.

These *F. graminearum* Affymetrix data-sets are now being prepared for full statistical and functional analysis using the Bioconductor software.

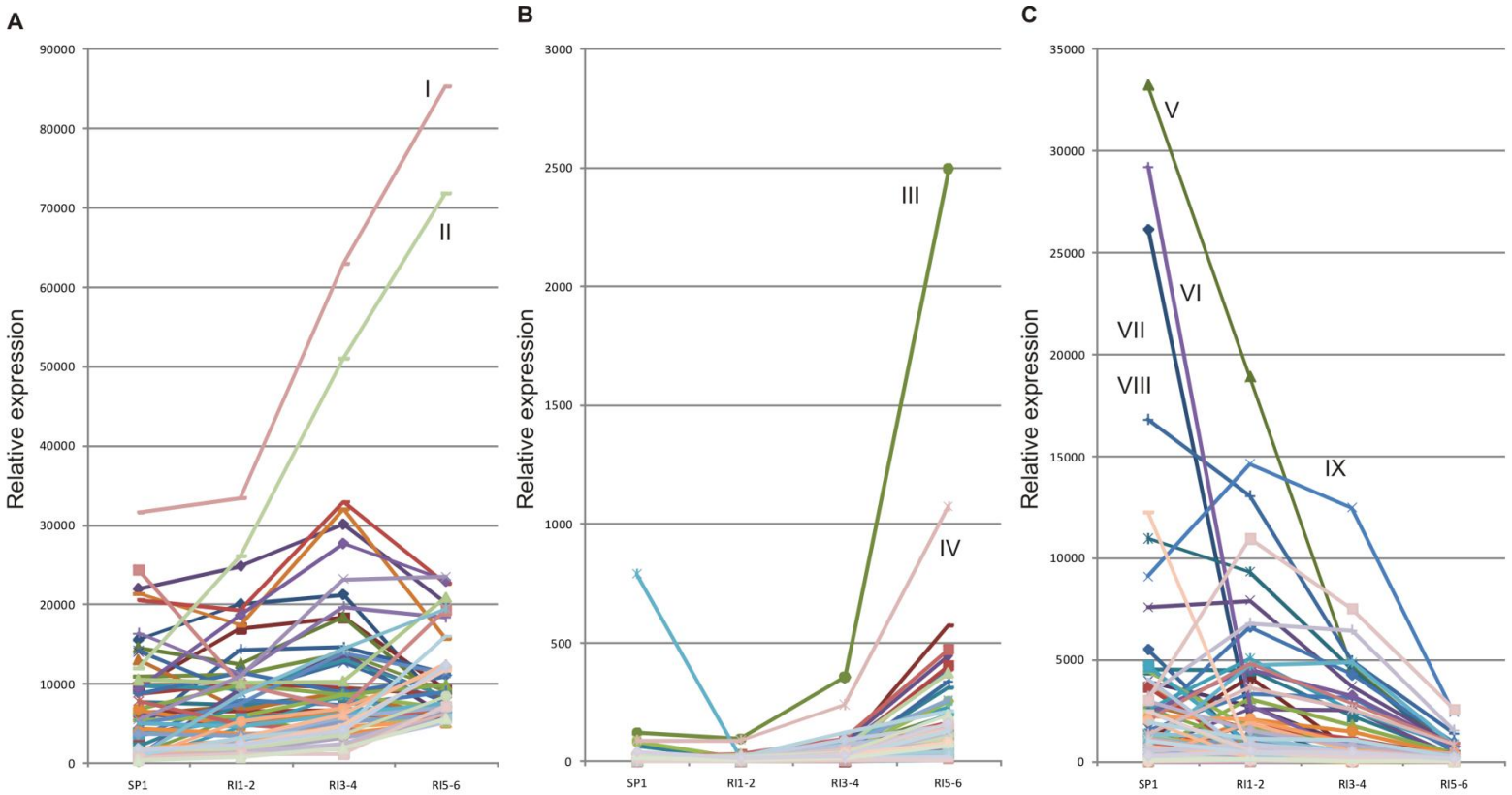

Figure 48 The expression pattern of genes that encode proteins of unknown function, from the point of inoculation (SP-1) through the rachis (RI1-2, RI3-4) to the advancing front of infection (RI5-6). The infection front alone represents symptomless infection. Relative expression is representative of the mean Affymetrix hybridisation values across the three biological replicates. The most highly **(A)** and differentially expressed genes, up **(B)** or down **(C)** regulated at the advancing front of infection, were identified. The FGSG_ID for the genes labelled with roman numerals can be found in table 14.

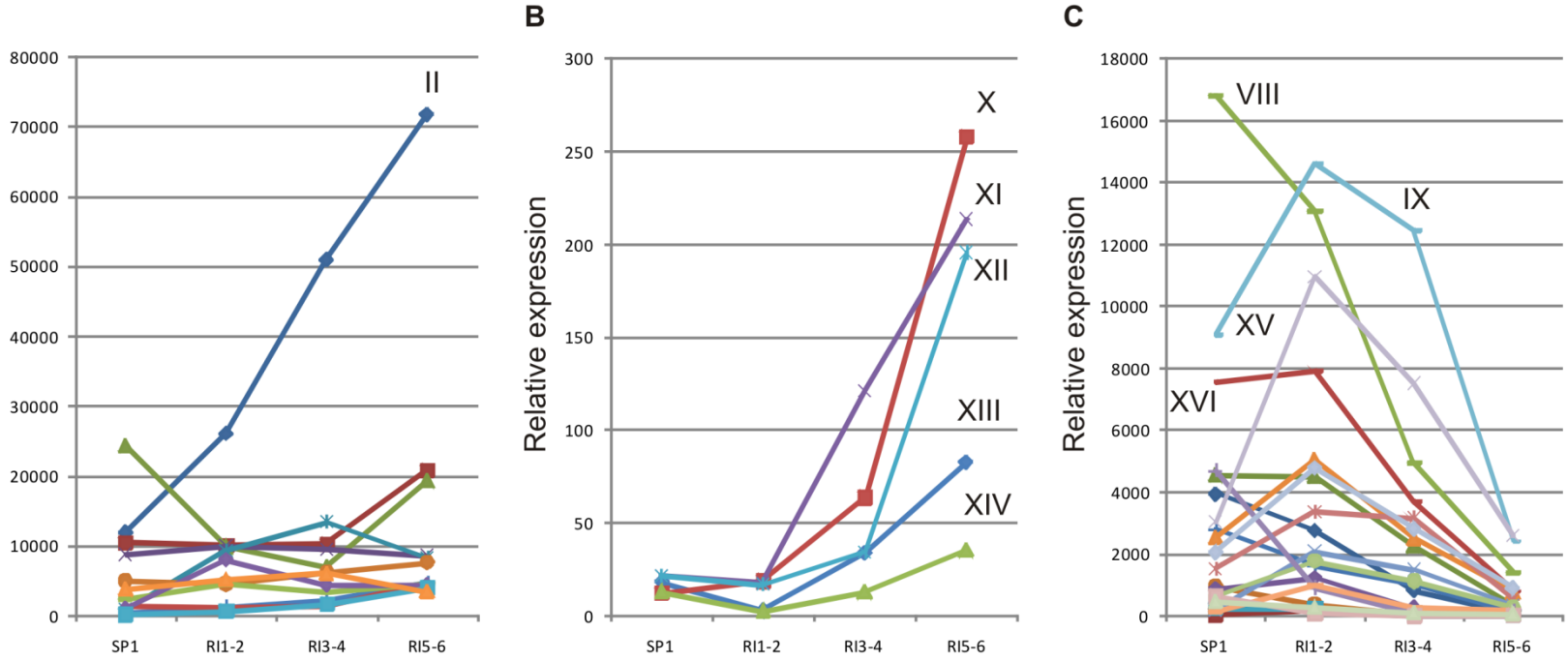

Figure 49 The expression pattern of genes that encode secreted proteins of unknown function, from the point of inoculation (SP-1) through the rachis (RI1-2, RI3-4) to the advancing front of infection (RI5-6). The infection front alone represents symptomless infection. Relative expression is representative of the mean Affymetrix hybridisation values across the three biological replicates. The most highly **(A)** and differentially expressed genes, up **(B)** or down **(C)** regulated at the advancing front of infection, were identified. The FGSG_ID for the genes labelled with roman numerals can be found in table 14.

Table 14 The characteristics of the proteins of unknown function that were identified via monitoring fungal gene expression throughout symptomless and symptomatic infection of the wheat ear. Features included: the length of the mature protein, the number of introns, cysteine residues (C), transmembrane domains (TM), internal amino acid repeats (RADAR), an extracellular localisation prediction (WoLFPSORT, WolLFP), the presence of a nuclear export signal (NES), Pfam domains, whether the gene is specific to *F. graminearum* (e-5).

Figure label	FGSG_ID	Expression pattern	Secreted protein	No. introns	Mature protein length	No. C	TMs	RADAR	WoLFP	NES	Pfam domain	FG specific
I	FGSG_12666	UP	N	1	84	-	-	-	-	-	-	Y
II	FGSG_05046	UP	Y	1	112	8	0	-	extra=27	0	-	N
III	FGSG_00379	UP	Y	1	424	6	1	3	mito=11	1	-	N
IV	FGSG_06418	UP	N	3	620	-	-	-	-	-	-	N
V	FGSG_07152	DOWN	N	2	69	-	-	-	-	-	-	N
VI	FGSG_09072	DOWN	N	1	108	-	-	-	-	-		N
VII	FGSG_09741	DOWN	N	0	96	-	-	-	-	-	-	N
VIII	FGSG_03599	DOWN	Y	1	77	10	0	3	extra=21	0	-	N
IX	FGSG_04583	DOWN	Y	0	130	4	0	-	extra=24	0	-	N
X	FGSG_03960	UP	Y	2	153	9	0	2	extra=25	1	01185	N
XI	FGSG_12504	UP	Y	3	101	7	0	-	extra=18	1	-	Y
XII	FGSG_10554	UP	Y	2	180	9	0	2	extra=19	0	-	N
XII	FGSG_06993	UP	Y	4	184	4	0	2	extra=25	0	09352	N
XIV	FGSG_10622	UP	Y	2	98	5	0	-	extra=26	0	08881	Y
XV	FGSG_06469	DOWN	Y	2	466	6	0	2	extra=24	0	-	N
XVI	FGSG_08825	DOWN	Y	3	238	1	0	2	extra=19	2	01738	N

7.3.3. Pilot high throughput RNA-sequencing study

The total number of reads between rachis internodes or treatments did not differ significantly (Table 15). Fungal transcripts detected within the infected RI2 and RI3 internodes accounted for 9 % and 5.2 % of the total reads, respectively. Therefore, the rachis internode that represented the advancing front of infection, RI3, possessed 37.2 % fewer fungal reads, reflecting the reduction in fungal biomass within this plant tissue. However, the number of *Fusarium* genes detected in RI3 did not drop significantly (4.8 %). The total number of reads that aligned to the 19, 200 full length cDNAs so far predicted from the sequenced wheat genome (sourced from the Riken Institute, Japan) did not differ significantly between individual mock or infected internodes (Table 15). However, dramatic differences between the mock and infected treatments were detected and indicate that there had been a considerable transcriptional response of the host cells to the infection. The proportion of reads aligned to wheat genome dropped 14.4 % (RI2) and 7.2 % (RI3), respective of the rachis internode, demonstrating the existence of novel wheat sequences involved in the response to *Fusarium* infection, which are not within the Riken full length dataset. The greater amount of unmapped reads in RI2 may indicate a novel wheat response following the recognition of fungal infection and DON mycotoxin. The late acquisition of this data means that the analysis of the wheat transcriptome is ongoing and is not presented in this thesis.

Table 15 The total number of reads generated by RNA-sequencing of the infected (PH1) and non-infected (Mock), second (RI2) and third (RI3) rachis internode below the point of inoculation at 5 dpi. Wheat and *F. graminearum* reads were aligned to the respective genomes. Reads that did not align were classified unmapped. * In the two mock inoculated samples 5 FGSG genes and an unannotated region at the far end of chromosome 4 were strongly identified as aligning to the wheat only samples. These were FGSG_00639, FGSG_01956, FGSG_08768, FGSG_10941 and FGSG_09530. In each case only a part of the sequence aligned.

Sample	Total reads	Wheat alignment				*Fusarium* alignment			
		Aligned	%	Unmapped	%	Aligned	%	Unmapped	%
RI2-PH1	33,961,229	19,666,432	57.9	13,943,753	41.1	3,043,176	9	30,470,005	89.7
RI2-Mock	32,239,797	23,317,750	72.3	8,325,950	25.8	52,107	0.2*	31,971,927	99.2
RI3-PH1	36,720,935	24,021,043	65.4	12,222,028	33.3	1,894,808	5.2	34,703,937	94.5
RI3-Mock	38,402,612	27,866,662	72.6	9,788,169	25.5	54,423	0.1*	38,130,441	99.3

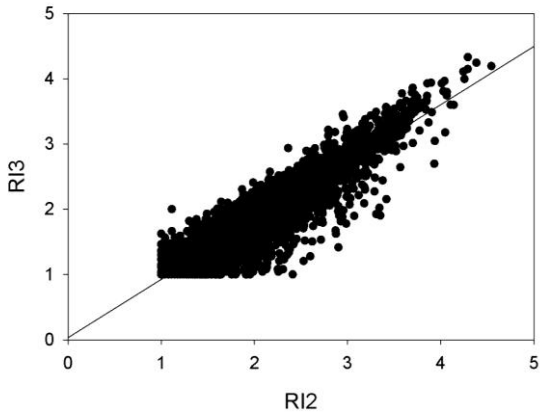

Figure 50 Scatter plot representation of the transcriptome of individual symptomless rachis internodes RI2 and RI3 at 5 dpi, assessed by RNA-sequencing. Log_{10} expression values are present.

Fungal genes with read counts higher than 1000 accounted for the upper 4.69 % and 2.99 % of genes detected and 55.01 % and 48.08 % of total *Fusarium* reads, respective to RI2 and RI3. Genome wide correlation in fungal gene expression between the two symptomless rachis internodes was very high (Figure 50, correlation 0.9036, $p<0.001$). No significant transcriptional alterations (> 2 fold) were observed in the expression of the *TRI* genes between the hyphae within the two symptomless

rachis internodes. The pattern of *TRI* gene expression depicted by the Affymetrix and RNA-sequencing studies was the same. The highest expressed (*TRI1*, *TRI4*, *TRI14* and FGSG_10397) and lowest expressed (*TRI6* and *VE1*) genes being constant between experimental approaches. Only genes I, II, IX and XV, of 12 genes of unknown function identified as differentially expressed in the Affymetrix study, were detected above negligible level via RNA-sequencing.

The MIPS functional categories were determined for the top 100 most highly or differentially expressed genes (Figure 51). A sub-set of fungal genes predicted to encode secreted proteins (Chapter 6) were analysed independently. The functional profile of the individual sub-sets of genes was compared. The functional profile of the most highly expressed genes within the different rachis internodes did not alter drastically, with a wide spread of categories represented. The two most frequently represented functional categories in both rachis internodes involved in protein-binding and protein synthesis and collectively accounted for 32.6 % (RI2) and 32.4 % (RI3). Proteins involved in metabolism, cellular transport, cell virulence, defence and rescue also featured highly and accounted for 23.3 % (RI2) and 22.8 % (RI3), while proteins of unknown function represented 11.1 % (RI2) and 10.7 % (RI3). However, the functional profile of the secretome changed dramatically between the internodes. The number of functional categories represented in the secretome dropped from 18 in both internodes to 10 and 5 in RI2 and RI3, respectively. The proportion of proteins with unknown function increased, especially at the advancing front of infection, where they accounted for 50 % of the transcripts. The three next most frequently represented functional categories detected in RI3, metabolism, protein-binding and cellular transport, accounted for another 42.9 % of transcripts. The highly expressed secreted proteins at the advancing front of symptomless infection (Table 16) included small cysteine-rich proteins of which some contained internal amino acid repeats that are not specific to *F. graminearum*. Therefore, transcriptional differences between hyphae within symptomless plant tissue exist, with the advancing front of infection being distinct, especially in the secretion of an array of proteins with unknown function.

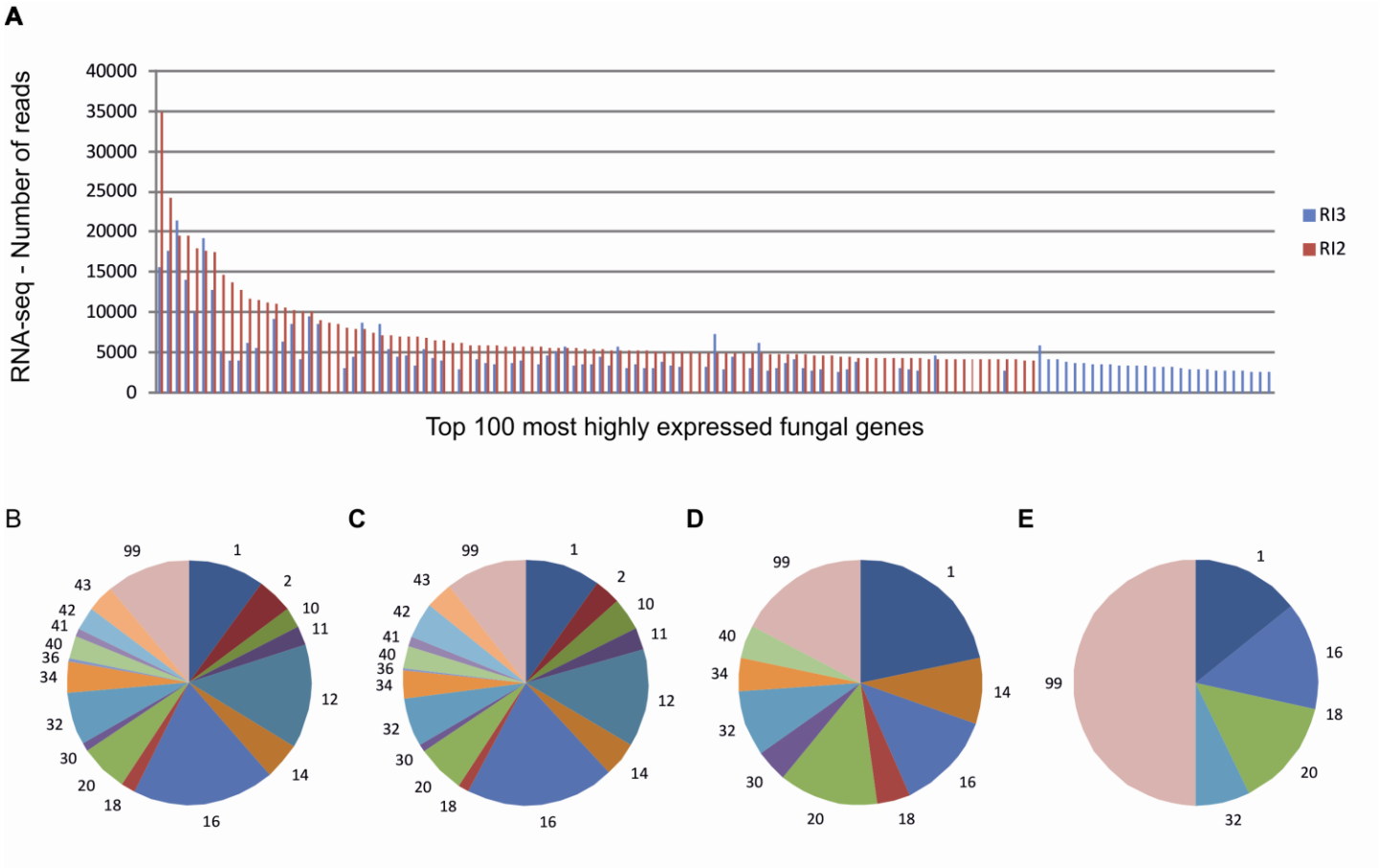

Figure 51 The 100 most highly expressed (number of reads) genes in RI2 and RI3 **(A)**. The MIPS functional categories of the most highly expressed genes in RI2 **(B)** and RI3 **(D)**. The MIPS functional categories of the genes predicted to encode secreted proteins, in RI2 **(C)** and **(E)**. The MIPS codes are described in Appendix 2.

Table 16 The characteristics of the secreted proteins of unknown function that were identified via monitoring fungal gene expression by RNA-sequencing during symptomatic infection of the wheat ear. The expression (number of reads) in the two symptomless rachis internode, RI2 and RI3, is presented. Traits include: the length of the mature protein, the number of introns, cysteine residues (C), transmembrane domains (TM), internal amino acid repeats (RADAR), an extracellular localisation prediction (WoLFPSORT), the presence of a nuclear export signal (NES), Pfam domains, whether the gene is specific to *F. graminearum.*

FGSG_ID	MIPs Annotation	Expression (No. reads)		No. introns	Mature protein length	No. C	RADAR	WoLFP	NES	Pfam domain	FG specific
		RI3	RI2								
FGSG_03632	Related to cellulose binding protein CEL1	9,905	17,992	-	-	-	-	-	-	-	-
FGSG_05046	Conserved hypothetical protein	8,479	7,171	1	112	8	-	extr=27	0	-	N
FGSG_09390	Related to circumsporozoite protein precursor	6,151	4,909	-	-	-	-	-	-	-	-
FGSG_09353	Related to gEgh 16 protein	5,066	14,683	-	-	-	-	-	-	-	-
FGSG_07988	Conserved hypothetical protein	3,851	3,615	0	161	4	-	extr=22	0	-	N
FGSG_09066	Conserved hypothetical protein	2,843	891	1	64	8	2	extr=24	0	-	N
FGSG_11101	Hypothetical protein	2,734	3,426	5	455	15	2	extr=26	1	-	N

7.3.4. A comparison of the *Fusarium* Affymetrix and *Fusarium* RNA-sequencing data-sets

The Affymetrix study of the day 7 time-point combined rachis internodes which appears symptomatically the same, while the RNA-sequencing investigation evaluated two symptomless internodes individually at the day 5 time-point. This experimental design was carefully planned to explore the dynamics at the hyphal front. Genome wide correlation in gene expression, assessed by RNA-sequencing, was very high between the two symptomless rachis internodes, which justified pooled rachis internode pairs in the Affymetrix study. Overall, the functional profiles of the transcriptome generated by the Affymetrix and RNA-sequencing studies were similar, with protein-binding, protein synthesis and metabolism functions accounting for the majority of the profile. The infection front at 5 and 7 dpi was hypothesised to be similar (Chapter 3). The Affymetrix data-set acquired from the symptomless infection front was individually compared with the RNA-sequencing data-sets from the two symptomless rachis internodes. The correlation in gene expression across all genes detected in both experiments was poor, irrespective of the internodes compared (Table 17, Figure 52). In the 5 dpi RNA-sequencing data-set a considerable number of genes had a value lower than 10 assigned (equal to the mean number of reads per gene in the mock infected control) and were excluded, whereas in the 7 dpi Affymetrix data, hybridisation values were assigned to most of these genes. A comparison of the reads generated by RNA-sequencing with the predicted gene model, on which the Affymetrix array was based, revealed numerous cases where sequenced mRNA transcripts were detected beyond the gene model (Figure 53). In addition, regions of several plant genes of highly conserved function, such as β tubulin, demonstrated significant homology to the fungal gene and were incorrectly detected as belonging to *Fusarium* in the non-infected controls. Therefore, the variation in the experimental approach appeared to cause significant alterations to the transcriptional profile.

Table 17 The correlation coefficient of the expression of genes detected in all the RNA-sequencing and Affymetrix data-sets, compared across samples (n = 5510). The analysis was repeated separately with the 1000 highest and lowest expressed genes. P values for all correlations were < 0.001.

		Affymetrix array			
		SP1	RI1-2	RI3-4	RI5-6
RNA-seq	RI2	0.4736	0.6014	0.6072	0.5956
	RI3	0.4161	0.5401	0.5622	0.6287

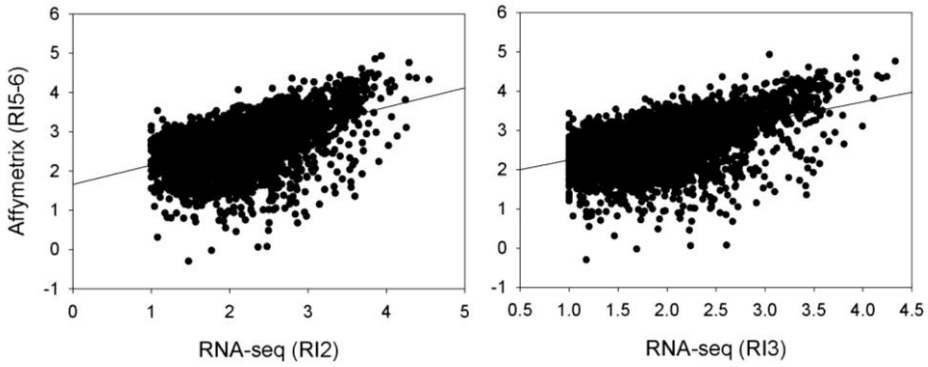

Figure 52 Scatter plot representation of the transcriptome of symptomless rachis internode infection assessed by Affymetrix arrays and RNA-sequencing techniques. The two individual symptomless internodes (RI2 and RI3 from the RNA-sequencing 5 dpi study) were compared with the symptomless pooled internodes (RI5-6 from the Affymetrix 7 dpi study). Log_{10} expression values are present.

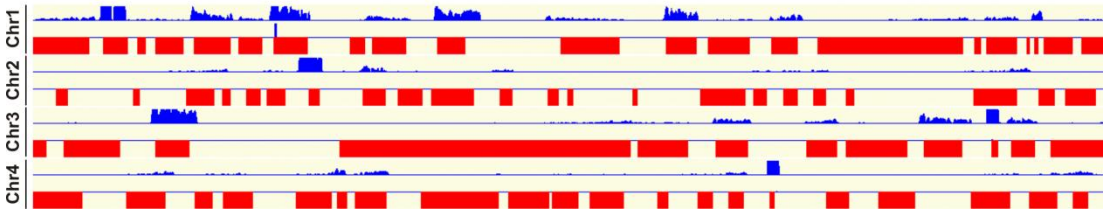

Figure 53 The alignment of the RNA-sequencing reads (blue histogram relative to number of reads where the range displayed is 0-500), from the *F. graminearum*-infected (lane 1) and the mock control (lane 2) alongside the FG3 predicted gene model (red, lane 3). This is representative of the RI2 transcriptome. Display generated using novel software under development by John Antoniw, RRes.

7.4. Discussion

The transcriptome investigation of the transition from latent symptomless to symptomatic *F. graminearum* wheat ear infection revealed the distinct expression profile of the advancing infection front. The Affymetrix analysis revealed that 48.9 % (6,440/13,158) of *F. graminearum* genes were differentially expressed between, and identified the functional profile of, the two infection phases. The number of genes up regulated during symptomless infection (5,347) was far greater than the number down regulated (1,093). In the presence of symptomless *F. graminearum* infection, the total number of unmapped wheat transcripts detected in the RNA-sequencing investigation rose 14.4 % and 7.2 %, representing the wide scale transcriptional response, and possible manipulation of the host by the pathogen. These two large transcriptomic data-sets were generated within the last month of the project. As a consequence, the presented analysis represents a first examination of the expression pattern of known genes of interest. A simplistic comparison of the top 100 most highly expressed, representing the upper 1 % of the transcriptome, during the two phases of infection and the fully symptomatic spikelet was undertaken. Of the top 100 most highly expressed fungal genes, 68 % were in agreement in the Affymetrix analysis of symptomless and symptomatic infection. The Affymetrix analysis also revealed that 27.2 % (3,584/13,158) *F. graminearum* genes were differentially expressed between rachis and spikelet infection, with 1,331 and 2,253 genes up and down regulated, respectively. The correlation between the top 100 most highly expressed genes during symptomatic infection of the spikelet and rachis was 51 %. This demonstrates that a degree of tissue specificity, and an alteration of the micro-environment, also exists within the wheat ear. However, a greater degree of transcriptional alteration occurs between the different phases of infection. This investigation demonstrates the flexibility of the *F. graminearum* transcriptome, and the dramatic alteration of the interaction between pathogen and host, over just a few centimetres.

Genome wide statistical analyses and the comparison with the other published transcriptomic data-sets, in particular the whole wheat ear investigation (Lysoe *et al.*, 2011b), are scheduled. The Awk Script is being prepared to incorporate the transcriptomic data-sets into Bioconductor (www.bioconductor.org) which will

subsequently link to the KEGG biosynthetic pathways database (http://www.genome.jp/kegg-bin/show_organism?org=fgr), enabling the analysis of the metabolic state of the fungal cell within the different phases of the interaction. This data could then be utilised in the generation of an electronic *F. graminearum* cell, as it captures the developmental progress of wheat infection. After rigorous statistical analysis of these data-sets will be used to identify candidate fungal genes, possibly involved in the establishment of symptomless infection or mycotoxin production for genetic investigation and therefore represent possible targets for fungicide intervention. The transcriptomic data generated may also assist in the construction of *Fusarium* only, and *Fusarium* plus wheat, protein-protein interaction networks, through the presence of known binding domains and correlated transcriptional regulation. Further analysis of the RNA-sequencing data may also be utilised to improve the *F. graminearum* gene models. A subsequent, comparative analysis of the identical tissue samples may reveal a better correlation between the Affymetrix and RNA-sequencing data-sets.

The Affymetrix and RNA-sequencing approaches were successful in evaluating the transcriptome of the advancing infection front, detecting 98.7 % (13,158) and 82.9 % (11,058) of the fungal genome (FG3 predicted 13,331 genes on which the Affymetrix array was based), respectively. The cell biology and *TRI* gene expression studies implied that the interaction at the symptomless infection front was repeated as infection advanced throughout the wheat ear (Chapters 3 and 4). Different time points after infection were selected for analysis by the two transcriptomic approaches, in an attempt to maximise the data-sets generated. Despite the *TRI* gene expression profile being similar between the Affymetrix and RNA-sequencing data-sets, genome wide correlation was poor. The lack of correlation could be explained by; 1) the length of infection influenced the transcriptome and the hypothesis that a cyclic repetition of the interaction occurred at the infection front was incorrect, or 2) technical differences in the approach, such as inaccurate gene models, or that the RNA-sequencing at the day 5 time point should have been to a greater depth to be able to detect the rarer transcripts, accounted for the poor correlation. To determine the cause of such variation, the pilot RNA-sequencing study would have to be extended and possibly deepened. A 5 dpi study of

the two infection phases, comparative to the Affymetrix study, would prove essential.

Previously, the prolonged period of latent infection was shown to be accompanied by maximal expression of several *TRI* genes (Brown *et al.*, 2011) (Chapter 4). Therefore, the expression profile of genes known to be involved in DON production or regulation was assessed. The enhanced transcription of all the *TRI* genes during symptomless infection was confirmed and correlated with the up regulation of the positive transcriptional regulators of *TRI* gene expression, *TRI6*, *TRI10* and *VE1*. The inverse expression profile was observed for negative transcriptional regulator, *TRI15*. Single gene deficient strains lacking either FGSG_00007 or FGSG_10397 are greatly augmented in virulence and DON production *in planta* (Gardiner *et al.*, 2009a). These two genes were dramatically up regulated at the advancing front of symptomless infection. A secreted lactonohydrolase (FGSG_10675) that could potentially detoxify the DON mycotoxin (Takahashi-Ando *et al.*, 2002, Takahashi-Ando *et al.*, 2004) (Chapter 6) was also up regulated at the advancing front. Further bioinformatic analyses may identify novel genes co-ordinately regulated with mycotoxin gene expression.

The communication between pathogen and host is, at least in part, mediated by secreted proteins. In many pathogenic interactions, secreted proteins are known to influence the outcome of the interaction (Boller & He, 2009, Stergiopoulos & de Wit, 2009). Genes that encode secreted proteins represented 11 % of the 100 most highly expressed genes detected during symptomless infection, which is similar to the genome as a whole (12.8 %). However, the 100 most differentially expressed genes where enriched in secreted proteins at 21.5 %. A *F. graminearum* gene that encodes a secreted circumsporozoite related protein (FGSG_09390), which is produced by *Plasmodium* parasites to inhibit host protein synthesis (Menard *et al.*, 1997), was maximally transcribed at the advancing front of infection. Many of the *F. graminearum* genes up regulated during symptomless infection encode small cysteine-rich secreted proteins of unknown function, of which some contained internal amino acid repeats. Conversely, these candidate *Fusarium* effectors were expressed at a far lower level during symptomatic infection. Molecular genetic studies of these candidate *Fusarium* genes are required to further elucidate function.

The intracellular gEgh16 proteins from powdery mildew fungi *B. graminis* f. sp. *hordei* and Gas proteins from *M. oryzae* are expressed during early infection and localises to the cytoplasm of developing appressoria (Xue *et al.*, 2002). A *F. graminearum* homologue of *GEGH16* was highly expressed at the hyphal front and during the remaining phases of active colonisation, but was expressed at a minimal level in the fully colonised spikelet. Determining the sub-cellular localisation of the gEgh16 homologues in *F. graminearum*, a non-appressoria producing pathogen, would therefore prove informative.

Snodprot1 is a known phytotoxin from *S. nodorum* (Hall *et al.*, 1999). Coinciding with the onset of host cell death and disease symptoms in the *F. graminearum* - wheat floral interaction was the expression of two *Fusarium* genes that encode Snodprot1 related proteins (FGSG_10212, FGSG_11205). Also in association with the onset of disease symptoms was the up regulation and secretion of an array of PCWDEs. The highly expressed PCWDEs were previously down regulated during symptomless growth. The lipase, Fgl1, is the only *F. graminearum* secreted protein experimentally proven to be essential for full virulence on wheat and maize (Voigt *et al.*, 2005). However, *FGL1* was expressed at low level at the advancing front of symptomless infection and was only up regulated within the fully symptomatic tissue, in association with wide scale intracellular colonisation. Therefore, due to the substantial distance between the infection front and the high level of *FGL1* expression, it would appear that Fgl1 functions as a traditional lipase and is possibly involved in lipid metabolism and does not play a role as a secreted effector.

Pathogens commit a lot of resources and energy into creating a hospitable environment for infection. In doing so, the host becomes more susceptible to colonisation by microbial competitors. The four genes that encode antifungal proteins, including three *KP4* homologues, where identified by a bioinformatic analysis of the secretome (Chapter 6). The antifungal protein (FGSG_04745) was highly expressed throughout, but was up regulated during the symptomatic phase of rachis infection, in association with host cell death, while the *KP4* homologues (FGSG_00060, FGSG_00061, FGSG_00062), which were expressed at a lower level, were up regulated during the last phase of infection. This is in agreement with

the whole wheat ear transcriptomic study (Lysoe *et al.*, 2011b) (Chapter 6) and could reflect the vulnerability of the niche created to infection by different competitors.

This investigation demonstrated that genome wide transcriptional alterations occur between the different phases of infection and depicts a situation where the symptomless infection front was the most distinct, especially in terms of the expression of genes that encode secreted proteins. The biphasic model of *F. graminearum* wheat floral infection must now be considered in the design and assessment of all future genetic or 'omic' studies of infection. The RNA-sequencing study revealed that this technique can be used successfully to study the *Fusarium* - wheat interaction. In addition to providing information on the pathogen, RNA-sequencing also generated the first data-set on the transcriptional alterations of the susceptible wheat ear to *F. graminearum* infection. In combination these studies provide a unique comparative resource for future transcriptomic studies and have identified many fungal and plant genes of interest for future genetic evaluation.

Chapter 8. Exploring the *Fusarium graminearum* cell-type specific transcriptome during wheat ear infection

8.1. Introduction

The laser capture microdissection (LCM) procedure originated from, and is an established technique in, the field of human pathology (Emmert-Buck *et al.*, 1996). Initially developed to isolate and study specific cancer cells, LCM has now been widely adopted by research communities studying microbial and plant systems (Asano *et al.*, 2002, Ramsay *et al.*, 2006). The ability of LCM to successfully harvest individual cell populations for DNA, RNA or protein extraction greatly enhances the resolution of the biological question that can be asked. This enables research to connect the observed sub-cellular alterations with the molecular status of a specific cell population, excluding the noise from other cells undergoing different processes. Whereas previous methods that utilised amalgamated tissues, including whole plants or organs, represent an average of all the different sub-populations of cells within the tissue.

Different LCM systems are available, all of which are based upon two approaches, utilising either ultraviolet (UV) or infrared (IR) lasers. The UV laser beam cuts through the specimen and membrane on a slide. Then the targeted cells either fall by gravity (Leica) or are catapulted by a defocused laser beam (PALM), into a microcentrifuge cap. While the IR laser system (Veritas) melts a themoplastic onto the sample attaching the desired region to the cap, which is then torn from the section as the cap is lifted. The heat generated by either laser system does not damage the nucleic acids or proteins (Jain, 2002), as it uses a higher wavelength than their absorption range (Day *et al.*, 2005). Many successful studies utilising both systems have been published (Asano *et al.*, 2002, Kerk *et al.*, 2003, Nakazono *et al.*, 2003, Tang *et al.*, 2006).

Coupling LCM with genome wide transcriptome studies enables the identification of genes and pathways associated with specific processes evident in the micrograph, providing additional gene function and regulation information. A balance between the preservation of cell integrity and RNA therefore exists. Precipitative fixatives (ethanol) provide better RNA preservation, while cross-linking

fixatives (aldehydes) demonstrate better cell integrity but lower RNA yields. Cryo-sectioning frozen fresh tissue yields the highest amount of RNA. However, ice crystals formed during the freezing process disrupt cell integrity, as is the case for plant tissue. Consequently, a fixation step is required to stop the biological process prior to infiltration with a cryo-protectant such as sucrose. Alternatively, a microwave based parafilm embedding procedure was developed to reduce the reliance on fixatives (Inada & Wildermuth, 2005). Again there is a range of publications that utilise different sample preparation procedures. Finally, for the extraction of small quantities of RNA from microdissected cells several commercial affinity column based kits are now available, for example, Ambion - RNAqueous, Arcturus - Picopure, RNeasy Plant Mini - Qiagen.

In the analysis of plant-microbe interactions LCM has been used sparsely compared to the frequent use in plant-nematode research and explorations of the feeding sites (Fosu-Nyarko *et al.*, 2009, Nakashima *et al.*, 2008, Portillo *et al.*, 2009, Ramsay *et al.*, 2004). The majority of transcriptome studies on plant-fungal associations, including *Fusarium* infections of wheat (Reviewed in Chapter 7) rely upon time course experiments using whole tissues. Increasingly, LCM is being used for the isolation of sexual fruiting bodies from cultures and the surface of leaves (Tremblay *et al.*, 2009). The few examples that use LCM to study fungal infections only assess a single cell-type at one time point and compare this to *in vitro* or whole tissue studies (Chandran *et al.*, 2010, Gomez *et al.*, 2009, Tang *et al.*, 2006). Reporter proteins GFP or GUS, produced by the modified fungus or plant in response to colonisation, facilitated localisation of infection. Fluorescent *Colletotrichum graminicola* hyphae were isolated during the early stage of maize silk infection, identifying 437 and 370 fungal genes that were up or down regulated respectively, compared to *in vitro* hyphae (Tang *et al.*, 2006). To enable site-specific sampling of *Golovinomyces orontii* infections, *Arabidopsis thaliana* was transformed with the *PR-1:GUS* reporter construct. LCM of GUS expressing plant cells, indicative of infection, increased the sensitivity of the gene expression assay enabling the identification of the response of 67 transcription factors and the localised host induced endoreduplication of the Arabidopsis genome (Chandran *et al.*, 2010). Isolation of arbuscule mycorrhizal fungus *G. intraradices* from

fluorescing cortical cells of *Medicago truncatula MtSCP1:GFP* roots, also indicative of infection, revealed spatial gene expression patterns (Gomez *et al.*, 2009). However, studies that utilise LCM to assess transcriptome changes in different host cell-types throughout the progression of infection have so far not been published.

In the presented work *F. graminearum* infected wheat tissues were prepared by precipitative fixation, cryo-protection and cryo-sectioning to preserve both cell integrity and RNA. The PALM Microbeam system (Zeiss) was used to isolate individual cell-types and the RNeasy Plant Mini Kit (Qiagen) to extract total RNA (Figure 54). The PALM Microbeam system (Zeiss) at Rothamsted Research was acquired on a BBSRC grant however, the principal investigator left Rothamsted before utilising the system to its potential. Due to the difference in composition, the diverse range of tissues that can be studied using this system required different sample preparation and LCM conditions. Consequently, the expertise and a working procedure for LCM of wheat was lacking at Rothamsted. The objective of this project was to develop a working procedure for a cell-type specific investigation of *Fusarium* infections of wheat ears. The development of a functional procedure was achieved in the duration of the project and is presented below. Unfortunately, due to time constraints and sample size constraints, the application of the technique in the investigation of a biological hypothesis was not undertaken.

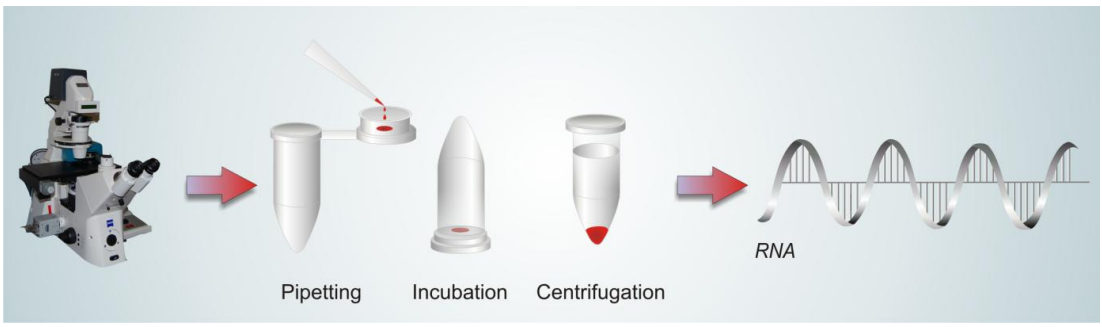

Figure 54 The PALM Microbeam laser capture microdissection system (Zeiss).

8.2. Experimental Procedures

8.2.1. Development of a procedure applicable to the *Fusarium* – wheat rachis system

Optimal cryo-sectioning was found to be paramount for successful LCM. The cryo-preservation, embedding and mounting process would determine the outcome

of the downstream procedures. Time was required to develop the technical skills needed, and a sense of how to manipulate the conditions for individual samples, to successfully operate the Cryostat CM1850 (Leica) and generate high quality frozen sections. The optimisation of the LCM procedure will be discussed and the successful application of the final procedure presented.

8.2.2. Embedding, mounting and sample temperature equilibration

Post cryo-protection, individual tissues were plunge frozen in liquid nitrogen within a 0.5 ml tube half full with TissueTek OCT (Sakura Finetek, USA). The embedded samples were removed from the tube and mounted onto a cryo-stub using TissueTek OCT. Freezing the TissueTek OCT placed around the embedded sample by plunging into liquid nitrogen fractured the embedded sample. To avoid this occurring, a droplet of TissueTek OCT was placed onto a cold cryo-stub, on the freezing stage within the Cryostat, and the embedded sample placed on top. Subsequently, additional TissueTek OCT was placed around the base of the sample and returned to the Cryostat to freeze. The frozen mounted sample was left within the Cryostat for 30 mins to equilibrate the tissue to -20^{o}C, ready for cryo-sectioning (Figure 55).

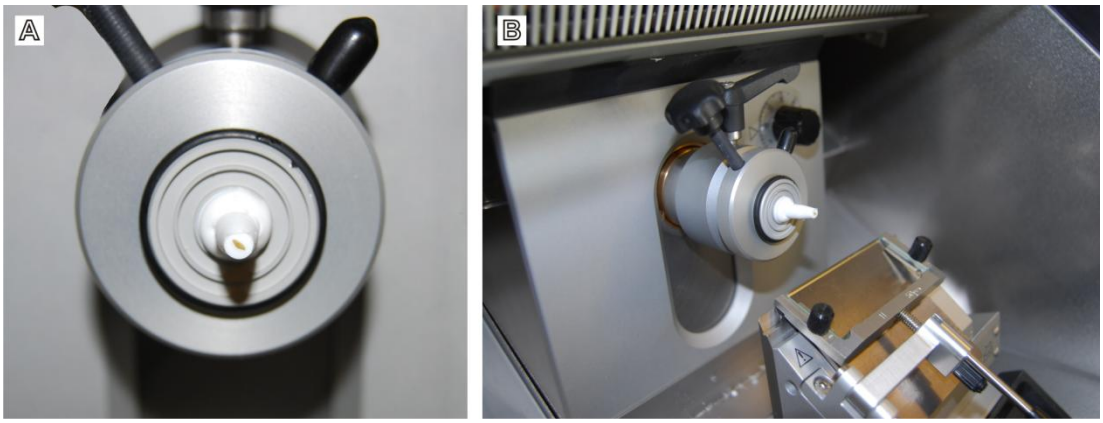

Figure 55 The optimal method for embedding and mounting the infected rachis internodes onto the cryo-stub, encased in TissueTek OCT **(A)** and subsequently sectioned, frozen at -20^{o}C, within the Cryostat **(B)**.

8.2.3. Cryo-preservation and Cryostat sectioning

In order to optimise cryo-preservation, equivalent rachis internodes (RI-1) at 5 dpi were infiltrated with a range of sucrose solutions, from 0.5 M to 2.3 M. The tissues containing different concentration of the cryo-protectant were sectioned in the

Cryostat set at -20^{o}C, with minor modifications to temperature and cutting angle depending on the sample. Frozen 10 µm sections collected from the start (initial 100 µm) and further into the sample (~ 500 µm) were inspected by light microscopy on a Zeiss Axiophot to assess tissue preservation.

8.2.4. Laser microdissection and pulse catapulting

For the purpose of removing the embedding medium surrounding the section and inhibiting RNase activity when the sections were bought to room temperature, frozen cryo-sections were washed and desiccated in an ethanol series increasing from 30-100 %. The percentage of ethanol, the temperature of the solution and the length of each wash were investigated. The success rate for the collection of microdissected samples was then determined. Cryo-section thickness also strongly influenced the success of the LCM procedure.

The energy of the UV laser beam, focal plane, speed of cutting and number of repeats, used during microdissection and pulse catapulting was optimised for the wheat rachis tissue. The energy of the beam was kept to a minimum to limit the damage caused. However, unlike the other published studies, the wheat rachis represented a heavily lignified resilient tissue.

Microscopy was used to confirm that the laser pulse catapulted cells were being collected in the microcentrifuge cap. Direct PCR was used to confirm that nucleic acids were detectable within the LCM collected cells. Individually whole desiccated cryo-section, LCM cells and gDNA (40 ng) were boiled at 95^{o}C in 0.25 N NaOH, then neutralised with 0.25 N HCl in 0.5 M Tris-HCl, pH 8, containing 0.25 % nonidet P40. The solutions were boiled for 2 min at 95^{o}C and put directly into a PCR reaction to determine whether nucleic acids could still be harvested. The PCR analysis was performed in a final volume of 25 µl and consisted of 12.5 µl of HotStarTag master mix (Promega), 1 µl of each primer (10 mM) (Chapter 2, Table 3), 5.5 µl of dH_2O and 5 µl of the 1/10 or 1/100 dilution of the nucleic acid template. The non template, dH_2O only, and the untreated gDNA (40 ng) controls were performed in parallel. Thermal cycling conditions were as follows: [95^{o}C 2 min, (95^{o}C 15 sec, 62^{o}C 20 sec, 72^{o}C 45 sec) x40].

8.2.5. Application of the final LCM experimental procedure for the extraction of RNA

The first rachis internode below the inoculated spikelet on the *F. graminearum* infected wheat ear, at 5 dpi, was excised, immersed in 5 vols *RNALater* (Ambion) vacuum infiltrated at room temperature for 15 min and incubated 16 h at 4^{o}C. Samples were fixed twice using fresh cold 75 % ethanol: 25 % acetic acid, vacuum infiltrate on ice for 15 min, rotated 20 min at room temperature and then incubated for 40 min at 4^{o}C. Samples were cryo-preserved by immersing fixed tissues in a 0.25 M sucrose solution, vacuum infiltrated for 15 min on ice, incubated for 4 h at 4^{o}C. Immersion, infiltration and incubation were repeated with 0.5 M sucrose solution. Finally samples were transferred into a 0.5 ml microcentrifuge tube half full with TissueTek OCT, plunge frozen in liquid nitrogen and stored at -80^{o}C. Embedded samples were removed from the microcentrifuge tube, mounted onto a cryo-stub using TissueTek OCT and equilibrated to -20^{o}C for 30 min within a Leica Cryostat CM1850 and then 10 µm thick sections were collected onto a cold PEN membrane covered slides (Zeiss). Mounted sections were immersed for 2 min in 50 %, 70 %, and 100 % ethanol solutions in deithylpyrocarbonate treated water kept at -20^{o}C. Dehydrated sections were dried inside the Cryostat at -20^{o}C, sealed within a 50 ml air tight tube and brought up to room temperature.

A PALM Microbeam system (Zeiss) was used to isolate infected wheat cells from the prepared slides. LCM was performed using the 10x objective, energy 60, and focus 80, cut once at speed 5. The robotic arm holding the microcentrifuge cap was brought over and down onto the slide. Laser pulse catapulting (LPC) was performed using the 10x objective, energy 80, and focus 78 with a single LPC dot in the centre of each group of cells. The collected cells were stored at -80^{o}C. RNA was extracted from the LCM cells using RNeasy Plant Mini Kit (Qiagen) according to manufacturer's instructions and eluted in 20 µl dH_2O.

8.2.6. RT-qPCR gene expression analysis

Individual vascular bundles from sections of three 5 dpi rachis internodes were harvested, pooled and the total RNA extracted. Approximately, 17.6 mm^2 of cells were collected (176 LPC harvested vascular bundles, each of 100 µm^2)

compared to the 15 mm^2 recommended (RNeasy Plant Mini Kit instructions, Qiagen). RNA was treated with a DNA-*free*™ kit (Ambion) to remove contaminating DNA and the absence of gDNA confirmed by PCR using intergenic primers. The cDNA was synthesised from 1 µg of RNA (or 7 µl of RNA collected via LCM) using 500 ng of OligodT primers and 200 U Superscript III (Invitrogen) according to manufacturer's instructions. RT-qPCR was performed on a Real Time PCR System 7500 (Applied Biosystems). All the sense and antisense primers used are presented in table 3. A standard curve of gDNA, from an *in vitro* culture, with known concentrations ranging from 25 ng to 0.025 ng was created for each primer pair. Synthesised cDNA from mock infected rachis internodes and from LCM samples of infected rachis internodes, both at 5 dpi, were diluted 1/50 and 1/20 respectively, in dH_2O. The qPCR analysis was performed in a final volume of 20 µl and consisted of 10 µl of Jumpstart Taq Ready mix plus ROX (Invitrogen), 5 µl of 1.2 µM of each primer, and 5 µl of the relevant nucleic acid template. Thermal cycling conditions were as follows: [95°C 2 min, (95°C 15 sec, 62°C 20 sec, 72°C 45 sec) x40]. The dissociation curves were as follows: [95°C 15 sec, 60°C 1 min, 95°C 15 sec] x1. The average cycle threshold value for each sample was calculated from triplicate technical replicates.

8.3. Results

8.3.1. Development of the LCM procedure

Contrary to expectations, the higher concentrations of the cryo-protectant sucrose applied to wheat rachis tissue resulted in poor tissue preservation. This was at least in part caused by the sample generating additional friction and tear when passing over the microtome blade. The cellular preservation of samples at the lowest sucrose concentration was good, even 500 µm into the sample (Figure 56). To infiltrate the samples with higher concentrations of sucrose tissues must be passed through a series of solutions, increasing in concentration every step. It is therefore ideal that sufficient preservation is achieved from the lower concentration sucrose solution, speeding up the preparation process.

A compromise was found between the ease of producing thicker sections (> 12 µm) in the Cryostat and the strength of the PALM laser beam required to cut the

plant cell walls. A thickness of 10 µm facilitated the collection of sections while not impeding microdissection. The temperature of the ethanol solution determined if the cryo-sections remained on the slide. To avoid the solutions warming and the sections being lost, the ethanol solutions were kept in sterile coplin jars (Wheaton Industries Inc) within the Cryostat at -20^{o}C. Three washes, containing 50 %, 70 % and 100 % ethanol, proved the most suitable for laser microdissection and pulse catapulting. Ensuring cryo-sections had not moved on the slide to overlap the embedding medium, discarding those which had, greatly enhanced microdissection and pulse catapulting efficiency. Applying all the aforementioned optimised steps resulted in an LCM success rate of 75 %.

Cells collected in a droplet of water were observed to be intact (Figure 57). Direct PCR of entire sections and LCM cells was successful, demonstrating that the preparation of the cryo-sections and the LCM procedure had not removed or destroyed the DNA (Figure 58). The final test remaining was to determine if RNA could be successfully extracted from LCM cells

8.3.2. Laser capture microdissection of infected wheat cells

Post DNAse treatment, RT-qPCR was used to quantify the amount of each fungal transcript. LCM samples are expected to yield pico grams (pg) of RNA. For *F. graminearum* γ-actin and glyceraldehydes 3 phosphate dehydrogenase (GAPDH), 4.48 pg and 15.2 pg where detected, respectively. The mixture of RNA from live fungal cells and dead or dying plant cells prevents the use of the Agilent Bioanalyser to determine integrity. However, the location of the primers within the gene provides an idea of the specific integrity of the fungal RNA. The distance of the amplified region from the 3' end polyA tail of the actin and GAPDH transcripts, 1010 bp and 488 bp, respectively, suggests that up to 1000 bp of the mRNA transcripts was preserved. Similar conservation of the 5'cap would be expected. This result demonstrates that the LCM technique can be successfully applied to the wheat rachis system. The abundance of these two fungal transcripts suggests that more than sufficient total RNA was harvested for downstream linear amplification and genome wide transcriptomics. The refined LCM procedure is summarised in table 18

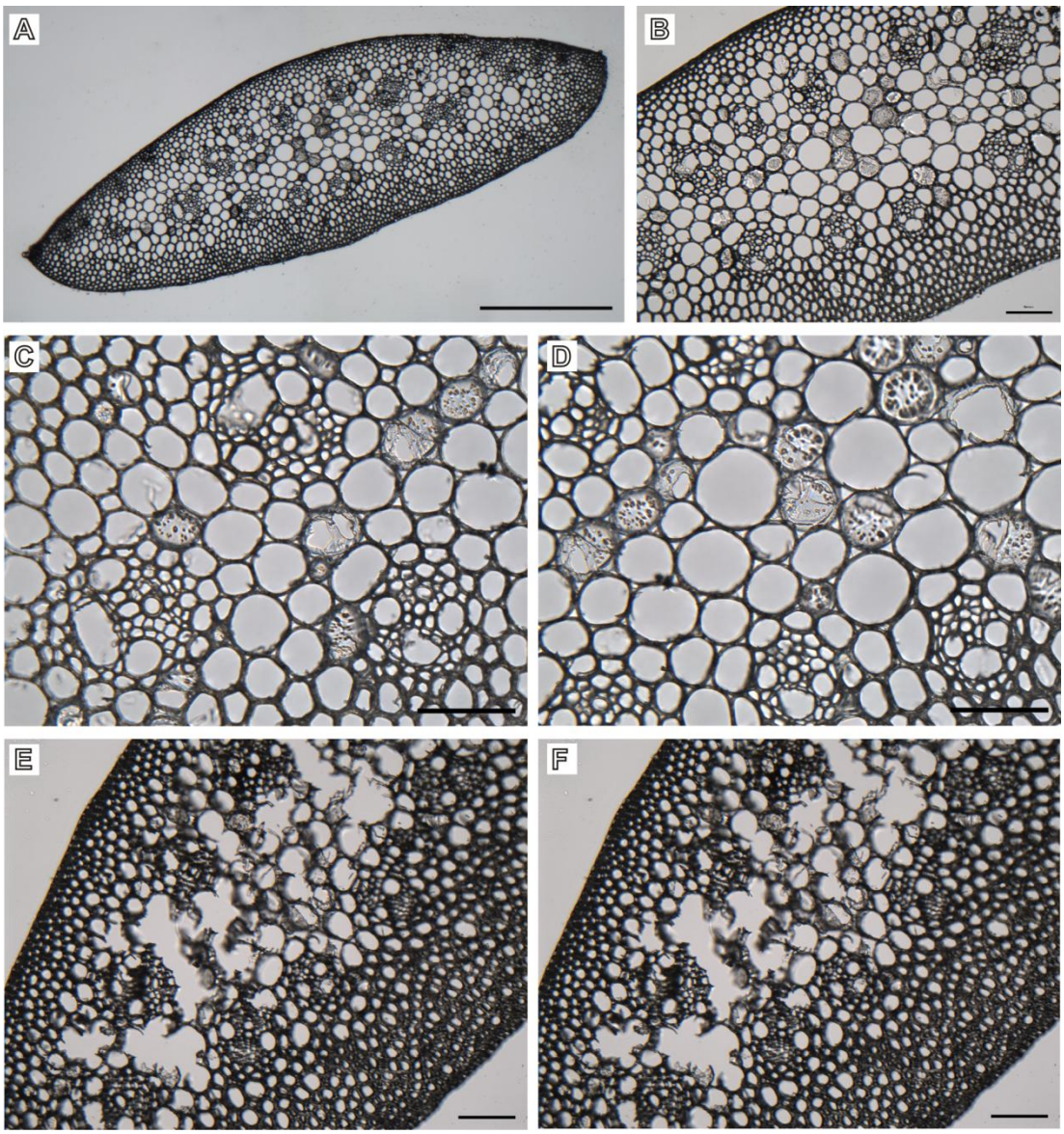

Figure 56 Optimisation of cryo-preservation of the *Fusarium* infected wheat rachis. All images are transverse, 10 µm thick, frozen section of a rachis internode at 5 dpi. Rachis tissues were infiltrated with different concentrations of sucrose prior to freezing in liquid nitrogen and cryo-sectioning. Tissue infiltrated with 0.5 M sucrose (**A** and **B**) alongside higher magnification images of the cortex and vasculature (**C** and **D**). Tissue infiltrated with 2.3 M sucrose (**E** and **F**). Bars = 500 µm (A), 100 µm (B, E, F) and 50 µm (C, D).

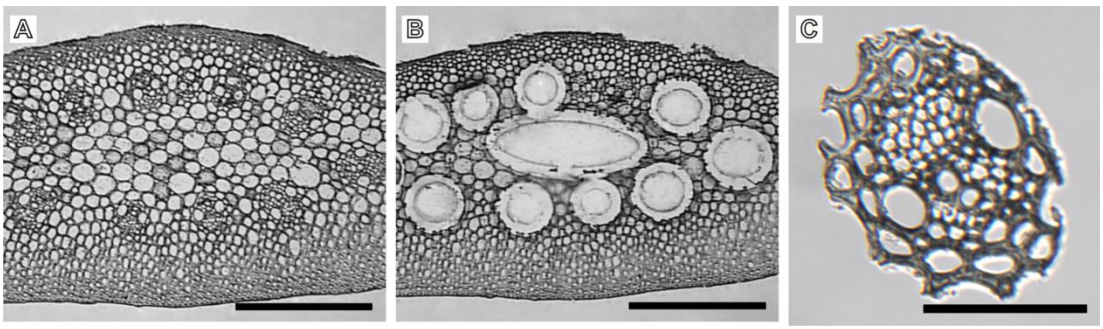

Figure 57 Optimising laser cutting and catapulting of the desired cells into the microcentrifuge cap. Light micrographs of a 10 µm thick, desiccated, cryo-section before **(A)** and after LCM **(B)** with a vascular bundle collected in the microcentrifuge cap **(C)**. Bars = 500 µm (A, B) and 100 µm (C).

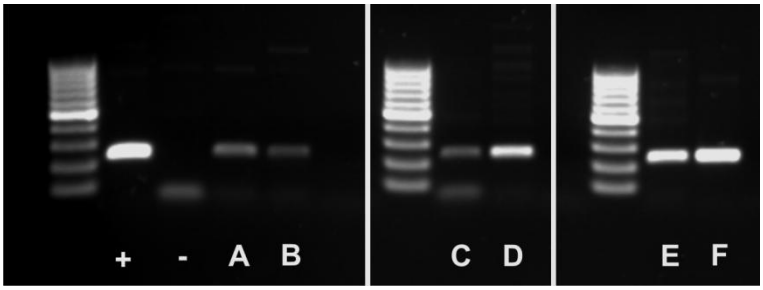

Figure 58 Direct PCR of the *F. graminearum* actin gene to confirm that sufficient LCM samples were successfully collected in the microcentrifuge cap. 20 LCM sampled vascular bundles (**A** and **B**) and ten whole cryo-sections (**C** and **D**) from an infected rachis internode at 5 dpi were assessed alongside 40 ng genomic *F. graminearum* DNA (**E** and **F**) using either a 1/10 (B, D, F) or 1/100 (A, C, E) dilution. Positive untreated gDNA control (+). Negative non template control (-).

Table 18 A summary of the working procedure for LCM of *F. graminearum* infected wheat rachis tissue and the time requirement and cost of each step of the process. * = Time required per sample.

Day 1	**Day 2**	**Day 3 (am)**	**Day 3 (pm)**	**Day 4-5**	**Day6**
Dissect tissue and immediately immerse in *RNAlater* (2 h)	Cold ethanol 75%: acetic acid 25% fixation (3 h)	Mount sample on cryo-stub with *TissueTek* (1/2 h)	Select regions for LCM (1/2 h*)	RNA extraction (2 h)	Two rounds of linear amplification (Convert pg to µg)
RNAlater infiltration (16 h)	Cryo-protection 0.2 M sucrose infiltration (5 h)	Equilibrate to -20^{0}C (1/2 h)	Cut (1/2 h*)	*RNaqueous (Ambion) is recommended*	*RiboAmp Plus (Arcturus) is recommended*
	0.5 M sucrose infiltration (5 h)	Section (1/2 h*)	Collection (1/2 h*)	DNAse treatment	
	Embed and freeze in liquid nitrogen (1 h)	Dehydrate and equilibrate to room temperature (1/2 h)	*Store LCM collected tissue at-80^{0}C*	*DNA-free (Ambion) is recommended*	
	Store at -80^{0}C	*Do not attempt more than 3 samples*			
RNAlater 100 ml £64	*TissueTek* 125 ml £15	Pack of 100, 1mm thick, PEN covered, slides £400	Pack of 200 AdhesiveCaps £168	*RNaqueous* 50 reactions £194 *DNA-free* 50 reactions £70	*RiboAmpPlus* 24 reactions £1,800

8.4. Discussion

The main objective to develop a working LCM procedure applicable to the study of the *Fusarium* – wheat ear interaction was achieved. The procedure was adapted from published investigations that used frozen plant tissue (Asano *et al.*, 2002, Nakazono *et al.*, 2003) and the commercial protocols provided by PALM (Zeiss). Tissue and nucleic acid preservation, cryo-sectioning and LCM was optimised for the wheat rachis system, previously developed to assess the dynamics of *Fusarium* infection (Chapters 4 and 7). RT-qPCR analysis confirmed the success of the developed procedure to collect RNA from microdissected wheat tissue. For the successful application of the procedure a degree of technical skill was required to generate viable cryo-sections and achieve a high LPC efficiency. The high cost of the procedure was evident, reaching approximately £3000 before the expense of any downstream transcriptome studies. LCM generated RNA has been used in many transcriptome investigations (Chandran *et al.*, 2010, Tang *et al.*, 2006) and the discussed issues of the poor conservation of the transcripts and the introduction of a 3' bias during linear amplification, are not envisaged to be an issue. The biological questions asked would have to merit the cost. The application of the procedure to the investigation of *Fusarium* infections of wheat is discussed.

8.4.1. Reduce complexity and enhance resolution of transcriptomic *Fusarium* studies by LCM

Profiling different wheat cell-types would enhance the sensitivity at detecting localised or site-specific responses during the different phases of *F. graminearum* wheat ear infection. Reducing the complexity of the harvested plant tissue from whole ears to individual rachis internodes (Chapter 7) has already proven successful in revealing the transcriptome changes masked in previous whole ear time-course studies (Brown *et al.*, 2011). A cell-type specific, LCM based, analysis of Arabidopsis infected with the powdery mildew fungus *G. orontii* identified site-specific processes and regulators which were previously expressed at too low a level to be detected in whole leaf experiments (Chandran *et al.*, 2010). Increasing the specificity to such a high level will enhance the understanding of how *F. graminearum* and wheat interact in different cell-types and may also aid in the

identification in low level changes, as is the case with genes coding for transcription factor.

The collection of *Fusarium* hyphal sub-populations over the duration of infection would capture how the two organisms interact within specific cell-types. Colonisation pattern and hyphal appearance is distinct and relevant to host cell-types and phase of infection (Chapter 3). Within the infected wheat ear hyphae differed in appearance, including the explorative within any host cell-type were thin and stained densely and the established hyphae that were larger in diameter, stained less intensely and were vesicle rich, while hyphae far behind the infection front lost cell content and often collapsed (Chapter 3). A three way comparison of the different hyphal types found during wheat infection, collected via LCM, could prove informative. Previously, the switch between thin haploid and thick dikaryotic hyphae has been observed within wheat stem infections (Guenther & Trail, 2005).

A comparison of the fungal transcriptome, isolated from cortical and vascular cells would determine how *F. graminearum* modulates its metabolism in these two nutritional distinct environments. *F. oxysporum* f. sp. *lycopersici* selectively secretes the SIX effectors into the xylem vessels of tomato roots, thus permitting successful infection (Ma *et al.*, 2010). *F. graminearum* may also up regulated virulence factor transcription and secretion within the vasculature in order to facilitate the systemic transport of effectors throughout the ear. Colonisation of the sclerenchyma and epidermis follows a different process to the cortex and vasculature due to the absence of intercellular space, the absence of autophagocytosis and the late development of asexual sporulation. LCM could be used to separate the early infected, cortex and vasculature, from the late infected sclerenchyma and epidermis. The heavily lignified sclenchyma tissue may still cause technical difficulties. Therefore, LCM could be used to remove the cortex and vasculature, avoiding such difficulties. Isolation of the sclerenchyma / epidermal cells that demonstrate signs of extreme cell wall degradation and sporulation could reveal how *F. graminearum* initiates and sustains reproduction.

Investigating alterations to the fungal transcriptome is really a study that has only explored half of the interaction. While a *F. graminearum* Affymetrix array is available, RNA-sequencing would double the data collected, permitting the analysis

of both organisms within the interaction from the same experiment. To date, the only published RNA-sequencing data from a plant pathogen interaction is on the *E. festucae* – Ryegrass system (Eaton *et al.*, 2010). No published data that combines RNA-sequencing and LCM in the study of a plant pathogen interaction exists. It is clear due to the change in physical appearance that host cell nuclei respond to the presence of intercellular *Fusarium* hyphae (Chapter 3). Therefore, RNA-sequencing would desirable as this would enhance the data produced from the same costly, linear amplified, LCM- preparation.

In other pathosystems involving hemibiotrophs, PCD has been shown to be closely associated with the death of the host tissue. For example, in the wheat – *M. graminicola* interaction (Keon *et al.*, 2007, Rudd *et al.*, 2008). *F. graminearum* produces a range of mycotoxins and there is some evidence to suggest that these may also lead to host cell death directly, or via PCD, at high concentrations (Desmond *et al.*, 2008). Traditional apoptosis kits, such as Tunel, which function via the exclusion of fluorescein-labelled nucleotides from the nucleus that otherwise bind to fragmented DNA, fail to discriminate between apoptosis and necrosis. Using the LCM technique to extract DNA extracted from cortical cells could be used to determine if DNA laddering occurs during the development of disease symptoms. In addition, isolated RNA could be used to monitor the transcriptional regulation of mitogen activated protein kinases, Mpk3 and Mpk6. These hallmarks of PCD and HR could be correlated with pathogenicity gene expression.

8.4.2. Isolation of sub-populations to study hyphal heterogeneity

Recently, within a fungal colony of *C. albicans* or *S. cerevisiae* individual cells have demonstrated heterogeneity in stress resistance and virulence (Avery, 2006). Heterogeneity in the enzyme, or the level of an enzyme, secreted has also been shown to exist in *Aspergillus niger* (Vinck *et al.*, 2005). *F. graminearum* colonises the wheat tissue by filamentous polarised growth at the apex and is predicted to secrete an array of fungal proteins and mycotoxins to manipulate the plant cell. Throughout the *Fusarium* colony, heterogeneity in metabolism and mycotoxin production could exist. This division of function may be modulated by environmental stimuli asserted on the hyphal apex. Conditions required for DON induction / production have already been established and detailed methods are now

available (Lowe *et al.*, 2011). Heterogeneity in mycotoxin production, under *in vitro* DON-inducing conditions, could be identified by using a fluorescent strain containing a *TRI5* promoter:GFP fusion construct. Corresponding to the induction of the *TRI5* gene, the hyphal population could be divided into two DON producing and non-DON producing categories by LCM extraction of the hyphal apex (front 100 μm). This system may again be utilised to study the influence of external stimuli such as nitrogen source, oxidative stress and fungicide application on DON induction and heterogeneity. This cell biology study of *TRI* gene transcription would provide a novel *in vitro* and *in planta* system to screen the impact of external compounds or stimuli on the dynamics of DON production and essential knowledge for the discovery of strategies for the inhibition of DON production.

Chapter 9. General Discussion

To support population growth global agricultural systems will need to produce more food from fewer resources through the incorporation of plant and microbial sciences, disease management, plant breeding and improved husbandry. Wheat provides one fifth of the world's total calorific intake and represents the most important carbohydrate source (Curtis *et al.*, 2002). Improved wheat germplasm and more appropriate agronomy are required to sustainably maintain and increase wheat productivity to meet global demand. Approximately half the global wheat cropping area is in developing countries that have lower annual yields per hectare (FAO, 2009), which in some cases represent the unfulfilled potential to maximise global output. Successful disease management has significantly contributed to the doubling of global food production over the last 40 years, yet 10-16 % of global output is still lost to disease (Chakraborty & Newton, 2011). High crop yields alone do not define food security since they must also be safe and nutritious.

Climate change will be beneficial for some wheat cropping regions but also detrimental to others. The greatest abiotic impact of climate change is predicted to occur in areas of low potential, reducing food security in already vulnerable regions. Climate change also influences biotic stresses exerted upon crops, leading to alterations in disease range and severity, through water availability and temperature, creating better conditions for infection, reproduction, dispersal, inoculum build-up and the introduction of additional host species (Garrett *et al.*, 2006, Paterson & Lima, 2010, Sanchis & Magan, 2004). Climate models predict that the UK will have warmer winters accompanied by drier summers with increasingly frequent extreme weather events, for example thunderstorms. Temporary drought stress can increase disease susceptibility and may become an important factor for consideration.

Increasingly throughout Europe, Asia and the Americas, Fusarium ear blight (FEB) disease is now leading to the severe losses in wheat grain yield and quality (McMullen *et al.*, 1997). The reasons for this rises are complex and include climate change, the banning of stubble burning, reduced ploughing and tilling, the increased cultivation of maize a highly susceptible host. Simultaneously, the species *F. graminearum* has increased in prevalence in the cooler regions of Northern Europe (Jennings *et al.*, 2004, Miedaner *et al.*, 2008, Waalwijk *et al.*, 2003) replacing the

previously predominant species of *F. culmorum* and *M. nivale* that produced less and no mycotoxin, respectively (Leonard & Bushnell, 2003). The rise in atmospheric CO_2 could also affect FEB, as it does for *F. pseudograminearum* crown rot where it results in increased inoculum pressure and a breakdown of wheat resistance (Melloy *et al.*, 2010). This could result in more frequent mycotoxin contaminations events. FEB favours warm wet conditions at anthesis. The flowering and maturation of the wheat crop is predicted to be brought forward, however, the adaptive *Fusarium* species are predicted to respond. Climate change models forecast increased FEB incidence in southern England by 2050 (Madgwick *et al.*, 2011). The increase in the number of rainy days during the critical wheat growth period in the UK and South America may result in more frequent crop rejections (Madgwick *et al.*, 2011, Ponte *et al.*, 2004).

Currently, regional forecasting of disease risk only gives farmers a broad indication of disease likelihood. The HGCA risk assessment tool and DONCAST, supported by Bayer CropScience, calculate the number of rainy, humid (>75 %) and warm (between 12^{o}C and 32^{o}C) days, while considering crop history, to predict the potential for mycotoxin contamination (Schaafsma & Hooker, 2007). Due to the sporadic nature of the disease and the rapid growth of symptomless infection, inoculum monitoring systems need to be developed that enable farmers to spray a preventative fungicide onto the clean, emerging ears with confidence that it is required. Development of this type of 'in field' sensor technology may be several years away.

Post-harvest conditions must be controlled to ensure the potential of the harvest is reached. Grain moisture, largely determined by its content at harvest, and temperature are the most influential factors affecting quality during storage and transport. To protect consumers, there are now strict legal limits in the USA, EU and elsewhere as to the levels of the DON mycotoxin permitted to enter into the food chain via unprocessed or processed grain products. Despite best practices, highly contaminated grains still slip through to cause production difficulties, product rejection and even product withdrawal. The presence of pink or symptomless grain either put into storage or transported elsewhere is a major concern to the farmers, millers, bakers, feed processors, brewers and the bioethanol fermentation industries.

F. graminearum and *F. culmorum* are important competitors of molds in stored grain, with *F. graminearum* being the more aggressive (Paterson & Lima, 2010). High moisture during storage can lead to increased mycotoxin contamination (Magan *et al.*, 2010). In addition, the light weight and exceptionally FEB contaminated grain left in the fields post-harvest are of growing concern to environmental agencies due to the health risk to wildlife and game birds.

The identification of new *Fusarium* species, strains and hosts is revealing the diverse agricultural impact of this taxonomic group. The rapid spread of a more toxigenic and vigorous *F. graminearum* strain in North America has caused anxiety (Ward *et al.*, 2008). *F. langsethiae* remains symptomless for long periods in oats and barley, while producing T-2 and HT-2 mycotoxins (Edwards *et al.*, 2009). This presents both pre- and post-harvest issues, similar to *F. graminearum* on wheat, due to the problems involved in identifying infection. The isolation of mycotoxin producing *F. culmorum* and *F. graminearum* strains from new hosts such as sugar beet (Rivera *et al.*, 2008, Schneider & Musters van Oorschot, 2008) and potato (Delgado *et al.*, 2010) present an agronomic problem for crop rotation and residue management. The aforementioned ecological issues demonstrate that in order to develop any effective prediction model or pre- and post-harvest control strategy, the entire agricultural system needs to be considered. Reliable and consistent monitoring of the local and regional climatic conditions, the presence of fungal spores and the history of the cultivated land would be highly beneficial.

Harvesting of *Fusarium* and mycotoxin contaminated cereal grains costs time and money at every step in the processing chain. The best method of control is to stop infection before it takes hold. However, *F. graminearum* has so far proven exceptionally difficult to control through the use of fungicides and / or partially resistant wheat cultivars (Trail, 2009). Cultural and cropping practices remain the best local options to reduce FEB disease incidence and severity. The presented research, undertaken during this PhD project, has revealed that the *F. graminearum* is able to establish, within a few days of germination on the plant surface, a very high density of both intercellular and intracellular hyphae in almost every cell-type in the wheat spikelet and rachis (Chapter 3). The majority of this early wheat infection (< 5 dpi) is also symptomless. To be fully effective, new fungicides will need to be

applied shortly before or immediately after infective spores are detected within the flowering crop. The chemistry also needs to be persistent and to have excellent systemic movement within ear tissue. Both the apoplast and the vasculature were confirmed as the key routes of infection. However, the production of a chemistry that is able to persist in the apoplast and vasculature currently presents one of the major challenges in fungicide design and formulation.

A significant outbreak of FEB in any major wheat producing region could lead to spikes in wheat commodity prices and national protectionism, affecting the food security of millions of people, particularly in economically unstable regions. Developing countries are major importers of wheat (FAO, 2009) with the majority of domestic produce being consumed locally. In these situations, prolonged consumption of trichothecene mycotoxin contaminated grain would have a chronic detrimental effect on local human and animal health.

The major findings of this PhD project are summarised below. Advances in biological techniques for studying pathogenicity and the new understanding of the *Fusarium* system are discussed. The infection biology of *F. graminearum* is compared with other cereal and grass infecting ascomycetes and a model for *F. graminearum* infection of susceptible wheat ears is presented. Finally, the impact of the discoveries made throughout this project in terms of crop protection, industrial application and the direction of future *Fusarium* research are discussed.

9.1. Summary of key findings and developments

- **Prolonged latent period of symptomless infection**

  The detailed microscopy investigation of the infection biology of *F. graminearum* on fully susceptible hexaploid wheat ears with a semi-dwarfing habit (Chapter 3) revealed that a substantial phase of symptomless intercellular hyphal growth was maintained at the advancing infection front. This symptomless growth established infection throughout the wheat ear and in the early phases of infection represents the majority of the colonised tissue. As early as five dpi one third of the ear may be colonised yet appear healthy. This represents a non necrotrophic mode of infection and supports hypothesis one.

- **Maximal *TRI* gene expression during symptomless infection**

  A follow up study revealed maximal transcription of several *TRI* genes essential for DON mycotoxin biosynthesis at the advancing front of symptomless infection at 5 and 7 dpi (Chapter 4). In these tissues, the biomass of *Fusarium* hyphae is far lower than in the lesion centre. The later intracellular symptomatic infection was accompanied by an increase in fungal biomass and basal, low level, *TRI* gene expression. The infection phase specific production of a secreted virulence factor that inhibits plant defence also supports the hypothesis that *F. graminearum* colonises susceptible wheat ears via a non necrotrophic mode of infection, as stated in hypothesis one.

- **Identification of possible *Fusarium* effectors that may, in combination with DON, promote symptomless infection**

  The analysis of wheat infection by *tri5* and *top1* single gene deficient strains implicated the existence of additional *F. graminearum* secreted effectors that in combination with DON may permit symptomless infection (Chapter 5). The combined bioinformatic analysis of the predicted *F. graminearum* secretome (Chapter 6) and two different approaches of evaluating the transcriptome of wild-type infection (Chapter 7) have led to the identification of a list of candidate *Fusarium* effectors for future investigations.

- **Pathogenicity requirements and plant defence responses to infection are tissue specific**

  Wheat floral infection by the *F. graminearum top1* deficient strain induced a plant tissue specific defence response in the rachis node, at distance from the debilitated hyphal growth which was constrained within the floret. This demonstrated that the pathogenicity requirements for floret and rachis infection are different, in support of hypothesis two. The plant defence response in the rachis node that occurred ahead of the infection, demonstrates that this tissue has the ability to recognise a diffuse signal of pathogen or plant origin which induces the reaction. This supports hypothesis three, which states that tissue specificity exists in pathogenicity and plant defence.

- **Identification of the wheat response to symptomless *Fusarium* infection**

  The transcriptome analysis of the susceptible wheat host, once fully analysed will reveal how the plant responds to symptomless *F. graminearum* infection (Chapter 7) and provides a resource for future investigations. Follow up studies could examine hypothesis three by comparing this data-set to the response of the wheat spikelet to symptomless infection.

- **'Ghost' hyphae and the importance of autophagocytosis**

  F. graminearum hyphae which were devoid of all cell content and often appeared collapsed were identified during late infection within the central region of the rachis but not towards the plant surface (Chapter 3). Single gene deletion of the autophagocytosis gene, *ATG15*, dramatically reduced *F. graminearum* pathogenicity (Long Nam *et al.*, 2011). It therefore appears that autophagocytosis plays an important role in the remobilisation of nutrition to the active region of the hyphal colony and at this late phase of infection this is towards the surface in preparation for asexual sporulation.

- **A flexible and forceful ability to degrade lignocelluloses**

  The observation of the sequential degradation of the different polysaccharides of the wheat cell wall within specific locations and the bioinformatic analysis of PCWDEs demonstrated the flexible, as well as forceful, ability of the *F. graminearum* hydrolytic arsenal (Chapter 3 and 6). The importance of this degradation being localised in close proximity of asexual sporulation requires further investigation. The phase specific expression of the PCWDEs is reminiscent of non necrotrophic infection, in support of hypothesis one.

- **Subtle cell-to-cell passage via pit fields**

  Intracellular *F. graminearum* hyphae were able to dramatically constrict hyphal diameter in order to pass between thick walled sclerenchyma cells via the pit fields (Chapter 3). This subtle form of cell-to-cell passage is not representative of necrotrophic infection, providing further support for hypothesis one.

- **Establishment of LCM procedure for the *Fusarium* – wheat floral pathosystem**

  The development of a working LCM procedure applicable to the *Fusarium* infected wheat rachis will enable the cell-type specific evaluation of the plant and fungal transcriptome during the different phases of the interaction (Chapter 8). This technology will enable hypothesis two and three, which are related to plant tissue specificity, to be analysed in greater detail.

9.2. Major advances in pathogenomics

9.2.1. Advances in biological techniques and their benefit to unravelling pathogenesis

Next generation sequencing (NSG) has reduced the cost and increased the speed at generating gigabases of sequence data that can be applied, in various ways, to the study of microbes and pathogenicity. The utilisation of short reads (70-140 bp) by the majority of these new technologies and the preferential requirement of a reference genome has put an emphasis on re-sequencing genomes. Draft genomes have proven a cost efficient tool for exploring the genetics underling observed phenotypic difference by the analysis of core / dispensable gene sets and polymorphisms between strains. Single nucleotide polymorphisms (SNP) commonly result in the disruption of endonuclease restriction sites and their identification is used during genetic mapping. Now NGS can be used to sequence restriction site sequence tags to map genetic loci faster than traditional methods. An approach successfully applied when mapping the genetic loci responsible for the methylation-deficient phenotype of a reverse genetics *N. crassa* mutant (Baird *et al.*, 2008). In addition to the identification of genetic polymorphisms next generation re-sequencing permits the study of the selection pressures underlying the mutations, through the calculation of synonymous to non-synonymous mutation ratio. Genes under positive selection, as represented by a higher rate of non-synonymous mutations, have been implicated in playing a role in the interaction with the host (Oliver & Solomon, 2010). Whole genome comparisons of different bacterial strains facilitated by NGS has been used to investigate drug resistance (Loman & Pallen, 2008) and may soon become a diagnostic tool for the study of the development of

fungicide resistance that cannot be explained simply by target site mutations such as multidrug resistance (Kretschmer *et al.*, 2009).

Transcript analysis to identify genes or quantify abundance by pyrosequencing EST libraries or using genome wide microarrays has proved effective. However, NGS of the transcriptome may replace these approaches and is now being referred to as RNA-seq, as it can produce tens of millions of transcript reads at lower costs. The use of RNA-seq is now becoming increasing common in the study of plant-microbe interactions, as it can provide information on both pathogen and host (Eaton *et al.*, 2010) (J. Rudd, RRes, UK, pers. com.). Chromatin immunoprecipitation (ChIP) combined with genome wide microarrays have also been used to study the role of transcription factors, however direct sequencing of the protein bound DNA is now possible by ChIP-seq. This approach is proving particularly useful for the analysis of epigenetic influences on histone modification and transcription. A combination of ChIP-seq and RNA-seq was used to investigate the influence of the white collar complex in *N. crassa*, identifying hundreds of Wc-2 targets, including 24 transcription factors (Dekhang *et al.*, 2011). A combined ChIP-seq and bioinformatic analysis of *F. graminearum* revealed the targets of the *TRI6* mycotoxin gene regulator and a consensus binding sequence (Nasmith *et al.*, 2011). The application of ChIP-seq provides a link between the environment and the genome that in turn may enable the construction of holistic systems biology models of cellular physiology.

The Genomes Online Database (www.genomesonline.org) lists ~ 450 completed fungal genomes. The application of this comparative knowledge has been particularly fruitful in the bioinformatic prediction of fungal effectors. Homology in functional protein domains identified apoplastic effectors with LysM domains that were predicted to bind chitin fragments in a wide range of fungi. For some of these LysM containing effectors this function has now been experimentally confirmed (de Jonge *et al.*, 2010, Marshall *et al.*, 2011). Re-sequencing genes that encode cell surface proteins from multiple strains of *M. graminicola* also revealed how novel traits, such as internal amino acid repeats, could play a role in assisting the pathogen avoid host recognition (Rudd *et al.*, 2010). Advances in the bioinformatic identification of effectors have been accompanied by the development of new assays,

utilising fluorescent fusion proteins, to evaluate effector target location. The attachment of a nuclear localisation signal (NLS) to an effector fusion protein, concentrated the signal and enabled the distance that intracellular effector diffused ahead of infection to be quantified for the rice blast fungus (Khang *et al.*, 2010). Bioinformatic identification, experimental confirmation and microscopic localisation of fungal effectors are now standard.

Oomycete *Phytophthora* species possess hundreds of candidate effector genes (Tyler *et al.*, 2006). NGS of multiple strains and the identification of polymorphisms driven by positive selection aided the prioritisation of candidate genes for further investigation (Liu *et al.*, 2005). After demonstrating the effector resided within the plant cell, the mode of effector uptake needed to be determined. The RxLR motif in *Phytophthora* has been shown to bind to phosphotidyl-inositol-3-phosphate (PI-3-P) on the host cell membrane which is then taken up by endocytosis. Applying a blocking agent inhibited the uptake of the effector into the plant cell (Kale *et al.*, 2010). This mechanism has also been applied to a disease control strategy, where transformed cacao transiently secreted PI-3-P, binding the extracellular effector, inhibiting its uptake. The modified cacao leaves challenged with *P. palmivora* showed a reduction in lesion size, demonstrating the successful application of this concept to lessen the impact of this devastating fungal disease of the developing world (Tyler *et al.*, 2011). Following on this work, researchers are now searching for a highly degenerative RxLR-like motif in a wide range of fungi including plant, insect and mammalian pathogens, while attempting to prove conservation of this mode of effector uptake.

The transformation of fungal strains of differing virulence with effectors, to convert a non adapted pathogen into a pathogen or to reduce the impact of a pathogen on its host represents a powerful tool to prove function. The tomato infecting *F. oxysporum* f. sp. *lycopersici* is known to secrete various taxon specific effectors called the SIX (secreted in xylem) proteins which can trigger effector-triggered immunity (ETI) if the tomato plant possesses the corresponding resistance gene (Houterman *et al.*, 2008, Houterman *et al.*, 2009). In addition, transfer of the lineage-specific chromosome containing numerous genes, including some predicted to be effectors, can alter host specificity and instantly turn a non-pathogenic strain

into a pathogen (Ma *et al.*, 2010). Effectors are not confined to pathogenic fungi. Work on mycorrhizal fungi identified a small secreted fungal protein that possessed a signal peptide, a NLS and a sequence of short and long amino acid repeats. The effector fusion protein was translocated to the plant nucleus where it down regulated a plant transcription factor involved in the ethylene response pathway, normally associated with pathogens. Proof that the secreted protein, Sp7, from *G. intraradices* promotes mutualism was obtained by transforming *SP7* into the pathogenic fungus *M. oryzae*, where the fusion protein still localised to the plant cell nucleus. Root infected with the transformed *M. oryzae* strain showed less necrosis, less impact on root development and a reduction in PR gene expression, compared to the wild-type *M. oryzae* interaction, demonstrating the ability of this mycorrhizal effector (Kloppholz *et al.*, 2011).

The macroscopic and cellular phenotypes observed are the result of a large network of interacting macromolecular and metabolites. Therefore, cell function is determined by thousands of gene products. In order to understand the interacting network, a systems biology approach that incorporate 'omic' data into mathematical models, is required. High-throughput transcript, protein and metabolite screening has made this possible. In yeast, transcriptome and metabolome data have been assembled to create a view of a working cell (Laxman & Tu, 2010). The reduced cost of NGS has enabled large-scale network reconstruction that underlies cellular regulation and provided the ability to achieve greater temporal resolution, revealing oscillations in transcription that are more frequent than the circadian rhythm (Baggs & Hogenesch, 2010). Screening transcription factor binding has permitted the quick identification of specific gene regulators, removing the need for the laborious construction of mutant libraries (McClung & Gutiérrez, 2010). The state of the interacting macromolecules, such as the phosphorylation and dephosphorylation status of a protein which influences binding activity, must also be taken into consideration. Network construction has commonly focused upon protein-protein and DNA-protein interactions. However, lipids are bioactive metabolites and in *S. cerevisiae* over 500 lipid-protein interactions have been identified of which ~ 70 % were novel (Gallego *et al.*, 2010). How cells respond to external stimuli is influenced by the intensity, duration and timing of exposure. The application of the systems

biology approach will enable the theoretical, analytical and computational construction of testable hypothesis that would not be possible without the advances made in the production of 'omic' data, which in turn could explain how pathogen and host are responding to one another.

9.2.2. Advances made by the Fusarium research community

Genomic comparisons have proven a powerful tool for understanding the molecular determinants and evolution of fungal pathogenicity. Comparisons of four cereal and non-cereal infecting *Fusarium* species (*F. graminearum*, *F. solani*, *F. verticillioides* and *F. oxysporum* f. sp. *lycopersici*) have been discussed previously (Chapter 1) (Ma *et al.*, 2010, Rep & Kistler, 2010) and represents an essential comparative resource for the molecular study of *Fusarium* pathogenicity. The genomes of additional strains of each of these species with distinct biological properties are currently being sequenced. In addition, the genomes of several *F. oxysporum* formae specialis, with different host ranges, will soon become available (L. Ma and M. Repp, unpublished). Other groups within the Fusarium community have sequenced the genomes of five other species (discussed later).

The development of community bases resources has, and will continue, to assist in the advancement of *Fusarium* research. All *F. graminearum* transcriptome Affymetrix data-sets are available on the PLEXdb interface (www.plexdb.org), providing a valuable comparative tool. The continued manual annotation by MIPS of the *F. graminearum* genome is constantly improving gene predictions with the latest version released in 2011 (Wong *et al.*) and with the introduction of RNA-seq data, such as that generated by this project, will continue to do so. The *F. graminearum* genome has also become available on KEGG (http://www.genome.jp/kegg-bin/show_organism?org=fgr) providing a link between the genome and enzymatic pathways, which will be integral to future systems biology approaches.

Advances in the understanding of trichothecene induction and regulation have proven paramount in determining what mediates the synthesis of the key virulence factor which is also so detrimental to human and animal health. The synthesis of DON is higher during pathogenic growth than in saprotrophic cultures, suggesting that plant derived compound(s) stimulate mycotoxin production. DON production is known to be higher under nutrient-rich conditions. A large-scale nutrient profiling

study identified amines as being inducers of *TRI5* gene expression and DON production (Gardiner *et al.*, 2009b). Analyses of the intracellular basal metabolome revealed increased γ-aminobutyric acid under DON-inducing conditions implicating a role for nitrogen status in regulating DON production (Lowe *et al.*, 2010). Within *in vitro* cultures, specific polyamines (putrescine / agmatine) and amino acids (arginine / ornithine) are potent inducers of DON (Gardiner *et al.*, 2009b). These plant derived nitrogen containing compounds were detected within an infected wheat ear, as early as 1 dpi, along with the two up regulated wheat genes for putrescine biosynthetic enzymes (Gardiner *et al.*, 2010). Collectively it would appear that the hosts stress response, in the form of polyamine synthesis, induces *F. graminearum* to produce DON. Within the NGS data generated in Chapter 7, it will be interesting to identify whether a similar wheat stress response is identified in rachis tissue. The induction of DON production *in vitro* is accompanied by a drop in pH, while buffering or alkalisation of the culture stops *TRI* gene expression and DON synthesis (Merhej *et al.*, 2010). Nitrogen uptake and pH are intimately linked and the pH drop *in vitro* could result in the consumption of ammonium instead of nitrates. *AREA* homologues in *F. graminearum* have not been experimentally identified, however *TRI* gene promoters appear to contain the AreA binding motif (C. Barreau, INRA, France, pers. com.). Extracellular pH is managed by the PacC transcription factor that also influences secondary metabolite production. The *pac1*-deficient *F. graminearum* strain showed reduced growth under neutral or alkaline conditions, increased sensitivity to H_2O_2 and earlier *TRI* gene expression / DON accumulation in acid conditions, demonstrating that *PACC* negatively regulates mycotoxin production (Merhej *et al.*, 2011). Similar to *TRI15*, another negative regulator of DON production, *PAC1* was maximally expressed during symptomatic infection (Chapter 7). A lag exists between the exposure to polyamines or the application of oxidative stresses, including H_2O_2 and sub-lethal doses of azole fungicides, and the induction of *TRI* gene expression or DON production (Gardiner *et al.*, 2009b, Ponts *et al.*, 2009, Ponts *et al.*, 2007) suggesting that intermediate regulators may play a role in nitrogen and pH mediated DON induction.

Epigenetic regulation of chromatin structure and secondary metabolism has attracted attention concerning its role in coordinating *TRI* gene expression. The

acetylation of histones has been associated with increased secondary metabolite production. While secondary metabolism gene clusters are silenced by heterochromatic histone marks, a process that can be reversed by the master epigenetic regulator LaeA (Bok & Keller, 2004, Strauss & Reyes-Dominguez, 2011). A histone deacetylase *HDF1* in *F. graminearum* has been demonstrated to be important for conidiation, sexual reproduction and pathogenesis on wheat ears or maize cobs (Li *et al.*, 2011). Deletion of the *LAEA* homologues in *F. fujkuroi* and *F. verticillioides* resulted in repression of secondary metabolite gene clusters (Butchko *et al.*, 2011, Wiemann *et al.*, 2010). The role chromatin regulation plays in *F. graminearum* is still under investigation. The light sensitive velvet complex, consisting of VelB/VelA/LaeA in *Aspergillus*, has been demonstrated to be involved in the activation / inhibition of sexual / asexual development, respectively (Sproete & Brakhage, 2007, Yager, 1992). Velvet has also been shown to repress aflatoxin production when exposed to light (Duran *et al.*, 2007, Joffe & Lisker, 1969). Deletion of the *VELA* component in *F. graminearum*, termed *VE1*, reduced aerial hyphae, *TRI* gene expression, DON production and virulence on wheat ears (Barreau *et al.*, 2011). Conservation in function among fungi suggests that epigenetic, upper-hierarchal, regulation of secondary metabolite cluster expression will soon be shown to play a pivotal role in the regulation of trichothecene biosynthesis. The chromosomal localisation of a wide range of pathogenicity genes to distinct regions of the genome suggests chromatin structure and DNA topology plays an important function in determining the outcome of these host-pathogen interactions.

The understanding of how plant genetics contributes to the outcome of *Fusarium* infection has been enhanced through the study of the floral infection of the model species *Arabidopsis thaliana*. The response of the Arabidopsis salicylic acid (SA), jasmonic acid (JA) and ethylene (ET) defences signalling pathways to *Fusarium* infections has attracted attention. The assessment of *F. culmorum* infection of mutant Arabidopsis lines, impaired in different defence signalling pathways, identified *eds11* and *npr1* of the SA pathway as having enhanced susceptibility and increased DON production (Cuzick *et al.*, 2008a). The SA pathway was also implicated in mediating the *F. graminearum* Arabidopsis interaction (Makandar *et al.*, 2010). Over expression of non-expressor of PR-1 (*NPR1*) enhanced *F.*

graminearum resistance and increased SA accumulation. Other studies using the Arabidopsis pathosytem have revealed that gene disruption of SA-induction deficient (*sid2*), salicylate hydroxylase *nahg*, *npr1* and pathogen-induced transcription factor *wrky18* increased susceptibility. In addition to SA signalling, *NPR1* over expression activated the JA pathway, while disruption of the 12-oxo-phytodienoic acid reductase *opr3*, the phytotoxin coronatine-insensitive *coi1* and jasmonate resistant *jar1* increased resistance. However, the studies with the JA mutant have to be interpreted with caution, because the loss of this signalling pathway also leads to a loss of viable pollen and female sterility. In wheat, physical removal of the anthers is known to dramatically reduce the ability of *Fusarium* to infect and colonise the wheat ear (Strange *et al.*, 1972). In Arabidopsis, disruption of both *npr1* and *jar1* resulted in a cumulative affect with the double mutant line being more susceptible than *npr1* alone. Therefore, SA appears to play a role in basal defence of floral tissue, while JA may / may not contribute to some extent. *F. graminearum* has also been suggested to exploit the ET signalling pathway. In the first Arabidopsis mutant line study, ET signalling was found to have no influence on the outcome of the floral interaction (Cuzick *et al.*, 2008a). In a second Arabidopsis mutant study, which used detached leaves, wounding and DON application, lines with enhanced or reduced ET signalling were either more susceptible or resistant, respectively (Chen *et al.*, 2009). A single transgenic wheat plants with reduced *EIN2*, a component in the ET signalling pathway, was shown to have reduced visible disease and DON contamination (Chen *et al.*, 2009). However, a newer and more comprehensive wheat study has re-evaluated the role of ET signalling and contradicts this original publication. In the new study, virus induced gene silencing (VIGS) was used to study the various components of the ET defence signalling pathway in a resistant wheat cultivar and demonstrated that by impairing ET signalling resistance was reduced (S. Scofield, USDA Laboratory, Purdue University, USA, pers. com.). These results were re-enforced using chemical inhibitors and inducers of the ethylene pathway.

A combined transcriptome / proteome approach revealed that the SA and calcium signalling pathways were activated within 6 hours of *F. graminearum* infection on a resistant wheat cultivar and then ET signalling began before JA-mediated defences were initiated at 12 hpi. A delay in SA signalling was associated

with cultivars of increased susceptibility (Ding *et al.*, 2011). An Arabidopsis line deficient in the defence signalling gene, *SGT1A*, but not *SGT1B* both of which are involved in hypersensitive response (HR) and are upstream of SA signalling, was more resistant to *F. culmorum* floral infection, while DON accumulation was wild-type (Cuzick *et al.*, 2009). This contradictory result was explained by the requirement of the pathogen for competent plant cells able to activate programmed cell death (PCD) to facilitate the infection process. Collectively, plant defence signalling pathways characteristic of both biotrophic and necrotrophic infections appear to play a role in determining the outcome of the disease.

All the aforementioned advances in the molecular understanding of *Fusarium* infections have direct implications on the presented research on the infection biology of *F. graminearum*. These topics have been taken into consideration, and will be included, within the proposed model for *F. graminearum* infections of susceptible wheat ears.

9.3. A comparison *F. graminearum* infection with other Ascomycete pathogens and endophytes of cereals and grasses

F. culmorum represents a closely related pathogen to *F. graminearum* that requires the same environmental parameters to cause FEB on cereals but is less aggressive and produces DON under a different range of conditions (Hope & Magan, 2003). The infection biology of *F. culmorum* is strikingly similar to *F. graminearum* (Kang & Buchenauer, 1999, 2000a, 2000b, Wanjiru *et al.*, 2002). A substantial symptomless phase of wheat ear infection has now been identified using a GFP tagged *F. culmorum* strain (A. van de Meene and K. Hammond-Kosack, unpublished 2011). Young *F. culmorum* hyphae demonstrate higher mycotoxin immunolabelling compared to older hyphae *in planta* (Kang & Buchenauer, 1999) which suggests that *F. culmorum* may also up regulate mycotoxin production at the advancing front of infection. Recently, *F. culmorum* has also been discovered to colonise endophytically cereal roots, providing a mutualistic benefit to the plant in the form of drought and salt stress tolerance (Rodriguez *et al.*, 2008). *F. avenaceum* also causes FEB on cereals in the cooler regions of northern Europe, but unlike the other two aforementioned *Fusarium* species does not produce DON, instead producing the

toxic secondary metabolites moniliformin and fusarin (Desjardins & Proctor, 2001). Despite being less pathogenic, *F. avenaceum* appears to adopt a similar pattern of colonisation. However, the detailed cytological *F. avenaceum* study described infection as necrotrophic (Kang *et al.*, 2005) and symptomless infection has not been identified.

The closely related intercellular endophytic species, *E. festucae*, which infects all aerial regions of specific grass species, provides an interesting comparative system. *E. festucae* naturally forms a mutualistic interaction with ryegrass (Schardl, 2001). Initially the seed transmitted fungus establishes a colony via proliferative highly branched growth in apical meristem. Fungal growth is then tightly coordinated with plant development and the hyphae go through a long phase of mutualistic, unbranched, intercalary growth, parallel to, but not entering, the vasculature. The redistribution of resources at flowering causes the fungus to switch from its mutualistic asexual cycle to proliferative growth in the pathogenic sexual cycle (Eaton *et al.*, 2011). Disruption in the fungus of reactive oxygen species (ROS) production (*noxA, noxR, racA*), the osmotic stress activated MAPK (*sakA*) or intercellular iron availability (*sidN*), via genetic manipulation, inhibits the switch from proliferative to mutualistic growth (Eaton *et al.*, 2010, Johnson *et al.*, 2007, Takemoto *et al.*, 2006, Tanaka *et al.*, 2006, Tanaka *et al.*, 2008). Continued proliferative growth, sustained by infection of the vasculature, results in a higher fungal biomass and a loss of mutualism. During the wild-type interaction the plant is either unable to respond or detect the presence of infection, while the pathogenic association with the *sakA* deficient strain results in the up regulation of ET signalling and plant defences (Eaton *et al.*, 2010). Post initial penetration *F. graminearum* also undergoes a short lived phase of hyper-branching and produces a coralline sub-cuticular hyphal mat (Rittenour & Harris, 2010). This is followed by intercellular growth, which like *E. festucae*, is infrequently branched and parallel to, but not entering, the vasculature. The subsequent colonisation of the vasculature is associated with an increase in fungal biomass and intracellular symptomatic infection. The final switch to a reproductive cycle in *F. graminearum* is also linked to a change in pathogenicity with the up regulation of hydrolases (Chapter 3 and 7). ROS production is required for polarised hyphal growth (Scott & Eaton, 2008) and

pathogenicity in *B. cinerea*, *C. purpurea* and *M. oryzae* (Egan *et al.*, 2007, Giesbert *et al.*, 2008, Rolke & Tudzynski, 2008, Segmueller *et al.*, 2008). Both ROS and the osmotic stress MAPK have been linked with increased DON and pathogenicity in *F. graminearum* (Ochiai *et al.*, 2007, Ponts *et al.*, 2007) while the siderophore *SID1* is also required for full virulence on wheat but the impact on DON production is not known (Greenshields *et al.*, 2007).

M. graminicola (*Septoria tritici*), the number one pathogen of wheat in the UK (www.cropmonitor.co.uk), undergoes a transition from budding to hyphal growth in order to penetrate the leaf stomata. Extensive intercellular symptomless infection occurs for ~ 10 days, during which hyphae do not enter the vasculature. Infection is sustained by apoplastic exudates, prior to the onset of host cell death, exclusively in the mesophyll L2 leaf layer, and then visible disease symptoms and the development of pycnidia (Kema *et al.*, 1996, Keon *et al.*, 2007). During this prolonged symptomless phase, which is up to 9 days in duration, the host does not respond to infection and PAMPs-triggered immunity (PTI) is prevented by the secretion of an apoplastic LysM effector that collates chitin fragments (Deller *et al.*, 2011, Marshall *et al.*, 2011). This enables the pathogen to establish a large colony before unmasking infection, secreting hydrolytic enzymes and inducing widespread PCD. During the development of *M. graminicola* disease symptoms mitochondrial cytochrome C is released into the cytosol, representative of PCD, while the apoplast is also enriched in amino acids and sugars that support increased growth and sporulation (Keon *et al.*, 2007). *F. graminearum* also establishes an intercellular colony prior to host cell death (Chapter 3), while DON alone is not sufficient to inhibit plant defence thus suggesting the occurrence of additional effectors (Chapter 5). The nuclei of host cells, surrounded by intercellular hyphae, were enlarged and round, while the cytoplasm becomes condensed (Chapter 3), characteristics which are hallmarks of PCD (Pennell & Lamb, 1997). Chitin-binding LysM effectors are proposed to be widespread in the fungal kingdom (de Jonge *et al.*, 2010) but to date no homologous genes have been predicted in the sequenced *F. graminearum* genome. However, several *F. graminearum* cysteine-rich, internal amino acid containing proteins were up regulated during symptomless infection.

S. nodorum is a true necrotrophic pathogen of wheat and secretes an array of host-selective proteinaceous toxins, now referred to as necrotrophic effectors (Friesen *et al.*, 2008, Friesen *et al.*, 2007). The recognition of the necrotrophic effectors by the corresponding host gene results in host cell death in advance of infection, liberating nutrition for the invading pathogen and promoting disease, a process now termed effector-triggered susceptibility (ETS). Absence of the necrotrophic effector or the host gene results in an incompatible interaction (Liu *et al.*, 2009). In the wheat – *S. nodorum* pathosystem five effectors (ToxA, Tox1, Tox2, Tox3 and Tox4) are matched by five host genes (*TSN1*, *SNN1*, *SNN2*, *SNN3* and *SNN4*) of which the Tsn1-ToxA and Snn3-Tox3 are the best characterised (Faris & Friesen, 2009). The *TSN1* gene has now been identified and encodes a NB-LRR protein with many motifs in common with R proteins that control ETI (Faris *et al.*, 2010). In contrast, *F. graminearum* does not appear to produce a proteinaceous host-selective toxin and instead produces the non-proteinaceous toxin, DON, which has a universal target of the ribosomal complex (Ueno, 1984). However in Chapter 6, within the predicted secretome several *F. graminearum* sequences with high similarity to *S. nodorum* necrotrophic effectors were identified. The function of the *F. graminearum* gene is currently not known. In addition, a protein related to the *S. nodorum* phytotoxin was transcriptional up regulated in *F. graminearum* and coincided with the onset of host cell death. High concentrations of DON (200 mg/L) have been associated with PCD following the apoplastic infiltrated of wheat leaves (Desmond *et al.*, 2008). However, the concentrations that occur *in planta* are not predicted to be sufficient alone to induce PCD. The existence, and phase specific secretion, of other unknown effector(s) that triggers host cell death cannot be ruled out for the wheat – *F. graminearum* interaction.

The division of fungi into biotrophic and non-biotrophic, or across a continuum, is not a trivial task as phytopathogenicity has independently evolved many times (Oliver & Solomon, 2010). This is evident in the previous comparisons of *F. graminearum* infection biology with endophytes, hemibiotrophs and necrotrophs. Most pathogens are host-adapted and colonise either a very narrow to slightly wider range of host taxa due to the evolution and requirement of specific virulence factors. *F. graminearum* naturally infects a range of cultivated cereal

species and some wild grass species (Francis & Burgess, 1977, Goswami & Kistler, 2004). However, a level of host specificity does exist, as depicted by the different outcome of a single floret inoculation of wheat and barley, suggests the possible existence of an interaction between gene products in barley. Whether unknown effector(s) trigger susceptibility, mask infection, or both are produced during *F. graminearum* infections of wheat, remains to be seen. Host cell death in all the aforementioned systems is accompanied by increased pathogen growth and is associated with sporulation. Non-self recognition and toxin sensitivity both conclude with the activation of *Mapk3* and plant cell death (Pandelova *et al.*, 2009, Rudd *et al.*, 2008). In either circumstance the plant is responding to infection and the inhibition of transcription or protein synthesis can prevent cell death (Kwon *et al.*, 1998). Fungi have independently evolved, and horizontally transferred, effectors that target the conserved plant defence signalling pathways (Friesen *et al.*, 2006). The genomic and transcriptomic comparisons of phytopathogens will aid in the identification of conserved and unique candidate effectors for experimental investigation. In chapter 6, nineteen possible *F. graminearum* specific putative effectors were identified. The thorough analysis of the different phases of *F. graminearum* infection has provided novel effector candidates and the subsequent genetic manipulation of the interaction will prove insightful. All fungi are required to interact with their host. The comparison of infection by a range of ascomycetes, including mutualists and necrotrophs, demonstrates that a period, however short, of interaction with live host cells and their immune system is required to establish a successful infection.

9.4. A model for *F. graminearum* pathogenicity on wheat

The simplified schematic of how *F. graminearum* infects a susceptible wheat ear, as perceived prior to the start of this project, is given in Figure 59. How infection is now perceived to be established and maintained, as a result of the discoveries made in this project, is given in Figure 60. The different phases of infection and the possible molecular mechanisms responsible for the observed phenotypes are presented in turn. Secretion of the low molecular weight toxic metabolite, DON, alone is not sufficient to permit full infection, as demonstrated by the *top1* and *fgl1* deficient strains (Baldwin *et al.*, 2010, Voigt *et al.*, 2005) and therefore secreted

proteins and potentially other secreted metabolites are proposed to play a role in pathogenicity. The regulation and possible function of secreted virulence factors are discussed.

During a prolonged latent period, intercellular hyphae establish symptomless infection throughout the susceptible wheat ear. This interaction between live plant and fungal cells is maintained for 2-3 days and extends for ~ 20 mm. By the time a tiller comes into flower, physiologically the ear has become the main sink tissue supported by the upper leaves and a separate root system is dedicated to this tiller. Rapid intercellular growth therefore occurs in a nutrient-rich environment within the ear apoplast, as DON production and *TRI* gene expression has been shown to be maximal under such conditions (Lowe *et al.*, 2011). To maintain the symptomless ear interaction with live plant cells the infecting hyphae secrete an array of proteins and metabolites that diffuse ahead of infection. The key metabolite DON and possibly a related circumsporozoite protein may function synergistically to inhibit transcription and protein synthesis within the plant cell, hampering the plant cell's ability to respond. Activation of various plant defence signalling pathways converge on Mapk3 and result in HR. Inhibition of these processes may prevent PCD from occurring too early, enabling the establishment of the fungal colony prior to host cell death. Abundant small cysteine-rich proteins of unknown function, characteristic of known fungal apoplastic effectors, are secreted by *F. graminearum*, while limited PCWDEs are produced. In combination apoplastic effectors and limited PCWDE production may prevent the induction of PTI mediated basal defence during symptomless infection. A secreted catalase enzyme that is highly expressed during symptomless infection, could break down H_2O_2, possible produced by the oxidative burst. This may assist the fungal hyphae by preventing PCD occurring too early.

Plant derived signals or compounds have been implicated in inducing DON production. Genetic manipulation of the MAPKs signalling pathways in *F. graminearum* results in reduced DON production, and in some cases a loss of pathogenicity, suggesting that the recognition of external stimuli is involved in the induction of DON, implicating nutrient availability and osmotic stress. Polyamines, ammonia and acidity have been linked to DON induction *in vitro* (Gardiner *et al.*, 2009b, Gardiner *et al.*, 2009c). The enhanced transcription of all the *TRI* genes

during symptomless infection correlated with the up regulation of the positive transcriptional regulators of *TRI* gene expression, *TRI6*, *TRI10* and *VE1*. The positive regulation of *VE1* suggests that light sensing, and possibly a diurnal cycle, plays a role in mycotoxin regulation. Disruption of *VE1* in *F. graminearum* also results in the abolition of DON synthesis, aerial hyphae formation and conidia production (Barreau *et al.*, 2011). A circadian rhythm in the production of plant defence compounds exists with increased synthesis during the day (Wang *et al.*, 2011). It is currently unknown if there is a circadian rhythm in DON production and / or the secretion of fungal proteins. The inverse expression profile was observed for negative transcriptional regulators, *TRI15* and *PAC1*.

Two genes of unknown function (FGSG_00007, FGSG_10397) contain *TRI6* binding sites in the promoter regions, were down regulated in a *tri6*-deficient strain and were up regulated under DON-inducing agmatine containing conditions (Gardiner *et al.*, 2009a). Single gene deficient strains lacking either FGSG_00007 or FGSG_10397 were greatly augmented in virulence and DON production *in planta* (Gardiner *et al.*, 2009a). Subsequently, both genes were proposed to be negative regulators of DON synthesis, which either directly limit DON production or form part of a competitive metabolic pathway. The two genes, FGSG_00007 and FGSG_10397, were dramatically up regulated at the advancing front of infection, possibly by Tri6. This suggests that these two negative regulators of DON production are involved in a competitive pathway also required during symptomless infection and therefore, regulated by the same mechanisms. Alternatively, the up regulation of these two negative regulators could reflect a transcriptional response to the high turnover of the gene products, which may be specifically ubiquitinated to prevent the inhibition of DON synthesis. Further research is required to determine the exact role these two protein play in the regulation of DON biosynthesis. Interestingly, a secreted lactonohydrolase (FGSG_10675) that could potentially detoxify the DON mycotoxin (Takahashi-Ando *et al.*, 2002, Takahashi-Ando *et al.*, 2004) (Chapter 6 and 7) was also up regulated at the advancing front. The localised secretion of a mycotoxin detoxifying protein may represent a self protection mechanism.

After two to three days the host wheat cells surrounded by intercellular hyphae begin to die (Brown *et al.*, 2010) (Chapter 3), while the cause and type of

host cell death remains unknown. What causes the transition between symptomless and symptomatic infection is also unknown. High levels of DON have been associated with PCD (Desmond *et al.*, 2008), therefore when a concentration of, or length of exposure to, the stable mycotoxin is reached, host cell death may occur. Alternatively, *SGT1A R*-gene mediated HR has been demonstrated to be essential to the successful outcome of the interaction in Arabidopsis (Cuzick *et al.*, 2009) suggesting that a gene-for-gene interaction may also exist. Either the phase specific absence of an unknown fungal effector that previously blocked pathogen recognition mediated HR, or the phase specific secretion of a necrotrophic effector, may initiate PCD and assist *F. graminearum* during the necrotrophic phase of disease cycle. Coinciding with the onset of host cell death and disease symptoms was the expression of two *Fusarium* genes that encode Snodprot1 related proteins (FGSG_10212, FGSG_11205). Snodprot1 is a known phytotoxin from *S. nodorum* (Hall *et al.*, 1999). The small secreted cysteine-rich *F. graminearum* proteins, highly expressed during symptomless infection, were expressed at a far lower level as symptoms developed. Inversely, an array of PCWDEs that degrade the plant cell wall assisting intercellular colonisation and liberating cell wall fragments, which may act as elicitors PAMP-triggered host cell death, were up regulated during symptomatic infection. The action of the PCWDEs, including feruloyl esterase, on the host will increase exposure to ferulic acid, a plant cell wall component that is an efficient inhibitor of DON biosynthesis and *TRI* gene expression (Boutigny *et al.*, 2009). The increased secretion of proteinaceous phytotoxins and PCWDEs, accompanied by a reduction in DON, circumsporozoite and possible apoplastic effectors may allow the host to detect and respond to infection, inducing wide scale PCD to the benefit of *F. graminearum*.

Once full symptoms appear, the plant tissue is dead and all cells are intracellularly colonised. Hyphae within fully disease tissue alter the primary axis of growth, increasing growing towards the plant surface (Chapter 3). Hyphae accumulate *en masse* in the outer cell layers where dramatic plant cell wall degradation and asexual sporulation is eminent. During the saprotrophic growth in dead plant material significant up regulation of PCWDEs is required to liberate the remaining nutrition stored within the plant cell walls, while additional DON

production is surplus to requirements, now the host cells are dead and as a consequence returns to basal levels (Chapter 7). The lipase, Fgl1, is the only *F. graminearum* secreted protein experimentally proven to be essential for fully virulence on wheat and maize (Voigt *et al.*, 2005). Despite *fgl1*-deficient strains demonstrating enhanced DON production, infection was still constricted to the spikelet (Voigt *et al.*, 2007). During wild-type infections of wheat ears, callose synthase activity and callose deposition was reduced, while linolenic acid was elevated (Voigt *et al.*, 2011). It is proposed that the increased level of long-chain fatty acids produced by Fgl1, such as linolenic acid, inhibits callose synthase activity, thereby facilitating infection. However, *FGL1* was expressed at a low level at the advancing front of symptomless infection and was only up regulated within the fully symptomatic tissue, in association with wide scale intracellular colonisation. Therefore, due to the substantial distance between the infection front and the high level of *FGL1* expression, it would appear that Fgl1 functions as a traditional lipase and is possibly involved in lipid metabolism and does not play a role as a secreted effector. As the colony re-mobilises to the surface, abundant hyphae devoid of content appear in the centre of infection, reminiscent of autophagocytosis. Disruption of *ATG15*, blocks autophagocytosis and reduces virulence (Long Nam *et al.*, 2011) suggesting that nutrient re-cycling plays an important role in the final phase of infection.

Pathogens commit a lot of resources and energy into creating a hospitable environment for infection. In doing so, the host becomes more susceptible to colonisation by microbial competitors. The four genes that encode antifungal proteins, including three *KP4* homologues, where identified by a bioinformatic analysis of the secretome (Chapter 6). The antifungal protein was highly expressed throughout, but was up regulated during the symptomatic phase of infection, in association with host cell death, while the three *KP4* homologues, which were expressed at a lower level, were up regulated during the last phase of infection. This is in agreement with the whole wheat ear transcriptomic study (Lysoe *et al.*, 2011a) (Chapter 6) and could reflect the vulnerability of the niche created to infection by different competitors. Additional genes that encode proteins of unknown function were up regulated during the final phase of infection, including a protein that

contained a dienelactone hydrolase domain, involved in aromatic compound degradation, including phenolics such as lignin (Harwood & Parales, 1996). This coincides with the dramatic degradation of the host cell wall (Brown *et al.*, 2010).

Therefore, *F. graminearum* would appear to sequentially circumvent, manipulate and exploit the host's defences to permit successful infection. Circumventing PTI, manipulating the plant cell by preventing protein synthesis and exploiting the plants own defence to liberate nutrition once a colony has been established appear to be the three major requirements for successful floral infection. Finally *F. graminearum* saprotrophically degrades the dead plant tissue to initially support asexual, and later, sexual sporulation. This investigation demonstrated that genome wide transcriptional alterations occur between the different phases of infection and depicts a situation where the symptomless infection front was the most distinct, especially in terms of the expression of genes that encode secreted proteins. The biphasic model of *F. graminearum* wheat floral infection must now be considered in the design and assessment of all future genetic or 'omic' studies of infection.

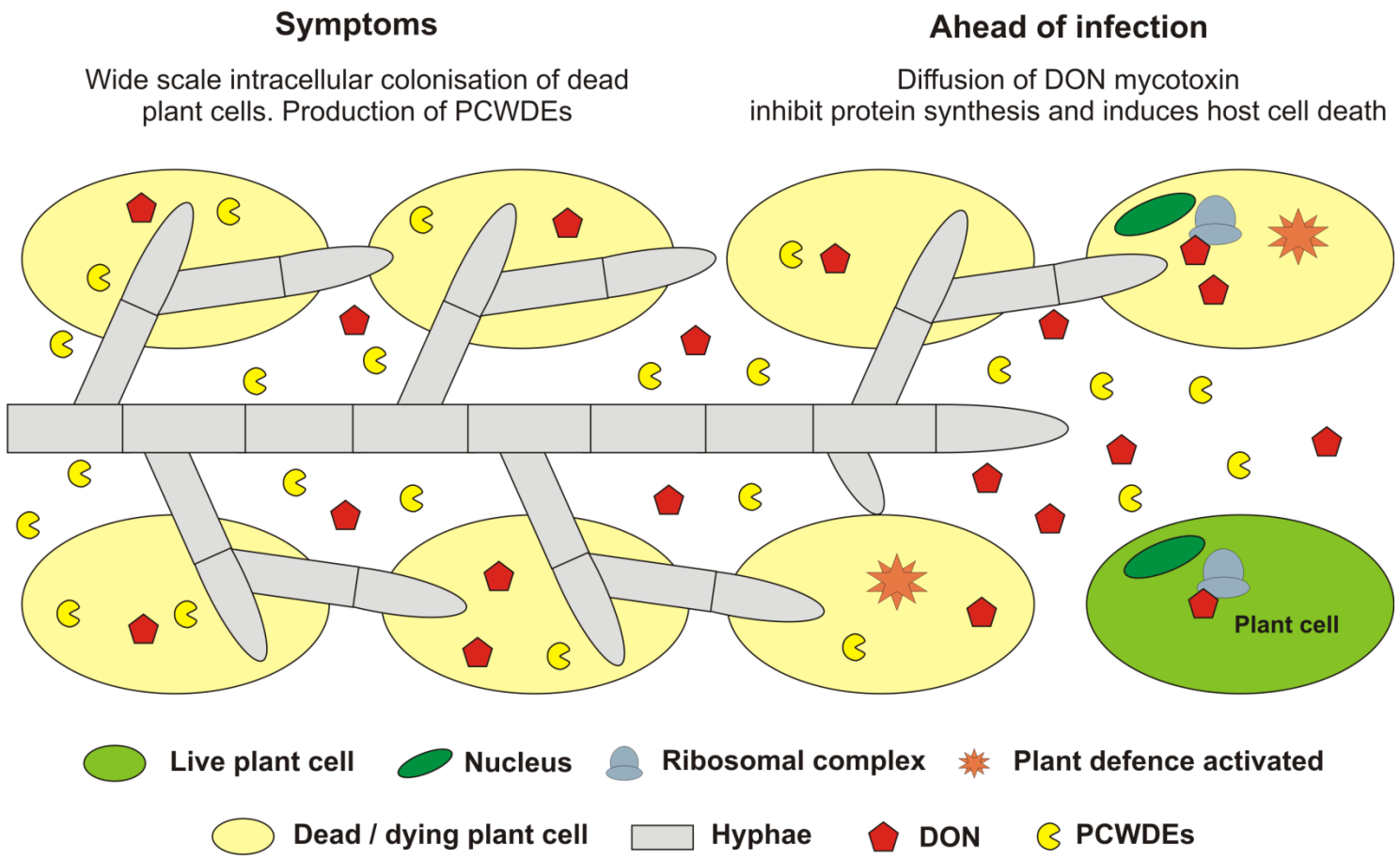

Figure 59 A schematic of how *F. graminearum* was perceived to infect a susceptible wheat ear when this project commenced in 2007.

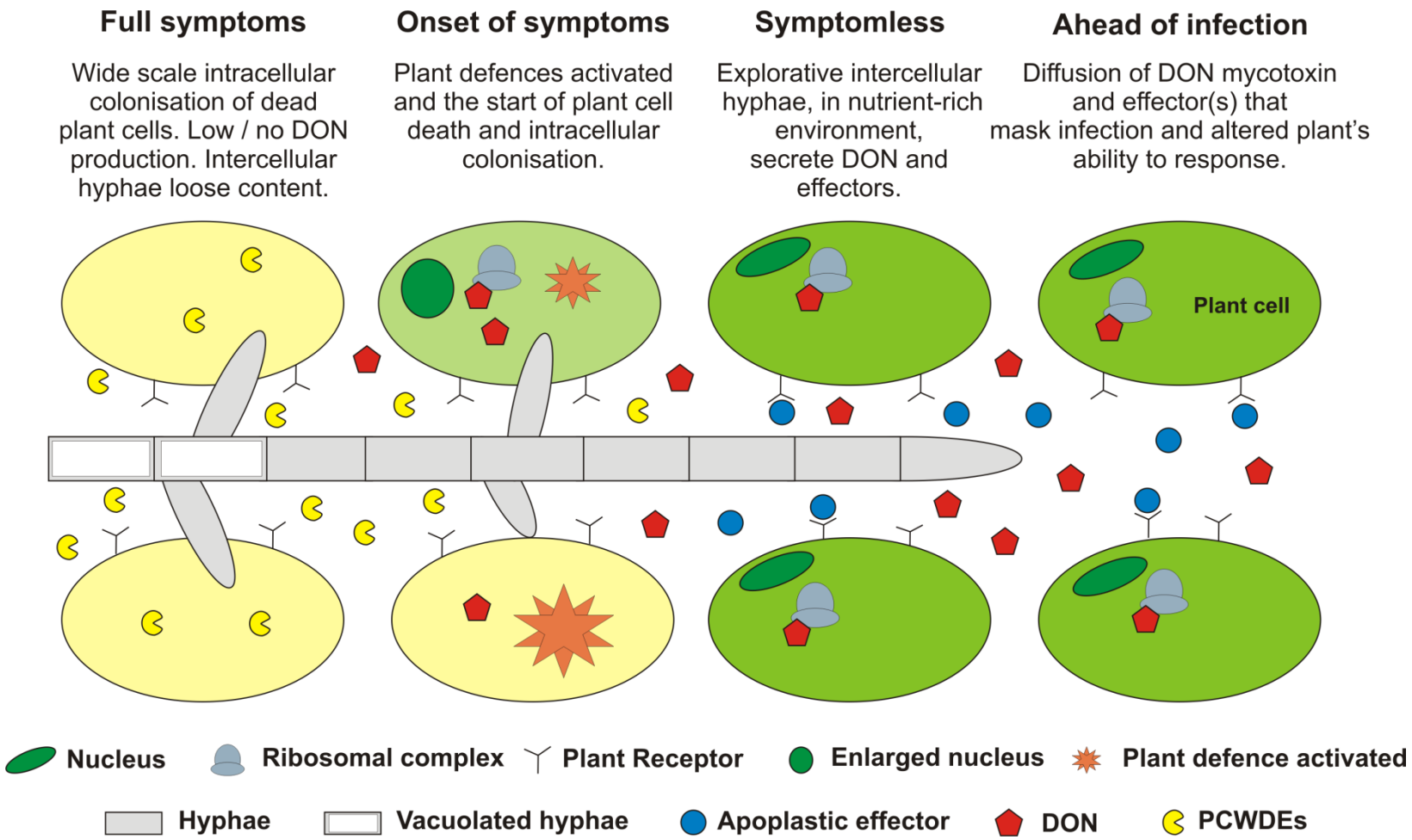

Figure 60 A schematic of how *F. graminearum* establishes and maintains infection of a susceptible wheat ear, based on the data generated in this project.

9.5. Future directions for *F. graminearum* research

Accurate genomic information is fundamental to molecular biology, molecular genetic and bioinformatic analysis. An improved genomic resource for *F. graminearum* will enhance the progression of research carried out by the global scientific community. Sequencing the genome of a wild-type *F. graminearum* strains that demonstrate reduced or increased disease causing abilities, but are still able to produce DON to a similar level as the sequenced wild-type PH-1 strain, will assist in the identification of novel *Fusarium* effectors and / or novel clusters of genes coding for additional secondary metabolites. Sequencing multiple strains will also assist in the determination of the type of selective pressure exerted upon genes, which for the case of secreted proteins, will greatly assist in the identification of possible effector proteins that have been shown to be exposed to positive selection in other pathogenic systems (Oliver & Solomon, 2010). New genomic sequence and transcriptome data-sets will provide a highly enriched annotated genome and improve gene calling throughout the *F. graminearum* genome. Such a revised genome can be achieved by inter-comparing with the now available but unpublished sequenced genomes of *F. asiaticum* (Korea), *F. fujikuroi* (Germany), *F. culmorum* (RRes / University of Liverpool, UK), *F. langsethiae* (Norway), *F. pseudograminearum* (Australia), *F. circinatum* (South Africa) and various *F. oxysporum* formae specialis (USA and Netherlands). Collectively, these new genomic resources will permit the global Fusarium community to define the minimal core *Fusarium* genome and identify for each species the unique predicted taxon specific gene sets. This information along with a growing number of *in planta* and *in vitro* transcriptome analyses can then be used to link specific genes and pathways to the various pathogenic lifestyles displayed by the members of the *Fusarium* clade. In light of the advances made in the understanding of epigenetic regulation of transcription and toxic biosynthetic or secreted effector clusters, improved information on gene location is vital, as these traits could determine phenotypic differences between strains. For *F. graminearum* these comparative studies will assist in defining additional key events during the symptomless phase of infection.

The combined analyses of the *F. graminearum* secretome and transcriptome during symptomless infection have lead to the identification of candidate fungal

effectors that may permit apoplastic colonisation without triggering a host defence response capable of arresting hyphal growth. Identification of novel secreted fungal proteins required for full virulence via single gene deletion and a cell biology study of infection will further elucidate the pathogenic role of these fungal proteins. Construction of double mutant strains that are deficient in specific effector(s) and/or DON production may reveal the accumulative effect of their removal from the interaction. By exploring the sub-sets of genes which exhibit coordinated patterns of expression, specific common motifs within their promoters may be recognised. These may provide clues as to the protein(s) involved in the transcriptional up regulation of the genes expressed at the hyphal front. A comparison of the wheat transcriptome during symptomless / symptomatic wild-type infection with that of single gene deletion strains, such as the *tri5* (DON-minus) and effector-minus strains, may assist the identification of the targets of the fungal virulence factors. However, most *R* genes and pattern recognition receptor genes are not induced during infection or only very weakly. Information on the plant genes either induced or suppressed would enable new hypothesis and investigations to be designed that could be linked to the new information simultaneously acquired on the pathogen. For example, cellular localisation of fluorescent fusion proteins, PAMP / effector detection using the VIGS vector as a transient *in planta* expression system and PAMP-binding assays.

The majority of the RNA-sequencing data generated in the study of the wheat – *Fusarium* interaction is from the wheat transcriptome. Assembly of this large quantity of wheat transcript information will enable a transcriptome comparison of the healthy and symptomless wheat tissue and assist in the identification of the wheat processes that are influenced by the *Fusarium* secreted proteins and DON mycotoxin. At present time, the annotation associated with the full length wheat cDNA collection is very modest. A future analysis could focus on identifying the wheat genes specifically up or down regulated at the apex of explorative hyphae during colonisation by either a highly or less aggressive isolates. A similar study comparing infection by strains deficient in single or multiple pathogenicity factors would determine the different types of defence responses activated in the absence of virulence factors. These changes to the wheat transcriptome could then be compared

to the spatial and temporal changes to the wild-type *F. graminearum* PH-1 transcriptome already defined in this project. By interlinking the two transcriptomes, the first clues of how the two interacting organisms respond and counter-respond should be revealed. Genetic studies of hexaploid wheat are difficult and time consuming, therefore, such a transcriptome study will enable the selection of wheat genes for testing for function via VIGS. Also genes which have been shown to play a pivotal role in determining the outcome of other fungal – cereal host interactions can be directly tested using the VIGS system. Ideal candidates would be *CERK1* and *CeBiP* which recognise chitin fragments leading to the triggering of PTI in rice (Shimizu *et al.*, 2010).

Heterogeneity in stress resistance, enzyme production and virulence exists within a single fungal colony (Avery, 2006, Vinck *et al.*, 2005). *F. graminearum* colonises the plant by polarised filamentous growth and secretes an array of virulence factors to promote infection. Throughout the *F. graminearum* colony, heterogeneity in metabolism and a division of function could exist. DON synthesis and regulation is now predicted to occur at the apex of explorative hyphae and heterogeneity in the local environment may control the extent of mycotoxin induction. The development of an *in vitro* and / or *in planta* assay to localise fluorescently labelled DON mycotoxin biosynthetic enzymes and regulatory proteins at the advancing hyphal apex would be very informative. Fungal genes of interest would include; *MAP1* (mating MAPK) (Urban *et al.*, 2003), *OS2* (osmotic stress MAPK) (M. Jubault, unpublished, RRes, UK), *VE1* (light response)(Barreau *et al.*, 2011), *TRI6* (positive regulator), *TRI10* (positive regulator), *TRI14* (positive regulator) (Dyer *et al.*, 2005) and *TRI15* (negative regulator) (M. Jubault, unpublished RRes, UK).

Characterising hyphal heterogeneity in the production and localisation of the key components in DON synthesis at the hyphal apex and in different host cell-types at differing phase of infection would provide new insights into how DON production is controlled. An *in vitro* assay could be used to observe variation in the regulation of DON synthesis between multiple hyphal apexes within a single colony grown on agar coated slides in the presence of different DON inducing chemistries namely; agmatine, putreseine, H_2O_2, ferulic acid, ammonium salts, high glucose and sub-

lethal doses of an azole fungicide. Using this system would enable the alterations in DON synthesis throughout the course of the day, *in vitro* and *in planta* within different host cell-types, to be monitored and the influence of light or circadian rhythms on mycotoxin production determined. A floret epidermal peel assay, infected with the transgenic strains containing the DON synthesis / regulation fluorescent fusion proteins could be used to determine the sub-cellular localisation of these proteins. This system would be used to explore the sequence of events controlling the production of the mycotoxin at the advancing hyphal apex and determine if hyphal heterogeneity in DON regulation exists during different phases in the infection cycle. The histochemical stain 3, 3'-Diaminobenzidine staining could determine if H_2O_2, indicative of the oxidative burst, coincides with the production of DON at the hyphal apex of explorative hyphae.

The interaction between fungal effectors and the presence of their cognate host receptors determines host range and potentially also pathogen tissue specificity. Within the ear tissue, the interaction between *F. graminearum* secreted proteins and the relevant wheat receptors may enable infection. The breakdown or lack of an interaction between effector(s) and receptor(s) which inhibits infection could explain the tissue specificity of *F. graminearum* infections of wheat. A comparison of cereal infecting fungal pathogens with differing tissue specificity (root, leaf, stem and /or floral tissue), host range (single species / multiple species), mode of obtaining nutrition (biotrophs / non-biotrophs / necrotrophs) and pattern of hyphal growth (haustoria forming / intracellular / extracellular) may reveal how the repertoire of candidate effectors that regulate tissue specific infection and *in planta* lifestyles. *F. graminearum* genes found to be up regulated or specifically expressed at the advancing hyphal front that have orthologous genes expressed during extracellular plant colonisation in other cereal-fungal interactions could be characterised further. This will reveal the species distribution, the expansion / contraction of specific gene families, and genome location.

9.6. The impact of this research

The discovery of the symptomless phase of *Fusarium* ear infection has already had an impact on UK and European agriculture. Previous assessments of the disease causing ability of a fungal strain and the efficacy of a fungicide or germplasm have relied upon scoring visible disease symptoms. The screening of single gene-deficient fungal strains for attenuated virulence and wheat germplasm or antifungal chemistries for an ability to reduce infection will now have to take symptomless infection phase into account. Existing germplasm and fungicides may also require re-screening. When this novel result was first publicised to the farming community at the UK Cereals event in June 2010, this lead to an interview broadcast on the Radio 4 Farming today programme within a week, articles in the Farmers Guardian, an invited presentation at CropWorld in October 2010, with additional exposure within the BBSRC's own food security video of this event, and another invited presentation at the AAB Crop Protection conference at Cambridge in February 2011. During this period several articles in Farmers Weekly have also been published. In addition, the HGCA recommendation to growers on how to control FEB will be rewritten in 2011, as a direct result of this research, with the advice being to spray wheat ears earlier. This new advice should start to improve the performance of some of the triazoles fungicide. But two main problems remain, namely, that various *Fusarium* species are intrinsically resistant to most of the fungicides available and secondly that good sources of genetic resistance to FEB, which are compatible with high wheat yields in commercial crops, have not been identified.

9.6.1. Future methods for combating *F. graminearum*

The genome wide transcriptome investigation of the pathogen and host during the symptomless and symptomatic phases of infection has identified possible determinants of symptomless infection and elevated mycotoxin production. Molecular genetic studies are still required to confirm hypothesis generated by this project. However, in the near future, targeting the determinants of symptomless infection with novel chemistries or introducing novel genes into the plant that impede symptomless infection could prevent the establishment of the disease and curtail the spread of infection and / or mycotoxin accumulation. Transcriptome

studies of the late phase of infection and sporulation could reveal targets for the intervention of asexual sporulation and reduced the spread of fungal spores from tiller to tiller and / or the contamination of the crop residues / grain at harvest. The comparative analysis of the predicted gene repertoire from the genomes of several related *Fusaria* identified a core set of fungal processes essential for infection. Such information could lead to the development of a single approach for combating multiple wheat ear attacking *Fusarium* species.

A transgenic approach to disease control, though publically unacceptable at present, may in future become a necessity. The fringe of living host cells could be utilised to continuously deliver antifungals directly onto the intercellular advancing hyphae. Alternatively, these living host cells could deliver a series of chemical signals, which when taken up by hyphae either reduce or block the production of the DON mycotoxin. The same approach could be applied to limit the production of any other fungal suppressor or effector that assists *Fusarium* infection. Living host cells in advance of the infection could also be induced, upon perception of *Fusarium* hyphae, to secrete an excess of wall polymers that would block the entire apoplastic spaces creating a barrier, similar to the outcome of the *tri5*-wheat interaction (Chapter 5). These types of induced responses may slow the rate at which the initial intercellular infection proceeds.

Finally, this study has revealed that new infections into each successive spikelet of the ear, both above and below the initial point of infection, occur via the cortex and not the vasculature. If effective induced plant defences could be localised to the cortex and not to the vasculature then there should be minimal risk to the growth and development of the wheat grain. The transgenic defensive response targeted to floral and rachis tissue, excluding the grain and vasculature, via the careful choice of promoters, would thereby avoid the issue of human consumption. From field observations, it is well established that the infection of florets at the base of the ear pose the greater risk of high grain losses, because of the subsequent loss of vascular integrity. Therefore, it is especially important that novel defence options are effective in the cortex of the spikelets situated at the ear base and thereby minimise the risk to the vascular supply of the ear.

The information collected from the various cell biology and transcriptome investigations will assist the development of a combination of new chemistries specific to *Fusaria*, improved wheat genotypes via traditionally breeding and / or transgenically modified wheat varieties that; stop or minimise the establishment of symptomless deep infection, the induction of the mycotoxin production and the spread of infection throughout the crop canopy.

9.6.2. Comparative tool for studying cereal pathogenesis

Traditionally most fundamental cereal pathology research has investigated the biotrophs (powdery mildews, smuts and rust) and *M. oryzae.* This research has mainly focussed on signalling and events occurring at the host surface, during appressorium formation, penetration, haustorium formation and early colonisation. However, many globally important cereal pathogens have different infection biology, e.g. *Claviceps purpurea*, *Fusarium* species, *M. graminicola* and *S. nodorum*. Through comparative species studies, both the generic as well as the species-specific molecular and biochemical processes controlling pathogenesis can be pinpointed.

Over the past decade, significant advances have been made in understanding the molecular mechanisms by which non-cereal infecting biotrophic and non-biotrophic pathogens manipulate the host plant to permit infection (Jones & Dangl, 2006, Stergiopoulos & de Wit, 2009). Far more limited is our understanding of how cereal hosts are successfully invaded by biotrophic and non-biotrophic pathogens and how the surrounding plant cells are manipulated to the advantage of the invading pathogen (Hueckelhoven & Schweizer, 2011). Many non-biotrophic pathogens are now known to interact with live plant cells during the initial phase of infection (the latent period) and may be required to adapt to the plant's defensive response (Deller *et al.*, 2011). An understanding of the molecular determinants of the latent period of infection by non-biotrophic cereal infecting fungi is progressing. However, overall there is only a limited understanding of the mechanisms deployed by pathogens which cause disease on non-leaf cereal tissues and the maintenance of healthy cereal floral tissue is essential for grain production. Therefore, the study of *F. graminearum* represents a useful comparative tool.

The commonality between all the different pathosystems described above is the need for the pathogen to circumvent the plants defensive response in order to

prevail. The secretion of effector proteins that prevent, manipulate or utilise the plant's defence response to the benefit of the pathogen appear conserved across different fungal lifestyles. In some pathosystems, the pathogen has in addition evolved the ability to produce a range of non-proteinaceous secondary metabolites to aid the infection process. As is the case for *F. graminearum* which requires DON synthesis to be induced to ensure infection and disease formation throughout the wheat floral tissue (Cuzick *et al.*, 2008b, Proctor *et al.*, 1997). However, DON production is not required for the successful colonisation of barley ears, maize cobs or Arabidopsis floral tissue (Cuzick *et al.*, 2008b, Harris *et al.*, 1999, Maier *et al.*, 2006, Proctor *et al.*, 1995a, Proctor *et al.*, 1995b). Although the target of DON, the 60S ribosomal subunit, is universal, the role for DON in disease formation is somehow host-species selective. This research suggests that it is highly likely that *F. graminearum* uses a combination of DON mycotoxin production and the secretion of an array of effectors and other metabolites to establish and maintain the advancing front of hyphal growth through the apoplast between living wheat cells. In effect, using a dual approach to successfully perturb and / or suppress basal plant defences in floral tissue. It is also highly likely, that at later stages in the infection process the communication events between the *F. graminearum* hyphae and the host cells change and this leads to a switch to intracellular colonisation, massive wheat cell death and macroscopically visible disease symptom formation (Brown *et al.*, 2010). This later phase may in part be achieved by the selective activation *en masse* of specific defence signalling pathways normally required for mounting a successful resistance response.

This research has provided an enhanced molecular understanding of the cereal host-pathogen interactions occurring during the latent period of infection, when most host cells remain alive. The various data-sets generated during this project will be invaluable for comparative analyses with cereal and non-cereal infecting biotrophic, non-biotrophic and necrotrophic pathogens. By using an RNA-sequencing approach the transcriptomes of both the fungus and the wheat host have been captured during the communicative phase of the interaction. The wider Affymetrix study enabled the temporal and spatial exploration of the interaction. The discovery of the symptomless apoplastic colonisation route which underlies the

Fusarium wheat ear infection process means that direct comparisons with the *M. graminicola* – wheat leaf infection process (Kema *et al.*, 1996, Marshall *et al.*, 2011) as well as the exceptionally well studied *C. fulvum* – tomato leaf model system (Bolton *et al.*, 2008) are appropriate. Within this triad of pathogenic species, three key apoplastic lifestyles are well represented.

9.6.3. Potential industrial use of *F. graminearum* for industrial hydrolytic enzyme production

Plant pathogenic fungi produce PCWDEs to breakdown the host cell wall to obtain nutrition and also to gain entry into the cell to assist colonisation of the plant tissue. Agricultural wastes from cereal crops such as straw and spent grain from the brewing process represent an abundant low cost fuel stock for the production of bioethanol. Straw is the most abundant crop residue and briefly consists of cellulose (40 %), hemicellulose (30 %) and lignin (20 %) (Lequart *et al.*, 1999). Spent grain is variable in composition but mainly consists of hemicelluloses (Mussatto & Roberto, 2006, Santos *et al.*, 2003, Xiros *et al.*, 2008). Pretreatment of lignocellulosic biomass converts it from its recalcitrant form into a state where enzymatic hydrolysis is effective (Alvira *et al.*, 2010). However, high enzyme loading is required to release the fermentable sugars. This represents the most expensive step in conversion of biomass into fermentable sugars and the major goal is to make the cell wall more openly accessible to enzymatic degradation. *T. reesei* is widely investigated and used for bioethanol production (Mathew *et al.*, 2008, Parawira & Tekere, 2011, Xu *et al.*, 2009), because of its ability to produce large amounts of cellulases. However, it only possesses a weak ability to degrade hemicellulose and lignin.

F. graminearum is a natural pathogen of all cereal species and has an impressive arsenal of PCWDEs (Chapter 6). The efficient hydrolysis of hemicellulose by bacteria producing high yields of *F. graminearum* enzymes has been achieved (Carapito *et al.*, 2009a). However, the plant cell wall is a highly complex structure. The simplicity of utilising a single organism that; can penetrate all plant cell-types, is able degrade every cell wall layer, will increase the porosity and accessibility for enzymatic hydrolysis of the cell wall would be highly beneficial. Figure 20 in chapter 3 indicates exactly what *F. graminearum* hyphae can do. The proven ability of *F. graminearum* to colonise and digest the lignocellulosic biomass

of wheat, straw or grain, coupled with the organism's pathogenic and saprotrophic nature make it an exciting candidate for investigation. Understanding the induction, regulation and production of the *F. graminearum* PCWDEs during wheat cell wall degradation will enable the engineering of safe, reproductively sterile and efficient strains for industrial biomass conversion. The analysis of the fungal transcriptome specifically during wheat cell wall degradation by LCM will enable; 1) the identification of new, efficient, stable enzymes and helper enzymes, such as cinnamoyl esterase which will increase enzyme access to cellulose, 2) the construction of strains which simultaneously produce higher levels of the enzymes required, and 3) the identification of any biochemical bottlenecks in the degradation process.

Chapter 10. Bibliography

Agrios, G. N., (1997) *Plant Pathology*. Academic Press, London.

Alexander, N. J., S. P. McCormick & T. M. Hohn, (1999) TRI12, a trichothecene efflux pump from *Fusarium sporotrichioides*: gene isolation and expression in yeast. *Molecular and General Genetics* **261**: 977-984.

Alexander, N. J., S. P. McCormick, C. Waalwijk, T. van der Lee & R. H. Proctor, (2011) The genetic basis for 3-ADON and 15-ADON trichothecene chemotypes in Fusarium. *Fungal Genetics and Biology* **48**: 485-495.

Alspaugh, J. A., R. Pukkila-Worley, T. Harashima, L. M. Cavallo, D. Funnell, G. M. Cox, J. R. Perfect, J. W. Kronstad & J. Heitman, (2002) Adenylyl cyclase functions downstream of the G alpha protein Gpa1 and controls mating and pathogenicity of *Cryptococcus neoformans*. *Eukaryotic Cell* **1**: 75-84.

Alvira, P., E. Tomas-Pejo, M. Ballesteros & M. J. Negro, (2010) Pretreatment technologies for an efficient bioethanol production process based on enzymatic hydrolysis: A review. *Bioresource Technology* **101**: 4851-4861.

Antoniw, J., A. Beacham, T. Baldwin, M. Urban, J. Rudd & K. Hammond-Kosack, (2011) OmniMapFree: A new tool to visualise and explore sequenced genomes. *BMC Bioinformatics*: Submitted.

Asakura, M., S. Ninomiya, M. Sugimoto, M. Oku, S.-i. Yamashita, T. Okuno, Y. Sakai & Y. Takano, (2009) Atg26-Mediated Pexophagy Is Required for Host Invasion by the Plant Pathogenic Fungus *Colletotrichum orbiculare*. *Plant Cell* **21**: 1291-1304.

Asano, T., T. Masumura, H. Kusano, S. Kikuchi, A. Kurita, H. Shimada & K. Kadowaki, (2002) Construction of a specialized cDNA library from plant cells isolated by laser capture microdissection: toward comprehensive analysis of the genes expressed in the rice phloem. *Plant Journal* **32**: 401-408.

Audenaert, K., E. Callewaert, M. Hofte, S. De Saeger & G. Haesaert, (2010) Hydrogen peroxide induced by the fungicide prothioconazole triggers deoxynivalenol (DON) production by *Fusarium graminearum*. *BMC Microbiology* **10**: 112.

Avery, S. V., (2006) Microbial cell individuality and the underlying sources of heterogeneity. *Nature Reviews Microbiology* **4**: 577-587.

Baggs, J. E. & J. B. Hogenesch, (2010) Genomics and systems approaches in the mammalian circadian clock. *Current Opinion in Genetics & Development* **20**: 581-587.

Bai, G. & G. Shaner, (2004a) Management and resistance in wheat and barley to Fusarium head blight. *Annual Review of Phytopathology* **42**: 135-161.

Bai, G. H. & G. Shaner, (2004b) Management and resistance in wheat and barley to Fusarium head blight. *Annual Review of Phytopathology* **42**: 135-161.

Baird, N. A., P. D. Etter, T. S. Atwood, M. C. Currey, A. L. Shiver, Z. A. Lewis, E. U. Selker, W. A. Cresko & E. A. Johnson, (2008) Rapid SNP Discovery and Genetic Mapping Using Sequenced RAD Markers. *Plos One* **3**.

Bakan, B., D. Melcion, D. Richard-Molard & B. Cahagnier, (2002) Fungal growth and Fusarium mycotoxin content in isogenic traditional maize and genetically modified maize grown in France and Spain. *Journal of Agricultural and Food Chemistry* **50**: 728-731.

Baldwin, T., (2007) *Fusarium graminearum* and *F. culmorum* pathogenicity on wheat ears. University of Exeter, Exeter, UK

Baldwin, T. K., M. Urban, N. Brown & K. E. Hammond-Kosack, (2010) A Role for Topoisomerase I in *Fusarium graminearum* and *F. culmorum* Pathogenesis and Sporulation. *Molecular Plant-Microbe Interactions* **23**: 566-577.

Bardwell, L., (2005) A walk-through of the yeast mating pheromone response pathway. *Peptides* **26**: 337.

Barreau, C., J. Merhej, L. Saint-Felix, M. Urban, K. E. Hammond-Kosack & F. Forget-Richard, (2011) The *velvet* gene of *Fusarium graminearum* positively regulates virulence and trichothecenes biosynthesis. In: 26th Fungal Genetics Conference. Asilomar, CA, USA, pp. 237.

Bayer, (2006) Technical bulletin: Prosaro. Bayer CropScience. http://bayercropwest.com/=file:Bulletins/1154976798272961 0a02022132198867/pdf. [20.06.2008]

Beacham, A., (2010) Pathogenicity determinants of *Fusarium graminearum* on wheat ears. University of Exeter, Exeter, UK

Beacham, A., J. Antoniw & K. E. Hammond-Kosack, (2009) A genomic fungal foray. *Biologist* **56**: 98-105.

Beck, T. & M. N. Hall, (1999) The TOR signalling pathway controls nuclear localization of nutrient-regulated transcription factors. *Nature* **402**: 689-692.

Belien, T., S. Van Campenhout, M. Van Acker & G. Volckaert, (2005) Cloning and characterization of two endoxylanases from the cereal phytopathogen *Fusarium graminearum* and their inhibition profile against endoxylanase inhibitors from wheat. *Biochemical and Biophysical Research Communications* **327**: 407-414.

Bhattacharjee, S., N. L. Hiller, K. Liolios, J. Win, T. D. Kanneganti, C. Young, S. Kamoun & K. Haldar, (2006) The malarial host-targeting signal is conserved in the Irish potato famine pathogen. *Plos Pathogens* **2**: 453-465.

Binder, E. M., (2007) Managing the risk of mycotoxins in modern feed production. *Animal Feed Science and Technology* **133**: 149-166.

Bluhm, B. H., X. Zhao, J. E. Flaherty, J. R. Xu & L. D. Dunkle, (2007) Ras2 regulates growth and pathogenesis in *Fusarium graminearum*. *Molecular Plant-Microbe Interactions* **20**: 627-636.

Boenisch, M. J. & W. Schäfer, (2011) *Fusarium graminearum* forms mycotoxin producing infection structures on wheat (*Triticum aestivum L.*). *BMC Plant Biology*: In Press.

Bok, J. W. & N. P. Keller, (2004) LaeA, a regulator of secondary metabolism in *Aspergillus spp*. *Eukaryotic Cell* **3**: 527-535.

Boller, T. & S. Y. He, (2009) Innate Immunity in Plants: An Arms Race Between Pattern Recognition Receptors in Plants and Effectors in Microbial Pathogens. *Science* **324**: 742-744.

Bolton, M. D., B. Thomma & B. D. Nelson, (2006) *Sclerotinia sclerotiorum* (Lib.) de Bary: biology and molecular traits of a cosmopolitan pathogen. *Molecular Plant Pathology* **7**: 1-16.

Bolton, M. D., H. P. van Esse, J. H. Vossen, R. de Jonge, I. Stergiopoulos, I. J. E. Stulemeijer, G. C. M. van den Berg, O. Borras-Hidalgo, H. L. Dekker, C. G. de Koster, P. de Wit, M. Joosten & B. Thomma, (2008) The novel *Cladosporium fulvum* lysin motif effector Ecp6 is a virulence factor with orthologues in other fungal species. *Molecular Microbiology* **69**: 119-136.

Both, M., M. Csukai, M. P. H. Stumpf & P. D. Spanu, (2005) Gene expression profiles of *Blumeria graminis* indicate dynamic changes to primary metabolism during development of an obligate biotrophic pathogen. *Plant Cell* **17**: 2107-2122.

Boutigny, A.-L., C. Barreau, V. Atanasova-Penichon, M.-N. Verdal-Bonnin, L. Pinson-Gadais & F. Richard-Forget, (2009) Ferulic acid, an efficient inhibitor of type B trichothecene biosynthesis and Tri gene expression in Fusarium liquid cultures. *Mycological Research* **113**: 746-753.

Brakhage, A. A. & V. Schroeckh, (2011) Fungal secondary metabolites - Strategies to activate silent gene clusters. *Fungal Genetics and Biology* **48**: 15-22.

Broders, K. D., P. E. Lipps, P. A. Paul & A. E. Dorrance, (2007) Evaluation of *Fusarium graminearum* associated with corn and soybean seed and seedling disease in Ohio. *Plant Disease* **91**: 1155-1160.

Brown, D. W., S. P. McCormick, N. J. Alexander, R. H. Proctor & A. E. Desjardins, (2001) A genetic and biochemical approach to study trichothecene diversity in *Fusarium sporotrichioides* and *Fusarium graminearum*. *Fungal Genetics and Biology* **32**: 121-133.

Brown, N. A., C. Bass, T. Baldwin, M. Urban, A. M. L. Van de Meene & K. E. Hammond-Kosack, (2011) Characterisation of the *Fusarium graminearum* - wheat floral interaction. *Journal Of Pathogens*: In Press.

Brown, N. A., M. Urban, A. M. L. van de Meene & K. E. Hammond-Kosack, (2010) The infection biology of *Fusarium graminearum*: Defining the pathways of spikelet to spikelet colonisation in wheat ears. *Fungal Biology* **114**: 555-571.

Browne, R. A. & B. M. Cooke, (2004) Development and evaluation of an in vitro detached leaf assay for pre-screening resistance to *Fusarium* head blight in wheat. *European Journal of Plant Pathology* **110**: 91-102.

Bruckmann, A., P. J. Hensbergen, C. I. A. Balog, A. M. Deelder, H. Y. Steensma & G. P. H. van Heusden, (2007) Post-transcriptional Control of the *Saccharomyces cerevisiae* proteome by 14-3-3 proteins. *Journal of Proteome Research* **6**: 1689-1699.

Buerstmayr, H., T. Ban & J. A. Anderson, (2009) QTL mapping and marker-assisted selection for Fusarium head blight resistance in wheat: a review. *Plant Breeding* **128**: 1-26.

Burlakoti, R. R., R. Estrada, V. V. Rivera, A. Boddeda, G. A. Secor & T. B. Adhikari, (2007) Real-time PCR quantification and mycotoxin production of *Fusarium graminearum* in wheat inoculated with isolates collected from potato, sugar beet, and wheat. *Phytopathology* **97**: 835-841.

Bushnell, W. R., B. E. Hazen & C. Pritsch, (2003) Histological and physiology of Fusarium Head Blight. In: Fusarium Head Blight of wheat and barley. K. J. Leonard & W. R. Bushnell (eds). Minnesota: The American Phytopathological Society, pp. 44-83.

Butchko, R. A. E., S. P. McCormick, M. Busman, B. Tudyznski & P. Wiemann, (2011) Regulation of secondary metabolite production in *Fusarium* species by the global regulator LAE1. In: 26th Fungal Genetics Conference. Asilomar, CA, USA, pp. 161.

Carapito, R., C. Carapito, J. M. Jeltsch & V. Phalip, (2009a) Efficient hydrolysis of hemicellulose by a *Fusarium graminearum* xylanase blend produced at high levels in *Escherichia coli*. *Bioresource Technology* **100**: 845-850.

Carapito, R., D. Hatsch, S. Vorwerk, E. Petkovski, J. M. Jeltsch & V. Phalip, (2008) Gene expression in *Fusarium graminearum* grown on plant cell wall. *Fungal Genetics and Biology* **45**: 738-748.

Carapito, R., A. Imberty, J. M. Jeltsch, S. C. Byrns, P. H. Tam, T. L. Lowary, A. Varrot & V. Phalip, (2009b) Molecular Basis of Arabinobio-hydrolase Activity in Phytopathogenic Fungi. Crystal structure and catalytic mechanism of *F. graminearum* GH93 exo-alpha-L-arabinanase. *Journal of Biological Chemistry* **284**: 12285-12296.

Carlson, M., (1999) Glucose repression in yeast. *Current Opinion in Microbiology* **2**: 202-207.

Cessna, S. G., V. E. Sears, M. B. Dickman & P. S. Low, (2000) Oxalic acid, a pathogenicity factor for *Sclerotinia sclerotiorum*, suppresses the oxidative burst of the host plant. *Plant Cell* **12**: 2191-2199.

Chakraborty, S. & A. C. Newton, (2011) Climate change, plant diseases and food security: an overview. *Plant Pathology* **60**: 2-14.

Champoux, J. J., (2001) DNA topoisomerases: Structure, function, and mechanism. *Annual Review of Biochemistry* **70**: 369-413.

Chandran, D., N. Inada, G. Hather, C. K. Kleindt & M. C. Wildermuth, (2010) Laser microdissection of Arabidopsis cells at the powdery mildew infection site reveals site-specific processes and regulators. *Proceedings of the National Academy of Sciences of the United States of America* **107**: 460-465.

Chang, L. F. & M. Karin, (2001) Mammalian MAP kinase signalling cascades. *Nature* **410**: 37-40.

Chen, R. E. & J. Thorner, (2007) Function and regulation in MAPK signaling pathways: Lessons learned from the yeast *Saccharomyces cerevisiae*. *Biochimica Et Biophysica Acta-Molecular Cell Research* **1773**: 1311-1340.

Chen, X., A. Steed, S. Travella, B. Keller & P. Nicholson, (2009) *Fusarium graminearum* exploits ethylene signalling to colonize dicotyledonous and monocotyledonous plants. *New Phytologist* **182**: 975-983.

Chi, Y., M. J. Huddleston, X. L. Zhang, R. A. Young, R. S. Annan, S. A. Carr & R. J. Deshaies, (2001) Negative regulation of Gcn4 and Msn2 transcription factors by Srb10 cyclin-dependent kinase. *Genes & Development* **15**: 1078-1092.

Christensen, M. J., R. J. Bennett, H. A. Ansari, H. Koga, R. D. Johnson, G. T. Bryan, W. R. Simpson, J. P. Koolaard, E. M. Nickless & C. R. Voisey, (2008) Epichloe endophytes grow by intercalary hyphal extension in elongating grass leaves. *Fungal Genetics and Biology* **45**: 84-93.

Clark, B., L. N. Jorgensen, D. Antichi, T. CGoral, D. Gouache, L. Hornok, M. Jahn, P. Lucas, B. Rolland & H. Schepers, (2009) From science to field: Wheat case study - guide number 2. Strategies to control *Fusarium* Ear Blight and mycotoxin production in wheat. In. R. Research (ed). ENDURE, pp. 1-4.

Coleman, J. J., S. D. Rounsley, M. Rodriguez-Carres, A. Kuo, C. C. Wasmann, J. Grimwood, J. Schmutz, M. Taga, G. J. White, S. G. Zhou, D. C. Schwartz, M. Freitag, L. J. Ma, E. G. J. Danchin, B. Henrissat, P. M. Coutinho, D. R. Nelson, D. Straney, C. A. Napoli, B. M. Barker, M. Gribskov, M. Rep, S. Kroken, I. Molnar, C. Rensing, J. C. Kennell, J. Zamora, M. L. Farman, E. U. Selker, A. Salamov, H. Shapiro, J. Pangilinan, E. Lindquist, C. Lamers, I. V. Grigoriev, D. M. Geiser, S. F. Covert, E. Temporini & H. D. VanEtten, (2009) The Genome of *Nectria haematococca*: Contribution of Supernumerary Chromosomes to Gene Expansion. *Plos Genetics* **5**.

Cordell, D., J.-O. Drangert & S. White, (2009) The story of phosphorus: Global food security and food for thought. *Global Environmental Change-Human and Policy Dimensions* **19**: 292-305.

Cuomo, C. A., U. Gueldener, J. R. Xu, F. Trail, B. G. Turgeon, A. Di Pietro, J. D. Walton, L. J. Ma, S. E. Baker, M. Rep, G. Adam, J. Antoniw, T. Baldwin, S. Calvo, Y. L. Chang, D. DeCaprio, L. R. Gale, S. Gnerre, R. S. Goswami, K. Hammond-Kosack, L. J. Harris, K. Hilburn, J. C. Kennell, S. Kroken, J. K. Magnuson, G. Mannhaupt, E. Mauceli, H. W. Mewes, R. Mitterbauer, G. Muehlbauer, M. Munsterkotter, D. Nelson, K. O'Donnell, T. Ouellet, W. H. Qi, H. Quesneville, M. I. G. Roncero, K. Y. Seong, I. V. Tetko, M. Urban, C. Waalwijk, T. J. Ward, J. Q. Yao, B. W. Birren & H. C. Kistler, (2007) The *Fusarium graminearum* genome reveals a link between localized polymorphism and pathogen specialization. *Science* **317**: 1400-1402.

Curtis, B. C., S. Rajaram & H. G. Macpherson, (2002) *Wheat in the world. In: Bread wheat: improvement and production*. FAO, Rome, Italy.

Cuzick, A., S. Lee, S. Gezan & K. E. Hammond-Kosack, (2008a) *NPR1* and *EDS11* contribute to host resistance against *Fusarium culmorum* in Arabidopsis buds and flowers. *Molecular Plant Pathology* **9**: 697-704.

Cuzick, A., K. Maguire & K. E. Hammond-Kosack, (2009) Lack of the plant signalling component SGT1b enhances disease resistance to *Fusarium culmorum* in Arabidopsis buds and flowers. *New Phytologist* **181**: 901-912.

Cuzick, A., M. Urban & K. Hammond-Kosack, (2008b) *Fusarium graminearum* gene deletion mutants *map1* and *tri5* reveal similarities and differences in the pathogenicity requirements to cause disease on Arabidopsis and wheat floral tissue. *New Phytologist* **177**: 990-1000.

Day, R. C., U. Grossniklaus & R. C. Macknight, (2005) Be more specific! Laser-assisted microdissection of plant cells. *Trends in Plant Science* **10**: 397-406.

de Jonge, R., H. P. van Esse, A. Kombrink, T. Shinya, Y. Desaki, R. Bours, S. van der Krol, N. Shibuya, M. Joosten & B. Thomma, (2010) Conserved Fungal LysM Effector Ecp6 Prevents Chitin-Triggered Immunity in Plants. *Science* **329**: 953-955.

Dean, R. A., N. J. Talbot, D. J. Ebbole, M. L. Farman, T. K. Mitchell, M. J. Orbach, M. Thon, R. Kulkarni, J. R. Xu, H. Q. Pan, N. D. Read, Y. H. Lee, I. Carbone, D. Brown, Y. Y. Oh, N. Donofrio, J. S. Jeong, D. M. Soanes, S. Djonovic, E. Kolomiets, C. Rehmeyer, W. X. Li, M. Harding, S. Kim, M. H. Lebrun, H. Bohnert, S. Coughlan, J. Butler, S. Calvo, L. J. Ma, R. Nicol, S. Purcell, C. Nusbaum, J. E. Galagan & B. W. Birren, (2005) The genome sequence of the rice blast fungus *Magnaporthe grisea*. *Nature* **434**: 980-986.

Deising, H. B., S. Werner & M. Wernitz, (2000) The role of fungal appressoria in plant infection. *Microbes and Infection* **2**: 1631-1641.

Dekhang, R., K. M. Smith, E. L. Bredeweg, J. M. Emerson, M. S. Sachs, J. C. Dunlap, M. Freitag & D. Bell-Pedersen, (2011) Characterization of Circadian Clock Output Pathways Regulated by Adv-1 in *Neurospora Crassa* Using Chip-se. In: 26th Fungal Genetic Conference Asilomar, CA, USA, pp. 165.

Delgado, J. A., P. B. Schwarz, J. Gillespie, V. V. Rivera-Varas & G. A. Secor, (2010) Trichothecene Mycotoxins Associated with Potato Dry Rot Caused by *Fusarium graminearum*. *Phytopathology* **100**: 290-296.

Deller, S., K. E. Hammond-Kosack & J. J. Rudd, (2011) The complex interactions between host immunity and non-biotrophic fungal pathogens of wheat leaves. *Journal of Plant Physiology* **168**: 63-71.

Desjardins, A. E., (2006) *Fusarium mycotoxins: Chemistry, Genetics and Biology*. APS Press, St Paul, MN, USA.

Desjardins, A. E. & R. H. Proctor, (2001) *Biochemistry and genetics of Fusarium toxins*, p. 50-69.

Desjardins, A. E. & R. H. Proctor, (2007) Molecular biology of Fusarium mycotoxins. *International Journal of Food Microbiology* **119**: 47-50.

Desmond, O. J., J. M. Manners, A. E. Stephens, D. J. Maclean, P. M. Schenk, D. M. Gardiner, A. L. Munn & K. Kazan, (2008) The *Fusarium* mycotoxin deoxynivalenol elicits hydrogen peroxide production, programmed cell death and defence responses in wheat. *Molecular Plant Pathology* **9**: 435-445.

Di Pietro, A., F. I. Garcia-Maceira, E. Meglecz & M. I. G. Roncero, (2001) A MAP kinase of the vascular wilt fungus *Fusarium oxysporum* is essential for root penetration and pathogenesis. *Molecular Microbiology* **39**: 1140-1152.

Dignani, M. C. & E. Anaissie, (2004) Human fusariosis. *Clin. Microbiol. Infect.* **10**: 67-75.

Dilova, I., S. Aronova, J. C. Y. Chen & T. Powers, (2004) Tor signaling and nutrient-based signals converge on Mks1p phosphorylation to regulate expression of Rtg1p center dot Rtg3p-dependent target genes. *Journal of Biological Chemistry* **279**: 46527-46535.

Ding, L. N., H. B. Xu, H. Y. Yi, L. M. Yang, Z. X. Kong, L. X. Zhang, S. L. Xue, H. Y. Jia & Z. Q. Ma, (2011) Resistance to Hemi-Biotrophic *F-graminearum* Infection Is Associated with Coordinated and Ordered Expression of Diverse Defense Signaling Pathways. *Plos One* **6**.

Doehlemann, G., P. Berndt & M. Hahn, (2006) Trehalose metabolism is important for heat stress tolerance and spore germination of *Botrytis cinerea*. *Microbiology-Sgm* **152**: 2625-2634.

Doehlemann, G., K. van der Linde, D. Amann, D. Schwammbach, A. Hof, A. Mohanty, D. Jackson & R. Kahmann, (2009) Pep1, a Secreted Effector Protein of *Ustilago maydis*, Is Required for Successful Invasion of Plant Cells. *Plos Pathogens* **5**.

Dohlman, H. G. & J. W. Thorner, (2001) Regulation of G protein-initiated signal transduction in yeast: Paradigms and principles. *Annual Review of Biochemistry* **70**: 703-754.

Dorman, C. J., (1991) DNA supercoiling and environmental regulation of gene expression in pathogenic bacteria. *Infection and Immunity* **59**: 745-749.

Dorman, C. J. & C. P. Corcoran, (2009) Bacterial DNA topology and infectious disease. *Nucleic Acids Research* **37**: 672-678.

Dowd, P. F., (2001) Biotic and abiotic factors limiting efficacy of Bt corn in indirectly reducing mycotoxin levels in commercial fields. *Journal of Economic Entomology* **94**: 1067-1074.

Dublin, H. J., L. Glichrist, J. Reeves & A. McNab, (1997) *Fusarium Head Scab: Global Status and Prospects*. CIMMYT, Mexico.

Duran, R. M., J. W. Cary & A. M. Calvo, (2007) Production of cyclopiazonic acid, aflatrem, and aflatoxin by *Aspergillus flavus* is regulated by veA, a gene necessary for sclerotial formation. *Applied Microbiology and Biotechnology* **73**: 1158-1168.

Duyvesteijn, R. G. E., R. van Wijk, Y. Boer, M. Rep, B. J. C. Cornelissen & M. A. Haring, (2005) Frp1 is a *Fusarium oxysporum* F-box protein required for pathogenicity on tomato. *Molecular Microbiology* **57**: 1051-1063.

Dyer, R. B., R. D. Plattner, D. F. Kendra & D. W. Brown, (2005) *Fusarium graminearum* TRI14 is required for high virulence and DON production on wheat but not for DON synthesis in vitro. *Journal of Agricultural and Food Chemistry* **53**: 9281-9287.

Eaton, C. J., M. P. Cox, B. Ambrose, M. Becker, U. Hesse, C. L. Schardl & B. Scott, (2010) Disruption of Signaling in a Fungal-Grass Symbiosis Leads to Pathogenesis. *Plant Physiology* **153**: 1780-1794.

Eaton, C. J., M. P. Cox & B. Scott, (2011) What triggers grass endophytes to switch from mutualism to pathogenism? *Plant Science* **180**: 190-195.

Edwards, S. G., B. Barrier-Guillot, P. E. Clasen, V. Hietaniemi & H. Pettersson, (2009) Emerging issues of HT-2 and T-2 toxins in European cereal production. *World Mycotoxin J.* **2**: 173-179.

Egan, M. J., Z.-Y. Wang, M. A. Jones, N. Smirnoff & N. J. Talbot, (2007) Generation of reactive oxygen species by fungal NADPH oxidases is required for rice blast disease. *Proceedings of the National Academy of Sciences of the United States of America* **104**: 11772-11777.

Eisenhaber, B., G. Schneider, M. Wildpaner & F. Eisenhaber, (2004) A sensitive predictor for potential GPI lipid modification sites in fungal protein sequences and its application to genome-wide studies for *Aspergillus nidulans, Candida albicans Neurospora crassa, Saccharomyces cerevisiae* and *Schizosaccharomyces pombe*. *Journal of Molecular Biology* **337**: 243-253.

Emanuelsson, O., S. Brunak, G. von Heijne & H. Nielsen, (2007) Locating proteins in the cell using TargetP, SignalP and related tools. *Nature Protocols* **2**: 953-971.

Emanuelsson, O., H. Nielsen, S. Brunak & G. von Heijne, (2000) Predicting subcellular localization of proteins based on their N-terminal amino acid sequence. *Journal of Molecular Biology* **300**: 1005-1016.

Emmert-Buck, M. R., R. F. Bonner, P. D. Smith, R. F. Chuaqui, Z. P. Zhuang, S. R. Goldstein, R. A. Weiss & L. A. Liotta, (1996) Laser capture microdissection. *Science* **274**: 998-1001.

Estrada, R., N. C. Gudmestad, V. V. Rivera & G. A. Secor, (2010) *Fusarium graminearum* as a dry rot pathogen of potato in the USA: prevalence, comparison of host isolate aggressiveness and factors affecting aetiology. *Plant Pathology* **59**: 1114-1120.

Estrada, R. E., V. V. Rivera & G. A. Secor, (2007) Pathogenicity of *Fusarium graminearum* to potato, sugarbeet and wheat. *Phytopathology* **97**: S160-S160.

Evans, C. K., W. Xie, R. Dill-Macky & C. J. Mirocha, (2000) Biosynthesis of deoxynivalenol in spikelets of barley inoculated with macroconidia of *Fusarium graminearum*. *Plant Disease* **84**: 654-660.

Faris, J. D. & T. L. Friesen, (2009) Reevaluation of a Tetraploid Wheat Population Indicates that the Tsn1-ToxA Interaction Is the Only Factor Governing *Stagonospora nodorum* Blotch Susceptibility. *Phytopathology* **99**: 906-912.

Faris, J. D., Z. Zhang, H. Lu, S. Lu, L. Reddy, S. Cloutier, J. P. Fellers, S. W. Meinhardt, J. B. Rasmussen, S. S. Xu, R. P. Oliver, K. J. Simons & T. L. Friesen, (2010) A unique wheat disease resistance-like gene governs effector-triggered susceptibility to necrotrophic pathogens. *Proceedings of the National Academy of Sciences of the United States of America* **107**: 13544-13549.

Fellbrich, G., A. Romanski, A. Varet, B. Blume, F. Brunner, S. Engelhardt, G. Felix, B. Kemmerling, M. Krzymowska & T. Nurnberger, (2002) NPP1, a Phytophthora-associated trigger of plant defense in parsley and Arabidopsis. *Plant Journal* **32**: 375-390.

Feng, J., R. Hwang, K. F. Chang, S. F. Hwang, S. E. Strelkov, B. D. Gossen, R. L. Conner & G. D. Turnbull, (2010) Genetic variation in *Fusarium avenaceum* causing root rot on field pea. *Plant Pathology* **59**: 845-852.

Feng, J., G. S. Liu, G. Selvaraj, G. R. Hughes & Y. D. Wei, (2005) A secreted lipase encoded by LIP1 is necessary for efficient use of saturated triglyceride lipids in *Fusarium graminearum*. *Microbiology-Sgm* **151**: 3911-3921.

Folcher, L., M. Delos, E. Marengue, M. Jarry, A. Weissenberger, N. Eychenne & C. Regnault-Roger, (2010) Lower mycotoxin levels in Bt maize grain. *Agronomy for Sustainable Development* **30**: 711-719.

Foster, A. J., J. M. Jenkinson & N. J. Talbot, (2003) Trehalose synthesis and metabolism are required at different stages of plant infection by *Magnaporthe grisea*. *Embo Journal* **22**: 225-235.

Fosu-Nyarko, J., M. G. K. Jones & Z. Wang, (2009) Functional characterization of transcripts expressed in early-stage Meloidogyne javanica-induced giant cells isolated by laser microdissection. *Molecular Plant Pathology* **10**: 237-248.

Francis, R. G. & L. W. Burgess, (1977) Characteristics of 2 populations of *Fusarium roseum graminearum* in Eastern Australia. *Transactions of the British Mycological Society* **68**: 421-427.

Friesen, T. L., J. D. Faris, P. S. Solomon & R. P. Oliver, (2008) Host-specific toxins: effectors of necrotrophic pathogenicity. *Cellular Microbiology* **10**: 1421-1428.

Friesen, T. L., S. W. Meinhardt & J. D. Faris, (2007) The *Stagonospora nodorum*-wheat pathosystem involves multiple proteinaceous host-selective toxins and corresponding host sensitivity genes that interact in an inverse gene-for-gene manner. *Plant Journal* **51**: 681-692.

Friesen, T. L., E. H. Stukenbrock, Z. Liu, S. Meinhardt, H. Ling, J. D. Faris, J. B. Rasmussen, P. S. Solomon, B. A. McDonald & R. P. Oliver, (2006) Emergence of a new disease as a result of interspecific virulence gene transfer. *Nature Genetics* **38**: 953-956.

Gaffoor, I., D. W. Brown, R. Plattner, R. H. Proctor, W. H. Qi & F. Trail, (2005) Functional analysis of the polyketide synthase genes in the filamentous fungus *Gibberella zeae* (Anamorph *Fusarium graminearum*). *Eukaryotic Cell* **4**: 1926-1933.

Gaffoor, I. & F. Trail, (2006) Characterization of two polyketide synthase genes involved in zearalenone biosynthesis in *Gibberella zeae*. *Applied and Environmental Microbiology* **72**: 1793-1799.

Galan, J. E. & A. Collmer, (1999) Type III secretion machines: Bacterial devices for protein delivery into host cells. *Science* **284**: 1322-1328.

Galan, J. E. & R. Curtiss, (1990) Expression of *Salmonella typhimurim* genes required for invasion is regulated by changes in DNA supercoiling. *Infection and Immunity* **58**: 1879-1885.

Gallego, O., M. J. Betts, J. Gvozdenovic-Jeremic, K. Maeda, C. Matetzki, C. Aguilar-Gurrieri, P. Beltran-Alvarez, S. Bonn, C. Fernandez-Tornero, L. J. Jensen, M. Kuhn, J. Trott, V. Rybin, C. W. Mueller, P. Bork, M. Kaksonen, R. B. Russell & A.-C. Gavin, (2010) A systematic screen for protein-lipid interactions in *Saccharomyces cerevisiae*. *Molecular Systems Biology* **6**.

Gan, P. H. P., M. Rafiqi, A. R. Hardham & P. N. Dodds, (2010) Effectors of biotrophic fungal plant pathogens. *Functional Plant Biology* **37**: 913-918.

Gancedo, J. M., (2001) Control of pseudohyphae formation in *Saccharomyces cerevisiae*. *Fems Microbiology Reviews* **25**: 107-123.

Gardiner, D. M., K. Kazan & J. M. Manners, (2009a) Novel Genes of *Fusarium graminearum* That Negatively Regulate Deoxynivalenol Production and Virulence. *Molecular Plant-Microbe Interactions* **22**: 1588-1600.

Gardiner, D. M., K. Kazan & J. M. Manners, (2009b) Nutrient profiling reveals potent inducers of trichothecene biosynthesis in *Fusarium graminearum*. *Fungal Genetics and Biology* **46**: 604-613.

Gardiner, D. M., K. Kazan, S. Praud, F. J. Torney, A. Rusu & J. M. Manners, (2010) Early activation of wheat polyamine biosynthesis during Fusarium head blight implicates putrescine as an inducer of trichothecene mycotoxin production. *Bmc Plant Biology* **10**.

Gardiner, D. M., S. Osborne, K. Kazan & J. M. Manners, (2009c) Low pH regulates the production of deoxynivalenol by *Fusarium graminearum*. *Microbiology-Sgm* **155**: 3149-3156.

Garrett, K. A., S. P. Dendy, E. E. Frank, M. N. Rouse & S. E. Travers, (2006) Climate change effects on plant disease: Genomes to ecosystems. *Annual Review of Phytopathology* **44**: 489-509.

Garvey, G. S., S. P. McCormick & I. Rayment, (2008) Structural and functional characterization of the TRI101 trichothecene 3-O-acetyltransferase from *Fusarium sporotrichioides* and *Fusarium graminearum* - Kinetic insights to combating fusarium head blight. *Journal of Biological Chemistry* **283**: 1660-1669.

Giesbert, S., T. Schurg, S. Scheele & P. Tudzynski, (2008) The NADPH oxidase Cpnox1 is required for full pathogenicity of the ergot fungus *Claviceps purpurea*. *Molecular Plant Pathology* **9**: 317-327.

Gilbert, J. & W. G. D. Fernando, (2004) Epidemiology and biological control of *Gibberella zeae Fusarium graminearum*. *Canadian Journal of Plant Pathology-Revue Canadienne De Phytopathologie* **26**: 464-472.

Gomez, S. K., H. Javot, P. Deewatthanawong, I. Torres-Jerez, Y. Tang, E. B. Blancaflor, M. K. Udvardi & M. J. Harrison, (2009) *Medicago truncatula* and *Glomus intraradices* gene expression in cortical cells harboring arbuscules in the arbuscular mycorrhizal symbiosis. *Bmc Plant Biology* **9**.

Gonzalez, A., A. Ruiz, A. Casamayor & J. Arino, (2009) Normal Function of the Yeast TOR Pathway Requires the Type 2C Protein Phosphatase Ptc1. *Molecular and Cellular Biology* **29**: 2876-2888.

Goodwin, P. H. & G. Y. Chen, (2002) High expression of a sucrose non-fermenting (SNF1)-related protein kinase from *Colletotrichum gloeosporoides* f. sp *malvae* is associated with penetration of Malva pusilla. *Fems Microbiology Letters* **215**: 169-174.

Goodwin, S. B., S. Ben M'Barek, B. Dhillon, A. H. J. Wittenberg, C. F. Crane, J. K. Hane, A. J. Foster, T. A. J. Van der Lee, J. Grimwood, A. Aerts, J. Antoniw, A. Bailey, B. Bluhm, J. Bowler, J. Bristow, A. van der Burgt, B. Canto-Canche, A. C. L. Churchill, L. Conde-Ferraez, H. J. Cools, P. M. Coutinho, M. Csukai, P. Dehal, P. De Wit, B. Donzelli, H. C. van de Geest, R. C. H. J. van Ham, K. E. Hammond-Kosack, B. Henrissat, A. Kilian, A. K. Kobayashi, E. Koopmann, Y. Kourmpetis, A. Kuzniar, E. Lindquist, V. Lombard, C. Maliepaard, N. Martins, R. Mehrabi, J. P. H. Nap, A. Ponomarenko, J. J. Rudd, A. Salamov, J. Schmutz, H. J. Schouten, H. Shapiro, I. Stergiopoulos, S. F. F. Torriani, H. Tu, R. P. de Vries, C. Waalwijk, S. B. Ware, A. Wiebenga, L.-H. Zwiers, R. P. Oliver, I. V. Grigoriev & G. H. J. Kema, (2011) Finished Genome of the Fungal Wheat Pathogen *Mycosphaerella graminicola* Reveals Dispensome Structure, Chromosome Plasticity, and Stealth Pathogenesis. *Plos Genetics* **7**.

Goswami, R. S. & H. C. Kistler, (2004) Heading for disaster: *Fusarium graminearum* on cereal crops. *Molecular Plant Pathology* **5**: 515-525.

Govrin, E. M. & A. Levine, (2000) The hypersensitive response facilitates plant infection by the necrotrophic pathogen *Botrytis cinerea*. *Current Biology* **10**: 751-757.

Greenshields, D. L., G. S. Liu, J. Feng, G. Selvaraj & Y. D. Wei, (2007) The siderophore biosynthetic gene *SID1*, but not the ferroxidase gene *FET3*, is required for full *Fusarium graminearum* virulence. *Molecular Plant Pathology* **8**: 411-421.

Guenther, J. C., H. E. Hallen-Adams, H. Bucking, Y. Shachar-Hill & F. Trail, (2009) Triacylglyceride Metabolism by *Fusarium graminearum* During Colonization and Sexual Development on Wheat. *Molecular Plant-Microbe Interactions* **22**: 1492-1503.

Guenther, J. C. & F. Trail, (2005) The development and differentiation of *Gibberella zeae* (anamorph: *Fusarium graminearum*) during colonization of wheat. *Mycologia* **97**: 229-237.

Guldener, U., K. Y. Seong, J. Boddu, S. H. Cho, F. Trail, J. R. Xu, G. Adam, H. W. Mewes, G. J. Muehlbauer & H. C. Kistler, (2006) Development of a *Fusarium graminearum* Affymetrix GeneChip for profiling fungal gene expression in vitro and in planta. *Fungal Genetics and Biology* **43**: 316-325.

Gustin, M. C., J. Albertyn, M. Alexander & K. Davenport, (1998) MAP kinase pathways in the yeast *Saccharomyces cerevisiae*. *Microbiology and Molecular Biology Reviews* **62**: 1264-+.

Gutleb, A. C., E. Morrison & A. J. Murk, (2002) Cytotoxicity assays for mycotoxins produced by Fusarium strains: a review. *Environmental Toxicology and Pharmacology* **11**: 309-320.

Haas, B. J., S. Kamoun, M. C. Zody, R. H. Y. Jiang, R. E. Handsaker, L. M. Cano, M. Grabherr, C. D. Kodira, S. Raffaele, T. Torto-Alalibo, T. O. Bozkurt, A. M. V. Ah-Fong, L. Alvarado, V. L. Anderson, M. R. Armstrong, A. Avrova, L. Baxter, J. Beynon, P. C. Boevink, S. R. Bollmann, J. I. B. Bos, V. Bulone, G. H. Cai, C. Cakir, J. C. Carrington, M. Chawner, L. Conti, S. Costanzo, R. Ewan, N. Fahlgren, M. A. Fischbach, J. Fugelstad, E. M. Gilroy, S. Gnerre, P. J. Green, L. J. Grenville-Briggs, J. Griffith, N. J. Grunwald, K. Horn, N. R. Horner, C. H. Hu, E. Huitema, D. H. Jeong, A. M. E. Jones, J. D. G. Jones, R. W. Jones, E. K. Karlsson, S. G. Kunjeti, K. Lamour, Z. Y. Liu, L. J. Ma, D. MacLean, M. C. Chibucos, H. McDonald, J. McWalters, H. J. G. Meijer, W. Morgan, P. F. Morris, C. A. Munro, K. O'Neill, M. Ospina-Giraldo, A. Pinzon, L. Pritchard, B. Ramsahoye, Q. H. Ren, S. Restrepo, S. Roy, A. Sadanandom, A. Savidor, S. Schornack, D. C. Schwartz, U. D. Schumann, B. Schwessinger, L. Seyer, T. Sharpe, C. Silvar, J. Song, D. J. Studholme, S. Sykes, M. Thines, P. J. I. van de Vondervoort, V. Phuntumart, S. Wawra, R. Weide, J. Win, C. Young, S. G. Zhou, W. Fry, B. C. Meyers, P. van West, J. Ristaino, F. Govers, P. R. J. Birch, S. C. Whisson, H. S. Judelson & C. Nusbaum, (2009) Genome sequence and analysis of the Irish potato famine pathogen *Phytophthora infestans*. *Nature* **461**: 393-398.

Hall, D. W., (1970) Handling and storage of food grains in tropical and sub-tropical areas. In: FAO Agricultural Development Paper. F. a. A. Organisatioin (ed). Rome, Italy, pp. 1-375.

Hall, N., J. P. R. Keon & J. A. Hargreaves, (1999) A homologue of a gene implicated in the virulence of human fungal diseases is present in a plant fungal pathogen and is expressed during infection. *Physiological and Molecular Plant Pathology* **55**: 69-73.

Hallen, H. E. & F. Trail, (2008) The L-type calcium ion channel, Cch1, affects ascospore discharge and mycelial growth in the filamentous fungus *Gibberella zeae* (anamorph *Fusarium graminearum*). *Eukaryotic Cell* **7**: 415-424.

Han, Y. K., M. D. Kim, S. H. Lee, S. H. Yun & Y. W. Lee, (2007) A novel F-box protein involved in sexual development and pathogenesis in *Gibberella zeae*. *Molecular Microbiology* **63**: 768-779.

Han, Y. K., T. Lee, K. H. Han, S. H. Yun & Y. W. Lee, (2004) Functional analysis of the homoserine O-acetyltransferase gene and its identification as a selectable marker in *Gibberella zeae*. *Current Genetics* **46**: 205-212.

Hane, J. K., R. G. T. Lowe, P. S. Solomon, K. C. Tan, C. L. Schoch, J. W. Spatafora, P. W. Crous, C. Kodira, B. W. Birren, J. E. Galagan, S. F. F. Torriani, B. A. McDonald & R. P. Oliver, (2007) Dothideomycete-plant interactions illuminated by genome sequencing and EST analysis of the wheat pathogen *Stagonospora nodorum*. *Plant Cell* **19**: 3347-3368.

Hardie, D. G., D. Carling & M. Carlson, (1998) The AMP-activated/SNF1 protein kinase subfamily: Metabolic sensors of the eukaryotic cell? *Annual Review of Biochemistry* **67**: 821-855.

Hardy, T. A., D. Q. Huang & P. J. Roach, (1994) Interactions betweencAMP-dependent and SNF1 protein kinases in the control of glycogen accumulation in *Saccharomyces cerevisiae*. *Journal of Biological Chemistry* **269**: 27907-27913.

Harris, L. J., N. J. Alexander, A. Saparno, B. Blackwell, S. P. McCormick, A. E. Desjardins, L. S. Robert, N. Tinker, J. Hattori, C. Piche, J. P. Schernthaner, R. Watson & T. Ouellet, (2007) A novel gene cluster in *Fusarium graminearum* contains a gene that contributes to butenolide synthesis. *Fungal Genetics and Biology* **44**: 293-306.

Harris, L. J., A. E. Desjardins, R. D. Plattner, P. Nicholson, G. Butler, J. C. Young, G. Weston, R. H. Proctor & T. M. Hohn, (1999) Possible role of trichothecene mycotoxins in virulence of *Fusarium graminearum* on maize. *Plant Disease* **83**: 954-960.

Harwood, C. S. & R. E. Parales, (1996) The beta-ketoadipate pathway and the biology of self-identity. *Annual Review of Microbiology* **50**: 553-590.

Heger, A. & L. Holm, (2000) Rapid automatic detection and alignment of repeats in protein sequences. *Proteins-Structure Function and Genetics* **41**: 224-237.

Hensel, M., (2000) Salmonella pathogenicity island 2. *Molecular Microbiology* **36**: 1015-1023.

Hirschman, J. E., R. Balakrishnan, K. R. Christie, M. C. Costanzo, S. S. Dwight, S. R. Engel, D. G. Fisk, E. L. Hong, M. S. Livstone, R. Nash, J. Park, R. Oughtred, M. Skrzypek, B. Starr, C. L. Theesfeld, J. Williams, R. Andrada, G. Binkley, Q. Dong, C. Lane, S. Miyasato, A. Sethuraman, M. Schroeder, M. K. Thanawala, S. Weng, K. Dolinski, D. Botstein & J. M. Cherry, (2006) Genome Snapshot: a new resource at the Saccharomyces Genome Database (SGD) presenting an overview of the *Saccharomyces cerevisiae* genome. *Nucleic Acids Research* **34**: D442-D445.

Hohmann, S., (2002) Osmotic stress signaling and osmoadaptation in Yeasts. *Microbiology and Molecular Biology Reviews* **66**: 300.

Hohn, T. M. & F. Vanmiddlesworth, (1986) Purification and characterization of the sesquiterpene cyclase trichodiene synthetase from *Fusarium sporotrichioides*. *Archives of Biochemistry and Biophysics* **251**: 756-761.

Holdgate, S., (2009) Improving the diversity of resistance mechanisms available in wheat to combat Fusarium ear blight disease. Cranfield University, UK, Cranfield

Hong, S.-Y., J. So, J. Lee, K. Min, H. Son, C. Park, S.-H. Yun & Y.-W. Lee, (2010) Functional analyses of two syntaxin-like SNARE genes, GzSYN1 and GzSYN2, in the ascomycete *Gibberella zeae*. *Fungal Genetics and Biology* **47**: 364-372.

Hook, S., R. Williams, C. Edwards & G. Dodgson, (2007) Guidelines to minimise risk of fusarium mycotoxins in cereals. In. London: HGCA, pp. 1-8.
Hope, R. & N. Magan, (2003) Two-dimensional environmental profiles of growth, deoxynivalenol and nivalenol production by *Fusarium culmorum* on a wheat-based substrate. *Letters in Applied Microbiology* **37**: 70-74.
Horton, P., K. J. Park, T. Obayashi & K. Nakai, (2006) Protein subcellular localization prediction with WOLF PSORT. *Proceedings of the 4th Asia-Pacific Bioinformatics Conference* **3**: 39-48.
Hou, Z. M., C. Y. Xue, Y. L. Peng, T. Katan, H. C. Kistler & J. R. Xu, (2002) A mitogen-activated protein kinase gene (*MGV1*) in *Fusarium graminearum* is required for female fertility, heterokaryon formation, and plant infection. *Molecular Plant-Microbe Interactions* **15**: 1119-1127.
Houterman, P. M., B. J. C. Cornelissen & M. Rep, (2008) Suppression of plant resistance gene-based immunity by a fungal effector. *PLoS Pathog* **4**: e1000061.
Houterman, P. M., L. Ma, G. van Ooijen, M. J. de Vroomen, B. J. C. Cornelissen, F. L. W. Takken & M. Rep, (2009) The effector protein Avr2 of the xylem-colonizing fungus *Fusarium oxysporum* activates the tomato resistance protein I-2 intracellularly. *Plant Journal* **58**: 970-978.
Howlett, B. J., (2006) Secondary metabolite toxins and nutrition of plant pathogenic fungi. *Current Opinion in Plant Biology* **9**: 371-375.
Hueckelhoven, R. & P. Schweizer, (2011) Quantitative disease resistance and fungal pathogenicity in Triticeae. *Journal of Plant Physiology* **168**: 1-2.
Hungria, M., J. C. Franchini, R. J. Campo, C. C. Crispino, J. Z. Moraes, R. N. R. Sibaldelli, I. C. Mendes & J. Arihara, (2006) Nitrogen nutrition of soybean in Brazil: Contributions of biological N-2 fixation and N fertilizer to grain yield. *Canadian Journal of Plant Science* **86**: 927-939.
Idnurm, A., D. C. Warnecke, E. Heinz & B. J. Howlett, (2003) Characterisation of neutral trehalase and UDP-glucose : sterol glucosyltransferase genes from the plant pathogenic fungus Leptosphaeria maculans. *Physiological and Molecular Plant Pathology* **62**: 305-313.
Igawa, T., N. Takahashi-Ando, N. Ochiai, S. Ohsato, T. Shimizu, T. Kudo, I. Yamaguchi & M. Kimura, (2007) Reduced contamination by the Fusarium mycotoxin zearalenone in maize kernels through genetic modification with a detoxification gene. *Applied and Environmental Microbiology* **73**: 1622-1629.
Ilgen, P., B. Hadeler, F. J. Maier & W. Schafer, (2009) Developing kernel and rachis node induce the trichothecene pathway of *Fusarium graminearum* during wheat head infection. *Mol Plant Microbe Interact* **22**: 899-908.
Inada, N. & M. C. Wildermuth, (2005) Novel tissue preparation method and cell-specific marker for laser microdissection of Arabidopsis mature leaf. *Planta* **221**: 9-16.
Inderbitzin, P., T. Asvarak & B. G. Turgeon, (2010) Six New Genes Required for Production of T-Toxin, a Polyketide Determinant of High Virulence of Cochliobolus heterostrophus to Maize. *Molecular Plant-Microbe Interactions* **23**: 458-472.
Ingham, J. L., B. J. Deverall, J. Kuc, D. T. Coxon, A. Stoessl, H. D. VanEtten, D. E. Matthews & D. A. Smith, (1982) *Phytoalexins*.

Jain, K. K., (2002) Application of laser capture microdissection to proteomics. *Laser Capture Microscopy and Microdissection* **356**: 157-167.

Jansen, C., D. von Wettstein, W. Schafer, K. H. Kogel, A. Felk & F. J. Maier, (2005) Infection patterns in barley and wheat spikes inoculated with wild-type and trichodiene synthase gene disrupted *Fusarium graminearum*. *Proceedings of the National Academy of Sciences of the United States of America* **102**: 16892-16897.

Jenczmionka, N. J. & W. Schafer, (2005) The Gpmk1 MAP kinase of *Fusarium graminearum* regulates the induction of specific secreted enzymes. *Current Genetics* **47**: 29-36.

Jennings, P., M. E. Coates, K. Walsh, J. A. Turner & P. Nicholson, (2004) Determination of deoxynivalenol- and nivalenol-producing chemotypes of *Fusarium graminearum* isolated from wheat crops in England and Wales. *Plant Pathology* **53**: 643-652.

Jiang, L., J. Yang, F. Fan, D. Zhang & X. Wang, (2010) The Type 2C protein phosphatase FgPtc1p of the plant fungal pathogen *Fusarium graminearum* is involved in lithium toxicity and virulence. *Molecular Plant Pathology* **11**: 277-282.

Jiang, W. D., D. Gerhold, E. B. Kmiec, M. Hauser, J. M. Becker & Y. Koltin, (1997) The topoisomerase I gene from *Candida albicans*. *Microbiology-Uk* **143**: 377-386.

Jiao, F., A. Kawakami & T. Nakajima, (2008) Effects of different carbon sources on trichothecene production and Tri gene expression by *Fusarium graminearum* in liquid culture. *Fems Microbiology Letters* **285**: 212-219.

Jochum, C. C., L. E. Osborne & G. Y. Yuen, (2006) Fusarium head blight biological control with Lysobacter enzymogenes. *Biological Control* **39**: 336-344.

Joffe, A. Z. & N. Lisker, (1969) Effects of light, temperature and pH value on aflatoxin production *in vitro*. *Applied Microbiology* **18**: 517-&.

Johnson, R., C. Voisey, L. Johnson, J. Pratt, D. Fleetwood, A. Khan & G. Bryan, (2007) Distribution of NRPS gene families within the Neotyphodium/Epichloe complex. *Fungal Genetics and Biology* **44**: 1180-1190.

Jones, J. D. G. & J. L. Dangl, (2006) The plant immune system. *Nature* **444**: 323-329.

Jonkers, W. & M. Rep, (2009) Mutation of *CRE1* in *Fusarium oxysporum* reverts the pathogenicity defects of the *FRP1* deletion mutant. *Molecular Microbiology* **74**: 1100-1113.

Josefsen, L., J. Svensson, S. Olsson & H. Giese, (2008) The role of autophagy in *Fusarium graminearum* during infection of cereals. In: 9th European Conference on Fungal Genetics. University of Edinburgh: Fungal Genetic Ltd, pp. 104.

Kale, S. D., B. A. Gu, D. G. S. Capelluto, D. L. Dou, E. Feldman, A. Rumore, F. D. Arredondo, R. Hanlon, I. Fudal, T. Rouxel, C. B. Lawrence, W. X. Shan & B. M. Tyler, (2010) External Lipid PI3P Mediates Entry of Eukaryotic Pathogen Effectors into Plant and Animal Host Cells. *Cell* **142**: 284-295.

Kämper, J., R. Kahmann, M. Boelker, L.-J. Ma, T. Brefort, B. J. Saville, F. Banuett, J. W. Kronstad, S. E. Gold, O. Mueller, M. H. Perlin, H. A. B. Woesten, R. de Vries, J. Ruiz-Herrera, C. G. Reynaga-Pena, K. Snetselaar, M. McCann, J.

Perez-Martin, M. Feldbruegge, C. W. Basse, G. Steinberg, J. I. Ibeas, W. Holloman, P. Guzman, M. Farman, J. E. Stajich, R. Sentandreu, J. M. Gonzalez-Prieto, J. C. Kennell, L. Molina, J. Schirawski, A. Mendoza-Mendoza, D. Greilinger, K. Muench, N. Roessel, M. Scherer, M. Vranes, O. Ladendorf, V. Vincon, U. Fuchs, B. Sandrock, S. Meng, E. C. H. Ho, M. J. Cahill, K. J. Boyce, J. Klose, S. J. Klosterman, H. J. Deelstra, L. Ortiz-Castellanos, W. Li, P. Sanchez-Alonso, P. H. Schreier, I. Haeuser-Hahn, M. Vaupel, E. Koopmann, G. Friedrich, H. Voss, T. Schlueter, J. Margolis, D. Platt, C. Swimmer, A. Gnirke, F. Chen, V. Vysotskaia, G. Mannhaupt, U. Gueldener, M. Muensterkoetter, D. Haase, M. Oesterheld, H.-W. Mewes, E. W. Mauceli, D. DeCaprio, C. M. Wade, J. Butler, S. Young, D. B. Jaffe, S. Calvo, C. Nusbaum, J. Galagan & B. W. Birren, (2006) Insights from the genome of the biotrophic fungal plant pathogen *Ustilago maydis*. *Nature* **444**: 97-101.

Kang, Z. & H. Buchenauer, (1999) Immunocytochemical localization of fusarium toxins in infected wheat spikes by *Fusarium culmorum*. *Physiological and Molecular Plant Pathology* **55**: 275-288.

Kang, Z. & H. Buchenauer, (2000a) Cytology and ultrastructure of the infection of wheat spikes by *Fusarium culmorum*. *Mycological Research* **104**: 1083-1093.

Kang, Z. & H. Buchenauer, (2000b) Ultrastructural and cytochemical studies on cellulose, xylan and pectin degradation in wheat spikes infected by *Fusarium culmorum*. *Journal of Phytopathology-Phytopathologische Zeitschrift* **148**: 263-275.

Kang, Z. & H. Buchenauer, (2000c) Ultrastructural and immunocytochemical investigation of pathogen development and host responses in resistant and susceptible wheat spikes infected by *Fusarium culmorum*. *Physiological and Molecular Plant Pathology* **57**: 255-268.

Kang, Z. S., H. Buchenauer, L. L. Huang, Q. M. Han & H. C. Zhang, (2008) Cytological and immunocytochemical studies on responses of wheat spikes of the resistant Chinese cv. Sumai 3 and the susceptible cv. Xiaoyan 22 to infection by *Fusarium graminearum*. *European Journal of Plant Pathology* **120**: 383-396.

Kang, Z. S., I. Zingen-Sell & H. Buchenauer, (2005) Infection of wheat spikes by *Fusarium avenaceum* and alterations of cell wall components in the infected tissue. *European Journal of Plant Pathology* **111**: 19-28.

Kankanala, P., K. Czymmek & B. Valent, (2007) Roles for rice membrane dynamics and plasmodesmata during biotrophic invasion by the blast fungus. *Plant Cell* **19**: 706-724.

Kema, G. H. J., D. Z. Yu, F. H. J. Rijkenberg, M. W. Shaw & R. P. Baayen, (1996) Histology of the pathogenesis of *Mycosphaerella graminicola* in wheat. *Phytopathology* **86**: 777-786.

Keon, J., J. Antoniw, R. Carzaniga, S. Deller, J. L. Ward, J. M. Baker, M. H. Beale, K. Hammond-Kosack & J. J. Rudd, (2007) Transcriptional adaptation of *Mycosphaerella graminicola* to programmed cell death (PCD) of its susceptible wheat host. *Molecular Plant-Microbe Interactions* **20**: 178-193.

Kerk, N. M., T. Ceserani, S. L. Tausta, I. M. Sussex & T. M. Nelson, (2003) Laser capture microdissection of cells from plant tissues. *Plant Physiology* **132**: 27-35.

Khan, N. I., D. A. Schisler, M. J. Boehm, P. J. Slininger & R. J. Bothast, (2001) Selection and evaluation of microorganisms for biocontrol of Fusarium head blight of wheat incited by Gibberella zeae. *Plant Disease* **85**: 1253-1258.

Khang, C. H., R. Berruyer, M. C. Giraldo, P. Kankanala, S. Y. Park, K. Czymmek, S. Kang & B. Valent, (2010) Translocation of *Magnaporthe oryzae* Effectors into Rice Cells and Their Subsequent Cell-to-Cell Movement. *Plant Cell* **22**: 1388-1403.

Khush, G. S., (2001) Green revolution: the way forward. *Nature Reviews Genetics* **2**: 815-822.

Kim, J., H. Lee, J. Lee, K. Kim, S. Yun, W. B. Shim & Y. Lee, (2009) *Gibberella zeae* chitin synthase genes, *GzCHS5* and *GzCHS7*, are required for hyphal growth, perithecia formation, and pathogenicity. *Current Genetics* **55**: 449-459.

Kim, J. E., K. Myong, W. B. Shim, S. H. Yun & Y. W. Lee, (2007) Functional characterization of acetylglutamate synthase and phosphoribosylamine-glycine ligase genes in *Gibberella zeae*. *Current Genetics* **51**: 99-108.

Kim, Y. T., Y. R. Lee, J. M. Jin, K. H. Han, H. Kim, J. C. Kim, T. Lee, S. H. Yun & Y. W. Lee, (2005) Two different polyketide synthase genes are required for synthesis of zearalenone in *Gibberella zeae*. *Molecular Microbiology* **58**: 1102-1113.

Kimura, M., H. Anzai & I. Yamaguchi, (2001) Microbial toxins in plant-pathogen interactions: Biosynthesis, resistance mechanisms, and significance. *Journal of General and Applied Microbiology* **47**: 149-160.

Kimura, M., I. Kaneko, M. Komiyama, A. Takatsuki, H. Koshino, K. Yoneyama & I. Yamaguchi, (1998) Trichothecene 3-O-acetyltransferase protects both the producing organism and transformed yeast from related mycotoxins - Cloning and characterization of *Tri101*. *Journal of Biological Chemistry* **273**: 1654-1661.

Kimura, M., T. Tokai, N. Takahashi-Ando, S. Ohsato & M. Fujimura, (2007) Molecular and genetic studies of *Fusarium* trichothecene biosynthesis: Pathways, genes, and evolution. *Bioscience Biotechnology and Biochemistry* **71**: 2105-2123.

Kloppholz, S., H. Kuhn & N. Requena, (2011) A Secreted Fungal Effector of *Glomus intraradices* Promotes Symbiotic Biotrophy. *Current Biology* **21**: 1204-1209.

Koltin, Y. & P. R. Day, (1976) Inheritance of killer phenotypes and double stranded RNA in *Ustilago maydis*. *Proceedings of the National Academy of Sciences of the United States of America* **73**: 594-598.

Kretschmer, M., M. Leroch, A. Mosbach, A.-S. Walker, S. Fillinger, D. Mernke, H.-J. Schoonbeek, J.-M. Pradier, P. Leroux, M. A. De Waard & M. Hahn, (2009) Fungicide-Driven Evolution and Molecular Basis of Multidrug Resistance in Field Populations of the Grey Mould Fungus *Botrytis cinerea*. *Plos Pathogens* **5**.

Kuchin, S., V. K. Vyas & M. Carlson, (2002) Snf1 protein kinase and the repressors Nrg1 and Nrg2 regulate FLO11, haploid invasive growth, and diploid pseudohyphal differentiation. *Molecular and Cellular Biology* **22**: 3994-4000.

Kwon, C. Y., J. B. Rasmussen & S. W. Meinhardt, (1998) Activity of Ptr ToxA from *Pyrenophora tritici-repentis* requires host metabolism. *Physiological and Molecular Plant Pathology* **52**: 201-212.

Laxman, S. & B. P. Tu, (2010) Systems approaches for the study of metabolic cycles in yeast. *Current Opinion in Genetics & Development* **20**: 599-604.

Lee, N., C. A. D'Souza & J. W. Kronstad, (2003) Of smuts, blasts, mildews, and blights: cAMP signaling in phytopathogenic fungi. *Annual Review of Phytopathology* **41**: 399-427.

Lee, S.-H., Y.-K. Han, S.-H. Yun & Y.-W. Lee, (2009a) Roles of the Glyoxylate and Methylcitrate Cycles in Sexual Development and Virulence in the Cereal Pathogen *Gibberella zeae*. *Eukaryotic Cell* **8**: 1155-1164.

Lee, S. H., J. Lee, S. Lee, E. H. Park, K. W. Kim, M. D. Kim, S. H. Yun & Y. W. Lee, (2009b) GzSNF1 Is Required for Normal Sexual and Asexual Development in the Ascomycete *Gibberella zeae*. *Eukaryotic Cell* **8**: 116-127.

Lee, T., Y. K. Han, K. H. Kim, S. H. Yun & Y. W. Lee, (2002) Tri13 and Tri7 determine deoxynivalenol- and nivalenol-producing chemotypes of *Gibberella zeae*. *Applied and Environmental Microbiology* **68**: 2148-2154.

Lee, T., D. W. Oh, H. S. Kim, J. Lee, Y. H. Kim, S. H. Yun & Y. W. Lee, (2001) Identification of deoxynivalenol- and nivalenol-producing chemotypes of *Gibberella zeae* by using PCR. *Applied and Environmental Microbiology* **67**: 2966-2972.

Lemmens, M., K. Haim, H. Lew & P. Ruckenbauer, (2004) The effect of nitrogen fertilization on Fusarium head blight development and deoxynivalenol contamination in wheat. *Journal of Phytopathology* **152**: 1-8.

Lengeler, K. B., R. C. Davidson, C. D'Souza, T. Harashima, W. C. Shen, P. Wang, X. W. Pan, M. Waugh & J. Heitman, (2000) Signal transduction cascades regulating fungal development and virulence. *Microbiology and Molecular Biology Reviews* **64**: 746.

Leonard, K. J. & W. R. e. Bushnell, (2003) *Fusarium head blight of wheat and barley*. The American phytopathology society, Minnesota, USA.

Leonard, K. J. & L. J. Szabo, (2005) Stem rust of small grains and grasses caused by Puccinia graminis. *Molecular Plant Pathology* **6**: 99-111.

Lequart, C., J. M. Nuzillard, B. Kurek & P. Debeire, (1999) Hydrolysis of wheat bran and straw by an endoxylanase: production and structural characterization of cinnamoyl-oligosaccharides. *Carbohydrate Research* **319**: 102-111.

Levdansky, E., J. Romano, Y. Shadkchan, H. Sharon, K. J. Verstrepen, G. R. Fink & N. Osherov, (2007) Coding tandem repeats generate diversity in *Aspegillus fumigatus* genes. *Eukaryotic Cell* **6**: 1380-1391.

Levin, D. E., (2005) Cell wall integrity signaling in *Saccharomyces cerevisiae*. *Microbiology and Molecular Biology Reviews* **69**: 262.

Li, G. L. & Y. Yen, (2008) Jasmonate and ethylene signaling pathway may mediate Fusarium head blight resistance in wheat. *Crop Science* **48**: 1888-1896.

Li, X., J. B. Zhang, B. Song, H. P. Li, H. Q. Xu, B. Qu, F. J. Dang & Y. C. Liao, (2010) Resistance to Fusarium Head Blight and Seedling Blight in Wheat Is Associated with Activation of a Cytochrome P450 Gene. *Phytopathology* **100**: 183-191.

Li, Y., C. Wang, W. Liu, G. Wang, Z. Kang, H. C. Kistler & J.-R. Xu, (2011) The HDF1 Histone Deacetylase Gene Is Important for Conidiation, Sexual Reproduction, and Pathogenesis in *Fusarium graminearum*. *Molecular Plant-Microbe Interactions* **24**: 487-496.

Lievens, B., P. M. Houterman & M. Rep, (2009) Effector gene screening allows unambiguous identification of *Fusarium oxysporum* f.sp *lycopersici* races and discriminationfrom other formae speciales. *Fems Microbiology Letters* **300**: 201-215.

Liggitt, J., P. Jenkinson & D. W. Parry, (1997) The role of saprophytic microflora in the development of Fusarium ear blight of winter wheat caused by *Fusarium culmorum*. *Crop Prot.* **16**: 679-685.

Liu, X.-H., J.-P. Lu, L. Zhang, B. Dong, H. Min & F.-C. Lin, (2007) Involvement of a *Magnaporthe grisea* serine/threonine kinase gene, *MgATG1*, in appressorium turgor and pathogenesis. *Eukaryotic Cell* **6**: 997-1005.

Liu, X., F. Yu, G. Schnabel, J. Wu, Z. Wang & Z. Ma, (2011) Paralogous *cyp51* genes in *Fusarium graminearum* mediate differential sensitivity to sterol demethylation inhibitors. *Fungal Genetics and Biology* **48**: 113-123.

Liu, Z., J. D. Faris, R. P. Oliver, K.-C. Tan, P. S. Solomon, M. C. McDonald, B. A. McDonald, A. Nunez, S. Lu, J. B. Rasmussen & T. L. Friesen, (2009) SnTox3 Acts in Effector Triggered Susceptibility to Induce Disease on Wheat Carrying the Snn3 Gene. *Plos Pathogens* **5**.

Liu, Z. Y., J. I. B. Bos, M. Armstrong, S. C. Whisson, L. da Cunha, T. Torto-Alalibo, J. Win, A. O. Avrova, F. Wright, P. R. J. Birch & S. Kamoun, (2005) Patterns of diversifying selection in the phytotoxin-like *scr74* gene family of *Phytophthora infestans*. *Molecular Biology and Evolution* **22**: 659-672.

Loman, N. J. & M. J. Pallen, (2008) XDR-TB genome sequencing: a glimpse of the microbiology of the future. *Future Microbiology* **3**: 111-113.

Long Nam, N., J. Bormann, L. Giang Thi Thu, C. Staerkel, S. Olsson, J. D. Nosanchuk, H. Giese & W. Schaefer, (2011) Autophagy-related lipase FgATG15 of *Fusarium graminearum* is important for lipid turnover and plant infection. *Fungal Genetics and Biology* **48**: 217-224.

Lotito, L., A. Russo, G. Chillemi, S. Bueno, D. Cavalieri & G. Capranico, (2008) Global transcription regulation by DNA topoisomerase I in exponentially growing *Saccharomyces cerevisiae* cells: Activation of telomere-proximal genes by *TOP1* deletion. *Journal of Molecular Biology* **377**: 311-322.

Lowe, R., M. Jubault, G. Canning, M. Urban & K. Hammond-Kosack, (2011) The induction of trichothecene mycotoxins by cereal-infecting *Fusarium* species *Methods in Molecular Biology*: In Press.

Lowe, R. G. T., J. W. Allwood, A. M. Galster, M. Urban, A. Daudi, G. Canning, J. L. Ward, M. H. Beale & K. E. Hammond-Kosack, (2010) A Combined (1)H Nuclear Magnetic Resonance and Electrospray Ionization-Mass Spectrometry Analysis to Understand the Basal Metabolism of Plant-Pathogenic *Fusarium spp*. *Mol Plant Microbe Interact* **23**: 1605-1618.

Lu, S. W., S. Kroken, B. N. Lee, B. Robbertse, A. C. L. Churchill, O. C. Yoder & B. G. Turgeon, (2003) A novel class of gene controlling virulence in plant pathogenic ascomycete fungi. *Proceedings of the National Academy of Sciences of the United States of America* **100**: 5980-5985.

Lutz, M. P., G. Feichtinger, G. Defago & B. Duffy, (2003) Mycotoxigenic Fusatium and deoxynivalenol production repress chitinase gene expression in the biocontrol agent *Trichoderma atroviride P1*. *Applied and Environmental Microbiology* **69**: 3077-3084.

Lysoe, E., S. S. Klemsdal, K. R. Bone, R. J. N. Frandsen, T. Johansen, U. Thrane & H. Giese, (2006) The *PKS4* gene of *Fusarium graminearum* is essential for zearalenone production. *Applied and Environmental Microbiology* **72**: 3924-3932.

Lysoe, E., M. Pasquali, A. Breakspear & H. C. Kistler, (2011a) The Transcription Factor FgStuAp Influences Spore Development, Pathogenicity, and Secondary Metabolism in *Fusarium graminearum*. *Molecular Plant-Microbe Interactions* **24**: 54-67.

Lysoe, E., K.-Y. Seong & H. C. Kistler, (2011b) The Transcriptome of *Fusarium graminearum* During the Infection of Wheat. *Molecular plant-microbe interactions : MPMI* **24**: 995-1000.

Ma, L. J., H. C. van der Does, K. A. Borkovich, J. J. Coleman, M. J. Daboussi, A. Di Pietro, M. Dufresne, M. Freitag, M. Grabherr, B. Henrissat, P. M. Houterman, S. Kang, W. B. Shim, C. Woloshuk, X. H. Xie, J. R. Xu, J. Antoniw, S. E. Baker, B. H. Bluhm, A. Breakspear, D. W. Brown, R. A. E. Butchko, S. Chapman, R. Coulson, P. M. Coutinho, E. G. J. Danchin, A. Diener, L. R. Gale, D. M. Gardiner, S. Goff, K. E. Hammond-Kosack, K. Hilburn, A. Hua-Van, W. Jonkers, K. Kazan, C. D. Kodira, M. Koehrsen, L. Kumar, Y. H. Lee, L. D. Li, J. M. Manners, D. Miranda-Saavedra, M. Mukherjee, G. Park, J. Park, S. Y. Park, R. H. Proctor, A. Regev, M. C. Ruiz-Roldan, D. Sain, S. Sakthikumar, S. Sykes, D. C. Schwartz, B. G. Turgeon, I. Wapinski, O. Yoder, S. Young, Q. D. Zeng, S. G. Zhou, J. Galagan, C. A. Cuomo, H. C. Kistler & M. Rep, (2010) Comparative genomics reveals mobile pathogenicity chromosomes in Fusarium. *Nature* **464**: 367-373.

Madgwick, J. W., J. S. West, R. P. White, M. A. Semenov, J. A. Townsend, J. A. Turner & B. D. L. Fitt, (2011) Impacts of climate change on wheat anthesis and fusarium ear blight in the UK. *European Journal of Plant Pathology* **130**: 117-131.

Magan, N. & D. Aldred, (2007) Post-harvest control strategies: Minimizing mycotoxins in the food chain. *International Journal of Food Microbiology* **119**: 131-139.

Magan, N., D. Aldred, K. Mylona & R. J. W. Lambert, (2010) Limiting mycotoxins in stored wheat. *Food Additives and Contaminants Part a-Chemistry Analysis Control Exposure & Risk Assessment* **27**: 644-650.

Maier, F. J., T. Miedaner, B. Hadeler, A. Felk, S. Salomon, M. Lemmens, H. Kassner & W. Schafer, (2006) Involvement of trichothecenes in fusarioses of wheat, barley and maize evaluated by gene disruption of the trichodiene synthase (Tri5) gene in three field isolates of different chemotype and virulence. *Molecular Plant Pathology* **7**: 449-461.

Maiorano, A., M. Blandino, A. Reyneri & F. Vanara, (2008) Effects of maize residues on the *Fusarium spp*. infection and deoxynivalenol (DON) contamination of wheat grain. *Crop Prot.* **27**: 182-188.

Makandar, R., V. Nalam, R. Chaturvedi, R. Jeannotte, A. A. Sparks & J. Shah, (2010) Involvement of Salicylate and Jasmonate Signaling Pathways in Arabidopsis Interaction with *Fusarium graminearum*. *Molecular Plant-Microbe Interactions* **23**: 861-870.

Marshall, R., A. Kombrink, J. Motteram, E. Loza-Reyes, J. Lucas, K. E. Hammond-Kosack, B. Thomma & J. J. Rudd, (2011) Analysis of Two in Planta Expressed LysM Effector Homologs from the Fungus *Mycosphaerella graminicola* Reveals Novel Functional Properties and Varying Contributions to Virulence on Wheat. *Plant Physiology* **156**: 756-769.

Martinez, A. T., M. Speranza, F. J. Ruiz-Duenas, P. Ferreira, S. Camarero, F. Guillen, M. J. Martinez, A. Gutierrez & J. C. del Rio, (2005) Biodegradation of lignocellulosics: microbial chemical, and enzymatic aspects of the fungal attack of lignin. *International Microbiology* **8**: 195-204.

MartinezPastor, M. T., G. Marchler, C. Schuller, A. MarchlerBauer, H. Ruis & F. Estruch, (1996) The *Saccharomyces cerevisiae* zinc finger proteins Msn2p and Msn4p are required for transcriptional induction through the stress-response element (STRE). *Embo Journal* **15**: 2227-2235.

Mathew, G. M., R. K. Sukumaran, R. R. Singhania & A. Pandey, (2008) Progress in research on fungal cellulases for lignocellulose degradation. *Journal of Scientific & Industrial Research* **67**: 898-907.

McClung, C. R. & R. A. Gutiérrez, (2010) Network news: prime time for systems biology of the plant circadian clock. *Current Opinion in Genetics & Development* **20**: 588-598.

McCormick, S. P. & N. J. Alexander, (2002) Fusarium Tri8 encodes a trichothecene C-3 esterase. *Applied and Environmental Microbiology* **68**: 2959-2964.

McCormick, S. P., N. J. Alexander, S. E. Trapp & T. M. Hohn, (1999) Disruption of *TRI101*, the gene encoding trichothecene 3-O-acetyltransferase, from *Fusarium sporotrichioides*. *Applied and Environmental Microbiology* **65**: 5252-5256.

McDonald, T., D. Brown, N. P. Keller & T. M. Hammond, (2005) RNA silencing of mycotoxin production in Aspergillus and Fusarium species. *Molecular Plant-Microbe Interactions* **18**: 539-545.

McMullen, M., R. Jones & D. Gallenberg, (1997) Scab of wheat and barley: A re-emerging disease of devastating impact. *Plant Disease* **81**: 1340-1348.

Melloy, P., G. Hollaway, J. Luck, R. Norton, E. Aitken & S. Chakraborty, (2010) Production and fitness of *Fusarium pseudograminearum* inoculum at elevated carbon dioxide in FACE. *Global Change Biology* **16**: 3363-3373.

Menard, R., A. A. Sultan, C. Cortes, R. Altszuler, M. R. vanDijk, C. J. Janse, A. P. Waters, R. S. Nussenzweig & V. Nussenzweig, (1997) Circumsporozoite protein is required for development of malaria sporozoites in mosquitoes. *Nature* **385**: 336-340.

Merhej, J., A. L. Boutigny, L. Pinson-Gadais, F. Richard-Forget & C. Barreau, (2010) Acidic pH as a determinant of TRI gene expression and trichothecene B biosynthesis in *Fusarium graminearum*. *Food Additives and Contaminants Part a-Chemistry Analysis Control Exposure & Risk Assessment* **27**: 710-717.

Merhej, J., F. Richard-Forget & C. Barreau, (2011) The pH regulatory factor PacC regulates Tri gene expression and trichothecene production in *Fusarium graminearum*. *Fungal Genetics and Biology* **48**: 275-284.

Mesterházy, A., (2003) Breeding wheat for Fusarium head blight resistance in Europe. In: Fusarium Head Blight of Wheat and Barley. K. J. Leonard & W. R. Bushnell (eds). St. Pauls, MN: APS Press, pp. 211-240.

Mesterhazy, A., T. Bartok, G. Kaszonyi, M. Varga, B. Toth & J. Varga, (2005) Common resistance to different *Fusarium spp*. causing Fusarium head blight in wheat. *European Journal of Plant Pathology* **112**: 267-281.

Michielse, C. B. & M. Rep, (2009) Pathogen profile update: *Fusarium oxysporum*. *Molecular Plant Pathology* **10**: 311-324.

Miedaner, T., C. J. R. Cumagun & S. Chakraborty, (2008) Population genetics of three important head blight pathogens *Fusarium graminearum, F-pseudograminearum* and *F-culmorum*. *Journal of Phytopathology* **156**: 129-139.

Miller, S. S., D. M. P. Chabot, T. Ouellet, L. J. Harris & G. Fedak, (2004) Use of a *Fusarium graminearum* strain transformed with green fluorescent protein to study infection in wheat (*Triticum aestivum*). *Canadian Journal of Plant Pathology-Revue Canadienne De Phytopathologie* **26**: 453-463.

Miller, S. S., L. M. Reid & L. J. Harris, (2007) Colonization of maize silks by *Fusarium graminearum*, the causative organism of gibberella ear rot. *Canadian Journal of Botany-Revue Canadienne De Botanique* **85**: 369-376.

Mosquera, G., M. C. Giraldo, C. H. Khang, S. Coughlan & B. Valent, (2009) Interaction transcriptome analysis identifies *Magnaporthe oryzae* BAS1-4 as biotrophy-associated secreted proteins in rice blast disease. *Plant Cell* **21**: 1273-1290.

Motteram, J., I. Kuefner, S. Deller, F. Brunner, K. E. Hammond-Kosack, T. Nuernberger & J. J. Rudd, (2009) Molecular Characterization and Functional Analysis of MgNLP, the Sole NPP1 Domain-Containing Protein, from the Fungal Wheat Leaf Pathogen *Mycosphaerella graminicola*. *Molecular Plant-Microbe Interactions* **22**: 790-799.

Muhitch, M. J., S. P. McCormick, N. J. Alexander & T. M. Hohn, (2000) Transgenic expression of the TRI101 or PDR5 gene increases resistance of tobacco to the phytotoxic effects of the trichothecene 4,15-diacetoxyscirpenol. *Plant Science* **157**: 201-207.

Muller, O., P. H. Schreier & J. F. Uhrig, (2008) Identification and characterization of secreted and pathogenesis-related proteins in *Ustilago maydis*. *Molecular Genetics and Genomics* **279**: 27-39.

Mussatto, S. I. & I. C. Roberto, (2006) Chemical characterization and liberation of pentose sugars from brewer's spent grain. *Journal of Chemical Technology and Biotechnology* **81**: 268-274.

Naef, A., T. Zesiger & G. Defago, (2006) Impact of transgenic Bt maize residues on the mycotoxigenic plant pathogen *Fusarium graminearum* and the biocontrol agent *Trichodearma atroviride*. *Journal of Environmental Quality* **35**: 1001-1009.

Nakashima, J., F. Chen, L. Jackson, G. Shadle & R. A. Dixon, (2008) Multi-site genetic modification of monolignol biosynthesis in alfalfa (*Medicago sativa*): effects on lignin composition in specific cell types. *New Phytologist* **179**: 738-750.

Nakazono, M., F. Qiu, L. A. Borsuk & P. S. Schnable, (2003) Laser-capture microdissection, a tool for the global analysis of gene expression in specific plant cell types: Identification of genes expressed differentially in epidermal cells or vascular tissues of maize. *Plant Cell* **15**: 583-596.

Nasmith, C. G., L. Wang, S. Walkowiak, Y. Gong, W. Leung, D. S. Guttman & G. Subramaniam, (2011) ChIP sequencing reveal dual role for the transcription regulator Tri6 in the phytopathogen *Fusarium graminearu*. In: 26th Fungal Genetics Conference. Asilomar, CA, USA, pp. 147.

Navarre, D. A. & T. J. Wolpert, (1999) Victorin induction of an apoptotic/senescence-like response in oats. *Plant Cell* **11**: 237-249.

Nelson, C., S. Goto, K. Lund, W. Hung & I. Sadowski, (2003) Srb10/Cdk8 regulates yeast filamentous growth by phosphorylating the transcription factor Ste12. *Nature* **421**: 187-190.

Nganje, W. E., D. D. Johnson, W. W. Wilson, F. L. Leistritz, D. A. Bangsund & N. M. Tiapo, (2001) Economic impacts of Fusarium Head Blight in wheat and barley: 1998-2000. *Agribusiness & Applied Economics Report - Department of Agribusiness and Applied Economics, North Dakota State University*: 49 pp.

Noda, T. & Y. Ohsumi, (1998) Tor, a phosphatidylinositol kinase homologue, controls autophagy in yeast. *Journal of Biological Chemistry* **273**: 3963-3966.

Nwaka, S. & H. Holzer, (1998) Molecular biology of trehalose and the trehalases in the yeast *Saccharomyces cerevisiae*. *Progress in Nucleic Acid Research and Molecular Biology, Vol 58* **58**: 197-237.

Nwaka, S., M. Kopp & H. Holzer, (1995) Expression and function of the Trehalase genes *NTH1* and *YBR0106* in *Saccharomyces cerevisiae*. *Journal of Biological Chemistry* **270**: 10193-10198.

O'Rourke, S. M. & I. Herskowitz, (2004) Unique and redundant roles for HOG MAPK pathway components as revealed by whole-genome expression analysis. *Molecular Biology of the Cell* **15**: 532-542.

O Croinin, T., R. K. Carroll, A. Kelly & C. J. Dorman, (2006) Roles for DNA supercoiling and the Fis protein in modulating expression of virulence genes during intracellular growth of *Salmonella enterica* serovar *Typhimurium*. *Molecular Microbiology* **62**: 869-882.

Ochiai, N., T. Tokai, T. Nishiuchi, N. Takahashi-Ando, M. Fujimura & M. Kimura, (2007) Involvement of the osmosensor histidine kinase and osmotic stress-activated protein kinases in the regulation of secondary metabolism in *Fusarium graminearum*. *Biochemical and Biophysical Research Communications* **363**: 639-644.

Ohsato, S., T. Ochiai-Fukuda, T. Nishiuchi, N. Takahashi-Ando, S. Koizumi, H. Hamamoto, T. Kudo, I. Yamaguchi & M. Kimura, (2007) Transgenic rice plants expressing trichothecene 3-O-acetyltransferase show resistance to the Fusarium phytotoxin deoxynivalenol. *Plant Cell Reports* **26**: 531-538.

Oide, S., W. Moeder, S. Krasnoff, D. Gibson, H. Haas, K. Yoshioka & B. G. Turgeon, (2006) NPS6, encoding a nonribosomal peptide synthetase involved in siderophore-mediated iron metabolism, is a conserved virulence determinant of plant pathogenic ascomycetes. *Plant Cell* **18**: 2836-2853.

Okubara, P. A., A. E. Blechl, S. P. McCormick, N. J. Alexander, R. Dill-Macky & T. M. Hohn, (2002) Engineering deoxynivalenol metabolism in wheat through the expression of a fungal trichothecene acetyltransferase gene. *Theoretical and Applied Genetics* **106**: 74-83.

Oliver, R. P., M. L. Farman, J. D. G. Jones & K. E. Hammond-Kosack, (1993) Use of fungal transformants expressing beta-glucuronidase activity to detect infection and measure hyphal biomass in infected plant tissue *Molecular Plant-Microbe Interactions* **6**: 521-525.

Oliver, R. P. & P. S. Solomon, (2010) New developments in pathogenicity and virulence of necrotrophs. *Current Opinion in Plant Biology* **13**: 415-419.

Orlova, M., E. Kanter, D. Krakovich & S. Kuchin, (2006) Nitrogen availability and TOR regulate the Snf1 protein kinase in *Saccharomyces cerevisiae*. *Eukaryotic Cell* **5**: 1831-1837.

Ospina-Giraldo, M. D., E. Mullins & S. Kang, (2003) Loss of function of the *Fusarium oxysporum SNF1* gene reduces virulence on cabbage and Arabidopsis. *Current Genetics* **44**: 49-57.

Pandelova, I., M. F. Betts, V. A. Manning, L. J. Wilhelm, T. C. Mockler & L. M. Ciuffetti, (2009) Analysis of Transcriptome Changes Induced by Ptr ToxA in Wheat Provides Insights into the Mechanisms of Plant Susceptibility. *Molecular Plant* **2**: 1067-1083.

Panstruga, R., (2003) Establishing compatibility between plants and obligate biotrophic pathogens. *Current Opinion in Plant Biology* **6**: 320-326.

Paper, J. M., J. S. Scott-Craig, N. D. Adhikari, C. A. Cuom & J. D. Walton, (2007) Comparative proteornics of extracellular proteins in vitro and in planta from the pathogenic fungus *Fusarium graminearum*. *Proteomics* **7**: 3171-3183.

Parawira, W. & M. Tekere, (2011) Biotechnological strategies to overcome inhibitors in lignocellulose hydrolysates for ethanol production: review. *Critical Reviews in Biotechnology* **31**: 20-31.

Parry, D. W., P. Jenkinson & L. McLeod, (1995) Fusarium ear blight (scab) in small grain cereals - a review. *Plant Pathology* **44**: 207-238.

Parry, M., C. Rosenzweig & M. Livermore, (2005) Climate change, and risk global food supply of hunger. *Philosophical Transactions of the Royal Society B-Biological Sciences* **360**: 2125-2138.

Paterson, R. R. M. & N. Lima, (2010) How will climate change affect mycotoxins in food? *Food Research International* **43**: 1902-1914.

Pazzagli, L., G. Cappugi, G. Manao, G. Camici, A. Santini & A. Scala, (1999) Purification, characterization, and amino acid sequence of cerato-platanin, a new phytotoxic protein from *Ceratocystis fimbriata* f. sp *platani*. *Journal of Biological Chemistry* **274**: 24959-24964.

Peng, J. R., D. E. Richards, N. M. Hartley, G. P. Murphy, K. M. Devos, J. E. Flintham, J. Beales, L. J. Fish, A. J. Worland, F. Pelica, D. Sudhakar, P. Christou, J. W. Snape, M. D. Gale & N. P. Harberd, (1999) 'Green revolution' genes encode mutant gibberellin response modulators. *Nature* **400**: 256-261.

Pennell, R. I. & C. Lamb, (1997) Programmed cell death in plants. *Plant Cell* **9**: 1157-1168.

Perez-Martin, J., S. Castillo-Lluva, C. Sgarlata, I. Flor-Parra, N. Mielnichuk, J. Torreblanca & N. Carbo, (2006) Pathocycles: *Ustilago maydis* as a model to study the relationships between cell cycle and virulence in pathogenic fungi. *Molecular Genetics and Genomics* **276**: 211-229.

Perez-Nadales, E. & A. Di Pietro, (2011) The Membrane Mucin Msb2 Regulates Invasive Growth and Plant Infection in Fusarium oxysporum. *Plant Cell* **23**: 1171-1185.

Pestka, J. J., (2007) Deoxynivalenol: Toxicity, mechanisms and animal health risks. *Animal Feed Science and Technology* **137**: 283-298.

Pestka, J. J., (2008) Mechanisms of deoxynivalenol-induced gene expression and apoptosis. *Food Additives and Contaminants Part a-Chemistry Analysis Control Exposure & Risk Assessment* **25**: 1128-1140.

Pestka, J. J., H. R. Zhou, Y. Moon & Y. J. Chung, (2004) Cellular and molecular mechanisms for immune modulation by deoxynivalenol and other trichothecenes: unraveling a paradox. *Toxicology Letters* **153**: 61-73.

Peters, J. C., A. K. Lees, D. W. Cullen, L. Sullivan, G. P. Stroud & A. C. Cunnington, (2008a) Characterization of *Fusarium spp*. responsible for causing dry rot of potato in Great Britain. *Plant Pathology* **57**: 262-271.

Peters, R. D., C. MacLeod, K. A. Seifert, R. A. Martin, L. R. Hale, C. R. Grau & S. MacInnis, (2008b) Pathogenicity to potato tubers of *Fusarium spp*. isolated from potato, cereal and forage crops. *American Journal of Potato Research* **85**: 367-374.

Phalip, V., F. Goubet, R. Carapito & J. M. Jeltsch, (2009) Plant Cell Wall Degradation with a Powerful *Fusarium graminearum* Enzymatic Arsenal. *Journal of Microbiology and Biotechnology* **19**: 573-581.

Ponte, E. M. d., J. M. C. Fernandes, C. R. Pierobom, G. C. Bergstrom & E. M. del Ponte, (2004) Fusarium head blight of wheat - epidemiological aspects and forecast models. *Fitopatologia Brasileira* **29**: 587-605.

Ponts, N., L. Couedelo, L. Pinson-Gadais, M. N. Verdal-Bonnin, C. Barreau & F. Richard-Forget, (2009) Fusarium response to oxidative stress by H2O2 is trichothecene chemotype-dependent. *Fems Microbiology Letters* **293**: 255-262.

Ponts, N., L. Pinson-Gadais, C. Barreau, F. Richard-Forget & T. Ouellet, (2007) Exogenous H2O2 and catalase treatments interfere with Tri genes expression in liquid cultures of *Fusarium graminearum*. *FEBS Letters* **581**: 443-447.

Portillo, M., K. Lindsey, S. Casson, G. Garcia-Casado, R. Solano, C. Fenoll & C. Escobar, (2009) Isolation of RNA from laser-capture-microdissected giant cells at early differentiation stages suitable for differential transcriptome analysis. *Molecular Plant Pathology* **10**: 523-535.

Pritsch, C., G. J. Muehlbauer, W. R. Bushnell, D. A. Somers & C. P. Vance, (2000) Fungal development and induction of defense response genes during early infection of wheat spikes by *Fusarium graminearum*. *Molecular Plant-Microbe Interactions* **13**: 159-169.

Proctor, R. H., T. M. Hohn & S. P. McCormick, (1995a) Reduced virulence of *Gibberella zeae* caused by disruption of a trichothecene toxin synthetic gene. *Molecular Plant-Microbe Interactions* **8**: 593-601.

Proctor, R. H., T. M. Hohn & S. P. McCormick, (1997) Restoration of wild-type virulence to Tri5 disruption mutants of Gibberella zeae via gene reversion and mutant complementation. *Microbiology-Uk* **143**: 2583-2591.

Proctor, R. H., T. M. Hohn, S. P. McCormick & A. E. Desjardins, (1995b) *TRI6* encodes an unusual zinc-finger protein involved in regulation of trichothecene biosynthesis in *Fusarium sporotrichioides*. *Applied and Environmental Microbiology* **61**: 1923-1930.

Pugh, G. W., (1933) Factors affecting infection of wheat heads by *Gibberella saubinetii*. *Journal of Agricultural Research* **46**: 771-797.

Qutob, D., S. Kamoun & M. Gijzen, (2002) Expression of a Phytophthora sojae necrosis-inducing protein occurs during transition from biotrophy to necrotrophy. *Plant Journal* **32**: 361-373.

Ramamoorthy, V., E. B. Cahoon, J. Li, M. Thokala, R. E. Minto & D. M. Shah, (2007a) Glucosylceramide synthase is essential for alfalfa defensin-mediated growth inhibition but not for pathogenicity of *Fusarium graminearum*. *Molecular Microbiology* **66**: 771-786.

Ramamoorthy, V., E. B. Cahoon, M. Thokala, J. Kaur, J. Li & D. M. Shah, (2009) Sphingolipid C-9 Methyltransferases Are Important for Growth and Virulence but Not for Sensitivity to Antifungal Plant Defensins in *Fusarium graminearum*. *Eukaryotic Cell* **8**: 217-229.

Ramamoorthy, V., X. H. Zhao, A. K. Snyder, J. R. Xu & D. M. Shah, (2007b) Two mitogen-activated protein kinase signalling cascades mediate basal resistance to antifungal plant defensins in *Fusarium graminearum*. *Cellular Microbiology* **9**: 1491-1506.

Ramirez, M. L., S. Chulze & N. Magan, (2006) Temperature and water activity effects on growth and temporal deoxynivalenol production by two Argentinean strains of *Fusarium graminearum* on irradiated wheat grain. *International Journal of Food Microbiology* **106**: 291-296.

Ramsay, K., M. G. K. Jones & Z. Wang, (2006) Laser capture microdissection: a novel approach to microanalysis of plant-microbe interactions. *Molecular Plant Pathology* **7**: 429-435.

Ramsay, K., Z. H. Wang & M. G. K. Jones, (2004) Using laser capture microdissection to study gene expression in early stages of giant cells induced by root-knot nematodes. *Molecular Plant Pathology* **5**: 587-592.

Rep, M. & H. C. Kistler, (2010) The genomic organization of plant pathogenicity in Fusarium species. *Current Opinion in Plant Biology* **13**: 420-426.

Reynolds, M. P. & N. E. Borlaug, (2006) Impacts of breeding on international collaborative wheat improvement. *J. Agric. Sci.* **144**: 3-17.

Ribichich, K. F., S. E. Lopez & A. C. Vegetti, (2000) Histopathological spikelet changes produced by *Fusarium graminearum* in susceptible and resistant wheat cultivars. *Plant Disease* **84**: 794-802.

Ridout, C. J., P. Skamnioti, O. Porritt, S. Sacristan, J. D. G. Jones & J. K. M. Brown, (2006) Multiple avirulence paralogues in cereal powdery mildew fungi may contribute to parasite fitness and defeat of plant resistance. *Plant Cell* **18**: 2402-2414.

Rispail, N., D. M. Soanes, C. Ant, R. Czajkowski, A. Grunler, R. Huguet, E. Perez-Nadales, A. Poli, E. Sartorel, V. Valiante, M. Yang, R. Beffa, A. A. Brakhage, N. A. R. Gow, R. Kahmann, M.-H. Lebrun, H. Lenasi, J. Perez-Martin, N. J. Talbot, J. Wendland & A. Di Pietro, (2009) Comparative genomics of MAP kinase and calcium-calcineurin signalling components in plant and human pathogenic fungi. *Fungal Genetics and Biology* **46**: 287-298.

Rittenour, W. & S. D. Harris, (2008) Characterisation of *Fusarium graminearum* Mes1 reveals roles in cell-surface organisation and virulence. *Fungal Genetics and Biology* **45**: 933-946.

Rittenour, W. R. & S. D. Harris, (2010) An *in vitro* method for the analysis of infection-related morphogenesis in *Fusarium graminearum*. *Molecular Plant Pathology* **11**: 361-369.

Rivera, V., J. Rengifo, M. Khan, D. M. Geiser, M. Mansfield & G. Secor, (2008) First Report of a Novel Fusarium Species Causing Yellowing Decline of Sugar Beet in Minnesota. *Plant Disease* **92**: 1589-1589.

Roberts, I. N., P. R. Oliver, P. J. Punt & C. A. M. J. J. van den Hondel, (1989) Expression of the *Escherichia coli* β-glucuronidase gene in industrial and phytopathogenic filamentous fungi. *Current Genetics* **15**: 177-180.

Rodriguez, R. J., J. Henson, E. Van Volkenburgh, M. Hoy, L. Wright, F. Beckwith, Y.-O. Kim & R. S. Redman, (2008) Stress tolerance in plants via habitat-adapted symbiosis. *Isme Journal* **2**: 404-416.

Rohde, J., J. Heitman & M. E. Cardenas, (2001) The TOR kinases link nutrient sensing to cell growth. *Journal of Biological Chemistry* **276**: 9583-9586.

Rokas, A., (2011) The birth, evolution and death of metabolic pathways in fungi. In: 26th Fungal Genetics Conference. Asilomar, USA, pp. 34.

Rolke, Y. & P. Tudzynski, (2008) The small GTPase Rac and the p21-activated kinase Cla4 in *Claviceps purpurea*: interaction and impact on polarity, development and pathogenicity. *Molecular Microbiology* **68**: 405-423.

Rollins, J. A., (2003) The *Sclerotinia sclerotiorum pac1* gene is required for sclerotial development and virulence. *Molecular Plant-Microbe Interactions* **16**: 785-795.

Rollins, J. A. & M. B. Dickman, (2001) PH signaling in *Sclerotinia sclerotiorum*: Identification of a pacC/RIM1 Homolog. *Applied and Environmental Microbiology* **67**: 75-81.

Rotter, B. A., D. B. Prelusky & J. J. Pestka, (1996) Toxicology of deoxynivalenol (vomitoxin). *Journal of Toxicology and Environmental Health* **48**: 1-34.

Roze, L. V., A. Chanda & J. E. Linz, (2011) Compartmentalization and molecular traffic in secondary metabolism: A new understanding of established cellular processes. *Fungal Genetics and Biology* **48**: 35-48.

Rudd, J. J., J. Antoniw, R. Marshall, J. Motteram, B. Fraaije & K. Hammond-Kosack, (2010) Identification and characterisation of *Mycosphaerella graminicola* secreted or surface-associated proteins with variable intragenic coding repeats. *Fungal Genetics and Biology* **47**: 19-32.

Rudd, J. J., J. Keon & K. E. Hammond-Kosack, (2008) The wheat mitogen-activated protein kinases TaMPK3 and TaMPK6 are differentially regulated at multiple levels during compatible disease interactions with *Mycosphaerella graminicola*. *Plant Physiology* **147**: 802-815.

Rupp, S., E. Summers, H. J. Lo, H. Madhani & G. Fink, (1999) MAP kinase and cAMP filamentation signaling pathways converge on the unusually large promoter of the yeast FLO11 gene. *Embo Journal* **18**: 1257-1269.
Ruzin, S. E., (1999) *Plant Microtechniques and Microscopy*. Oxford University Press, New York.
Sanchis, V. & N. Magan, (2004) *Environmental conditions affecting mycotoxins,* p. 174-189.
Santangelo, G. M., (2006) Glucose signaling in *Saccharomyces cerevisiae*. *Microbiology and Molecular Biology Reviews* **70**: 253.
Santos, M., J. J. Jimemez, B. Bartolome, C. Gomez-Cordoves & M. J. del Nozal, (2003) Variability of brewer's spent grain within a brewery. *Food Chemistry* **80**: 17-21.
Savard, M. E., R. C. Sinha, W. L. Seaman & G. Fedak, (2000) Sequential distribution of the mycotoxin deoxynivalenol in wheat spikes after inoculation with *Fusarium graminearum*. *Canadian Journal of Plant Pathology-Revue Canadienne De Phytopathologie* **22**: 280-285.
Schaafsma, A. W. & D. C. Hooker, (2007) Climatic models to predict occurrence of Fusarium toxins in wheat and maize. *International Journal of Food Microbiology* **119**: 116-125.
Schardl, C. L., (2001) Epichloe festucae and related mutualistic symbionts of grasses. *Fungal Genetics and Biology* **33**: 69-82.
Schneider, J. H. M. & P. M. S. Musters van Oorschot, (2008) Some characteristics of *Fusarium* species occurring in sugar beet in the Netherlands. *Journal of Plant Pathology* **90**: 88.
Schroeder, H. W. & J. J. Christensen, (1963) Factors affecting resistance of wheat to scab caused by *Gibberella zeae*. *Phytopathology* **53**: 831.
Schuller, H. J., (2003) Transcriptional control of nonfermentative metabolism in the yeast *Saccharomyces cerevisiae*. *Current Genetics* **43**: 139-160.
Schwarze, F. W. M. R., J. Engels & C. Mattheck, (2000) Fungal strategies of wood decay in trees. *Fungal strategies of wood decay in trees*: pp. xv + 185
Scott, B. & C. J. Eaton, (2008) Role of reactive oxygen species in fungal cellular differentiations. *Current Opinion in Microbiology* **11**: 488-493.
Secor, G. A. & B. Salas, (2001) Fusarium dry rot and Fusarium wilts. In: Compendium of Potato Disease. W. R. Stevenson (ed). St Paul, MN, USA: APS Press, pp. 43-53.
Segmueller, N., L. Kokkelink, S. Giesbert, D. Odinius, J. van Kan & P. Tudzynski, (2008) NADPH Oxidases are involved in differentiation and pathogenicity in *Botrytis cinerea*. *Molecular Plant-Microbe Interactions* **21**: 808-819.
Sels, J., J. Mathys, B. M. A. De Coninck, B. P. A. Cammue & M. F. C. De Bolle, (2008) Plant pathogenesis-related (PR) proteins: A focus on PR peptides. *Plant Physiology and Biochemistry* **46**: 941-950.
Seong, K.-Y., X. Zhao, J.-R. Xu, U. Gueldener & H. C. Kistler, (2008) Conidial germination in the filamentous fungus *Fusarium graminearum*. *Fungal Genetics and Biology* **45**: 389-399.
Seong, K., Z. M. Hou, M. Tracy, H. C. Kistler & J. R. Xu, (2005) Random insertional mutagenesis identifies genes associated with virulence in the wheat scab fungus *Fusarium graminearum*. *Phytopathology* **95**: 744-750.

Seong, K., L. Li, Z. M. Hou, M. Tracy, H. C. Kistler & J. R. Xu, (2006) Cryptic promoter activity in the coding region of the HMG-CoA rediactase gene in *Fusarium graminearum*. *Fungal Genetics and Biology* **43**: 34-41.

Seong, K. Y., M. Pasquali, X. Y. Zhou, J. Song, K. Hilburn, S. McCormick, Y. H. Dong, J. R. Xu & H. C. Kistler, (2009) Global gene regulation by Fusarium transcription factors Tri6 and Tri10 reveals adaptations for toxin biosynthesis. *Molecular Microbiology* **72**: 354-367.

Shifrin, V. I. & P. Anderson, (1999) Trichothecene mycotoxins trigger a ribotoxic stress response that activates c-Jun N-terminal kinase and p38 mitogen-activated protein kinase and induces apoptosis. *Journal of Biological Chemistry* **274**: 13985-13992.

Shim, W. B., U. S. Sagaram, Y. E. Choi, J. So, H. H. Wilkinson & Y. W. Lee, (2006) FSR1 is essential for virulence and female fertility in *Fusarium verticillioides* and *F-graminearum*. *Molecular Plant-Microbe Interactions* **19**: 725-733.

Shimizu, T., T. Nakano, D. Takamizawa, Y. Desaki, N. Ishii-Minami, Y. Nishizawa, E. Minami, K. Okada, H. Yamane, H. Kaku & N. Shibuya, (2010) Two LysM receptor molecules, CEBiP and OsCERK1, cooperatively regulate chitin elicitor signaling in rice. *Plant Journal* **64**: 204-214.

Simpson, D. R., G. E. Weston, J. A. Turner, P. Jennings & P. Nicholson, (2001) Differential control of head blight pathogens of wheat by fungicides and consequences for mycotoxin contamination of grain. *European Journal of Plant Pathology* **107**: 421-431.

Singh, R. P., D. P. Hodson, J. Huerta-Espino, Y. Jin, S. Bhavani, P. Njau, S. Herrera-Foessel, P. K. Singh, S. Singh & V. Govindan, (2011) The Emergence of Ug99 Races of the Stem Rust Fungus is a Threat to World Wheat Production. *Annual Review of Phytopathology* **49**: 465-481.

Skibbe, D. S., G. Doehlemann, J. Fernandes & V. Walbot, (2010) Maize Tumors Caused by *Ustilago maydis* Require Organ-Specific Genes in Host and Pathogen. *Science* **328**: 89-92.

Smith, A. M., G. Coupland, L. Dolan, N. P. Harberd, J. Jones, C. Martin, R. Sablowski & A. Amey, (2010) *Plant Biology*. Garland Science, New York, USA.

Soanes, D. M., T. A. Richards & N. J. Talbot, (2007) Insights from sequencing fungal and oomycete genomes: What can we learn about plant disease and the evolution of pathogenicity? *Plant Cell* **19**: 3318-3326.

Son, H., J. Lee, A. R. Park & Y.-W. Lee, (2011) ATP citrate lyase is required for normal sexual and asexual development in *Gibberella zeae*. *Fungal Genetics and Biology* **48**: 408-417.

Spanu, P. D., J. C. Abbott, J. Amselem, T. A. Burgis, D. M. Soanes, K. Stuber, E. V. L. van Themaat, J. K. M. Brown, S. A. Butcher, S. J. Gurr, M. H. Lebrun, C. J. Ridout, P. Schulze-Lefert, N. J. Talbot, N. Ahmadinejad, C. Ametz, G. R. Barton, M. Benjdia, P. Bidzinski, L. V. Bindschedler, M. Both, M. T. Brewer, L. Cadle-Davidson, M. M. Cadle-Davidson, J. Collemare, R. Cramer, O. Frenkel, D. Godfrey, J. Harriman, C. Hoede, B. C. King, S. Klages, J. Kleemann, D. Knoll, P. S. Koti, J. Kreplak, F. J. Lopez-Ruiz, X. L. Lu, T. Maekawa, S. Mahanil, C. Micali, M. G. Milgroom, G. Montana, S. Noir, R. J. O'Connell, S. Oberhaensli, F. Parlange, C. Pedersen, H. Quesneville, R. Reinhardt, M. Rott, S. Sacristan, S. M. Schmidt, M. Schon, P. Skamnioti, H.

Sommer, A. Stephens, H. Takahara, H. Thordal-Christensen, M. Vigouroux, R. Wessling, T. Wicker & R. Panstruga, (2010) Genome Expansion and Gene Loss in Powdery Mildew Fungi Reveal Tradeoffs in Extreme Parasitism. *Science* **330**: 1543-1546.

Spoel, S. H., J. S. Johnson & X. Dong, (2007) Regulation of tradeoffs between plant defenses against pathogens with different lifestyles. *Proceedings of the National Academy of Sciences of the United States of America* **104**: 18842-18847.

Sproete, P. & A. A. Brakhage, (2007) The light-dependent regulator velvet A of *Aspergillus nidulans* acts as a repressor of the penicillin biosynthesis. *Archives of Microbiology* **188**: 69-79.

Srinivasachary, N. Gosman, A. Steed, J. Simmonds, M. Leverington-Waite, Y. Wang, J. Snape & P. Nicholson, (2008) Susceptibility to Fusarium head blight is associated with the *Rht-D1b* semi-dwarfing allele in wheat. *Theoretical and Applied Genetics* **116**: 1145-1153.

Stephens, A. E., D. M. Gardiner, R. G. White, A. L. Munn & J. M. Manners, (2008) Phases of Infection and Gene Expression of *Fusarium graminearum* During Crown Rot Disease of Wheat. *Molecular Plant-Microbe Interactions* **21**: 1571-1581.

Stergiopoulos, I. & P. de Wit, (2009) Fungal Effector Proteins. *Annual Review of Phytopathology* **47**: 233-263.

Stergiopoulos, I., H. A. van den Burg, B. Okmen, H. G. Beenen, S. van Liere, G. H. J. Kema & P. de Wit, (2010) Tomato Cf resistance proteins mediate recognition of cognate homologous effectors from fungi pathogenic on dicots and monocots. *Proceedings of the National Academy of Sciences of the United States of America* **107**: 7610-7615.

Strange, R. N. & P. R. Scott, (2005) Plant disease: A threat to global food security. *Annual Review of Phytopathology* **43**: 83-116.

Strange, R. N., H. Smith & J. R. Majer, (1972) Choline, one of 2 fungal growth stimulants in anthers responsible for susceptibility of wheat to *Fusarium graminearum*. *Nature* **238**: 103-&.

Strauss, J., H. K. Horvath, B. M. Abdallah, J. Kindermann, R. L. Mach & C. P. Kubicek, (1999) The function of CreA, the carbon catabolite repressor of *Aspergillus nidulans*, is regulated at the transcriptional and post-transcriptional level. *Molecular Microbiology* **32**: 169-178.

Strauss, J. & Y. Reyes-Dominguez, (2011) Regulation of secondary metabolism by chromatin structure and epigenetic codes. *Fungal Genetics and Biology* **48**: 62-69.

Takahashi-Ando, N., M. Kimura, H. Kakeya, H. Osada & I. Yamaguchi, (2002) A novel lactonohydrolase responsible for the detoxification of zearalenone: enzyme purification and gene cloning. *Biochemical Journal* **365**: 1-6.

Takahashi-Ando, N., S. Ohsato, T. Shibata, H. Hamamoto, I. Yamaguchi & M. Kimura, (2004) Metabolism of zearalenone by genetically modified organisms expressing the detoxification gene from *Clonostachys rosea*. *Applied and Environmental Microbiology* **70**: 3239-3245.

Takano, Y., T. Kikuchi, Y. Kubo, J. E. Hamer, K. Mise & I. Furusawa, (2000) The *Colletotrichum lagenarium* MAP kinase gene *CMK1* regulates diverse aspects of fungal pathogenesis. *Molecular Plant-Microbe Interactions* **13**: 374-383.

Takemoto, D., A. Tanaka & B. Scott, (2006) A p67(Phox)-like regulator is recruited to control hyphal branching in a fungal-grass mutualistic symbiosis. *Plant Cell* **18**: 2807-2821.

Tan, K. C., R. P. Oliver, P. S. Solomon & C. S. Moffat, (2010) Proteinaceous necrotrophic effectors in fungal virulence. *Functional Plant Biology* **37**: 907-912.

Tanaka, A., M. J. Christensen, D. Takemoto, P. Park & B. Scott, (2006) Reactive oxygen species play a role in regulating a fungus-perennial ryegrass mutualistic interaction. *Plant Cell* **18**: 1052-1066.

Tanaka, A., D. Takemoto, G.-S. Hyon, P. Park & B. Scott, (2008) NoxA activation by the small GTPase RacA is required to maintain a mutualistic symbiotic association between *Epichloe festucae* and perennial ryegrass. *Molecular Microbiology* **68**: 1165-1178.

Tang, W. H., S. Coughlan, E. Crane, M. Beatty & J. Duvick, (2006) The application of laser microdissection to in planta gene expression profiling of the maize anthracnose stalk rot fungus *Colletotrichum graminicola*. *Molecular Plant-Microbe Interactions* **19**: 1240-1250.

Teter, S. A., K. P. Eggerton, S. V. Scott, J. Kim, A. M. Fischer & D. J. Klionsky, (2001) Degradation of lipid vesicles in the yeast vacuole requires function of Cvt17, a putative lipase. *Journal of Biological Chemistry* **276**: 2083-2087.

Thuvander, A., C. Wikman & I. Gadhasson, (1999) In vitro exposure of human lymphocytes to trichothecenes: Individual variation in sensitivity and effects of combined exposure on lymphocyte function. *Food and Chemical Toxicology* **37**: 639-648.

Tokai, T., H. Koshino, N. Takahashi-Ando, M. Sato, M. Fujimura & M. Kimura, (2007) Fusarium Tri4 encodes a key multifunctional cytochrome P450 monooxygenase for four consecutive oxygenation steps in trichothecene biosynthesis. *Biochemical and Biophysical Research Communications* **353**: 412-417.

Tonukari, N. J., J. S. Scott-Craig & J. D. Walton, (2000) The *Cochliobolus carbonum SNF1* gene is required for cell wall-degrading enzyme expression and virulence on maize. *Plant Cell* **12**: 237-247.

Trail, F., (2009) For blighted waves of grain: *Fusarium graminearum* in the postgenomics era. *Plant Physiology* **149**: 103-110.

Tremblay, A., S. Li, B. E. Scheffler & B. F. Matthews, (2009) Laser capture microdissection and expressed sequence tag analysis of uredinia formed by *Phakopsora pachyrhizi*, the causal agent of Asian soybean rust. *Physiological and Molecular Plant Pathology* **73**: 163-174.

Tu, D. S., (1950) Factors affecting the reaction of wheat varieties to head blight infection caused by *Gibberella zeae*. Ph.D. dissertation. Ohio State University, Ohio

Tyler, B. M., (2009) Entering and breaking: virulence effector proteins of oomycete plant pathogens. *Cellular Microbiology* **11**: 13-20.

Tyler, B. M., S. D. Kale, V. Antignani, J. Vega-Arreguin, R. Andreson, B. Gu, D. G. S. Capelluto, D. Dou, E. Feldman, A. Rumore, F. D. Arredondo, R. Hanlon, J. Plett, R. Aggarwal, I. Fudal, T. Rouxel, F. Martin, J. J. Stuart, J. McDowell & C. B. Lawrence, (2011) How oomycete and fungal effectors enter plant and animal cells. In: 26th Fungal Genetics Conference. Asilomar, CA, USA, pp. 41.

Tyler, B. M., S. Tripathy, X. Zhang, P. Dehal, R. H. Y. Jiang, A. Aerts, F. D. Arredondo, L. Baxter, D. Bensasson, J. L. Beynon, J. Chapman, C. M. B. Damasceno, A. E. Dorrance, D. Dou, A. W. Dickerman, I. L. Dubchak, M. Garbelotto, M. Gijzen, S. G. Gordon, F. Govers, N. J. Grunwald, W. Huang, K. L. Ivors, R. W. Jones, S. Kamoun, K. Krampis, K. H. Lamour, M.-K. Lee, W. H. McDonald, M. Medina, H. J. G. Meijer, E. K. Nordberg, D. J. Maclean, M. D. Ospina-Giraldo, P. F. Morris, V. Phuntumart, N. H. Putnam, S. Rash, J. K. C. Rose, Y. Sakihama, A. A. Salamov, A. Savidor, C. F. Scheuring, B. M. Smith, B. W. S. Sobral, A. Terry, T. A. Torto-Alalibo, J. Win, Z. Xu, H. Zhang, I. V. Grigoriev, D. S. Rokhsar & J. L. Boore, (2006) Phytophthora genome sequences uncover evolutionary origins and mechanisms of pathogenesis. *Science* **313**: 1261-1266.

Ueno, Y., (1984) Toxicological features of T-2 toxin and related trichothecenes. *Fundamental and Applied Toxicology* **4**: S124-S132.

Ullstrup, A. J., (1972) Impacts of southern corn leaf blight epidermics of 1970-1971. *Annual Review of Phytopathology* **10**: 37.

Urban, J., A. Soulard, A. Huber, S. Lippman, D. Mukhopadhyay, O. Deloche, V. Wanke, D. Anrather, G. Ammerer, H. Riezman, J. R. Broach, C. De Virgilio, M. N. Hall & R. Loewith, (2007) Sch9 is a major target of TORC1 in *Saccharomyces cerevisiae*. *Molecular Cell* **26**: 663-674.

Urban, M., S. Daniels, E. Mott & K. Hammond-Kosack, (2002) Arabidopsis is susceptible to the cereal ear blight fungal pathogens *Fusarium graminearum* and *Fusarium culmorum*. *Plant Journal* **32**: 961-973.

Urban, M., E. Mott, T. Farley & K. Hammond-Kosack, (2003) The *Fusarium graminearum MAP1* gene is essential for pathogenicity and development of perithecia. *Molecular Plant Pathology* **4**: 347-359.

Valent, B. & C. H. Khang, (2010) Recent advances in rice blast effector research. *Current Opinion in Plant Biology* **13**: 434-441.

Van der Hoorn, R. A. L., R. Roth & P. J. G. De Wit, (2001) Identification of distinct specificity determinants in resistance protein Cf-4 allows construction of a Cf-9 mutant that confers recognition of avirulence protein AVR4. *Plant Cell* **13**: 273-285.

van Esse, H. P., M. D. Bolton, L. Stergiopoulos, P. de Wit & B. Thomma, (2007) The chitin-binding *Cladosporium fulvum* effector protein Avr4 is a virulence factor. *Molecular Plant-Microbe Interactions* **20**: 1092-1101.

Veneault-Fourrey, C., M. Barooah, M. Egan, G. Wakley & N. J. Talbot, (2006) Autophagic fungal cell death is necessary for infection by the rice blast fungus. *Science* **312**: 580-583.

Verstrepen, K. J., A. Jansen, F. Lewitter & G. R. Fink, (2005) Intragenic tandem repeats generate functional variability. *Nature Genetics* **37**: 986-990.

Vincent, O., R. Townley, S. Kuchin & M. Carlson, (2001) Subcellular localization of the Snf1 kinase is regulated by specific beta subunits and a novel glucose signaling mechanism. *Genes & Development* **15**: 1104-1114.

Vinck, A., M. Terlou, W. R. Pestman, E. P. Martens, A. F. Ram, C. van den Hondel & H. A. B. Wosten, (2005) Hyphal differentiation in the exploring mycelium of *Aspergillus niger*. *Molecular Microbiology* **58**: 693-699.

Voegele, R. T., C. Struck, M. Hahn & K. Mendgen, (2001) The role of haustoria in sugar supply during infection of broad bean by the rust fungus *Uromyces fabae*. *Proceedings of the National Academy of Sciences of the United States of America* **98**: 8133-8138.

Voigt, C., C. Goebel, R. Bobe, I. Feussner & W. Schaefer, (2011) Pathogen-caused release of linolenic acid suppresses plant defense by inhibition of callose synthesis in wheat. In: 26th Fungal Genetics Conference. Asilomar, CA, USA, pp. 237.

Voigt, C. A., W. Schafer & S. Salomon, (2005) A secreted lipase of *Fusarium graminearum* is a virulence factor required for infection of cereals. *Plant Journal* **42**: 364-375.

Voigt, C. A., B. von Scheidt, A. Gacser, H. Kassner, R. Lieberei, W. Schaefer & S. Salomon, (2007) Enhanced mycotoxin production of a lipase-deficient *Fusarium graminearum* mutant correlates to toxin-related gene expression. *European Journal of Plant Pathology* **117**: 1-12.

von Tiedemann, A., (1997) Evidence for a primary role of active oxygen species in induction of host cell death during infection of bean leaves with *Botrytis cinerea*. *Physiological and Molecular Plant Pathology* **50**: 151-166.

Vyas, V. K., S. Kuchin, C. D. Berkey & M. Carlson, (2003) Snf1 kinases with different beta-subunit isoforms play distinct roles in regulating haploid invasive growth. *Molecular and Cellular Biology* **23**: 1341-1348.

Waalwijk, C., P. Kastelein, I. de Vries, Z. Kerenyi, T. van der Lee, T. Hesselink, J. Kohl & G. Kema, (2003) Major changes in *Fusarium spp.* in wheat in the Netherlands. *European Journal of Plant Pathology* **109**: 743-754.

Wang, W., J. Y. Barnaby, Y. Tada, H. Li, M. Toer, D. Caldelari, D.-u. Lee, X.-D. Fu & X. Dong, (2011) Timing of plant immune responses by a central circadian regulator. *Nature* **470**: 110-U126.

Wanjiru, W. M., Z. S. Kang & H. Buchenauer, (2002) Importance of cell wall degrading enzymes produced by *Fusarium graminearum* during infection of wheat heads. *European Journal of Plant Pathology* **108**: 803-810.

Ward, T. J., R. M. Clear, A. P. Rooney, K. O'Donnell, D. Gaba, S. Patrick, D. E. Starkey, J. Gilbert, D. M. Geiser & T. W. Nowicki, (2008) An adaptive evolutionary shift in Fusarium head blight pathogen populations is driving the rapid spread of more toxigenic *Fusarium graminearum* in North America. *Fungal Genetics and Biology* **45**: 473-484.

Warmka, J., J. Hanneman, J. Lee, D. Amin & I. Ota, (2001) Ptc1, a type 2C Ser/Thr phosphatase, inactivates the HOG pathway by dephosphorylating the mitogen-activated protein kinase Hog1. *Molecular and Cellular Biology* **21**: 51-60.

Westfall, P. J., D. R. Ballon & J. Thorner, (2004) When the stress of your environment makes you go HOG wild. *Science* **306**: 1511-1512.

Whingwiri, E. E., J. Kuo & W. R. Stern, (1981) The vascular system in the rachis of a wheat ear. *Annals of Botany* **48**: 189-201.
Wiemann, P., D. W. Brown, K. Kleigrewe, J. W. Bok, N. P. Keller, H.-U. Humpf & B. Tudzynski, (2010) FfVel1 and FfLae1, components of a velvet-like complex in *Fusarium fujikuroi*, affect differentiation, secondary metabolism and virulence. *Molecular Microbiology* **77**: 972-994.
Wingfield, M. J., A. Hammerbacher, R. J. Ganley, E. T. Steenkamp, T. R. Gordon, B. D. Wingfield & T. A. Coutinho, (2008) Pitch canker caused by *Fusarium circinatum* - a growing threat to pine plantations and forests worldwide. *Australasian Plant Pathology* **37**: 319-334.
Wolpert, T. J., L. D. Dunkle & L. M. Ciuffetti, (2002) Host-selective toxins and avirulence determinants: What's in a name? *Annual Review of Phytopathology* **40**: 251.
Wong, P., M. Walter, W. Lee, G. Mannhaupt, M. Munsterkotter, H. W. Mewes, G. Adam & U. Guldener, (2011) FGDB: revisiting the genome annotation of the plant pathogen *Fusarium graminearum*. *Nucleic Acids Research* **39**: D637-D639.
Wu, F. & G. P. Munkvold, (2008) Mycotoxins in ethanol co-products: modeling economic impacts on the livestock industry and management strategies. *Journal of Agricultural and Food Chemistry* **56**: 3900-3911.
Xiros, C., E. Topakas, P. Katapodis & P. Christakopoulos, (2008) Hydrolysis and fermentation of brewer's spent grain by *Neurospora crassa*. *Bioresource Technology* **99**: 5427-5435.
Xu, J. R., (2000) MAP kinases in fungal pathogens. *Fungal Genetics and Biology* **31**: 137-152.
Xu, J. R. & J. E. Hamer, (1996) MAP kinase and cAMP signaling regulate infection structure formation and pathogenic growth in the rice blast fungus *Magnaporthe grisea*. *Genes & Development* **10**: 2696-2706.
Xu, Q., A. Singh & M. E. Himmel, (2009) Perspectives and new directions for the production of bioethanol using consolidated bioprocessing of lignocellulose. *Current Opinion in Biotechnology* **20**: 364-371.
Xu, X. M., P. Nicholson, M. A. Thomsett, D. Simpson, B. M. Cooke, F. M. Doohan, J. Brennan, S. Monaghan, A. Moretti, G. Mule, L. Homok, E. Beki, J. Tatnell, A. Ritieni & S. G. Edwards, (2008) Relationship between the fungal complex causing Fusarium head blight of wheat and environmental conditions. *Phytopathology* **98**: 69-78.
Xue, C. Y., G. Park, W. B. Choi, L. Zheng, R. A. Dean & J. R. Xu, (2002) Two novel fungal virulence genes specifically expressed in appressoria of the rice blast fungus. *Plant Cell* **14**: 2107-2119.
Yager, L. N., (1992) Early developmental events during asexual and sexual sporulation in *Aspergillus nidulans*. *Biotechnology (Reading, Mass.)* **23**: 19-41.
Yazar, S. & G. Z. Omurtag, (2008) Fumonisins, Trichothecenes and Zearalenone in Cereals. *Int. J. Mol. Sci.* **9**: 2062-2090.
Ye, F., T. Brauer, E. Niehus, K. Drlica, C. Josenhans & S. Suerbaum, (2007) Flagellar and global gene regulation in *Helicobacter pylori* modulated by changes in DNA supercoiling. *International Journal of Medical Microbiology* **297**: 65-81.

Yorimitsu, T., S. Zaman, J. R. Broach & D. J. Klionsky, (2007) Protein kinase A and Sch9 cooperatively regulate induction of autophagy in *Saccharomyces cerevisiae*. *Molecular Biology of the Cell* **18**: 4180-4189.

Yu, H. Y., J. A. Seo, J. E. Kim, K. H. Han, W. B. Shim, S. H. Yun & Y. W. Lee, (2008) Functional analyses of heterotrimeric G protein G alpha and G beta subunits in Gibberella zeae. *Microbiology-Sgm* **154**: 392-401.

Yuen, G. Y. & S. D. Schoneweis, (2007) Strategies for managing Fusarium head blight and deoxynivalenol accumulation in wheat. *International Journal of Food Microbiology* **119**: 126-130.

Zahringer, H., M. Burgert, H. Holzer & S. Nwaka, (1997) Neutral trehalase Nth1p of *Saccharomyces cerevisiae* encoded by the *NTH1* gene is a multiple stress responsive protein. *Febs Letters* **412**: 615-620.

Zhang, D., F. Fan, J. Yang, X. Wang, D. Qiu & L. Jiang, (2010) FgTep1p is linked to the phosphatidylinositol-3 kinase signalling pathway and plays a role in the virulence of *Fusarium graminearum* on wheat. *Molecular Plant Pathology* **11**: 495-502.

Zheng, L., M. Campbell, J. Murphy, S. Lam & J. R. Xu, (2000) The *BMP1* gene is essential for pathogenicity in the gray mold fungus *Botrytis cinerea*. *Molecular Plant-Microbe Interactions* **13**: 724-732.

Zhou, X., C. Heyer, Y.-E. Choi, R. Mehrabi & J.-R. Xu, (2010) The *CID1* cyclin C-like gene is important for plant infection in *Fusarium graminearum*. *Fungal Genetics and Biology* **47**: 143-151.

Chapter 11. Appendices

Appendix 1 All the published single gene deletion strains of *F. graminearum* that demonstrated reduced pathogenicity or showed a loss of pathogenicity (marked *) on the ear of a susceptible wheat variety. All reference may be found in the PHI-base database via gene name or FG locus ID.

Gene	**FG3 locus**	**Host organism**	**Putative function (BROAD/MIPS)**	**MIPS functional characterisation**	**Hypothesised cellular location of gene products**	**Genes unique to *Fusarium spp.***	**Reference**
ACL1	FGSG_ 06039	Wheat	Hypothetical protein similar to ATP-citrat-lyase (3409 nt) / Probable ATP citrate lyase subunit 2	1	Mitochondria	No	(Son *et al.*, 2011)
ACL2	FGSG_ 12857	Wheat	ATP-citrate synthase subunit 1 (2283 nt)/ Probable ATP citrate lyase subunit 1	1	Mitochondria	No	(Son *et al.*, 2011)
ADE5	FGSG_ 02506	Barley	Phosphoribosylformylglycinamidine cyclo-ligase (2394 nt) / Bifunctional purine biosynthetic protein	1	Cytoplasm (ADE5)	No	(Kim *et al.*, 2007)
ARG2	FGSG_ 01939	Barley	Conserved hypothetical protein (2058 nt) / Amino-acid N-acetyltransferase	1	Mitochondrial matrix (ARG2)	No	(Kim *et al.*, 2007)
ATG8	FGSG_ 10740	Barley / Wheat	Hypothetical protein similar to E-117 protein (993 nt) / Autophagy protein AUT7	14, 16, 18, 20, 40	Not secreted	No	(Josefsen *et al.*, 2008)
CBL1	FGSG_ 01932	Maize / Wheat	Cystathionine beta-lyase (1391 nt)	1, 16	Cytoplasm (YHR112C)	No	(Seong *et al.*, 2005)

CID1	FGSG_ 04355	Wheat / Maize	Hypothetical protein similar to cyclin) (1363 nt) / Related to cyclin homolog UME3	1,10,11,18	Nucleus	No	(Zhou *et al.*, 2010)
CHS5	FGSG_ 01964	Barley	Hypothetical protein similar to class V chitin synthase (5703 nt) / Probable chitin synthase	1,42	Cytoplasm	No	(Kim *et al.*, 2009)
CHS7	FGSG_ 12039	Barley	Chitin synthase 6 (5305 nt) / Probable chitin synthase	1	Cytoplasm	No	(Kim *et al.*, 2009)
CCH1	FGSG_ 01364	Wheat	Conserved hypothetical protein (6528 nt) / Related to voltage gated Ca2+ channel	20, 34	Plasma membrane	No	(Hallen & Trail, 2008)
FBP1	FGSG_ 02095	Barley	Hypothetical protein similar to GRR1 protein (2375 nt)	1, 10	Cell bud neck contractile ring, cytoplasm, nucleus, SCF ubiquitin lgase complex (GRR1)	No	(Han *et al.*, 2007)
FCV1	FGSG_ 09907	Wheat	Conserved hypothetical protein (649 nt) / Conserved hypothetical protein	?	?	Yes	A. Beacham, RRes, UK, Unpublished
FGL1	FGSG_ 05906	Maize / Wheat	Hypothetical protein similar to extracellular lipase (1268 nt) / Triacylglycerol lipase precursor	1, 32	Secreted	Yes	(Voigt *et al.*, 2005)
FSR1	FGSG_ 01665	Barley	Striatin Pro11 (2581 nt) / Signal transduction scaffold protein, essential for virulence and fertility	30	Plasma membrane, cytoplasm	No	(Shim *et al.*, 2006)
GCS1	FGSG_ 05955	Maize / Wheat	Hypothetical protein similar to ceramide glucosyltransferase (1639 nt)	32	Secreted	No	(Ramamoorthy *et al.*, 2007a)

GzCPS1	FGSG_ 06631	Wheat	Conserved hypothetical protein (5808 nt) / Acyl CoA ligase-like protein	99	Not secreted	No	(Lu *et al.*, 2003)
GzGPA2	FGSG_ 09614	Barley	Guanine nucleotide-binding protein alpha-3 subunit (1354 nt) / G protein alpha subunit GNA-3	16, 30, 34, 40, 43	Plasma membrane, mitochondrion (GPA2)	No	(Yu *et al.*, 2008)
GzGPB1	FGSG_ 04104	Barley	Guanine nucleotide-binding protein subunit beta (2276 nt)	16, 30	Plasma membrane	No	(Yu *et al.*, 2008)
GzMetE	FGSG_ 05658	Wheat	Putative homoserine O-acetyltransferase (1668 nt)	1	Cytoplasm (MET2)	No	(Han *et al.*, 2004)
HDF1	FGSG_ 01353	Wheat / Maize	Histone deacetylase phd1 (1509 nt) / Probable histone deacetylase HosA	1,10,11,14,16,34, 40,42,43	Nucleus	No	(Li et al., 2011)
HDF2	FGSG_ 04324	Wheat / Maize	Histone deacetylase (2410 nt) / Related to histone deacetylase A	10,11,14,40	Nucleus	No	(Li et al., 2011)
HMR1	XP3893 73	Wheat	HMG-CoA reductase gene, mevalonate pathway	-	Endoplasmic reticulum membrane, mitochondrial matrix, nuclear envelope (HMG1)	No	(Seong et al., 2006)
ICL1 / MCL1	FGSG_ 09896 / 00176	Barley / Maize	Isocitrate lyase (2221 nt) / Probable isocitrate lyase (acu-3) : Isocitrate lyase (1926 nt) / Probable isocitrate lyase	1,2	Cytoplasm / Mitochondria	No	(Lee *et al.*, 2009a)
MAP1 (GPMK1)*	FGSG_ 06385	Arabidop sis / Tomato / Wheat	Pathogenicity mitogen-activated protein kinase 1 (1712 nt)	1, 10, 11, 14, 16, 18, 30, 32, 34	Nucleus (KSS1)	No	(Urban *et al.*, 2003)

MES1	FGSG_ 06680	Wheat	Hypothetical protein similar to MesA (2759 nt)	99	Not secreted	No	(Rittenour & Harris, 2008)
MGV1	FGSG_ 10313	Tomato / Wheat	Mitogen-activated protein kinase Spm1 (2100 nt)	1, 10, 14, 30, 32, 34, 40, 42, 43	Cytoplasm, Nucleus (SPM1)	No	(Hou *et al.*, 2002)
MT2	FGSG_ 05593	Wheat	Hypothetical protein similar to cyclopropane-fatty-acyl-phospholipid synthase (2084 nt) / Related to cyclopropane-fatty-acyl-phospholipid synthase	1	Membrane		(Ramamoorthy *et al.*, 2009)
MYS1	FGSG_ 10825	Maize / Wheat	5-methyltetrahydropteroyltriglutamate-homocysteine methyltransferase (2975 nt) / Methionine synthase	1, 14	Cytoplasm (MET6)	No	(Seong *et al.*, 2005)
NOS1	FGSG_ 00376	Maize / Wheat	NADH dehydrogenase iron-sulfur protein 2, mitochondrial precursor (2786 nt) / NADH dehydrogenase (ubiquinone) 49K chain	1, 2, 20	Mitochondrion	No	(Seong *et al.*, 2005)
NPS6	Unknown	Wheat	Nonribosomal peptide synthetase involved in sideophore-mediated iron metabolism	1, 2, 20	-	-	(Oide *et al.*, 2006)
NTH1	FGSG_ 09895	Wheat	Neutral trehalase, alpha,alpha-trehalose glucohydrolase (3117 nt)	1, 2, 32	Cytosol, cytoplasm (NTH1)	No	Unpublished
Os-2 (HOG1)	FGSG_ 09612	Wheat	Mitogen-activated protein kinase sty1 (2374 nt) / Osmotic sensitive-2 protein (putative mitogen-activated protein (MAP) kinase homolog)	1, 10, 11, 14, 16, 18, 30, 32, 34, 40, 42, 43	Cytoplasm, nucleus (HOG1)	No	(Ochiai *et al.*, 2007, Ramamoorthy *et al.*, 2007b)
PACC	FGSG_ 12970	Wheat	pH-response transcription factor pacC/RIM101 (2600 nt) / Related to pacC - transcription factor	11,16,34	Nucleus	No	(Merhej *et al.*, 2011)

PKAR	FGSG_ 09908	Wheat	cAMP-dependent protein kinase regulatory subunit (1666 nt) / Probable camp-dependent protein kinase regulatory chain (mcb)	1,11,14,16,18,20, 30,32,40,42,43,	Cytoplasm	No	A. Beacham, RRes, UK Unpublished
PTC1	FGSG_ 04111	Wheat	Hypothetical protein similar to protein phosphatase 2C (1781 nt) / Related to phosphoprotein phosphatase 2C	14,32	Cytoplasm, Nucleus	No	(Jiang *et al.*, 2010)
RAS2	FGSG_ 10114	Maize / Wheat	Ras-2 protein (786 nt)	1, 10, 12, 14, 16, 18, 20, 30, 32, 34, 40, 42, 43	Plasma membrane	No	(Bluhm *et al.*, 2007)
SID1	FGSG_ 05371	Wheat	Hypothetical protein similar to ornithine-N5-oxygenase (2312 nt) / Related to L-ornithine N5-hydroxylase	1	Not secreted	No	(Greenshields *et al.*, 2007)
SNF1	FGSG_ 09897	Barley / Wheat	Carbon catabolite derepressing protein kinase (2304 nt) / Serine/threonine protein kinase (SNF1)	1, 14, 16, 18, 30, 32, 34, 40, 43	Cytoplasm, fungal-type vacuole, nuclear envelope lumen, nucleus, mitochondrion (SNF1)	No	M. Urban, RRes, unpublished
STE7*	FGSG_ 09903	Tomato / Wheat	Protein kinase byr1 (1710 nt) / MAP kinase kinase	14, 30, 43	Cytoplasm (STE7)	No	(Ramamoorthy *et al.*, 2007b)
STE11*	FGSG_ 05484	Tomato / Wheat	Hypothetical protein similar to MAPKK kinase (2777 nt)	1, 14, 30, 32, 34, 43	Cytoplasm (STE11)	No	(Ramamoorthy *et al.*, 2007b)
STUA	FGSG_ 10129	Wheat	Hypothetical protein similar to transcription factor involved in conidiation (2550 nt) / Related to ascospore maturation 1 protein (Asm-1)	10,11,43	Nucleus	No	(Lysoe *et al.*, 2011a)

SYN1	FGSG_ 00950	Barley	Conserved hypothetical protein (1958 nt) / Related to putative snare protein syn	20,40,43	Membrane	No	(Hong *et al.*, 2010)
SYN2	FGSG_ 09928	Barley	Hypothetical protein similar to SSOI (1695 nt) / Related to putative snare protein syn	20,40,42,43	Membrane	No	(Hong *et al.*, 2010)
TBL1	FGSG_ 00332	Maize / Wheat	Conserved hypothetical protein (2377 nt) / Related to nuclear receptor co-repressor / HDAC3 complex subunit TBLR1	99	Not secreted	-	(Seong *et al.*, 2005)
TEP1	FGSG_ 04982	Wheat	Hypothetical protein similar to phosphoinositide 3-phosphate phosphatase (1747 nt) / Related to protein-tyrosine phosphatase	14,30	Cytoplasm	No	(Zhang *et al.*, 2010)
TOP1	FGSG_ 06874	Wheat	Hypothetical protein similar to DNA topoisomerase I (3124 nt)	10, 11	Nucleolus, nucleus	No	Unpublished
TRI5	FGSG_ 03537	Rye / Wheat	Trichodiene synthase (1368 nt) / Sesquiterpene cyclase	32	Not secreted	Yes	(Proctor *et al.*, 1995a)
TRI6	FGSG_ 03536	Wheat	Hypothetical protein similar to regulatory protein (756 nt) / Trichothecene biosynthesis positive transcription factor	32	Not secreted	Yes	(McDonald *et al.*, 2005)
TRI10	FGSG_ 03538	Wheat	Hypothetical protein similar to TRI10 (1353 nt) / Regulatory protein	32	Nucleus	Yes	(Seong *et al.*, 2009)
TRI14	FGSG_ 03543	Wheat	Hypothetical protein similar to TRI14 (1192 nt) / Putative trichothecene biosynthesis gene	32	Not secreted	Yes	(Dyer *et al.*, 2005)

VE1	FGSG_ 11955	Wheat	Hypothetical protein similar to VeA protein (2260 nt) / Probable sexual development activator VeA protein	34,43	Nucleus	No	J. Merhej, INRA, France, Unpublished
ZIF1	FGSG_ 01555	Maize / Wheat	Conserved hypothetical protein (2295 nt) / bZIP transcription factor	99	Not secreted	-	(Seong *et al.*, 2005)

Appendix 1 continued All the single gene deletion strains of *F. graminearum* that had demonstrated no difference in pathogenicity when compared to the wild type strain. All reference may be found in PHI-base via gene name or FG locus ID.

Gene	**FG3 locus**	**Host organism**	**Putative function (BROAD/MIPS)**	**MIPS functional characterisation**	**Hypothesised cellular location of gene products**	**Genes unique to *Fusarium spp***	**Reference**
AUR1	FGSG_ 00338	Wheat	Hypothetical protein similar to aureobasidin-resistance protein (2397 nt)	1, 32, 42	Golgi apparatus (AUR1)	No	(Gaffoor *et al.*, 2005)
Butenolide synthesis	FGSG_ 08079	Wheat	Conserved hypothetical protein (1747 nt) / Probable benzoate 4-monooxygenase cytochrome P450	1	Not secreted	Yes	(Harris et al., 2007)
FET3	FGSG_ 05159	Wheat	Iron transport multicopper oxidase FET3 precursor (2218 nt) / Probable FET3 - cell surface ferroxidase, high affinity	1, 20, 32, 34	High affinity iron permease complex, plasma membrane (FET3)	No	(Greenshields *et al.*, 2007)
Os-2 (HOG1)	FGSG_ 09612	Tomato	Mitogen-activated protein kinase sty1 (2374 nt) / Osmotic sensitive-2 protein (putative mitogen-activated protein kinase homolog)	1, 10, 11, 14, 16, 18, 30, 32, 34, 40, 42, 43	Cytoplasm, nucleus (HOG1)	No	(Ochiai *et al.*, 2007, Ramamoorthy *et al.*, 2007b)

GCS1	FGSG_ 05955	Tomato / Arabidopsis	Hypothetical protein similar to ceramide glucosyltransferase (1639 nt)	99	Secreted	No	(Ramamoorthy *et al.*, 2007a)
GIP1	-	Barley	Putative laccase (As suggested by the author)	-	-	-	(Kim *et al.*, 2005)
GRS1 (PKS14)	FGSG_ 03964	Wheat	Conserved hypothetical protein (6389 nt) / Polyketide synthase	99	Not secreted	No	(Gaffoor *et al.*, 2005)
GzFUS1 (PKS10)	FGSG_ 07798	Wheat	Hypothetical protein similar to polyketide synthase (11859 nt) / Probable polyketide synthase	99	Not secreted	No	(Gaffoor *et al.*, 2005)
GzGPA1	FGSG_ 05535	Barley	Conserved hypothetical protein (2248 nt) / Probable G protein alpha chain	1,14, 16, 18, 30, 34, 36, 40, 43	Endosome, heterotrimeric G-protein complex, plasma membrane (GPA1)	No	(Yu *et al.*, 2008)
GzGPA3	FGSG_ 09988	Barley	Guanine nucleotide-binding protein alpha-2 subunit (2395 nt) / Probable G protein alpha chain	1,14, 16, 18, 30, 34, 36, 40, 43	Heterotrimeric G-protein complex, plasma membrane	No	(Yu *et al.*, 2008)
HDF3	FGSG_ 05636	Wheat / Maize	Conserved hypothetical protein (3471 nt) / Related to histone deacetylase HOS3	10,14	Nucleus	No	(Li *et al.*, 2011)
KSA1	FGSG_ 07226	Wheat	3-oxoacyl-[acyl-carrier-protein] synthase, mitochondrial precursor (1495 nt) / Probable CEM1 - beta-keto-acyl-ACP synthase, mitochondrial	1, 2, 16	Mitochondrial	No	(Gaffoor *et al.*, 2005)
LIP1	FGSG_ 01603	Wheat	Hypothetical protein similar to sterol esterase precursor (1767 nt) / Probable triacylglycerol lipase V precursor	1	Secreted	No	(Feng *et al.*, 2005)

PGL1	FGSG_ 09182	Wheat	Hypothetical protein similar to polyketide synthase (6668 nt) / Related to sterigmatocystin biosynthesis polyketide synthase	99	Not secreted	No	(Gaffoor *et al.*, 2005)
PKS1	FGSG_ 10548	Wheat	Conserved hypothetical protein (7909 nt) / Polyketide synthase	99	Not secreted	No	(Gaffoor *et al.*, 2005)
PKS2	FGSG_ 04694	Wheat	Hypothetical protein similar to polyketide synthase (8208 nt) / Polyketide synthase	1, 32	Not secreted	No	(Gaffoor *et al.*, 2005)
PKS4 (related: ZEA1)	FGSG_ 12126	Barley / Wheat	Hypothetical protein similar to polyketide synthase (6876 nt) / Polyketide synthase	32	Not secreted	-	(Gaffoor & Trail, 2006, Lysoe et al., 2006)
PKS5	FGSG_ 05794	Wheat	Conserved hypothetical protein (10061 nt) / Related to polyketide synthase	-	Not secreted	No	(Gaffoor *et al.*, 2005)
PKS6	FGSG_ 08208	Wheat	Hypothetical protein similar to polyketide synthase (7772 nt) / Polyketide synthase	1, 32	Not secreted	No	(Gaffoor *et al.*, 2005)
PKS7	FGSG_ 08795	Wheat	Hypothetical protein similar to polyketide synthase (7426 nt) / Polyketide synthase	-	Not secreted	No	(Gaffoor *et al.*, 2005)
PKS9	FGSG_ 10464	Wheat	Hypothetical protein similar to polyketide synthase type I (8224 nt) / Polyketide synthase	-	Not secreted	No	(Gaffoor *et al.*, 2005)
PKS11	FGSG_ 01790	Wheat	Conserved hypothetical protein (7644 nt) / Polyketide synthase	1, 32	Not secreted	No	(Gaffoor *et al.*, 2005)
PKS13 (related:	FGSG_ 02395	Barley / Wheat	Hypothetical protein similar to polyketide synthase (6322 nt) /	99	Not secreted	-	(Gaffoor *et al.*, 2005, Kim

ZEA2)			Polyketide synthase				*et al.*, 2005)
PKS17 (renamed PKS8)	FGSG_ 03340	Wheat	Hypothetical protein similar to polyketide synthase (8525 nt) / Polyketide synthase	1, 32	Not secreted	No	(Gaffoor *et al.*, 2005)
PLSP1	FGSG_ 04488	Wheat	Conserved hypothetical protein (825 nt)	99	Not secreted	No	(Gaffoor *et al.*, 2005)
TRI5	FGSG_ 03537	Arabidopsis / Oat / Maize / Wheat*	Trichodiene synthase (1368 nt) / Sesquiterpene cyclase	32	Not secreted	Yes	(Proctor *et al.*, 1995a)
ZEB1	FGSG_ 02397	Barley	Hypothetical protein similar to isoamyl alcohol oxidase (895 nt) / Probable isoamyl alcohol oxidase	99	Not secreted	Yes	(Kim *et al.*, 2005)
ZEB2	FGSG_ 02398	Barley	Hypothetical protein similar to bZIP domain-containing transcription factor (1048 nt) / Hypothetical protein	99	Not secreted	Yes	(Kim *et al.*, 2005)

Appendix 2 Protein function characterisation and the relevant MIPS functional code.

MIPS Functional code	Protein functional characterisation
01	Metabolism
02	Energy
10	Cell cycle and DNA processing
11	Transcription
14	Protein fate (folding, modification and destination)
16	Protein with binding function or cofactor requirement (structural or catalytic)
18	Regulation of metabolism or protein function
20	Cellular transport, transport facilities and transport routes
30	Cellular communication / Signal transduction mechanism
32	Cell rescue, defence and virulence
34	Interaction with the environment
40	Cell fate
42	Biogenesis of cellular components
43	Cell type differentiation
99	Unclassified proteins

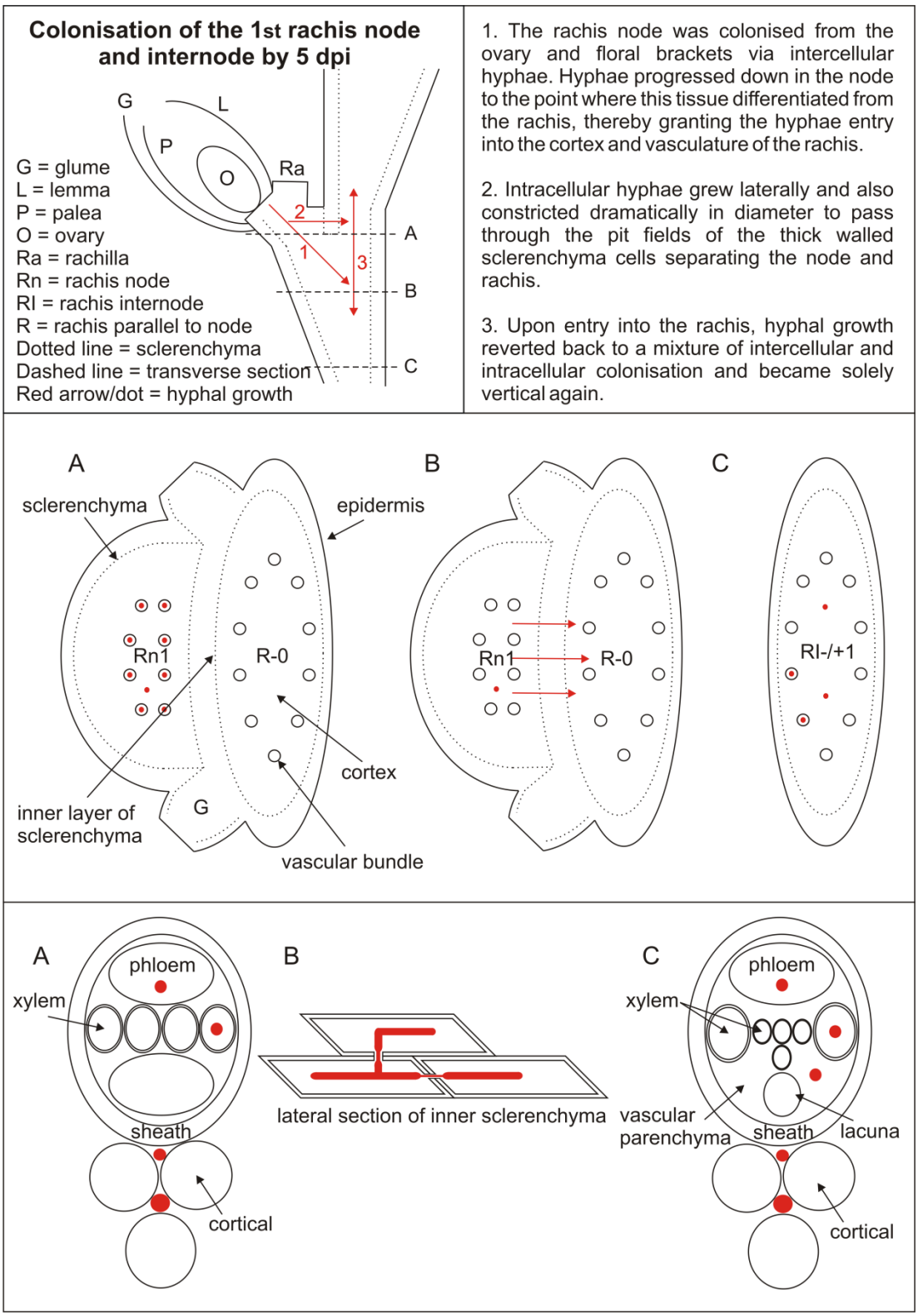

Appendix 3 A schematic of the initial colonisation of the rachis via two different routes, vertical intercellular and lateral intracellular growth by 5 dpi.

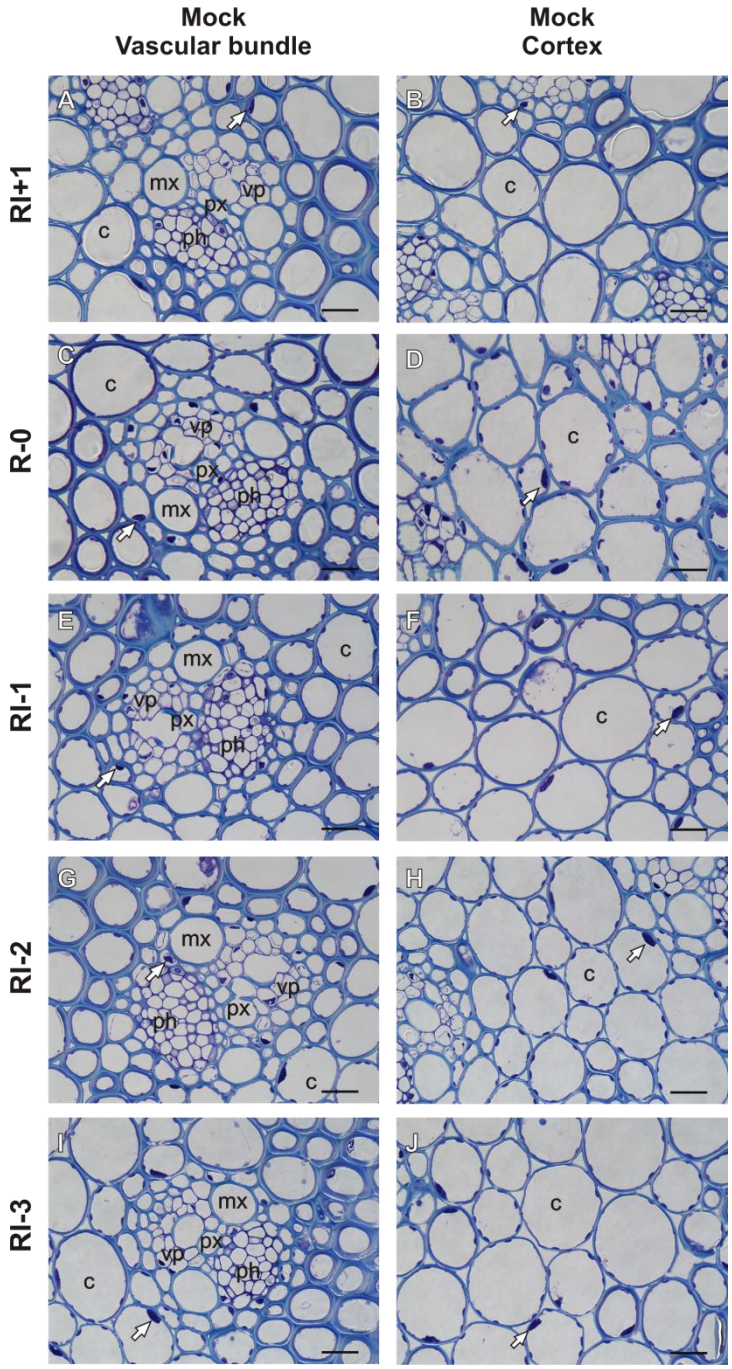

Appendix 4 The vascular bundles (**A**, **C**, **E, G** and **I**) and cortex (**B**, **D**, **F**, **H** and **J**) of sequential rachis internodes (RI+1 to RI-3) from a healthy wheat rachis at 5 dpi. Bar = 25 µm. All images in this figure are transverse 1 µm LR white sections stained with 0.1 % TBO, pH 9. Legend: c = cortex, mx = metaxylem, px = protoxylem, ph= phloem, vp = vascular parenchyma, white arrow = host nuclei.

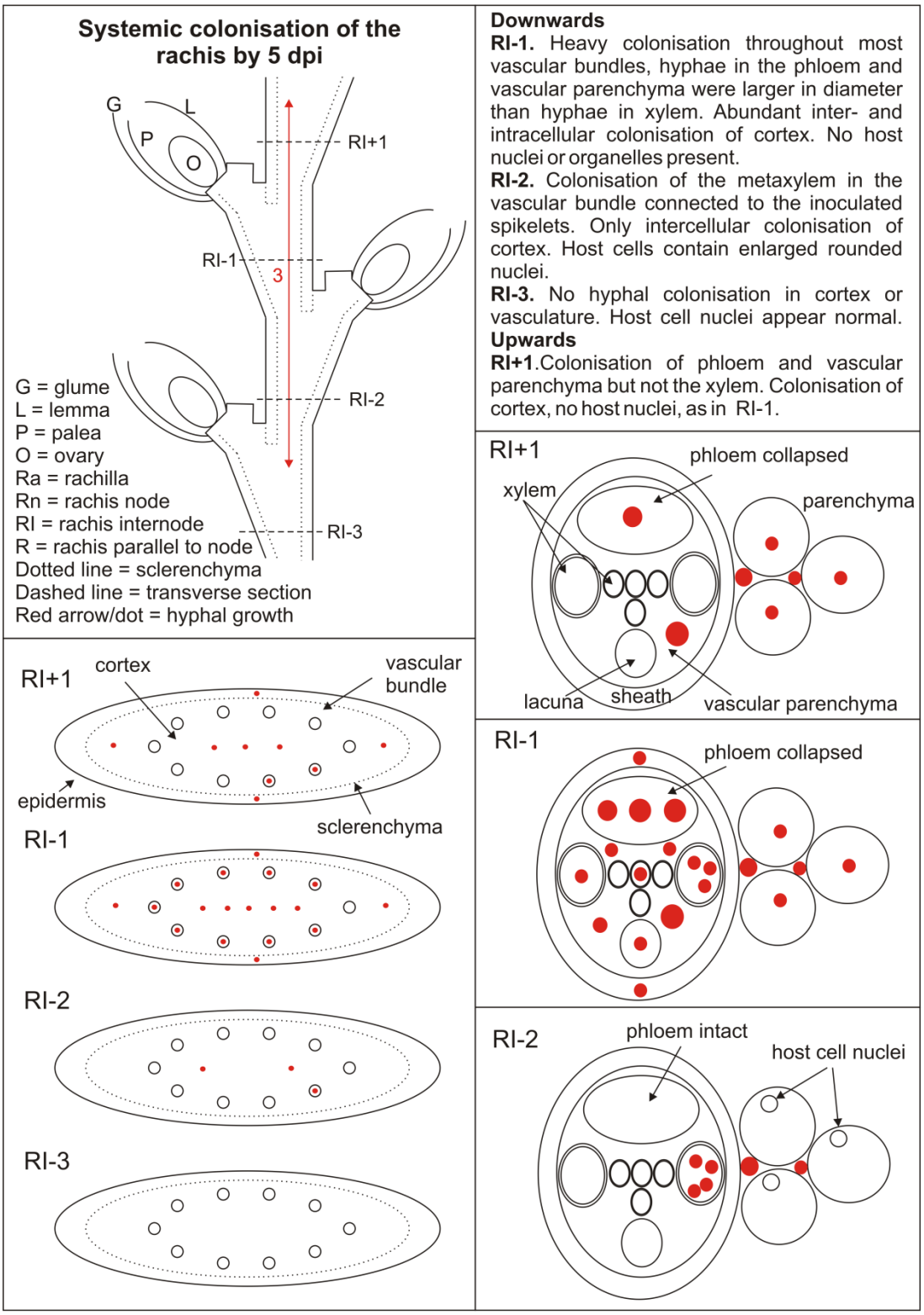

Appendix 5 A schematic of the systemic colonisation of the rachis via intercellular hyphal growth in the cortex and intracellular growth in the vasculature by 5 dpi.

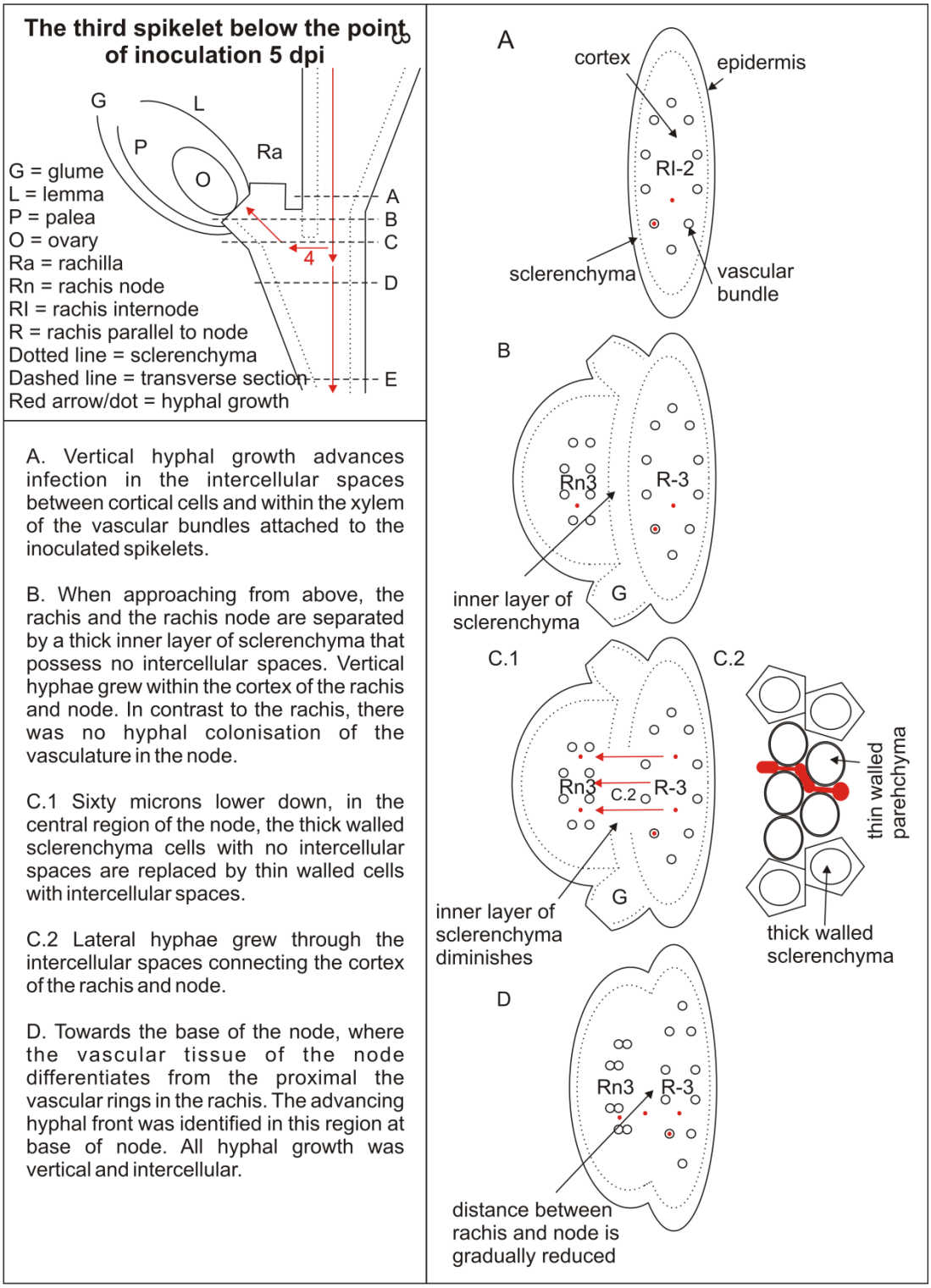

Appendix 6 A schematic of the colonisation of the rachis and rachis node connected to the third spikelet below the original point of inoculation by *Fusarium graminearum* at 5 dpi.

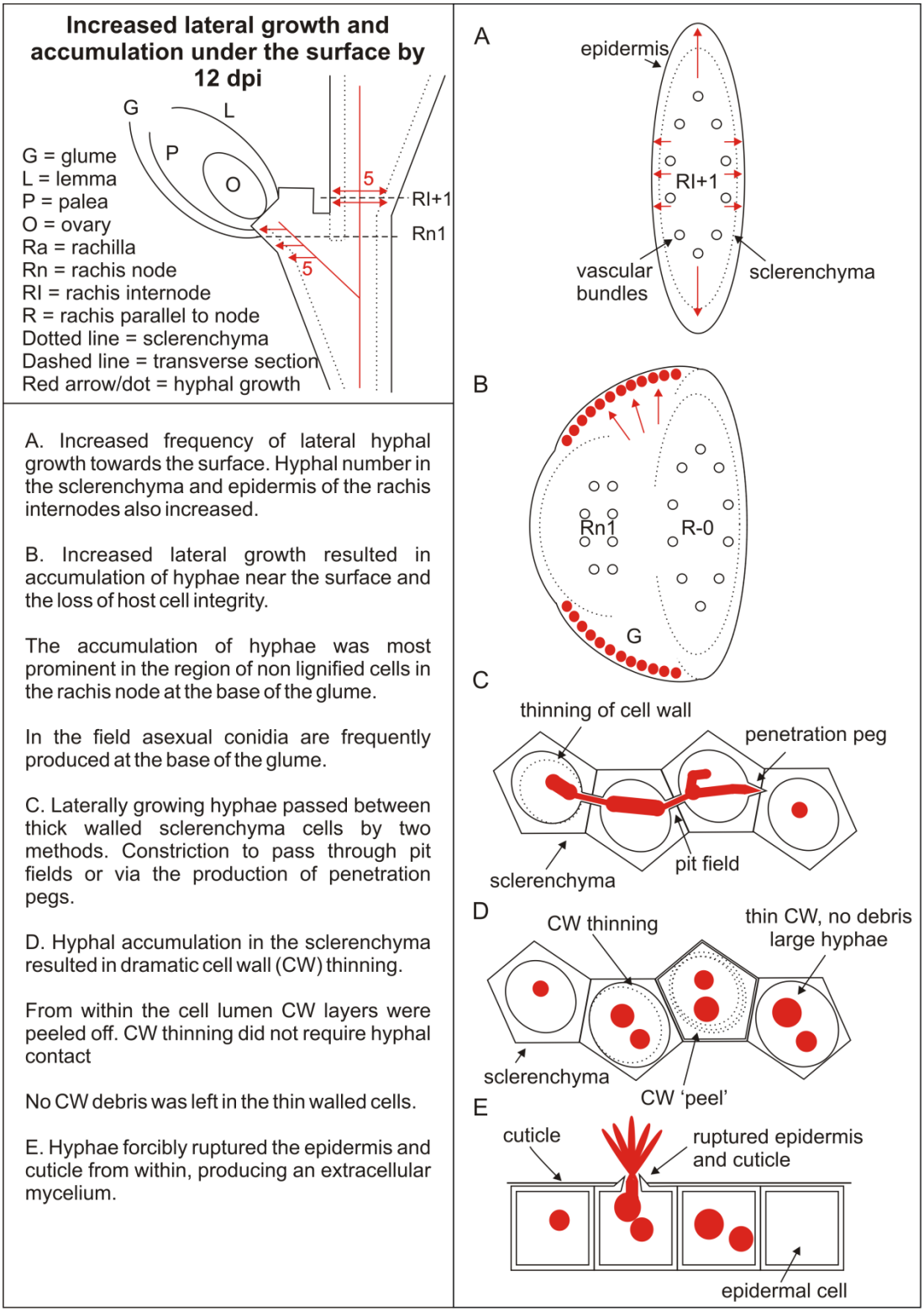

Appendix 7 A schematic of the increased lateral growth and hyphal accumulation immediately beneath the surface of the ear, and the rupture of the epidermis by 12 dpi.

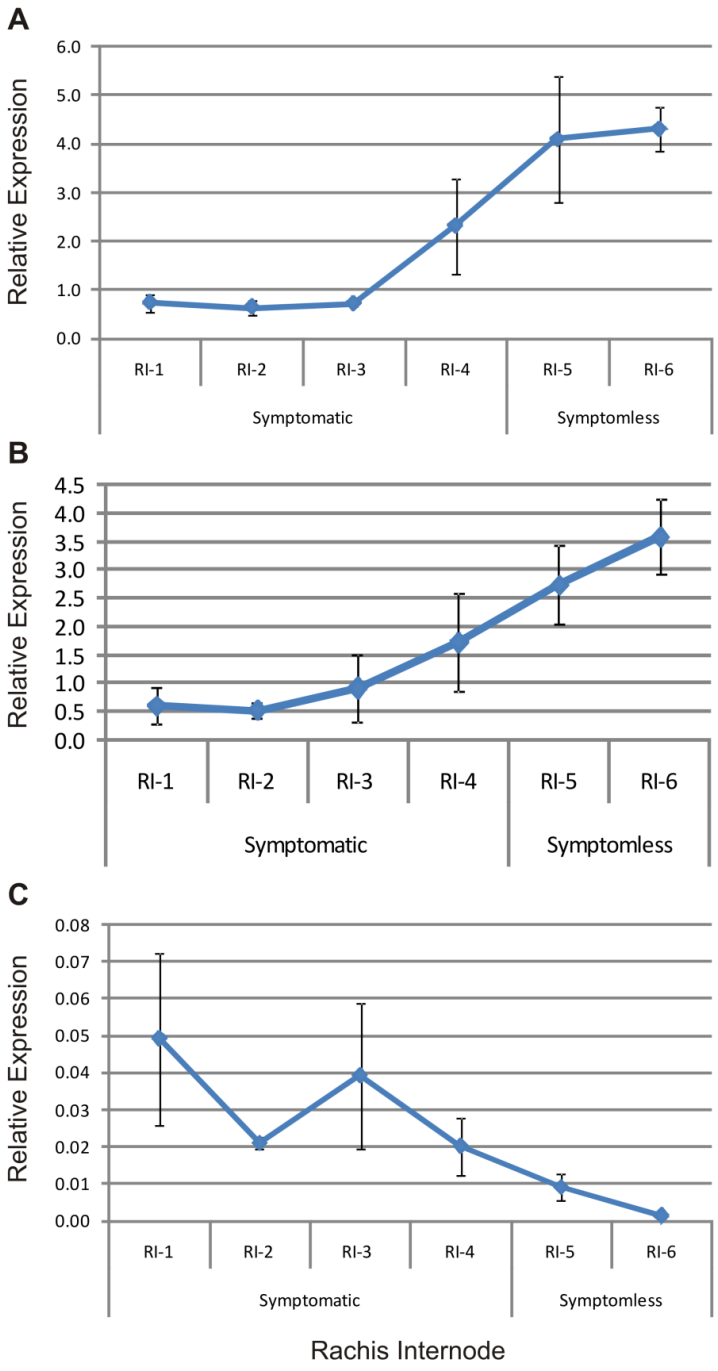

Appendix 8 Fungal *TRI4* (A) and *TRI5* (B) gene expression in the infected rachis internodes in which *F. graminearum* was detected at 7 dpi. Relative expression was measured by RT-qPCR and values normalised for fungal biomass relative to the expression of *F. graminearum* γ-actin and β-tubulin (C). Biological error is represented by one standard deviation from the mean.

Appendix 9 The fungal and oomycete genomes included within the 57 genomes that were screened for the presence of *F. graminearum* secretome genes, including A) plant pathogens, B) saprotrophs, C) animal pathogens and D) non-pathogens. Conservation data was generated according to sub-sets relevant to host / tissue specificity and pathogenic lifestyle.

Analysis	**Fungal / Oomycete genomes**	**Host**	**Cereal Path**	**Pathogenic lifestyle**	**Organ Specificity**
A	*Fusarium graminearum*	P,ICA	C,N	S, N	F,Se,St,E
	Fusarium oxysporum	P,ICA	C,N	S, N	R,St
	Fusarium solani	P,ICA	C,N	S, N	R
	Fusarium verticillioides	P,ICA	C,N	S, N	Se,St,E,R
	Alternaria brassicicola	P	C,N	N	L,Se,St,P
	Blumeria graminis[h]	P	C	B	L
	Botrytis cinerea	P	N	N	F
	Cochliobolus heterotrophus	P	C	N	L
	Hyaloperonospora arabidopsis[oh]	P	N	B	L
	Hyaloperonospora parasitica[oh]	P	N	B	L
	Leptosphaeria maculans	P	N	H	St,L
	Magnaporthe grisea	P	C	H	L,E
	Melampsora laricis-populina[b]	P	N	B	L
	Mycosphaerella fijiensis	P	N	H	L
	Mycosphaerella graminicola	P	C	H	L
	Phytophthora infestans[o]	P	N	H	T
	Phytophthora ramorum[o]	P	N	H	L,St
	Phytophthora sojae[o]	P	N	H	R, St
	Puccinia graminis[bh]	P	C	B	L,St
	Pyrenophora tritici repens	P	C	N	L,St,Se,E
	Sclerotinia sclerotiorum	P	N	N	L,F,St,P
	Sporisorium reilianum[b]	P	C	B	E,Se
	Stagonospora nodorum	P	C	N	L,E
	Ustilago maydis[b]	P	C	B	E,Se,St
	Verticillium dahliae	P	N	N	R,St,L
B	*Neurospora crassa*	S	-	S	-
	Phanerochaete chrysosporium[b]	S	-	S	-
	Trichoderma reesei	S	-	S	-

	Trichoderma virens	S	-	S	-
	Aspergillus nidulans	S,ICA	-	S	-
	Chaetomium globosum	S,ICA	-	S	-
	Rhizopus oryzae[m]	S,ICA	-	S	-
C	*Aspergillus fumigatus*	S,ICA	-	OP	-
	Candida albicans	ICA	-	OP	-
	Candida glabrata	ICA	-	OP	-
	Coccidioides immitis	ICA	-	OP	-
	Cryptococcus neoformans[b]	ICA	-	OP	-
	Histoplasma capsulatum	A,ICA	-	OP	-
	Batrachochytrium dendrobatidis[r]	A	-	P	-
	Blastomyces dermatitidis	A	-	OP	-
	Microsporum gypseum	A	-	OP	-
	Paracoccidioides brasiliensis	A	-	OP	-
D	*Saccharomyces cerevisiae*	N	-	S	-
	Schizosaccharomyces pombe	N	-	S	-

All organisms are fungal ascomycetes unless labelled otherwise. Phyla: b = basidiomycetes, o = oomycetes. Order: m = mucoraceae, r = rhizophydiales. Host: A = animal, ICA = immunocompromised animal, P = plant, S = saprotroph. Cereal Path: C = pathogen of cereal host, N = pathogen of non-cereal host. Plant pathogenic lifestyle: B = biotroph, H = hemibiotroph, N = necrotroph, S = saprotroph, OP = opportunistic pathogen, P = pathogen. Organ specificity: E = ear, F = flower, L = leaf, Se= seed, St = stem, P = petal, R = root, - = not applicable.

Appendix 10 The sub-set of *F. graminearum* genes that encode secreted proteins involved in the degradation of the plant cuticle and cell wall, divided according to substrate specificity.

Locus ID	Cell wall component	Mode of action	MIPS annotation	EC
FGSG_01621	Cellulose	hydrolysis, hydrolysis of O-glycosyl bond	probable cellulase precursor	3.2.1.4 / 3.2.1.6
FGSG_02202	Cellulose	hydrolysis of O-glycosyl bond	probable endoglucanase IV precursor	3.2.1.4
FGSG_02658	Cellulose	hydrolysis of O-glycosyl bond	probable endoglucanase	3.2.1.4
FGSG_03143	Cellulose	hydrolasis glycoside bond	related to glycosyl hydrolase	
FGSG_03632	Cellulose		related to cellulose binding protein CEL1	
FGSG_03695	Cellulose	hydrolysis of O-glycosyl bond	related to endoglucanase IV precursor	3.2.1.4
FGSG_03795	Cellulose	hydrolysis, hydrolysis of O-glycosyl bond	probable cellulase precursor	3.2.1.4 / 3.2.1.6
FGSG_04681	Cellulose	hydrolysis of O-glycosyl bond	probable endoglucanase IV precursor	3.2.1.4
FGSG_05851	Cellulose	hydrolysis of O-glycosyl bond, transglycosylation	related to endoglucanase I precursor	
FGSG_06110	Cellulose	hydrolysis of O-glycosyl bond	probable endoglucanase IV precursor	3.2.1.4
FGSG_06278	Cellulose	hydrolysis of O-glycosyl bond	probable glucan 1,4-alpha-glucosidase	3.2.1.1 / 3.2.1.3
FGSG_07944	Cellulose		related to glucanase	3.2.1.58
FGSG_08011	Cellulose		related to cellulose binding protein CEL1	
FGSG_11037	Cellulose	hydrolysis of O-glycosyl bond	probable endoglucanase I precursor	3.2.1.4
FGSG_11326	Cellulose	hydrolysis of O-glycosyl bond	probable glucan 1,4-alpha-glucosidase	3.2.1.1 / 3.2.1.3
FGSG_11488	Cellulose		related to cellulose binding protein CEL1	
FGSG_12160	Cellulose		probable cel1 protein precursor	
FGSG_13245	Cellulose	hydrolysis of O-glycosyl bond	probable endoglucanase IV	3.2.1.4
FGSG_01685	Cellulose / Cellobiose	hydrolysis of O-glycosyl bond	related to beta-glucosidase	3.2.1.21
FGSG_03387	Cellulose / Cellobiose	hydrolysis of O-glycosyl bond	probable beta-glucosidase precursor	3.2.1.21
FGSG_03570	Cellulose / Cellobiose	hydrolysis of O-glycosyl bond	probable beta-glucosidase 1 precursor	

FGSG_03628	Cellulose / Cellobiose	hydrolysis of O-glycosyl bond	probable cellulose 1,4-beta-cellobiosidase II precursor	3.2.1.91
FGSG_03858	Cellulose / Cellobiose	hydrolysis of O-glycosyl bond	probable beta-glucosidase precursor	
FGSG_04953	Cellulose / Cellobiose	hydrolysis of O-glycosyl bond	probable beta-glucosidase precursor	3.2.1.21
FGSG_06605	Cellulose / Cellobiose	hydrolysis of O-glycosyl bond	probable beta-glucosidase	3.2.1.21
FGSG_10615	Cellulose / Cellobiose	hydrolysis of O-glycosyl bond	related to beta-glucosidase precursor	
FGSG_11559	Cellulose / Cellobiose	hydrolysis of O-glycosyl bond	related to beta-glucosidase 1 precursor	3.2.1.21
FGSG_02917	Cellobiose	oxidation, redox reaction, reduction	related to cellobiose dehydrogenase	1.1.99.18
FGSG_05983	Cellobiose	oxidation, redox reaction, reduction	related to cellobiose dehydrogenase	1.1.99.18
FGSG_09085	Cellobiose	oxidation, redox reaction, reduction	probable cellobiose dehydrogenase	1.1.99.18
FGSG_00783	Hemicellulose	hydrolysis of carboxylic ester	related to acetylxylan esterase precursor	3.1.1.74
FGSG_00989	Hemicellulose		probable rhamnogalacturonase B precursor	3.2.1.113
FGSG_01803	Hemicellulose	hydrolysis of O-glycosyl bond	probable alpha-galactosidase C precursor	3.2.1.22
FGSG_02059	Hemicellulose	hydrolysis of O-glycosyl bond	related to alpha-galactosidase precursor	3.2.1.22
FGSG_02314	Hemicellulose	hydrolysis of O-glycosyl bond	related to beta-mannosidase	1.1.1.49 / 3.2.1.25 / 3.2.1.132
FGSG_03002	Hemicellulose	hydrolysis of O-glycosyl bond	related to arabinan endo-1,5-alpha-L-arabinosidase A precursor	3.2.1.99
FGSG_03003	Hemicellulose	hydrolysis of O-glycosyl bond	related to alpha-N-arabinofuranosidase / alpha-L-arabinofuranosidase	3.2.1.55
FGSG_03049	Hemicellulose	hydrolysis of O-glycosyl bond	related to alpha-L-arabinofuranosidase II precursor	3.2.1.55
FGSG_03194	Hemicellulose	hydrolysis of O-glycosyl bond	probable endopolygalacturonase	3.2.1.15
FGSG_03343	Hemicellulose	hydrolysis of O-glycosyl bond	related to beta-galactosidase	3.2.1.23
FGSG_03384	Hemicellulose	hydrolysis of O-glycosyl bond	probable exopolygalacturonase	3.2.1.67 / 3.2.1.82
FGSG_03569	Hemicellulose	oxidation, redox reaction, reduction	probable galactose oxidase	1.1.3.9
FGSG_03624	Hemicellulose	hydrolysis, hydrolysis of O-glycosyl bond	probable endo-1,4-beta-xylanase A precursor	3.2.1.8
FGSG_03629	Hemicellulose	hydrolysis, hydrolysis of O-glycosyl bond	probable alpha-glucuronidase precursor	3.2.1.131 / 3.2.1.139
FGSG_03813	Hemicellulose	hydrolysis of O-glycosyl bond	probable alpha-L-arabinofuranosidase	3.2.1.37 / 3.2.1.55
FGSG_03867	Hemicellulose	hydrolysis of carboxylic ester	probable acetylxylan esterase	3.1.1.1 / 3.1.1.72 / 3.1.1.73
FGSG_03904	Hemicellulose	hydrolysis of O-glycosyl bond	probable beta-galactosidase	3.2.1.23

FGSG_03905	Hemicellulose	hydrolysis of O-glycosyl bond	related to putative arabinase	3.2.1.99
FGSG_03922	Hemicellulose	hydrolysis of O-glycosyl bond	related to class I alpha-mannosidase 1B	3.2.1.25
FGSG_04678	Hemicellulose	hydrolysis of O-glycosyl bond	related to beta-mannanase	3.2.1.78
FGSG_04689	Hemicellulose		probable rhamnogalacturonase A precursor	3.2.1.15
FGSG_04848	Hemicellulose		probable rhamnogalacturonan acetylesterase precursor	
FGSG_06117	Hemicellulose		related to rhamnogalacturonate lyase precursor	
FGSG_06463	Hemicellulose	hydrolysis of O-glycosyl bond	related to alpha-L-arabinofuranosidase A precursor	3.2.1.55
FGSG_07625	Hemicellulose	hydrolysis of O-glycosyl bond	probable alpha-L-arabinofuranosidase precursor	3.2.1.8 / 3.2.1.55
FGSG_07639	Hemicellulose	hydrolysis of O-glycosyl bond	related to xylosidase/arabinosidase	3.2.1.37 / 3.2.1.55
FGSG_07993	Hemicellulose	hydrolysis of O-glycosyl bond	related to xylan 1,4-beta-xylosidase	3.2.1.37
FGSG_09093	Hemicellulose	oxidation, redox reaction, reduction	related to galactose oxidase precursor	1.1.3.9
FGSG_10670	Hemicellulose	hydrolysis of carboxylic ester	probable acetylxylan esterase precursor	3.1.1.72
FGSG_10999	Hemicellulose	hydrolysis, hydrolysis of O-glycosyl bond	endo-1,4-beta-xylanase	3.2.1.8
FGSG_11011	Hemicellulose	hydrolysis of O-glycosyl bond	probable PGU1 - Endo-polygalacturonase	3.2.1.15
FGSG_11032	Hemicellulose		galactose oxidase precursor [GAO]	1.1.3.9
FGSG_11048	Hemicellulose	hydrolysis of O-glycosyl bond	probable arabinogalactan endo-1,4-beta-galactosidase	3.2.1.89
FGSG_11066	Hemicellulose	hydrolysis of O-glycosyl bond	related to beta-mannanase	3.2.1.78
FGSG_11169	Hemicellulose	hydrolysis of O-glycosyl bond	related to alpha-galactosidase precursor	3.2.1.22
FGSG_11229	Hemicellulose	hydrolysis of carboxylic ester	related to acetylxylan esterase	3.1.1.72
FGSG_11304	Hemicellulose	hydrolysis, hydrolysis of O-glycosyl bond	related to endo-1,4-beta-xylanase	3.2.1.8 / 3.2.1.4
FGSG_11487	Hemicellulose	hydrolysis, hydrolysis of O-glycosyl bond	related to endo-1,4-beta-xylanase	3.2.1.8
FGSG_11548	Hemicellulose	hydrolysis of carboxylic ester	related to acetylxylan esterase precursor	3.1.1.72 / 3.1.1.74
FGSG_12047	Hemicellulose	hydrolysis, hydrolysis of O-glycosyl bond	probable endo-1,4-beta-xylanase A precursor	3.2.1.8
FGSG_13189	Hemicellulose	hydrolysis, hydrolysis of O-glycosyl bond	probable endo-1,4-beta-xylanase	3.2.1.8
FGSG_02987	Hemicellulose / Lignin	carboxylic ester hydrolysis	related to feruloyl esterase B precursor	3.1.1.20 / 3.1.1.72 / 3.1.1.73 / 3.5.1.11
FGSG_03217	Hemicellulose / Lignin	carboxylic ester hydrolysis	related to feruloyl esterase B precursor	3.1.1.20 / 3.1.1.73 / 3.5.1.11

FGSG_11428	Hemicellulose / Lignin	carboxylic ester hydrolysis	probable feruloyl esterase B precursor	3.1.1.20 / 3.1.1.72 / 3.1.1.73
FGSG_12548	Hemicellulose / Lignin	carboxylic ester hydrolysis	related to feruloyl esterase B precursor	3.1.1.20 / 3.1.1.72 / 3.1.1.73
FGSG_01607	Pectin	beta-elimination, elimination, ester hydrolysis	probable pectin lyase precursor	4.2.2.10
FGSG_02977	Pectin	elimination	probable pectate lyase	4.2.2.2
FGSG_03121	Pectin	beta-elimination, elimination, ester hydrolysis	probable pectin lyase precursor	4.2.2.10
FGSG_03131	Pectin	elimination	related to pectate lyase L precursor	4.2.2.2 / 4.2.2.9
FGSG_03406	Pectin	hydrolysis of carboxylic ester	probable pectinesterase precursor	3.1.1.11
FGSG_03908	Pectin	elimination	probable pectate lyase 1	4.2.2.2
FGSG_04439	Pectin	hydrolysis of carboxylic ester	related to pectinesterase	3.1.1.11
FGSG_04864	Pectin	elimination	probable pectate lyase	4.2.2.2
FGSG_07794	Pectin	elimination	probable pectate lyase 1	4.2.2.2
FGSG_09291	Pectin	elimination	probable pectate lyase 1	4.2.2.2
FGSG_11094	Pectin	elimination	probable pectate lyase	4.2.2.2
FGSG_11163	Pectin	elimination	probable pectate lyase 1	4.2.2.2
FGSG_02330	Lignin	oxidation, redox reaction, reduction	related to laccase precursor	1.10.3.3
FGSG_03507	Lignin	oxidation, redox reaction, reduction	related to laccase precursor	1.10.3.2
FGSG_09646	Lignin	oxidation, redox reaction, reduction	related to laccase precursor	1.10.3.2
FGSG_04434	Lignin		related to peroxidase	1.11.1.11 / 1.11.1.13
FGSG_03436	Lignin	oxidation, redox reaction, reduction	related to chloroperoxidase	1.11.1.10
FGSG_02651	Callose	hydrolysis of O-glycosyl bond	related to endo-1,3-beta-glucanase	3.2.1.6
FGSG_03529	Callose		related to glucan 1,3-beta-glucosidase	3.2.1.58
FGSG_03827	Callose	hydrolysis of O-glycosyl bond	related to endo-1,3-beta-glucanase	3.2.1.6
FGSG_04768	Callose	hydrolysis of O-glycosyl bond	related to endo-1,3-beta-glucanase	3.2.1.6
FGSG_06616	Callose		probable beta-1,3 exoglucanase precursor	3.2.1.58
FGSG_07238	Callose	hydrolysis of O-glycosyl bond	related to beta-1,3 exoglucanase	3.2.1.58
FGSG_08265	Callose	hydrolysis of O-glycosyl bond	related to SPR1 - exo-1,3-beta-glucanase precursor	3.2.1.75

FGSG_09445	Callose	hydrolysis of O-glycosyl bond	related to beta-1,3 exoglucanase precursor	3.2.1.58
FGSG_11006	Callose	hydrolysis of O-glycosyl bond, transglycosylation	probable glucan endo-1,3-beta-glucosidase bgn13.1 precursor	3.2.1.39 / 3.2.1.58
FGSG_02890	Cuticle	carboxylic ester hydrolysis	probable cutinase precursor	3.1.1.74
FGSG_03457	Cuticle	carboxylic ester hydrolysis	probable cutinase 1 precursor	

Appendix 11 The sub-set of *F. graminearum* genes that encode secreted proteins involved in the degradation of the plant cell, divided according to substrate specificity (starch, lipid and protein).

Locus ID	Cell component	Mode of action	MIPS annotation	EC
FGSG_03842	Starch	Hydrolysis of O-glycosyl bond	related to alpha-amylase A precursor	3.2.1.1
FGSG_04704	Starch	Hydrolysis of O-glycosyl bond	related to glucoamylase precursor	3.2.1.3
FGSG_03034	Starch	Oxidation, reduction	related to glucose dehydrogenase	1.1.3.7 / 1.1.99.1
FGSG_01240	Lipid	Hydrolysis, hydrolysis of carboxylic ester, acetylation	related to triacylglycerol lipase	3.1.1.3
FGSG_01603	Lipid	Hydrolysis, hydrolysis of carboxylic ester, acetylation	probable triacylglycerol lipase V precursor	3.1.1.13 / 3.1.1.3
FGSG_03012	Lipid	Hydrolysis, hydrolysis of carboxylic ester, acetylation	related to triacylglycerol lipase V precursor	3.1.1.3
FGSG_03095	Lipid	Hydrolysis, hydrolysis of carboxylic ester, acetylation	related to triacylglycerol lipase V precursor	3.1.1.3
FGSG_03209	Lipid	Hydrolysis, hydrolysis of carboxylic ester, acetylation	related to triacylglycerol lipase II precursor	3.1.1.3 / 3.1.1.7
FGSG_03243	Lipid	Hydrolysis, hydrolysis of carboxylic ester, acetylation	related to triacylglycerol lipase II precursor	3.1.1.3
FGSG_03583	Lipid	Hydrolysis, hydrolysis of carboxylic ester, acetylation	related to triacylglycerol lipase V precursor	3.1.1.3 / 3.1.1.42 / 3.1.1.8
FGSG_03687	Lipid	Hydrolysis, hydrolysis of carboxylic ester, acetylation	related to triacylglycerol lipase V precursor	3.1.1.3
FGSG_03846	Lipid	Hydrolysis, hydrolysis of carboxylic ester, acetylation	related to lipase 1	3.1.1.3
FGSG_04818	Lipid	Hydrolysis, hydrolysis of carboxylic ester, acetylation	related to triacylglycerol lipase precursor	3.1.1.3 / 3.1.1.73
FGSG_05906	Lipid	Hydrolysis, hydrolysis of carboxylic ester, acetylation	probable triacylglycerol lipase precursor	3.1.1.3
FGSG_06437	Lipid	Hydrolysis, hydrolysis of carboxylic ester, acetylation	related to triacylglycerol lipase V precursor	3.1.1.3
FGSG_09099	Lipid	Hydrolysis, hydrolysis of carboxylic ester, acetylation	related to triacylglycerol lipase V precursor	3.1.1.8

FGSG_09181	Lipid	Hydrolysis, hydrolysis of carboxylic ester, acetylation	related to triacylglycerol lipase II precursor	3.1.1.3
FGSG_10713	Lipid	Hydrolysis, hydrolysis of carboxylic ester, acetylation	related to triacylglycerol lipase V precursor	3.1.1.3
FGSG_11112	Lipid	Hydrolysis, hydrolysis of carboxylic ester, acetylation	related to lipase/acylhydrolase	3.2.1.4 / 3.1.1.72
FGSG_11227	Lipid	Hydrolysis, hydrolysis of carboxylic ester, acetylation	related to lipase B precursor	3.1.1.3
FGSG_11386	Lipid	Hydrolysis, hydrolysis of carboxylic ester, acetylation	related to triacylglycerol lipase II precursor	3.1.1.1
FGSG_11036	Lipid	Hydrolysis of carboxylic ester	related to esterase D	3.1.1.72
FGSG_02918	Protein	Hydrolysis of peptide bond	related to aspartic proteinase, pepstatin-sensitive	3.4.23.1 / 3.4.23.15 / 3.4.23.24
FGSG_04397	Protein	Hydrolysis of peptide bond	related to aspartic proteinase, pepstatin-sensitive	3.4.23.1 / 3.4.23.5
FGSG_04817	Protein	Hydrolysis of peptide bond	related to serine protease	
FGSG_06332	Protein	Ester bond hydrolysis, hydrolysis of peptide bond, transesterification, transpeptidation	related to subtilisin-like serine protease	3.4.21.62
FGSG_06895	Protein	Hydrolysis of peptide bond	probable PRC1 - carboxypeptidase y, serine-type protease	3.4.16.5
FGSG_07775	Protein	Hydrolysis of proteins, including elastin, by preferential cleavage	probable aspartic proteinase precursor	3.4.23.18 / 3.4.23.20 / 3.4.23.22
FGSG_08464	Protein	Hydrolysis of proteins with broad specificity	related to alkaline protease (oryzin)	3.4.21.62 / 3.4.21.63
FGSG_08583	Protein	Hydrolysis of peptide bond	related to aspartyl proteinase SAP3 precursor	3.4.23.24
FGSG_09382	Protein	Hydrolysis of proteins with broad specificity	probable alkaline protease (oryzin)	3.4.21.62 / 3.4.21.63
FGSG_10525	Protein	Ester bond hydrolysis, hydrolysis of peptide bond, transesterification, transpeptidation	related to subtilisin-like serine protease	3.4.21.62 / 3.4.21.63
FGSG_10595	Protein	Hydrolysis of proteins with broad specificity	related to alkaline protease (oryzin)	3.4.21.62 / 3.4.21.63
FGSG_10712	Protein	Hydrolysis of proteins with broad specificity	related to alkaline protease (oryzin)	3.4.21.62 / 3.4.21.63
FGSG_12544	Protein		related to proteinase R precursor	
FGSG_00806	Protein		probable endopeptidase K	3.4.21.62 / 3.4.21.63
FGSG_02976	Protein		probable endopeptidase K	3.4.21.64
FGSG_03315	Protein		related to endopeptidase K	3.4.21.62 / 3.4.21.63
FGSG_03975	Protein	Cleavage of hydrophobic, N-terminal signal from secreted proteins	related to aspartic-type signal peptidase	
FGSG_04546	Protein		related to serine-type carboxypeptidase f precursor	3.4.16.6

FGSG_05797	Protein		probable Serine-type carboxypeptidase F precursor	3.4.16.6
FGSG_12142	Protein	Hydrolysis of peptide bond, release of N-terminal residue from tripeptide	related to tripeptidyl-peptidase I	3.4.11.4 / 3.4.14.9
FGSG_11280	Protein	Hydrolysis of carboxylic ester, transesterification	probable acetylesterase	3.1.1.11
FGSG_02015	Protein	Acetylation, carboxylic ester hydrolysis, transesterification	related to esterase	3.1.1.3 / 3.1.1.42 / 3.1.1.8
FGSG_03331	Protein	Hydrolysis of peptide bond	related to YSP3 - subtilisin-like protease III	3.4.21.48
FGSG_03432	Protein	Hydrolysis of peptide bond	probable endothiapepsin precursor	3.4.23.18 / 3.4.23.20 / 3.4.23.22
FGSG_03467	Protein	Hydrolysis of peptide bond	probable extracellular elastinolytic metalloproteinase precursor	
FGSG_03769	Protein	Hydrolysis of peptide bond	related to carboxypeptidase	3.4.16.5 / 3.4.16.6
FGSG_04097	Protein		related to PRC1 - carboxypeptidase y, serine-type protease	3.2.1.21
FGSG_04527	Protein	Hydrolysis of peptide bond	related to carboxypeptidase	3.4.16.5 / 3.4.16.6
FGSG_05245	Protein	Hydrolysis of peptide bond	related to aminopeptidase	3.4.11.10
FGSG_06572	Protein		probable subtilisin-like serine protease	
FGSG_08196	Protein	Hydrolysis of peptide bond	related to aspergillopepsin II precursor	3.4.23.19 / 3.4.23.32
FGSG_10982	Protein	Hydrolysis of peptide bond	related to dipeptidyl aminopeptidase B	3.4.14.5
FGSG_11249	Protein	Hydrolysis of peptide bond	related to carboxypeptidase A	3.4.17.1 / 3.4.17.15
FGSG_11472	Protein		probable subtilisin-like serine protease	
FGSG_00028	Protein		probable metalloprotease MEP1	
FGSG_08289	Protein		related to neutral proteinase	
FGSG_08454	Protein	Hydrolysis of peptide bond	related to carboxypeptidase	3.4.16.5 / 3.4.16.6

Appendix 12 The sub-set of *F. graminearum* genes that encode MIPS annotated secreted proteins but not predicted to function in the degradation of plant cells.

FGSG_ID	MIPS Annotation
FGSG_00006	related to gEgh 16 protein
FGSG_00023	probable spherulin 1A precursor
FGSG_00060	related to KP4 killer toxin
FGSG_00061	related to KP4 killer toxin
FGSG_00062	related to KP4 killer toxin
FGSG_00100	related to 6-hydroxy-d-nicotine oxidase
FGSG_00642	related to spore coat protein SP96 precursor
FGSG_00742	related to S-adenosylmethionine:diacylglycerol 3-amino-3-carboxypropyl transferase
FGSG_01595	putative protein [EST hit]
FGSG_01660	putative protein [EST hit]
FGSG_01763	putative protein [EST hit]
FGSG_01818	related to bacterial leucyl aminopeptidase
FGSG_01829	related to aldose 1-epimerase
FGSG_01831	related to trihydrophobin precursor
FGSG_01988	related to monophenol monooxygenase (tyrosinase)
FGSG_02269	putative protein [EST hit]
FGSG_02339	related to SUC2 - invertase (sucrose hydrolyzing enzyme)
FGSG_02422	related to spore coat protein SP96 precursor
FGSG_02686	related to ribonucleases
FGSG_02893	related to protein-arginine deiminase type II
FGSG_03109	related to plant PR-1 class of pathogen related proteins
FGSG_03307	related to isoamyl alcohol oxidase
FGSG_03379	related to ribonucleases
FGSG_03526	OrfE - unknown, trichothecene gene cluster
FGSG_03531	monooxygenase
FGSG_03532	trichothecene 3-O-esterase
FGSG_03585	putative protein [EST hit]
FGSG_03616	related to isoamyl alcohol oxidase
FGSG_03816	probable lactonohydrolase
FGSG_03865	related to L-sorbosone dehydrogenase
FGSG_03916	related to Rds1 protein
FGSG_03954	related to S.fumigata Asp FII
FGSG_03972	related to isoamyl alcohol oxidase

FGSG_04504	related to acid phosphatase precursor
FGSG_04732	related to 6-hydroxy-d-nicotine oxidase
FGSG_04745	related to antifungal protein
FGSG_04980	related to palmitoyl-(protein) hydrolase
FGSG_05163	probable heterokaryon incompatibility Het-C protein
FGSG_05757	probable rAsp f 9 allergen
FGSG_05763	related to glyoxal oxidase precursor
FGSG_05933	related to acid phosphatase precursor
FGSG_06087	related to spore coat protein SP96 precursor
FGSG_06438	related to isoamyl alcohol oxidase
FGSG_06451	related to levanase
FGSG_06465	related to haloacetate dehalogenase H-1
FGSG_06610	related to alkaline phosphatase D precursor
FGSG_06612	related to oxalate decarboxylase
FGSG_06733	probable catalase-3
FGSG_07569	related to RF2 protein
FGSG_07608	related to acid phosphatase precursor
FGSG_07661	related to 6-hydroxy-d-nicotine oxidase
FGSG_07678	related to acid phosphatase Pho610
FGSG_07691	related to OrfH, unknown gene in trichothecene gene cluster
FGSG_07721	probable arylsulfatase
FGSG_07838	probable isoamyl alcohol oxidase
FGSG_07934	putative protein [EST hit]
FGSG_08007	related to monophenol monooxygenase (tyrosinase)
FGSG_08116	related to salicylate hydroxylase
FGSG_08150	related to PLB1 - phospholipase B (lysophospholipase)
FGSG_08549	related to pathogenesis-related protein PR5K (thaumatin family)
FGSG_08824	related to berberine bridge enzyme
FGSG_09353	related to gEgh 16 protein
FGSG_09358	related to phosphatidylcholine-sterol acyltransferase precursor
FGSG_09390	related to circumsporozoite protein precursor
FGSG_09586	probable phosphatidylglycerol/phosphatidylinositol transfer protein
FGSG_10206	putative protein [EST hit]
FGSG_10212	probable SnodProt1 PRECURSOR
FGSG_10495	putative protein [EST hit]
FGSG_10561	related to RF2 protein
FGSG_10587	related to peroxisomal amine oxidase (copper-containing)

FGSG_10609	related to 6-hydroxy-d-nicotine oxidase
FGSG_10611	related to 6-hydroxy-d-nicotine oxidase
FGSG_10656	related to OrfH - unknown, trichothecene gene cluster
FGSG_10675	related to lactonohydrolase
FGSG_10677	related to peroxisomal amine oxidase (copper-containing)
FGSG_10986	related to alcohol oxidase
FGSG_10998	related to 6-hydroxy-D-nicotine oxidase
FGSG_11095	related to carbonic anhydrase
FGSG_11097	related to glyoxal oxidase precursor
FGSG_11106	related to monophenol monooxygenase (tyrosinase)
FGSG_11164	probable trypsin precursor
FGSG_11190	probable ribonuclease T1
FGSG_11205	probable SnodProt1 precursor
FGSG_11236	related to non-hemolytic phospholipase C precursor
FGSG_11318	related to RF2 protein
FGSG_11517	related to monophenol monooxygenase (tyrosinase)
FGSG_11528	related to monophenol monooxygenase (tyrosinase)
FGSG_11602	probable brefeldin A resistance protein
FGSG_11645	related to proteoglycan
FGSG_11745	related to putative venom metalloproteinase jararhagin precursor
FGSG_12127	probable isoamyl alcohol oxidase
FGSG_12251	probable arylsulfatase
FGSG_12256	related to 6-hydroxy-d-nicotine oxidase
FGSG_12369	probable catalase 2
FGSG_12390	related to alcohol oxidase
FGSG_12414	related to conidiation-specific protein CON-13
FGSG_12492	related to cell wall mannoprotein
FGSG_13450	related to isoamyl alcohol oxidase
FGSG_13505	putative protein [EST hit]
FGSG_13840	probable isoamyl alcohol oxidase
FGSG_13992	related to peroxisomal short-chain alcohol dehydrogenase
FGSG_15003	related to dnase1 protein

Appendix 13 The sub-set of *F. graminearum* genes that encode secreted proteins with no MIPS annotation, but contain conserved protein functional (Pfam) domains.

FGSG-ID	Pfam domains
FGSG_10500	pfam00070,pfam07992
FGSG_02551	pfam00141
FGSG_03050	pfam00144
FGSG_04656	pfam00144
FGSG_07996	pfam00144
FGSG_08136	pfam00144
FGSG_09109	pfam00150
FGSG_02354	pfam00187,pfam00704
FGSG_00569	pfam00188
FGSG_08415	pfam00251,pfam08244
FGSG_03348	pfam00264
FGSG_03901	pfam00561
FGSG_12067	pfam00561,pfam08386
FGSG_02360	pfam00657
FGSG_03129	pfam00657
FGSG_03612	pfam00657
FGSG_12119	pfam00657
FGSG_13883	pfam00728
FGSG_01982	pfam00775
FGSG_04685	pfam00775
FGSG_11232	pfam00890,pfam01266,pfam01593,pfam03486,pfam07992
FGSG_12206	pfam00890,pfam03486
FGSG_10435	pfam01034,pfam01822,pfam03154,pfam03935,pfam03999,pfam04415,pfam04484,pfam04683,pfam05109,pfam05110,pfam05539,pfam05642,pfam05792,pfam05955,pfam06075,pfam06933,pfam07010,pfam07218,pfam07263,pfam08550,pfam08580,pfam08601,pfam08639,pfam08702,pfam08729,pfam09319,pfam09595,pfam09726,pfam09786,pfam10033
FGSG_08958	pfam01048
FGSG_03304	pfam01083
FGSG_01570	pfam01083,pfam04683,pfam05642
FGSG_03960	pfam01185
FGSG_03708	pfam01328
FGSG_02228	pfam01425
FGSG_09046	pfam01425

FGSG_05052	pfam01546,pfam07687
FGSG_02263	pfam01547
FGSG_08825	pfam01738
FGSG_03574	pfam01822
FGSG_03365	pfam03372
FGSG_03986	pfam03372
FGSG_09475	pfam03372
FGSG_06443	pfam03403
FGSG_00294	pfam03663
FGSG_03609	pfam04616
FGSG_07207	pfam04616
FGSG_07695	pfam04616
FGSG_08041	pfam04616
FGSG_11366	pfam04616
FGSG_00031	pfam05109
FGSG_02448	pfam05109
FGSG_02888	pfam05109
FGSG_15123	pfam05498
FGSG_04743	pfam05592
FGSG_11170	pfam05592
FGSG_03394	pfam05630
FGSG_06017	pfam05630
FGSG_11493	pfam05630
FGSG_10676	pfam05792,pfam10528
FGSG_03521	pfam06172
FGSG_11206	pfam06742,pfam06863
FGSG_08978	pfam07174
FGSG_08115	pfam07632
FGSG_12551	pfam07944
FGSG_07556	pfam07992
FGSG_03724	pfam08386
FGSG_01688	pfam08881
FGSG_10622	pfam08881
FGSG_10551	pfam09044
FGSG_03911	pfam09056
FGSG_06993	pfam09352
FGSG_01728	pfam09362

FGSG_06775	pfam09362
FGSG_01588	pfam09770
FGSG_04824	pfam09770
FGSG_11348	pfam10282
FGSG_04739	pfam10528
FGSG_04858	pfam10528

Appendix 14 The sub-set of *F. graminearum* genes that encode cysteine –rich (>5 %) unannotated secreted proteins.

FGSG_ID	**Mature peptide length**	**Cysteines**		**RADAR repeats**	**Pfam domains**
		Number	**Percent of peptide**		
FGSG_00002	714	70	9.8	15	-
FGSG_08978	199	12	6.03	2	pfam07174
FGSG_07899	197	10	5.08	-	-
FGSG_15251	47	6	12.77	-	-
FGSG_09132	189	10	5.29	2	-
FGSG_03599	77	10	12.99	3	-
FGSG_00847	48	4	8.33	-	-
FGSG_15437	53	8	15.09	-	-
FGSG_15123	59	4	6.78	-	pfam05498
FGSG_00260	60	6	10	-	-
FGSG_10554	180	9	5	2	-
FGSG_09066	64	8	12.5	2	-
FGSG_01688	222	12	5.41	2	pfam08881
FGSG_15448	71	8	11.27	-	-
FGSG_01754	212	14	6.6	2	-
FGSG_01776	212	14	6.6	2	-
FGSG_15142	71	8	11.27	-	-
FGSG_15469	74	6	8.11	2	-
FGSG_06712	129	16	12.4	3	-
FGSG_04239	186	14	7.53	3	-
FGSG_00114	82	6	7.32	-	-
FGSG_07755	86	6	6.98	-	-
FGSG_02898	1195	98	8.2	10	-
FGSG_05841	89	8	8.99	-	-

FGSG_07684	217	16	7.37	3	-
FGSG_11047	91	8	8.79	2	-
FGSG_11225	94	8	8.51	2	-
FGSG_08090	95	6	6.32	-	-
FGSG_09127	97	8	8.25	-	-
FGSG_04740	239	18	7.53	3	-
FGSG_02378	99	8	8.08	-	-
FGSG_02674	100	6	6	2	-
FGSG_11647	100	8	8	-	-
FGSG_00029	158	11	6.96	-	-
FGSG_03820	102	6	5.88	2	-
FGSG_08987	103	6	5.83	-	-
FGSG_05609	103	6	5.83	2	-
FGSG_08180	103	6	5.83	2	-
FGSG_03969	482	58	12.03	12	-
FGSG_03960	153	9	5.88	2	pfam01185
FGSG_04429	974	52	5.34	6	-
FGSG_10592	106	6	5.66	-	-
FGSG_00230	108	6	5.56	-	-
FGSG_05046	112	8	7.14	-	-
FGSG_00129	149	9	6.04	2	-
FGSG_03130	120	6	5	2	-
FGSG_12644	140	7	5	3	-
FGSG_02685	128	8	6.25	2	-
FGSG_02309	130	8	6.15	-	-
FGSG_08210	133	10	7.52	2	-
FGSG_03334	132	10	7.58	2	-
FGSG_07871	236	17	7.2	2	-
FGSG_11156	330	19	5.76	4	-
FGSG_12504	101	7	6.93	-	-
FGSG_12554	101	7	6.93	-	-
FGSG_12214	79	10	12.66	2	-
FGSG_12439	638	58	9.09	12	-
FGSG_10622	98	5	5.1	-	pfam08881
FGSG_12300	89	5	5.62	2	-
FGSG_15260	69	5	7.25	2	-
FGSG_15661	77	10	12.99	-	-

Appendix 15 The sub-set of *F. graminearum* genes that encode secreted proteins that are conserved ($p < e^{-5}$) within the three other *Fusaria* genomes.

FGSG_ID	MIPS Annotation	FGSG_ID	MIPS Annotation
FGSG_13436	hypothetical protein	FGSG_00131	hypothetical protein
FGSG_01660	putative protein [EST hit]	FGSG_04429	hypothetical protein
FGSG_04841	hypothetical protein	FGSG_00987	hypothetical protein
FGSG_00411	hypothetical protein	FGSG_09134	hypothetical protein
FGSG_07435	hypothetical protein	FGSG_04521	hypothetical protein
FGSG_12591	conserved hypothetical protein	FGSG_11276	hypothetical protein
FGSG_12434	hypothetical protein	FGSG_01595	putative protein [EST hit]
FGSG_12492	related to cell wall mannoprotein	FGSG_08026	hypothetical protein
FGSG_02674	conserved hypothetical protein	FGSG_00114	conserved hypothetical protein
FGSG_02269	putative protein [EST hit]	FGSG_11238	hypothetical protein
FGSG_02888	conserved hypothetical protein	FGSG_12210	hypothetical protein
FGSG_03958	hypothetical protein	FGSG_08090	hypothetical protein
FGSG_07629	hypothetical protein	FGSG_14020	hypothetical protein
FGSG_07684	hypothetical protein	FGSG_02448	conserved hypothetical protein
FGSG_03274	hypothetical protein	FGSG_11047	hypothetical protein
FGSG_04501	hypothetical protein		

Appendix 16 The sub-set of *F. graminearum* genes that encode secreted proteins which are specific to *F. graminearum* and were not detected ($p < e^{-5}$) within the other 55 fungal and oomycete genomes.

FGSG_ID	**MIPS Annotation**
FGSG_03096	hypothetical protein
FGSG_04646	hypothetical protein
FGSG_07221	hypothetical protein
FGSG_08210	hypothetical protein
FGSG_11136	hypothetical protein
FGSG_11156	hypothetical protein
FGSG_11647	hypothetical protein
FGSG_12300	hypothetical protein
FGSG_12504	hypothetical protein
FGSG_12514	hypothetical protein
FGSG_12554	hypothetical protein
FGSG_12644	hypothetical protein
FGSG_12873	hypothetical protein
FGSG_13412	hypothetical protein
FGSG_13628	hypothetical protein
FGSG_13692	hypothetical protein
FGSG_15048	hypothetical protein
FGSG_15142	hypothetical protein
FGSG_15437	hypothetical protein

Appendix 17 Images representative of the macroscopic appearance of the healthy non infected (Mock) and *F. graminearum* infected (PH-1) wheat ears over 12 days post infection.

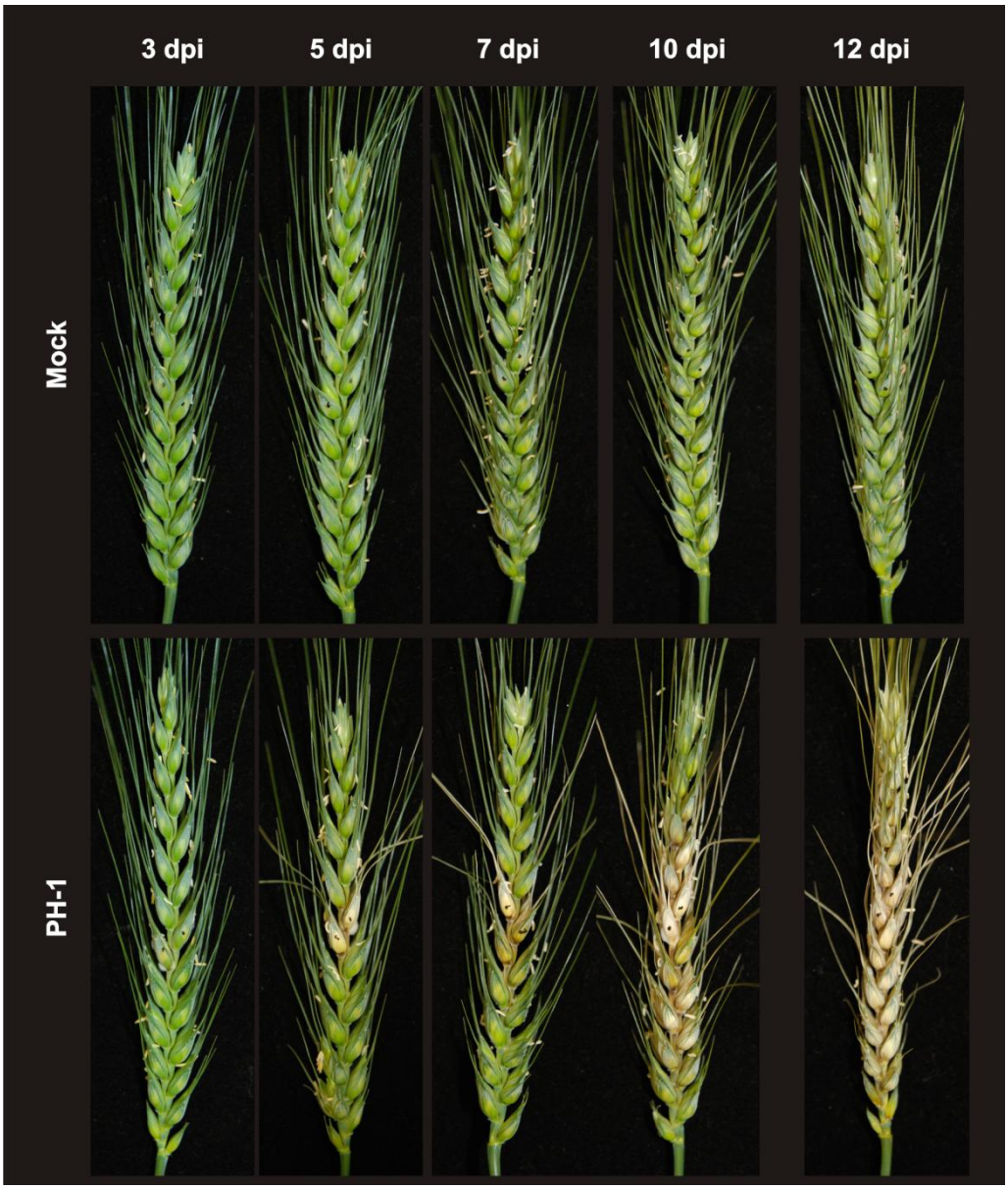

Appendix 18 Images representative of the macroscopic appearance of the healthy non infected (Mock) and *F. graminearum* infected (PH-1) sequential wheat rachis internodes below the point of infection over 12 days.